College of Social Sciences, Arts and Humanities

Graduate Program

Department of Geography and Environmental Studies

Spatiotemporal Trends of Climate Variability, Meteorological and Agricultural Droughts, and Their Effect on Land Surface Phenology in the Upper Gelana Watershed, Northeastern Highlands of Ethiopia

By Sileshi Tadesse Wodaje

June, 2025

Addis Ababa, Ethiopia

Addis Ababa University
አዲስ አበባ ዩኒቨርሲቲ
SEEK WISDOM, ELEVATE YOUR INTELLECT AND SERVE HUMANITY !

College of Social Sciences, Arts and Humanities
Graduate Program
Department of Geography and Environmental Studies

Spatiotemporal Trends of Climate Variability, Meteorological and Agricultural Droughts, and Their Effect on Land Surface Phenology in the Upper Gelana Watershed, Northeastern Highlands of Ethiopia

A Dissertation in Partial Fulfilment to the Requirements for the Degree of Doctor of Philosophy (PhD) in Environment and Natural Resources Management

By Sileshi Tadesse Wodaje
Supervisor: Asnake Mekuriaw (PhD, Associate Professor)

June, 2025
Addis Ababa, Ethiopia

Dissertation Approval

Addis Ababa University

College Of Social Sciences, Arts and Humanities

Graduate Program

This is to certify that this dissertation prepared and submitted by Sileshi Tadesse Wodaje entitled **"Spatiotemporal Trends of Climate Variability, Meteorological and Agricultural Droughts, Their Effect on Land Surface Phenology in the Upper Gelana Watershed, Northeastern Highlands of Ethiopia"** has been submitted for the Department of Geography and Environmental studies for the fulfilment of the requirements for the degree of Doctor of Philosophy in Geography and Environmental Studies (with specialization in Environment and Natural Resource Management) complies with the regulations of Addis Ababa University and meets the accepted standards with respect to originality and quality.

Signed by the Examining committee

Dr.Asmamaw Legass_____ _____
Chairman, the Examining committee Signature Date

Dr. Arragaw Alemayehu _____ _____
External Examiner Signature Date

Dr. Muluneh Abshare _____ _____
Internal Examiner Signature Date

Dr. Asnake Mekuriaw_____ _____
Main Supervisor Signature Date

Abstract

Climate change remains a pressing global challenge, significantly impacting socio-ecological systems and the livelihoods of millions, particularly in developing countries. In Ethiopia, unpredictable climate patterns and extreme droughts have severely threatened rain-fed agriculture, leaving many reliant on food assistance. As a result, understanding local climate variability, drought characteristics, and their impacts is crucial for devising appropriate adaptation strategies to safeguard smallholder farmers' livelihoods. This study explores climate variability and trends, meteorological and agricultural droughts, spatial and temporal variations in land surface phenology (LSP), and farmers' perceptions and adaptation strategies in response to climate variability and changeacross the *lower weina dega* (LWD), *upper weina dega* (UWD), and *dega* agroecological zones (AEZs) of the Upper Gelana watershed in the northeastern highlands of Ethiopia.

The first part of the study focusses on spatiotemporal climate variability and change across the AEZs of the data-scarce Upper Gelana watershed, where rain-fed agriculture is the primary livelihood source. We evaluated the performance of two widely used high-resolution satellite precipitation datasets, Tropical Applications of Meteorology using SATellite and ground-based observations (TAMSAT) and Climate Hazards Group Infrared Precipitation with Stations (CHIRPS), using various categorical and continuous validation statistics in R. The spatiotemporal variability was analyzed using TAMSAT rainfall and gridded temperature data from the Ethiopian Meteorological Institute (EMI) with coefficient of variation (CV), precipitation concentration index (PCI), and standardized rainfall anomaly (SRA). Trends were computed using the Mann-Kendall (MK) test, Sen's slope estimator, and innovative trend analysis (ITA). The findings reveal considerable inter-annual rainfall variability, with a significant positive trend in *kiremt* (main rainy season) rainfall and slight declines in *belg* (short rainy season) rainfall. Decadal increases in *kiremt* rainfall ranged from 96.1 to 104.8 mm, while *belg* rainfall declined by 14.0 to 16.4 mm across AEZs. The minimum and maximum annual temperatures showed significant decreasing and increasing trends, respectively, in LWD and UWD, while changes in *dega* were insignificant.

The second part investigates meteorological and agricultural droughts across the AEZs. Meteorological drought analysis was conducted using the Standardized Precipitation Index (SPI) with TAMSAT data, while agricultural drought was examined using Normalized Difference Vegetation Index (NDVI), Land Surface Temperature (LST), Evapotranspiration (ET), and Potential Evapotranspiration (PET). Drought characteristics such as intensity, severity, and duration were analyzed using run theory in R, and spatial correlation analysis assessed the relationship between meteorological and agricultural droughts. The findings indicate seasonal meteorological drought variability, with *kiremt* droughts occurring more frequently than *belg* season droughts between 1991 and 2021. Meteorological droughts were detected in *kiremt* during 1991, 1993, 2002, 2009, and

2015. Agricultural droughts, identified using ETDI and VHI, were more frequent during *belg* in LWD and UWD (2002, 2008, 2009, 2011, 2012, 2013, and 2021) and in *dega* (2008, 2012, 2013, and 2015). Agricultural droughts were also observed during *kiremt* in 2002, 2008, and 2009 across all AEZs. Pixel-wise correlation analysis revealed a statistically significant positive relationship between meteorological and agricultural drought indices during both the *belg* and *kiremt* seasons, indicating the potential translation of climatic stress to agricultural systems.

To assess the impact of climate change on vegetation ecosystems, we examined spatiotemporal changes in LSP across AEZs and their association with climate variability and drought events from 2001 to 2021. MODIS NDVI (250-meter resolution) was used to compute phenological metrics, including start of the season (SOS), end of the season (EOS), and length of the growing season (LOS), as well as key ecosystem condition indicators such as base value, peak value, and amplitude using MATLAB based TIMESAT software automated using Command Prompt (CMD) and R. Land use was classified for 2001 and 2021 using the Random Forest algorithm, and areas with changes were excluded from LSP trend detection to avoid misinterpretation. The relationship between LSP changes and climate variables was assessed using pixel-wise pearson correlation and partial correlation analyses. The results indicate that the *dega* AEZ experiences earlier SOS and longer LOS compared to LWD and UWD. A delay in SOS and EOS was observed in 71.3% and 82% of the study area, respectively, while LOS increased in nearly half of the area. The high spatial variability in the peak and amplitude values suggests ecosystem condition variations across AEZs. SOS exhibited a positive correlation with maximum temperature and a negative correlation with *belg* rainfall and drought indices across large portions of the study area. Shorter LOS was associated with rising temperatures, whereas increased rainfall extended LOS. The findings also indicate positive correlations between drought indices and EOS in more than half of the study area. Partial correlation analysis suggests that the negative impact of *belg* season meteorological drought on LSP is more pronounced when translated into agricultural drought.

Lastly, we explored farmers perceptions of climate change, its impacts, and the determinants influencing their adaptation choices using a multivariate probit model. The findings indicate that farmers widely perceive rising temperatures, declining rainfall, and increased droughts, partially aligning with statistical analyses. Adaptation strategies vary across AEZs: soil and water conservation dominate in *dega*, while irrigation, crop variety changes, and planting adjustments are prevalent in LWD and UWD. Education, extension services, and access to climate information significantly influence adaptation choices.

Overall,the findings of the study revealed local scale spatiotemporal patterns of climate variability, drought and their impact on LSP changes. Combined with the findings on perceived impacts and existing adaptation practices, it will helpto raise awareness and contribute to the development of AEZ-specific adaptation strategies to reduce the impacts of climate change on rain-fed agricultural dependent communities.

Keywords: climate variability, agricultural drought, meteorological drought, land surface phenology, remote sensing, perception, adaptation strategies

Acknowledgements

First and foremost, I would like to express my heartfelt gratitude to the Almighty God for His protection, guidance, and the strength He provided throughout my journey.

I am deeply grateful to my advisor, Dr. Asnake Mekuriaw, Associate Professor of GIS and Remote Sensing at Addis Ababa University, for his patient guidance, mentorship, and unwavering support throughout my journey, from the proposal stage to the completion of this work. Dr. Asnake's intellectual insight, humility, and encouragement have been invaluable to me. His timely and insightful feedback and constructive comments greatly improved this study, while his approachability and constant words of motivation helped me stay focused. I am truly fortunate to have had his guidance throughout this process.

Additionally, I extend my heartfelt appreciation to Professor Mohammed Assen for involving me in his thematic research project. The feedbacks that he provided have significantly enhanced the quality of my research, and his ongoing support has been vital to my academic journey. I am also grateful to all my teachers and staff members in the Department of Geography and Environmental Studies for their support and assistance during my study.

I would like to thank Addis Ababa University for providing financial support through the thematic research grant and Kotebe University of Education for granting me study leave and sponsoring my study. I am equally grateful to the Regional Centre for Mapping of Resources for Development (RCMRD)/GMES and Africa for their generous financial support, which made this study possible.

I would also like to express my deepest gratitude to the Tehuledere District Agricultural and Rural Development Office for the invaluable assistance during the field visit and data collection. I am also grateful to the enumerators and households who participated in the data collection. Special thanks go to Mohamed, Ali, and Yimam for their crucial role in facilitating the data collection process.

My heartfelt thanks go to all of my friends and colleagues at Addis Ababa University and Kotebe University for their encouragement and making challenging times more bearable.

No words can adequately express my gratitude to all my families, my wife and kids who have always supported me with love, care, and both moral and material assistance. Their belief in me has been a constant source of strength.

Table of contents

List of tables

List of figures

List of abbreviations and acronyms

ET	Evapotranspiration
SWC	Soil and water conservation
ACF	Autocorrelation function
AET	Potential evapotranspiration
AEZs	Agroecological zones
ANOVA	Analysis of variance
CCD	Cold Cloud Duration
CHIRPS	Climate Hazards Group Infrared Precipitation with Stations
CV	Coefficient of variation
DD	Duration of drought
DI	Intensity of the drought
DOY	Day of the Year
DS	Severity of drought
EMI	Ethiopian Meteorological Institute
EO	Earth Observation
EOS	End of the season
ETDI	Evapotranspiration Deficit Index
ETS	Enhanced treat score
FAR	False alarm ratio
FDRE	Federal Democratic Republic of Ethiopia
FGD	Focus group discussions
GEE	Google Earth Engine
GIS	Geographic Information Systems
GMAO	Global Modeling and Assimilation Office
GOs	Government organizations
GUI	Graphical User Interface
HH	Households
HSS	Heidke Skill Score
IPCC	Intergovernmental Panel on Climate Change
ITA	Innovative trend analysis
KII	Key informant interview
LOS	Length of the season
LSP	Land surface phenology
LULC	Land use and land cover
LWD	*Lower weina dega*
MAE	Mean absolute error
ME	Mean error
MK	Mann-Kendall
MLC	Maximum likelihood classification

MODIS	Moderate Resolution Imaging Spectroradiometer
MVP	Multivariate probit
NA	No-data
NASA	National Aeronautics and Space Administration
NDVI	Normalized Difference Vegetation Index
NetCDF	Network Common Data Form
NGOs	Nongovernmental organizations
NIR	Near-infrared
NSE	Nash–Sutcliffe Efficiency Coefficient
OLI	Operational land imager
PA	Producer accuracy
PCI	Precipitation concentration index
PET	Actual evapotranspiration
POD	Probability of detection
QA	Quality assessment
r	Pearson Correlation Coefficient
RCP	Representative Concentration Pathway
RMSE	Root mean square error
SCI	Standardized climate indices
SOS	Start of the season
SPI	Standardized precipitation index
SPSS	Statistical Package for the Social Sciences
SRA	Standardized rainfall anomaly
TAMSAT	Tropical Applications of Meteorology using SATellite and ground-based observations
TCI	Temperature Condition Index
TFP	Total factor productivity
TLU	Tropical livestock units
TS	Treat score
UA	User accuracy
UNCCD	United Nations Convention to Combat Desertification
UNDRR	UN Office for Disaster Risk Reduction
USD	US dollar
UWD	Upper weina dega
VCI	Vegetation Condition Index
VHI	Normalized Difference Vegetation Index
WS	Water stress
WSA	Monthly stress anomaly

List of publications

This dissertation is based on the following three published articles and one submitted manuscript.

Chapter Two: Tadesse, S., Mekuriaw, A., Assen, M., 2024. Spatiotemporal climate variability and trends in the Upper Gelana Watershed, northeastern highlands of Ethiopia. Heliyon 10, e27274. https://doi.org/10.1016/j.heliyon.2024.e27274.

Chapter Three: Tadesse, S., Mekuriaw, A., 2024. Agroecology-based analysis of meteorological and agricultural drought using time series remote sensing data in the upper Gelana watershed, Ethiopia. Geocarto Int. 39(1), 2417881. https://doi.org/10.1080/10106049.2024.2417881.

Chapter Four: Tadesse, S., Mekuriaw, A., Assen, M., 2024. Spatiotemporal dynamics of land surface phenology and its response to climate change in the upper Gelana watershed, northeastern highlands of Ethiopia. Environmental and Sustainability Indicators. 25. https://doi.org/10.1016/j.indic.2024.100574.

Chapter Five: Tadesse, S., Mekuriaw, A., Assen, M., 2025. Farmers' perception and choices of adaptation strategies to climate change in the upper Gelana watershed, northeastern highlands of Ethiopia. Theoretical and Applied Climatology. 156. https://doi.org/10.1007/s00704-025-05629-2.

CHAPTER ONE

1.GENERAL INTRODUCTION

1.1. Background

Climate change is one of the most pressing global concerns(Altieri & Nicholls, 2017). Since 1970, global surface temperatures have risen at an unprecedented rate, with 2011–2020 being the warmest decade in over six thousand years (IPCC, 2021). According to the Intergovernmental Panel on Climate Change (IPCC), the probability of exceeding the 1.5°C global warming threshold in the coming decades is high, and without significant reductions in greenhouse gas emissions, it will not be possible to limit the temperature rise to 1.5 °C or 2 °C (IPCC, 2021). Human-driven climate change is intensifying weather extremes such as heatwaves, heavy rainfall, droughts, and tropical cyclones, with growing evidence since 2014 linking these events to human activity (IPCC, 2021). The impacts of climate change on physical and ecological systems are already apparent (Adger et al., 2005), and extreme climate conditions increasingly threaten human well-being (Becker & Elliot, 2022).

Climate change accelerates biodiversity loss, drives species extinctions, shifts species distributions, and disrupts ecosystems, creating cascading effects on environmental balance (Muluneh, 2021; Saleem et al., 2024). Changes in rainfall and temperature patterns further deepen socioeconomic inequalities, especially in regions where agriculture serves as the main livelihood (Myers et al., 2017; Saleem et al., 2024). The changes are expected to intensify challenges in the agricultural sector, leading to declines in crop yields, shrinking pasture availability, and increasing occurrences of pests, diseases, and invasive species (Muluneh, 2021). According to Ortiz-Bobea et al. (2021), global total factor productivity (TFP) in agriculture has decreased by 21% since 1961 due to climate change, with warmer regions like Africa experiencing even steeper declinesestimated between 26% and 34%. Moreover, a rise in global temperatures will have dire consequences for major staple crops. Zhao et al. (2017) found that a 1°C increase in global temperature results in significant yield reductions: wheat (6.0%), rice (3.2%), maize (7.4%), and soybean (3.1%), unless urgent measures are implemented.

In Sub-Saharan Africa, the aforementioned challenges are compounded by intensified crop pest infestations, accelerated soil nutrient depletion, reduced soil moisture, and others, all of

which have severe economic implications (Bedeke, 2023). Millions of people in the region are already faced with and living with the impacts of climate change, and the situation is expected to deteriorate further, potentially affecting even more in the future (Muluneh, 2021).

Developing countries, including Ethiopia bear the brunt of the increasing impacts of global climate change, primarily due to their limited capacity to adapt and their heavy reliance on low-input, rainfed agriculture (Becker & Elliot, 2022; Mertz et al., 2009; Musemwa et al., 2012). Ethiopia is highly vulnerable to the impacts of climate variability and change, with recurring droughts and floods that pose critical challenges to agriculture-dependent rural communities. Changes in rainfall and temperature patterns have worsened problems such as excessive runoff, accelerated soil erosion, and increased evaporation(Sertse et al., 2021; Taye & Moges, 2021). These challenges have been more heightened in areas with unpredictable rainfall, resulting in sharp drops in yields and an increase in crop failures (Tibebe et al., 2022). For instance, projections show that maize yields could decline between 11 to 29 percent by the 2030 and 2050s based on RCP 4.5 and RCP 8.5 climate scenarios in Tehuledere and Kallu districts (Mohammed et al., 2022).

Climate-related extreme events, such as droughts, are becoming more frequent and severe, with profound environmental and socioeconomic consequences. Prolonged periods of insufficient rainfall, known as meteorological drought, disrupt the delicate climatic balance. This often leads to agricultural drought, where soil moisture becomes inadequate to support healthy crop growth. These conditions can have a significant impact on vegetation phenology, which is a key indicator to understand how plants respond to climate changes(Mbow et al., 2019). Research shows that climate change has a notable influence on phenology(Deng et al., 2020; Liu et al., 2021). Shifts in phenological patterns, such as the timing of greenness onset, the length of the growing season, and the end of the season, can disrupt ecosystem productivity. These changes also have serious implications for agricultural output(Liu et al., 2021; Ruml & Vulic, 2005), affecting food security and livelihoods.

The increasing impacts of climate change and extreme events underscore the urgent need for effective adaptation strategies to build resilience and promote sustainable development (Altieri et al., 2015; Zhao et al., 2017). This requires a thorough understanding of local scale variability and trends in climate change and its impacts (Bedeke, 2023). Equally important is recognizing the perceptions of smallholder farmers regarding climate variability and its

effects. The perception about climate change impacts varies across agroecological zones and the types of crops grown. Farmers in dry areas, for example, may perceive more significant changes in climate than those in wetter areas (Gezie, 2019). Understanding these varied perceptions is crucial to design effective adaptation strategies that directly address the impacts of the changing climate and helps to build resilience and foster sustainable agricultural practices (Ayal & Filho, 2017; Bedeke, 2023).

In recent years, the agroecological approach has gained wide acceptance as a promising solution to reduce the adverse effects of climate change on agriculture and ecosystems (Carolina et al., 2024; Wezel et al., 2020).Research highlights that adopting an agroecological framework provides holistic and effective solutions to climate change while addressing broader socioeconomic and environmental challenges(Carolina et al., 2024). Agroecological practices not only improve yields, but also minimize negative impacts on biodiversity (Altieri et al., 2015; Mbow et al., 2019). These practices prioritize locally relevant solutions, encourage participatory processes, and foster knowledge sharing, making them more adaptive to climate change compared to conventional agricultural systems (Snapp et al., 2023). A report by Dittmer et al. (2023) shows that in low and middle-income countries, agroecological approaches have led to increased crop yields while improving nutrient regulation, reducing pest infestations, and enhancing income stability, which are key indicators of adaptive capacity. This approach holds great promise for improving agriculture systems, particularly in the semi-arid and subhumid regions of Africa (Debray et al., 2019; Muluneh, 2021). By building resilience to climate change through sustainable practices, agroecological approaches reduces environmental stress and strengthens ecological processes, offering a viable pathway toward more resilient farming systems (Kerr et al., 2023; Mbow et al., 2019).

In this regard, geospatial technologies such as Geographic Information Systems (GIS) and Remote Sensing have emerged as indispensable tools for analyzing and addressing climate variability and change across agroecological zones (Bisht et al., 2020). The availability of spatial datasets such as elevation, land use/land cover, and satellite-derived climate data enabled us to capture the geographic variability of climate patterns in grid-based models. Researchers employ a variety of methods, from simple indices to advanced models, to assess climate variability, impacts, and implications. These tools are instrumental in unveiling climate dynamics and the impacts for instance on crop yields(Patel et al., 2019), flood risk

analysis(Hawchar et al., 2020; Sibandze et al., 2024), and spatiotemporal drought mapping (Ghazaryan et al., 2020; Houmma et al., 2022; Khorrami et al., 2023).

Commonly used precipitation-based drought indices such as the Standardized Precipitation Index (SPI) and vegetation-based metrics such as the Normalized Difference Vegetation Index (NDVI), Vegetation Health Index (VHI), and Evapotranspiration Deficit Index (ETDI) play an essential role in identifying drought. Remote sensing-based assessments of land surface phenology further enhance our understanding of climate change impacts on ecosystems. Together, these geospatial tools allow precise assessments, trend forecasts, and the development of tailored adaptation strategies. Integrating these approaches can help decision makers effectively address the complex challenges posed by climate change, reducing its socioeconomic and environmental consequences (Boulos & Wilson, 2023).

1.2. Statement of the problem

Ethiopia's economy is heavily reliant on rain-fed agriculture(Bewket et al., 2024; Conway & Schipper, 2011),which makes a significant contribution to increase revenues and employs a large proportion of the population (FDRE, 2015). This sector is highly sensitive to frequent disruptions caused by climate variability and extreme weather events, which have restricted agricultural productivity and hindered economic development (Conway & Schipper, 2011). A slight deviation in the average climate condition can result in significant losses in crop and livestock production, exacerbating food insecurity(Gonfa, 1996; Solomon et al., 2021).

Climate related shock such as droughts, have been catastrophic for Ethiopia. Historical data highlight severe impacts, including the highest drought-related death tolls in the 1970s and 1980s and affecting 14.2 million people in 2002 (World Bank, 2007) and nearly 10 million people in 2015(Mera, 2018). Chronic food insecurity persists, and approximately 10% of the population requires food assistance even during years with average rainfall(Conway & Schipper, 2011). These challenges disproportionately affect smallholder farmers who depend heavily on natural resources for their livelihoods(Alemayehu & Bewket, 2016; Echeverría & Terton, 2016; Gezie, 2019; Moges & Bhat, 2021).

Future projections indicate increasing climate variability and higher risks of environmental shocks, such as droughts(Alaminie et al., 2021; Degefie et al., 2019; Worku et al., 2020). In areas such as the Upper Gelana watershed, where mixed farming systems dominate

livelihoods, climate change could have various socioeconomic and environmental consequences (Bewket, 2012; Mohammed et al., 2022). Changes in land surface phenology due to climate change and drought can affect crop growth, leading to reduced yields and forage, increased vulnerability to pests and diseases, and heightened food insecurity(Lobell et al., 2008). Therefore, understanding changes in key vegetation phenological stages can serve as a vital indicator of ecosystem productivity and provide important information on responses to climate change and develop adaptation strategies(Piao et al., 2019). These responses vary across space, implying that the approaches successful in one area may not yield similar results elsewhere (Simane et al., 2016).

As a result, it is imperative to understand spatiotemporal climate variability, drought, and impacts on vegetation phenology. Equally important to understand is framer's perception and adaptation responses across different agroecological zones. This help to identify the sensitivity of the socioecological systems and design effective and sustainable interventions. Although the Ethiopian government has introduced sectoral adaptation strategies in agriculture, forest, energy, and water resources(Mamo, 2013; Tombe, 2016), there is a substantial gap in understanding localized impacts and formulating context-specific adaptation measures. The local-level interrelationships between climate change, drought, and land surface phenology are not well explored, making it challenging to properly understand and predict the impacts on the agriculture sector. Thus, exploring such interrelationships is essential to formulate proper adaptation measures in the agricultural sector and help minimize the impacts of climate change on rural livelihoods.

To address this gap, it is essential to follow an integrated approach that helps to categorize the heterogeneous landscape into homogeneous units based on the nature of climate and topography, which indirectly define socioeconomic activities such as agriculture activities. This can be properly addressed through the agroecology framework. Despite numerous studies on climate change and its impacts, there is a lack of comprehensive research that integrates local-level climate dynamics and its impact on the ecosystem, such as changes in vegetation phenology, through an agroecological lens. Furthermore, previous studies also overlooked taking into account the spatial dimension of these interactions, instead relying on aggregated data that do not adequately capture climate dynamics and their impact across the

agroecological zones. This lack of integrated and spatially explicit analysis hinders the development of targeted and effective adaptation interventions.

Therefore, using satellite precipitation and gridded temperature data, this study aimed to examine spatiotemporal climate variability and trends using Mann-Kendall and innovative trend analysis methods. We integrate various time-series remote sensing datasets to identify meteorological and agricultural drought events and their characteristics such as duration, intensity, and magnitude analyzed using run theory. Furthermore, this study explores the spatiotemporal changes in land surface phenology and its relationships with changes in rainfall, temperature, and drought. In addition, smallholder farmers' perceptions about climate variability and factors that determine the choice of adaptation strategies were examined. Overall, this study aims to provide actionable insights into local level climate variability and its impacts, supports evidence-based decision-making to develop tailored adaptation measures, and build resilience in the rural communities in the Upper Gelana watershed, northeastern highlands of Ethiopia.

1.3. Objectives of the study

The general objective of the study is to analyze the spatiotemporal variability and trends in climate, drought, and land surface phenology, as well as farmer perceptions and the determinant factors influencing the choice of adaptation strategies in the upper Gelana watershed, located in the northeastern highlands of Ethiopia. The study aimed to achieve the following specific objectives:

1. To examine the spatiotemporal climate variability and trends across the agroecological zones of the upper Gelana watershed.
2. To characterize meteorological and agricultural droughts using time-series remote sensing data across the agroecological zones of the upper Gelana watershed.
3. To explore the spatiotemporal dynamics of land surface phenology (LSP) and its relationship with rainfall, temperature, and drought across the agroecological zones of the upper Gelana watershed.
4. To analyze smallholder farmers' perceptions of climate variability and its impacts, as well as the factors influencing their choices of climate adaptation strategies in the study area.

1.4. Research questions

The study aimed to answer the following specific questions:

1. To what extent do rainfall and temperature vary across space and time in the different agroecological zones of the Upper Gelana watershed?
2. How do meteorological and agricultural drought manifest across the agroecological zones of the Upper Gelana watershed based on time-series remote sensing data?
3. Are there spatiotemporal dynamics in land surface phenology (SOS, EOS, LOS) across the different agroecological zones? How do these dynamics relate to rainfall, temperature, and drought across the agroecological zones of the Upper Gelana watershed?
4. How do smallholder farmers perceive climate change and its impacts across the agroecological zones in the Upper Gelana watershed? What adaptation strategies are used in the different agroecological zones, and what factors influence the choices of adaptation strategies in the study area?

1.5. Significance of the study

This study provides valuable insights on climate variability and change, as well as the potential impacts of climate-related hazards such as drought. The findings of this study are essential to understand the spatial and temporal dynamics of LSP and how this change affects agricultural activities in the study area and to adjust cropping calendars using LSP trends as a proxy. Furthermore, the study contributes to understanding the general perceptions of smallholder farmers about climate variability and impacts, including the factors that influence the choice of adaptation strategies. In general, the findings of this study will be useful to raise smallholder farmers' awareness about overall variability and trends in climate, drought, and the shifts in land surface phenology. It will help to understand how these changes might affect their livelihoods and support decision-making on the use of adaptation strategies. The findings are also essential to development partners, government and nongovernmental organizations (NGOs) to identify the specific gaps in the different agroecological zones and to support farmers' adaptation efforts. Furthermore, the findings of the study will help policymakers design appropriate agroecology-specific policy measures to reduce the impacts of climate

change on a local scale. Beyond this, the study will have a significant contribution to the scientific community on the spatiotemporal dynamics of climate, drought, phenology, and adaptation at the local level in agroecological zones. More specifically, the study will contribute to the procedures for processing remotely detected data for climate trend detection, calculating drought indices, and analyzing phenology using R programming.

1.6. Scope and limitation of the study

Climate change is a broad field that requires extensive time and resources for a comprehensive investigation. To maintain focus and feasibility, this study focuses on examining trends in climate, drought patterns, land surface phenology dynamics, and farmers' perceptions and adaptation strategies. Recognizing that climate dynamics can vary significantly in magnitude and impact across local, national, regional, and global scales, this study specifically investigates the localized climate dynamics across the agroecological zones in the upper Gelana watershed, with an emphasis on supporting smallholder farmers in the area.

Although satellite remote sensing is invaluable for studying land surface phenology, careful selection of remotely sensed data and validation with ground-based measurements are crucial to ensure the accuracy of the findings from remotely sensed image analysis. This study focusses on landscape-level phenology rather than crop-specific phenology due to limitations in field technology and security concerns in the area. Additionally, we relied on MODIS imagery, which offers high temporal but moderate spatial resolution. While spatial resolution could be enhanced by fusing MODIS data with higher-resolution satellite imagery, such as Landsat or Sentinel, computational limitations prevented us from pursuing this approach.

Furthermore, this study focused solely on recent climate dynamics; however, it is essential to examine how these dynamics will evolve in the future in relation to changes in socioeconomic and environmental factors. Consequently, researchers are encouraged to forecast changes in climate variables, drought, and their environmental impacts to support the implementation of adaptation strategies.

1.7. Research design

This study adopted a mixed research design, integrating both quantitative and qualitative methods to provide a comprehensive analysis. It largely relies on quantitative methods to

analyze variability and trends in climate, drought analysis, land surface phenology, and adaptation strategies. The quantitative data sources used in this study include remote sensing imagery, meteorological station records, and household surveys. The survey data were collected from 159 respondents that are selected using a simple random sampling technique, and proportionally distributed across the LWD, UWD, and dega agroecological zones based on their respective total household size. Moreover, the qualitative data were gathered through field observations and focus group discussions with key informants to complement the quantitative data. These qualitative findings were used to enrich and contextualize the quantitative results. The quantitative analysis employed a range of descriptive and inferential statistical techniques, including validation statistics, percentages, frequencies, machine learning algorithms, time series analysis, and a multivariate probit model. Detailed descriptions of these statistical methods and their applications are provided in the respective chapters.

The spatial and statistical software tools that were used in this study includes R programming, TIMESAT, Python, ArcGIS, OriginPro, Adobe Illustrator, SPSS, and STATA. R programming was used to perform many of the spatial analysis, such as land use and land cover (LULC) analysis using the random forest algorithm, satellite rainfall validation, variability and trend detection, and computation of drought indices. TIMESAT software was used to derive phenological metrics, while the preprocessing of MODIS NDVI data and subsequent processing of these metrics were also handled in R. For visualizing meteorological and agricultural drought trends, time series plots were prepared using the Matplotlib package. ArcGIS was also used to create many of the maps included in various sections of the study. Most graphical representations were prepared using OriginPro, ensuring clarity and visual appeal. SPSS was utilized to organize and manage the survey data, while advanced statistical analyses, including the multivariate probit model, were conducted in STATA.

1.8. Organization of the thesis

This dissertation is organized into six chapters that address different but related aspects of climate change and adaptation strategies. The first chapter is the introduction section. It discusses the background of the study, the problem statement, the objectives, the research question, the significance of the study, scope, and limitations of the study. The chapter also discusses the conceptual and theoretical frameworks of the study. The second chapter of this

study delves into the spatiotemporal variability and trends in climate using ground-based meteorological stations, satellite precipitation such as the TAMSAT and CHIRPS, and gridded temperature datasets. This chapter presents different validation statistics used to evaluate the performance of satellite precipitation in the study area. Then, it presents the spatiotemporal variability and trends in monthly, seasonal, and annual rainfall and temperature using the Mann Kendal and innovative trend analysis.

The third chapter of the dissertation focusses on meteorological and agricultural drought analysis using remote sensing time-series data. This chapter presents the severity, magnitude, and intensity of meteorological droughts based on the standardized precipitation index (SPI). It also discusses the occurrence and severity of agricultural drought using the vegetation condition index (VHI) and the evapotranspiration deficit index (ETDI). Furthermore, the correlations between the meteorological and agricultural drought indices were discussed to understand the possibilities of translations from the former to the latter.

In the fourth chapter, we present the spatiotemporal dynamics of land surface phenology (LSP) and its response to climate change. This chapter deals with the classification of land use and land cover with random forest classifiers and spatiotemporal variations in phenological metrics and trends for the unchanged land use and land cover classes. In addition, the correlations between phenological metrics and climate variables such as rainfall and temperature, as well as drought indices, are discussed in this chapter.

The fifth chapter discuss the perception of smallholder farmers about climate variability and the determinant factors that influence the choice of adaptation strategies. It discusses differences in the perceptions and adaptation strategies across the agroecological zones of the upper Galena watershed. Moreover, the chapter includes the determinant factors for the choice of adaptation strategies.

In the last chapter of this thesis, we discuss a summary of the findings, conclusions, and recommendations. This chapter highlights important insights that are useful to stakeholders, policymakers, and future researchers in the area. Organizing the chapters in this order maintains the coherence of the objectives and connects the narrative of climate trends, drought dynamics, phenological changes, farmers' perceptions, and adaptation strategies in a structured way.

1.9. Conceptual framework

Climate variability encompasses fluctuations in climatic conditions, including temperature, precipitation, wind, solar radiation and others, occurring at various temporal and spatial scales (Clinton et al., 2014a). Drought, a prolonged period of abnormally low precipitation, represents an extreme manifestation of climate variability (Vetter, 2009). The frequency, intensity, and duration of droughts are projected to increase under future climate change scenarios(Zarafshani et al., 2016), posing significant challenges to ecosystems and human societies. Different regions experience diverse drought characteristics, influenced by local geographical features and climatic patterns (Lv et al., 2022). Human activities can amplify the impact of drought(Zhu et al., 2022).

Climate change and extreme events such as droughts exert significant impacts on the ecosystem such as reduction in productivity and biodiversity loss and increasing risk of wildfires(de Beurs & Henebry, 2008; Maron et al., 2015; J. Wang & Zhang, 2017). These conditions also amplify the socioeconomic consequences such as food insecurity, migration, and conflict(Hoyer et al., 2023). As a result, assessing the spatiotemporal changes in climate and drought is essential to understanding the potential impact and devising possible adaptation strategies.

One of the best indicators of the impacts of climate change on the ecosystem and agriculture is the landscape-wide changes in seasonal timing of vegetation conditions referred to as land surface phenology. The phenological parameters such as the start of the season (SOS), end of the season (EOS), and length of the season (LOS) are valuable to understanding the onset of greenness, senescence, and the active photosynthesis or length of growing period(Verheggen & Defourny, 2012). Because of their sensitivity to the subtle changes in climate and drought events, they are valuable in identifying the impacts on the ecosystem and its productivity. Increasing temperature and shortage of rainfall may lead to a late start of the season, while droughts can lead to a short growing season and decreasing vegetation productivity(Zhou et al., 2023). However, such influence of changes in rainfall and temperature patterns varies geographically (Guo et al., 2021),for instance, between highlands and lowland areas.

Thus, quantifying the shifts in key phenological parameters and ecosystem indicators including their relationships with the spatial and temporal changes in temperature, rainfall,

and drought conditions is essential to formulate appropriate adaptation strategies. In this regard, the advancements in remote sensing products and techniques contribute substantially. The availability of satellite-based precipitation and gridded temperature data helped to maintain consistent results in rainfall and temperature changes at a high spatial and temporal resolution. In addition to this, freely available vegetation indices and evapotranspiration derived from satellite imageries such as MODIS play a crucial role in detecting agricultural drought and the changes in land surface phenology.

The identification of long-term trends or spatial variations in climate, drought conditions and land surface phenology help to design appropriate adaptation strategies that reduce the negative consequences of these changes on the environment and socioeconomic systems. These strategies can be implemented at various levels, from individual farmers to the national level(Cruz et al., 2018). Individual farmers can apply various agricultural practices to enhance resilience which may include soil conservation, water harvesting and irrigation, use of drought-resistant crop varieties(Araus et al., 2012; Karienye et al., 2020). However, the implementation and effectiveness of these adaptation strategies are determined various factors. For instance, farmers' perception of climate change and its impacts on agricultural activities and their overall livelihood is essential. In addition, demographic characteristics such as sex, age, socioeconomic factors such as education, income level, landholding size, availability of technologies and institutional factors such as, extension service, credit access and market linkage may affect the choices and implementation of adaptation strategies etc. The national-level policies also play a crucial role in supporting adaptation efforts (Cruz et al., 2018). In rural areas, communities are dependent on natural resource base and their livelihood is sensitive to the impacts of climate variability and change. Implementing effective adaptation strategies can help to reduce the impacts of drought for instance by improving water availability, it can also sustain the phenological phases or cyclic changes in vegetation dynamics at times of deficit rainfall. In agricultural communities, like the upper Gelana watershed, harnessing the adaptive potentials of nature is economically viable and effective to combat the impacts of climate change(Munang et al., 2013).

This study focuses on the analysis of climate variability, drought, and land surface phenology and their interactions as well as smallholder farmers' adaptation strategies. We utilized various satellite products and spatial analysis techniques to examine these problems

across the agroecology zones of the upper Gelana watershed, in Ethiopia. The various elements of the study and their interrelations are shown in the following conceptual framework (Fig.1.1).

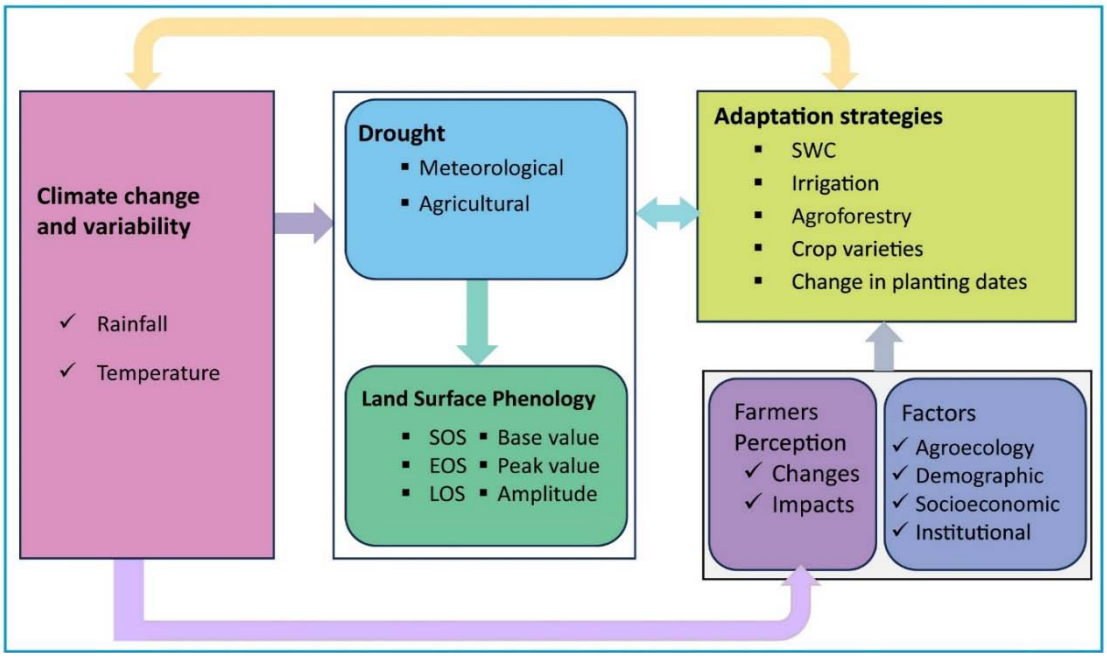

Fig. 1.1. Conceptual framework of the study

References

Adger, W. N., Arnell, N. W., & Tompkins, E. L. (2005). Successful adaptation to climate change across scales. *Global Environmental Change*, *15*, 77–86. https://doi.org/10.1016/j.gloenvcha.2004.12.005

Alaminie, A. A., Tilahun, S. A., Legesse, S. A., Zimale, F. A., Tarkegn, G. B., & Jury, M. R. (2021). Evaluation of Past and Future Climate Trends under CMIP6 Scenarios for the UBNB (Abay), Ethiopia. *Water*, *13*(15), 2110. https://doi.org/10.3390/W13152110

Alemayehu, A., & Bewket, W. (2016). Local climate variability and crop production in the central highlands of Ethiopia. *Environmental Development*, *19*, 36–48. https://doi.org/10.1016/j.envdev.2016.06.002

Altieri, M. A., & Nicholls, C. I. (2017). The adaptation and mitigation potential of traditional agriculture in a changing climate. *Climatic Change*, *140*, 33–45. https://doi.org/10.1007/s10584-013-0909-y

Altieri, M. A., Nicholls, C. I., Henao, A., & Lana, M. A. (2015). Agroecology and the design of climate change-resilient farming systems. *Agronomy for Sustainable Development*, *35*, 869–890. https://doi.org/10.1007/s13593-015-0285-2

Araus, J. L., Serret, M. D., & Edmeades, G. O. (2012). Phenotyping maize for adaptation to drought. *Frontiers in Physiology*, *3*(305). https://doi.org/10.3389/fphys.2012.00305

Becker, R., & Elliot, P. (2022). Climate change: a friend or foe to food security in Africa? *Environment, Development and Sustainability*, *24*, 4387–4412. https://doi.org/10.1007/s10668-021-01621-8

Bewket, W. (2012). Climate change perceptions and adaptive responses of smallholder farmers in central highlands of Ethiopia. *International Journal of Environmental Studies*, *69*(3), 507–523.

Bewket, W., Tibebe, D., Teferi, E., & Degefu, M. A. (2024). Changes in mean and extreme rainfall indices over a problemscape in central Ethiopia. *Environmental Challenges*, *15*, 100883. https://doi.org/10.1016/J.ENVC.2024.100883

Bisht, H., Gautam, S., Sarma, R., Mishra, A. K., & Prajapati, V. K. (2020). Integration of Geospatial Technology and Simulation Modelling for Climate Change Studies. In V. Venkatramanan, S. Shah, & R. Prasad (Eds.), *Global Climate Change: Resilient and Smart Agriculture* (pp. 221–247). Springer. https://doi.org/10.1007/978-981-32-9856-9_11

Boulos, M. N. K., & Wilson, J. P. (2023). Geospatial techniques for monitoring and mitigating climate change and its effects on human health. *International Journal of Health Geographics*, *22*(2). https://doi.org/10.1186/s12942-023-00324-9

Carolina, Q., Alejandra, A., & Nadine, A. (2024). Agroecology and Sustainable Food Systems Evidence of agroecology ' s contribution to mitigation , adaptation , and resilience under climate variability and change in Latin America. *Agroecology and Sustainable Food Systems*, *48*(2), 228–252. https://doi.org/10.1080/21683565.2023.2273835

Clinton, N., Yu, L., Fu, H. H., He, C. H., & Gong, P. (2014). Global-Scale Associations of Vegetation Phenology with Rainfall and Temperature at a High Spatio-Temporal Resolution. *Remote Sensing*, *6*, 7320–7338. https://doi.org/10.3390/rs6087320

Conway, D., & Schipper, E. L. F. (2011). Adaptation to climate change in Africa: Challenges and opportunities identified from Ethiopia. *Global Environmental Change*, *21*, 227–237. https://doi.org/10.1016/j.gloenvcha.2010.07.013

Cruz, G., Baethgen, W., Bartaburu, D., Bidegain, M., Giménez, A., Methol, M., Morales, H., Picasso, V., Podestá, G., Taddei, R., Terra, R., Tiscornia, G., & Vinocur, A. M. (2018). Thirty years of multilevel processes for adaptation of livestock production to droughts in

Uruguay. *Weather, Climate, and Society*, *10*(1), 59–74. https://doi.org/10.1175/WCAS-D-16-0133.1

de Beurs, K. M., & Henebry, G. M. (2008). War, drought, and phenology: Changes in the land surface phenology of Afghanistan since 1982. *Journal of Land Use Science*, *3*(2–3), 95–111. https://doi.org/10.1080/17474230701786109

Debray, V., Wezel, A., Lambert-derkimba, A., Roesch, K., Lieblein, G., & Francis, C. A. (2019). Agroecology and Sustainable Food Systems Agroecological practices for climate change adaptation in semiarid and subhumid Africa. *Agroecology and Sustainable Food Systems*, *43*(4), 429–456. https://doi.org/10.1080/21683565.2018.1509166

Degefie, D. T., Seid, J., Gessesse, B., & Bedada, T. B. (2019). Agricultural drought projection in Ethiopia from 1981 to 2050: Using coordinated regional climate downscaling experiment climate data for Africa. In Assefa M. Melesse, Wossenu Abtew, & Gabriel Senay (Eds.), *Extreme Hydrology and Climate Variability: Monitoring, Modelling, Adaptation and Mitigation* (pp. 311–323). Elsevier. https://doi.org/10.1016/B978-0-12-815998-9.00024-5

Deng, H., Yin, Y., Wu, S., & Xu, X. (2020). Contrasting drought impacts on the start of phenological growing season in Northern China during 1982 – 2015. *International Journal of Climatology*, *40*(7), 3330–3347. https://doi.org/10.1002/joc.6400

Dittmer, K. M., Rose, S., Snapp, S. S., Kebede, Y., Brickman, S., Shelton, S., Egler, C., Stier, M., & Wollenberg, E. (2023). Agroecology Can Promote Climate Change Adaptation Outcomes Without Compromising Yield In Smallholder Systems. *Environmental Management*, *72*, 333–342. https://doi.org/10.1007/s00267-023-01816-x

Echeverría, D., & Terton, A. (2016). *Review of Current and Planned Adaptation Action in Ethiopia* (CARIAA Working Paper no. 8).

FDRE. (2015). *Ethiopia's Climate-Resilient Green Economy. Climate Resilience Strategy: Agriculture and Forestry*. https://gggi.org/report/sectoral-climate-resilience-strategies-for-ethiopia/

Gezie, M. (2019). Farmer ' s response to climate change and variability in Ethiopia : A review. *Cogent Food & Agriculture*, *5*(1), 1613770. https://doi.org/10.1080/23311932.2019.1613770

Ghazaryan, G., Dubovyk, O., Graw, V., Kussul, N., & Schellberg, J. (2020). Local-scale agricultural drought monitoring with satellite-based multi-sensor time-series. *GIScience & Remote Sensing*, *57*(5), 704–718. https://doi.org/10.1080/15481603.2020.1778332

Gonfa, L. (1996). *Climate Classifications of Ethiopia*. http://localhost:8080/xmlui/handle/123456789/1492

Guo, J., Liu, X., Ge, W., Ni, X., Ma, W., Lu, Q., & Xing, X. (2021). Specific drivers and responses to land surface phenology of different vegetation types in the qinling mountains, central China. *Remote Sensing*, *13*(22). https://doi.org/10.3390/RS13224538

Hawchar, L., Naughton, O., Nolan, P., Stewart, M. G., & Ryan, P. C. (2020). Climate Risk Management A GIS-based framework for high-level climate change risk assessment of critical infrastructure. *Climate Risk Management*, *29*, 100235. https://doi.org/10.1016/j.crm.2020.100235

Houmma, I. H., Mansouri, L. El, Gadal, S., & Hadria, R. (2022). Modelling agricultural drought : a review of latest advances in big data technologies. *Geomatics, Natural Hazards and Risk*, *13*(1), 2737–2776. https://doi.org/10.1080/19475705.2022.2131471

Hoyer, D., Bennett, J., Reddish J, Holder S, Howard R, Benam M, Levine J, Ludlow F, Feinman G, & Turchin P. (2023). Navigating polycrisis: long-run socio-cultural factors shape response to changing climate. *Philos Trans R Soc Lond B Biol Sci.*, *378*(1889), 20220402. https://doi.org/10.1098/rstb.2022.0402

IPCC. (2021). Summary for Policymakers. In Masson-Delmotte, P. Z. V., A. Pirani, S. L. Connors, C. Péan, S. Berger, N. Caud, Y. Chen, L. Goldfarb, M. I. Gomis, M. Huang, K. Leitzell, E. Lonnoy, J. B. R. Matthews, T. K. Maycock, T. Waterfeld, O. Yelekçi, R. Yu, & B. Zhou (Eds.), *Climate Change 2021 The Physical Science Basis,Contribution of Working Group I to the Sixth Assessment Report of the Intergovernmental Panel on Climate Change* (pp. 3–33). https://doi.org/10.1017/9781009157896.001

Karienye, D. K., Nduru, G., & Kamiri, H. W. (2020). Factors that Influence Banana Farmers Adaptation Strategies to Climate Change in Meru County Kenya. *Journal of Arts and Humanities*, *9*(1), 104–115. https://doi.org/10.18533/JOURNAL.V9I1.1751

Kerr, R. B., Postigo, J. C., Smith, P., Cowie, A., Singh, K., Rivera-ferre, M., Tirado-von der Pahlen, Campbell, D., & Neufeldt, H. (2023). Agroecology as a transformative approach to tackle climatic , food , and ecosystemic crises. *Current Opinion in Environmental Sustainability*, *62*, 101275. https://doi.org/10.1016/j.cosust.2023.101275

Khorrami, B., Ali, S., & Gündüz, O. (2023). An appraisal of the local-scale spatio-temporal variations of drought based on the integrated GRACE/GRACE-FO observations and fine-resolution FLDAS model. *Hydrological Processes*, *37*(11), e15034. https://doi.org/10.1002/hyp.15034

Liu, Y., Zhang, J., Pan, T., & Ge, Q. (2021). Assessing the adaptability of maize phenology to climate change: The role of anthropogenic-management practices. *Journal of Environmental Management*, *293*. https://doi.org/10.1016/j.jenvman.2021.112874

Lobell, D. B., Burke, M. B., Tebaldi, C., Mastrandrea, M. D., Falcon, W. P., Naylor, R. L., & Investments. (2008). Prioritizing Climate Change Adaptation Needs for Food Security in 2030. *Science*, *319*, 607–610. https://doi.org/10.1126/science.1152339

Lv, W., Wu, C., Yeh, P. J. F., & Hu, B. X. (2022). Spatio-temporal variability of dryness and wetness based on standardized precipitation evapotranspiration index and standardized wetness index and its relation to the normalized difference vegetation index. *International Journal of Climatology*, *42*(2), 671–690. https://doi.org/10.1002/JOC.7266

Mamo, G. (2013). *Making Ethiopian Agriculture Climate Resilient: Towards Networking and Coordination to Mainstream Climate Change Adaptation into Food Security and Sustainable Development*.

Maron, M., Mcalpine, C. A., Watson, J. E. M., Maxwell, S., & Barnard, P. (2015). Climate-induced resource bottlenecks exacerbate species vulnerability: a review. *Diversity and Distributions*, *21*(7), 731–743. https://doi.org/10.1111/ddi.12339

Mbow, C., Rosenzweig, C., Barioni, L. G., Benton, T. G., Herrero, M., Krishnapillai, M., Liwenga, E., Pradhan, P., Rivera-Ferre, M. G., Sapkota, T., Tubiello, F. N., & Xu, Y. (2019). Food security. In P. R. Shukla, J. Skea, E. C. Buendia, V. Masson-Delmotte, H.-O. Pörtner, D. C. Roberts, P. Zhai, R. Slade, S. Connors, R. van Diemen, M. Ferrat, E. Haughey, S. N. S. Luz, M. Pathak, J. Petzold, J. P. Pereira, P. Vyas, E. Huntley, K. Kissick, … J. Malley (Eds.), *Climate Change and Land: an IPCC special report on climate change, desertification, land degradation, sustainable land management, food security, and greenhouse gas fluxes in terrestrial ecosystems* (pp. 437–550). https://doi.org/10.1017/9781009157988.007

Mera, G. A. (2018). Drought and its impacts in Ethiopia. *Weather and Climate Extremes*, *22*, 24–35. https://doi.org/10.1016/j.wace.2018.10.002

Moges, D. M., & Bhat, H. G. (2021). Climate change and its implications for rainfed agriculture in Ethiopia. *Journal of Water and Climate Change*, *12*(4), 1229–1244. https://doi.org/10.2166/wcc.2020.058

Mohammed, A., Yimer, E., Gessese, B., & Feleke, E. (2022). Predicting Maize (Zea mays) productivity under projected climate change with management options in Amhara region, Ethiopia. *Environmental and Sustainability Indicators*, *15*, 100185. https://doi.org/10.1016/j.indic.2022.100185

Muluneh, M. G. (2021). Impact of climate change on biodiversity and food security: a global perspective - a review article. *Agriculture & Food Security*, *10*(36). https://doi.org/10.1186/s40066-021-00318-5

Munang, R., Thiaw, I., Alverson, K., Mumba, M., Liu, J., & Rivington, M. (2013). Climate change and Ecosystem-based Adaptation : a new pragmatic approach to buffering climate

change impacts. *Current Opinion in Environmental Sustainability*, *5*, 67–71. https://doi.org/10.1016/j.cosust.2012.12.001

Patel, N. R., Akarsh, A., Ponraj, A., & Singh, J. (2019). Geospatial Technology for Climate Change Impact Assessment of Mountain Agriculture. In R. R. Navalgund et al. (Ed.), *Remote Sensing of Northwest Himalayan Ecosystems* (pp. 381–400). Springer Nature. https://doi.org/10.1007/978-981-13-2128-3_18

Piao, S., Liu, Q., Chen, A., Janssens, I. A., Fu, Y., Dai, J., Liu, L., Lian, X., Shen, M., & Zhu, X. (2019). Plant phenology and global climate change: Current progresses and challenges. *Global Change Biology*, *25*(6), 1922–1940. https://doi.org/10.1111/gcb.14619

Ruml, M., & Vulic, T. (2005). Importance of phenological observations and predictions in agriculture. *Journal of Agricultural Sciences*, *50*(2), 217–225. https://doi.org/10.2298/jas0502217r

Sertse, S. F., Khan, N. A., Shah, A. A., Liu, Y., & Naqvi, S. A. A. (2021). Farm households ' perceptions and adaptation strategies to climate change risks and their determinants : Evidence from Raya Azebo district , Ethiopia. *International Journal of Disaster Risk Reduction*, *60*, 102255. https://doi.org/10.1016/j.ijdrr.2021.102255

Sibandze, P., Kalumba, A. M., Aljaddani, A. H., Zhou, L., & Afuye, G. A. (2024). Geospatial Mapping and Meteorological Flood Risk Assessment: A Global Research Trend Analysis. *Environmental Management*. https://doi.org/10.1007/s00267-024-02059-0

Simane, B., Zaitchik, B. F., & Foltz, J. D. (2016). Agroecosystem specific climate vulnerability analysis : application of the livelihood vulnerability index to a tropical highland region. *Mitig Adapt Strateg Glob Change*, *21*(39), 39–65. https://doi.org/10.1007/s11027-014-9568-1

Snapp, S., Kebede, Y., Wollenberg, E., Dittmer, K. M., Brickman, S., Egler, C., & Shelton, S. (2023). Delivering Climate Change Outcomes with Agroecology in Low- and Middle-Income Countries: Evidence and Actions Needed. In J. von Braun et al. (Ed.), *Science and Innovations for Food Systems Transformation* (pp. 531–544). https://doi.org/10.1007/978-3-031-15703-5_28

Solomon, R., Simane, B., & Zaitchik, B. F. (2021). *The Impact of Climate Change on Agriculture Production in Ethiopia Application of a Dynamic Computable General Equilibrium Model*. 32–50. https://doi.org/10.4236/ajcc.2021.101003

Taye, T., & Moges, A. (2021). Implication of long-term watershed development on land use / land cover change and sediment loss in Maybar Sub-Watershed , South Wello Zone , Ethiopia Implication of long-term watershed development on land use / land cover change and sediment loss in Mayb. *Cogent Food & Agriculture*, *7*(1). https://doi.org/10.1080/23311932.2020.1863596

Tibebe, D., Teferi, E., Bewket, W., & Zeleke, G. (2022). Climate induced water security risks on agriculture in the Abbay river basin: A review. *Frontiers in Water*, *4*, 961948. https://doi.org/10.3389/frwa.2022.961948

Tombe, T. B. (2016). Climate Change Education for Climate Resilient Green Economy (CRGE) of Ethiopia. *International Journal of African and Asian Studies*, *20*.

Verheggen, A., & Defourny, P. (2012). A global scale land surface phenology reference dataset with 12 years of spot vegetation data. In Vanclooster M. (Ed.), *PhD Student Day ENVITAM* (p. 81).

Vetter, S. (2009). Drought, change and resilience in south africa's arid and semi-arid rangelands. *South African Journal of Science*, *105*(1–2), 29–33. https://doi.org/10.4102/SAJS.V105I1/2.35

Wakjira, M. T., Peleg, N., Anghileri, D., Molnar, D., Alamirew, T., Six, J., & Molnar, P. (2021). Rainfall seasonality and timing: implications for cereal crop production in Ethiopia. *Agricultural and Forest Meteorology*, *310*, 108633. https://doi.org/10.1016/J.AGRFORMET.2021.108633

Wang, J., & Zhang, X. (2017). Impacts of wildfires on interannual trends in land surface phenology: An investigation of the Hayman Fire. *Environmental Research Letters*, *12*(5). https://doi.org/10.1088/1748-9326/AA6AD9

Worku, G., Teferi, E., Bantider, A., & Dile, Y. T. (2020). Statistical bias correction of regional climate model simulations for climate change projection in the Jemma sub-basin, upper Blue Nile Basin of Ethiopia. *Theoretical and Applied Climatology*, *139*(3–4), 1569–1588. https://doi.org/10.1007/S00704-019-03053-X/FIGURES/12

World Bank. (2007). *Ethiopia: Accelerating Equitable Growth, Country Economic Memorandum. World Bank, Washington, DC*.

Zarafshani, K., Sharafi, L., Azadi, H., Van Passel, S., & Be, S. V. (2016). Vulnerability assessment models to drought: toward a conceptual framework. *Sustainability*, *8*(6), 588. https://doi.org/10.3390/su8060588

Zhou, Y., Ma, S., Wagle, P., & Gowda, P. H. (2023). Climate and Management Practices Jointly Control Vegetation Phenology in Native and Introduced Prairie Pastures. *Remote Sensing*, *15*(10). https://doi.org/10.3390/RS15102529

Zhu, Y., Li, B., Lian, L., Wu, T., Wang, J., Dong, F., & Wang, Y. (2022). Quantifying the Effects of Climate Variability, Land-Use Changes, and Human Activities on Drought Based on the SWAT–PDSI Model. *Remote Sensing*, *14*(16). https://doi.org/10.3390/RS14163895

CHAPTER TWO

2.SPATIOTEMPORAL CLIMATE VARIABILITY AND TRENDS IN THE UPPER GELANA WATERSHED, NORTHEASTERN HIGHLANDS OF ETHIOPIA

Tadesse, S., Mekuriaw, A., Assen, M., 2024. Spatiotemporal climate variability and trends in the Upper Gelana Watershed, northeastern highlands of Ethiopia. Heliyon 10, e27274. https://doi.org/10.1016/j.heliyon.2024.e27274.

2.SPATIOTEMPORAL CLIMATE VARIABILITY AND TRENDS IN THE UPPER GELANA WATERSHED, NORTHEASTERN HIGHLANDS OF ETHIOPIA

Abstract

The aim of this study was to evaluate the performance of CHIRPS and TAMSAT satellite rainfall data over the Upper Gelana watershed, where gauged meteorological data to understand the nature of the climate are scarce. In addition, variability and trends in rainfall and temperature were examined from 1983 to 2021. To evaluate satellite rainfall, categorical and continuous validation statistics were used. Trends were analyzed using Mann-Kendall, Sen's Slope estimator, and innovative trend analysis (ITA) methods. The study also utilized time-series geostatistical analysis techniques. The validation statistics show that TAMSAT performs better on the daily timescale, while the two products have comparable performance on the monthly timescale. TAMSAT was chosen for rainfall analysis because of its higher resolution and performance. The results reveal high inter-annual spatiotemporal variability and strong irregularities in monthly rainfall. The Mann-Kendall test indicates statistically significant positive trends in *kiremt* and annual rainfall, but *belg* rainfall exhibits an insignificant negative trend. In the *kiremt* season, we found a 96.1, 101.6 and 104.8 mm decadal rate of rainfall increment in the *lower weina dega* (*LWD*), *upper weina dega* (UWD), and *dega* agroecological zones, respectively. In contrast, *belg* season rainfall declined by 16.4, 16.2, and 14.0 mm per decade in the LWD, *UWD,* and *dega* agroecology zones, respectively. The pixel-wise trend analysis also revealed trends and magnitudes of monthly, seasonal, and annual rainfall that vary across the study area. In both *LWD* and *UWD* annual minimum and maximum temperatures, respectively, showed significant decreasing and increasing trends, but in *dega* agroecology the trends were insignificant. The findings of rainfall and temperature trends using the ITA method demonstrated its ability to discover some hidden trends that were not detected by the MK test.

Keywords: TAMSAT, CHIRPS, rainfall, temperature, climate variability, innovative trend analysis, spatiotemporal trend analysis

2.1. Introduction

Climate change is a global problem that attracts the attention of governments, non-government organizations, and researchers all over the world(IPCC, 2018). It affects both humans and the earth's ecosystem. Extreme events such as drought, heat waves, sea level rise and flooding endanger human health (Costello et al., 2009; Louis & Hess, 2008), damage infrastructure (Mirza, 2003a), and cause biodiversity loss throughout the globe (Bandh et al., 2021; Majedul Islam, 2022; Upadhyay, 2020). Though it is a global problem, the impacts vary from place to place with a more pronounced effect in developing countries (Mirza, 2003b).

Climate change is a serious threat to East Africa. The frequency of extreme events has been increasing at an alarming rate in the region (Ayanlade et al., 2022; Weber et al., 2020). The majority of East Africa's population relies on rainfed agriculture, making the region particularly vulnerable to the harmful effects of climate variability and change (Chapman et al., 2020). Climate change has impacted millions of people in East African countries over the last few decades (Funk et al., 2018; Joosten & Grey, 2017; Kew et al., 2021).

Being located in the East African region, Ethiopia is among the most vulnerable countries to the impacts of climate change (Conway & Schipper, 2011; Hamza & Iyela, 2012; Temesgen et al., 2014). Every year, a large number of people are affected by the direct impacts of climate extremes (Kassaye et al., 2021; Kew et al., 2021; Mera, 2018; World Bank, 2007). Climate change is affecting rainfed agricultural practices and crop yield, which would in turn affect food security (Asfaw et al., 2018; Joosten & Grey, 2017; Mekonen & Berlie, 2019; Suryabhagavan, 2017; Tadese et al., 2020). To lessen its effects, appropriate adaptation and mitigation measures should be implemented, which require adequate knowledge of local-level variability and trends in rainfall and temperature.

Many parts of Ethiopia receive rainfall in the *kiremt* (main) and *belg* (minor) seasons, which occur from June to September and February to May, respectively. Various studies have been conducted on rainfall variability in the country (Asfaw et al., 2018; Gummadi et al., 2017; Mekonen & Berlie, 2019; Mengistu et al., 2014; Suryabhagavan, 2017). However, the findings on the seasonal rainfall patterns are inconsistent in one way or another. For instance, Gummadi et al.(2017) reported general declining and increasing trends of rainfall over Ethiopia in the *belg* and *kiremt* seasons, respectively. Contrary to this, Suryabhagavan (2017) analyzed rainfall for

three decades in Ethiopia and found no significant trends in annual and seasonal rainfall amounts in Ethiopia. Disparities were also found in studies conducted at the regional level. A study conducted in the Amhara region of Ethiopia found a decreasing trend in *belg* rainfall and an increasing trend in *kiremt* season rainfall (Gedefaw et al., 2018). On the other hand, increasing trends of *belg* season rainfall were reported for the same region (Alemu & Bawoke, 2020). Similarly to the seasonal rainfall, the annual rainfall trends reported in previous studies are not uniform across the country. Among others, Mengistu et al. (2014) and Alemu & Bawoke (2020) found an increasing trend in annual rainfall in the northwestern Ethiopian highlands and over the Amhara region, respectively. Another study in the southern parts of Ethiopia found a decreasing trend in annual rainfall amounts (Gebremichael et al., 2014).

In the northeastern highlands of Ethiopia, where the present study area is located, a study over a century-long timescale found a significant decreasing trend in the *belg* season and annual rainfall amounts. Nevertheless, the decline in *kiremt* rainfall amount was not significant (Mekonen & Berlie, 2019). Similar results were reported by Asfaw et al. (2018) in the Woleka river basin in the northeastern highlands of Ethiopia, where they found a general decline in annual, *kiremt*, and *belg* rainfall on almost the same temporal scale. Yet, the trends in *kiremt* rainfall amounts in Asfaw et al. (2018) were *significant.* The same authors found an insignificant declining trend from metrological data analysis (Asfaw et al., 2018).

Generally, previous studies on climate variability and trends had discrepancies in their findings. According to Bewket & Conway (2007), such discrepancies are a result of factors that include differences in the data sources, the statistical method used for data analysis, and the study period covered. Most of these studies rely on observed data with a large number of missed values or very low-resolution gridded data and a single method of trend analysis. They were also carried out at the regional or country level and provide a generalized picture for policymakers at the national level. Undeniably, the climatic conditions of Ethiopia vary within a short distance, both in time and space. This demands a detailed investigation of local-level climate variability and change to help planners, decision-makers, and the local community develop and implement appropriate adaptation measures to reduce the impacts of climate variability and change. However, such studies are not available in the present study area, the upper Gelana Watershed.

Therefore, this study was aimed at filling the gaps that existed in previous studies on

climate variability and trends. First, to overcome the limitations pertinent to data, we examined the applications of high-resolution Earth Observation (EO) precipitation products, such as Tropical Applications of Meteorology using SATellite and ground-based observations (TAMSAT) and Climate Hazards Group Infrared Precipitation with Stations (CHIRPS), for local-level studies. The performance of satellite rainfall products varies based on topography, local climate, and the type of satellite (Ayehu et al., 2018; Dinku et al., 2018; Li et al., 2014). As a result, we assessed their suitability at the watershed level using various statistical techniques. Second, we employed a pixel-wise geostatistical approach to the well-known Mann-Kendall (MK) test. In addition, the recently developed innovative trend analysis (ITA) was used to refine the findings of the MK test(Ali et al., 2019; Caloiero et al., 2018; Cui et al., 2017; Girma et al., 2020; Saini & Sahu, 2021; Z. Sen, 2012; Yang et al., 2020). Moreover, variability and trends in rainfall and temperature were examined across the agroecological zones of the Upper Gelana watershed, in the northeastern highlands of Ethiopia.

2.2. Materials and methods

2.2.1. Description of the study area

The study was conducted in the Upper Gelana Watershed of Tehuledere district, in the northeastern highlands of Ethiopia. Geographically, it is found between 11.15^{o} N to 11.35^{o} N

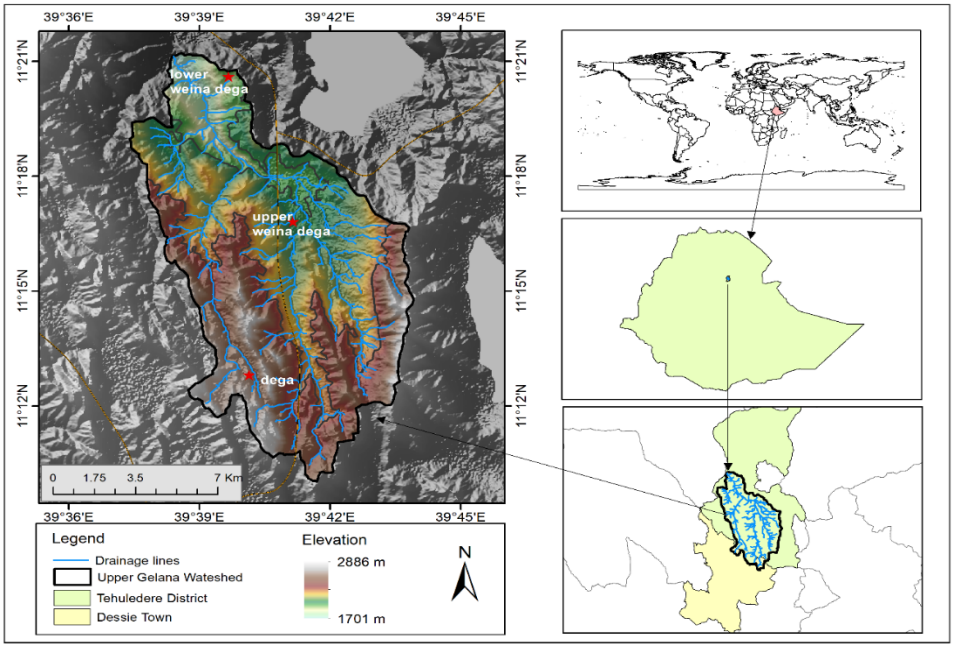

Fig. 2.1. Location map of the study area.

and 39.62^{o} E to 39.73^{o} E (Fig.2.1). It covers a total area of 134 km^{2}. The study area is characterized by rugged topography. The altitude of the study area ranges from 1701 meters to 2886 meters above mean sea level. The upper part of the study area is occupied by mountains dissected by a series of smaller streams that flow to the Gelana mainstream.

The study area has *dega* (cool and humid) and *weina dega* (semi-humid) traditional agroecological zones based on altitude and rainfall, which are the primary criteria to classify the agroecology zones in Ethiopia (Hurni, 1998; Negash, 1987). *Dega* agroecology is located above 2300 meters above sea level, while *weina dega* is located between 1701 and 2300 meters above sea level; both receive rainfall ranging from 900 to 1400mm. During our field observation, we have noted differences in plant and crop varieties grown in the lower and upper parts of the *weina dega* agroecology zone, mainly influenced by the climate conditions. To understand this distinction in climate conditions that exist within the *weina dega* agroecology zone of the study area, we have classified it into two equal parts based on the elevation: the lower *weina dega (LWD)* and upper *weina dega (UWD)* agroecology zones.

Major plant species found in the study area include planted *Eucalyptus* and naturally growing *Juniperus procera, Acacia abyssinica,* and*Euphorbia tirucalli.* A mixed traditional subsistence farming system consisting of both crop and animal production is the main source of livelihood in the study area. Major crops grown in the study area include *teff* (*Eragrostis tef*), wheat (*Triticum aestivum*), and sorghum (*Sorghum bicolor*) which are widely grown crops in the *dega* and *weina dega* zones. In addition to cereal crops, farmers produce *chat* (*Catha edulis*), a primary cash crop for the local community. The Upper Gelana watershed is among the most highly populated areas in Ethiopia, with limited cultivatable land in the South Wollo zone (Rosell et al., 2017).

2.2.2. Data sources

In this study, satellite precipitation data is the principal data source for rainfall variability and trend analysis. Ground-based or observed rainfall data were used to assess the performance of satellite rainfall products. In order to examine the variability and trends in temperature, gridded temperature data were used. Supportive qualitative data about the variability and trend of rainfall were also acquired through focus group discussions (FGDs) and key informant interviews (KIIs).

2.2.2.1. Satellite precipitation data

Satellite precipitation data is vital to overcome the data scarcity caused by the limited spatial coverage of ground-based observations. Among the various available satellite precipitation products (Dinku et al., 2007), two widely used satellite precipitation products, CHIRPS and TAMSAT version 3.1, were selected based on their long temporal coverage and relatively better spatial resolution.

CHIRPS is a satellite rainfall estimate derived from infrared Cold Cloud Duration (CCD) observations. It provides daily and monthly rainfall data from 1981 to the present with an average spatial resolution of 0.05 degrees (5.5 km). This precipitation data is essential, particularly in sparsely gauged locations (Funk et al., 2015). CHIRPS daily data (Funk et al., 2015) from 1983-2021 were retrieved from Google Earth Engine (GEE) Snippet ee.ImageCollection ("UCSB-CHG/CHIRPS/DAILY") using rgee, a package used to call GEE in the R environment (Aybar, 2021).

TAMSAT is another satellite rainfall data source. The product is delivered by the TAMSAT group (Maidment et al., 2014, 2017; Tarnavsky et al., 2014). The data is derived from Meteosat thermal infrared (TIR) imagery using cold cloud duration (CCD). The TAMSAT has provided long-term rainfall data since 1983 with an average spatial resolution of 0.0375 degrees (4 km) and temporal resolutions of daily, pentadal, dekadal, monthly, and seasonal time scales. The data in netCDF were retrieved from the TAMSAT website at http://www.tamsat.org.uk/data.

2.2.2.2. Observed rainfall data

Observed rainfall data from Haik station (found in the study area) as well as the Dessie, Ruga, and Kutaber stations found in the vicinity of the study area was obtained from the Ethiopian Meteorological Institute (EMI). The observed rainfall was used for validation of satellite precipitation data. To make a reliable comparison of the performances of satellite products across the stations, only precipitation records available on dates that are common to all four stations are considered, and missed values are disregarded. The location, elevation, and temporal coverage of stations used for satellite rainfall validation are presented in Table 2.1.

Table 2.1. List of meteorological stations used for validation and their locations based on the geographic coordinate system and Adindan datum.

No	Stations	Latitude	Longitude	Year	Elevation (m)
1	Ruga	11.17	39.58	1983-2007	2672
2	Dessie	11.12	39.63	1983-2007	2553
3	Haik	11.30	39.68	1983-2007	1985
4	Kutaber	11.27	39.53	1983-2007	1740

2.2.2.3. Gridded temperature data

We used gridded temperature data to examine the spatiotemporal variability and trends of temperature in the study area. The daily gridded temperature data with a spatial resolution of 0.0375 degrees (4km) over the study area were obtained from the EMI. Due to problems related to instruments and security issues that occurred in northern Ethiopia, including the study area, the metrological data for the Haik stations were not available in the last five years. Unfortunately, the gridded temperature from EMI is available only until 2018 for the whole of Ethiopia. As a result, we examined temperature from 1983 to 2018.

2.2.2.4. Interview and focus group discussion

To better understand farmers' perspectives on climate variability and change, three focus group discussions with five participants each were held in *lower weina dega (*LWD*), upper weina dega (*UWD*)* and *dega* agroecological zones. In addition, interviews were conducted with twelve key informants, four from each of the three agroecology zones, including community leaders, kebele heads, and agricultural extension workers. Participants for focus group discussions and key informant interviews were chosen based on their long-term residence in the area and familiarity with the issues under consideration.

2.2.3. Methods of data analysis

2.2.3.1. Validation methods

The performance of satellite precipitation is affected by several factors, including climate regimes, topography, and the type of satellite (Ayehu et al., 2018; Dinku et al., 2018; Li et al., 2014). Thus, it is essential to evaluate the accuracy of CHIRPS and TAMSAT in the Upper *Gelan* watershed before using them for further analysis. Several categorical and continuous-verification statistical tools were used to assess performance on daily and monthly timescales.

Continuous verification statistics were used to quantify the level of accuracy, or how well the satellite estimates rainfall amounts as compared to the ground observations. The continuous verification statistics used in this study include the multiplicative bias, mean error (ME), mean absolute error (MAE), root mean square error (RMSE), Pearson Correlation Coefficient (*r*), and Nash–Sutcliffe Efficiency Coefficient (NSE). Bias and NSE were used to validate the daily and monthly satellite rainfall, respectively, while the other statistics were applied to both timescales.

The multiplicative bias is the comparison of the magnitude of the average satellite-estimated rainfall to that of the average rainfall from ground-based observations. The value of multiplicative bias ranges from negative infinity to positive infinity, with one being the perfect score (Ebert, 2009).

$$\text{Bias (Multiplicative)} = \frac{\frac{1}{N}\sum_{i=1}^{N} Si}{\frac{1}{N}\sum_{i=1}^{N} Gi} \quad (1)$$

The mean error (ME) also called additive bias, measures the difference between the average satellite-estimated rainfall and the average ground observation (Ebert, 2007; Wilks, 2011). Higher average satellite measurements than the gauged rainfall yield a positive ME value, while the reverse results in a negative ME value (Wilks, 2011).

$$ME = \frac{1}{N}\sum_{i=1}^{N}(Si - Gi) \quad (2)$$

The Mean Absolute Error (MAE) measures the average magnitude of the errors between each pair of satellite-estimated and observed rainfall values. MAE values equal to zero imply that the satellite-estimated rainfall is accurate, and they rise as the differences between the estimated and observed rainfall become greater. It takes the same unit as the estimated rainfall (Wilks, 2011).

$$MAE = \frac{1}{N}\sum_{i=1}^{N}|Si - Gi| \quad (3)$$

The RMSE also measures the average magnitude of the errors but gives greater weight to the larger errors (E. Ebert, 2007). It has the same scale as the satellite-estimated rainfall (Wilks, 2011).

$$RMSE = \sqrt{\frac{1}{N}\sum_{i=1}^{N}(Si - Gi)^2} \quad (4)$$

The correlation coefficient (r) measures the degree of a linear relationship between the satellite-estimated rainfall and rain gauge data (Ebert, 2007). Its value ranges from +1 to -1, where the two upper and lower bounding values indicate a perfect linear relationship. If the value is zero, then it indicates no linear relationship (Wilks, 2011).

$$r = \frac{\sum(Si - \bar{S})(Gi - \bar{G})}{\sqrt{\sum(Si - \bar{S})^2}\sqrt{\sum(Gi - \bar{G})^2}} \quad (5)$$

Nash–Sutcliffe Efficiency (NSE) is a widely used index developed by (Nash & Sutcliffe, 1970) that measures the agreement between estimated and observed events. Its value ranges from minus infinity to one, where the latter indicates an excellent match between the estimated and observed event.

$$NSE = 1 - \frac{\sum_{i=1}^{N}(Si - Gi)^2}{\sum_{i=1}^{N}(Gi - \bar{G})^2} \quad (6)$$

In all the above formulas for continuous validation statistics, S*i* represents the satellite-estimated value, G*i* is the observed rain gauge value, N is the number of observed samples, $\bar{G}$ is the average observed rain gauge value, and $\bar{S}$ is the average satellite-estimated value. In the case of Bias and NSE the variables refer daily and monthly satellite rainfall, respectively, whereas in the other continuous statistics variables refer to both timescales.

Categorical verification statistics were also used to assess the match between rainfall incidences in the satellite estimate and ground observations. Categorical verification statistics are calculated from two-by-two contingency tables of yes/no events with four basic elements such as hit, misses, false alarms, and correct negatives (Ebert, 2007). A hit (a) refers to a matched record of rainfall events in both the satellite estimate and ground-based observations. A false alarm (b) refers to a rainfall event recorded by satellite where there is no corresponding recorded rainfall by the ground-based meteorological stations in the study area at any time during the study period. A miss (c) refers to a rainfall event recorded by ground observation but missed in the satellite estimate. A correct negative (d) refers to no rainfall

events in both satellite estimates and ground-based observations. In this study, we used categorical verification statistics such as the probability of detection (POD), false alarm ratio (FAR), treat score (TS), enhanced treat score (ETS), Heidke Skill Score (HSS), and frequency bias score to evaluate the daily satellite rainfall estimate. In computing these statistics, 0.1 mm was used as a threshold to separate the rain and non-rain events.

The probability of detection (POD) tells about the fraction of rain events recorded by the rain gauge, which was also correctly estimated by the satellite (Ebert, 2007; Wilks, 2011).

$$\mathrm{POD} = \frac{a}{a+c} \tag{7}$$

The false alarm ratio (FAR) measures the fraction of rain events estimated by the satellite that did not happen in reality (E. Ebert, 2007). The best value for POD is one, and for FAR it is zero.

$$\mathrm{FAR} = \frac{b}{a+b} \tag{8}$$

Heidke Skill Score (HSS) refers to the accuracy of the satellite rainfall estimate in relation to that of random chance. An HSS value of one indicates a perfect satellite estimate, and zero implies no skill. When the satellite rainfall products become worse than the reference data, the HSS value becomes negative (Wilks, 2011).

$$\mathrm{HSS} = \frac{a * d - b * c}{(a + c)(c + d)(a + b)\,(b + d)} \tag{9}$$

The threat score (TS) is the number of correct yes forecasts divided by the total number of occasions on which that event was forecast and/or observed. Its value ranges between 0 and 1, where zero indicates a poor estimate and 1 is the perfect threat score (Wilks, 2011).

$$\mathrm{TS} = \frac{a}{a+c+b} \tag{10}$$

The equitable threat score (ETS) is a modified version of the threat score (TS) that was developed to address the TS's flaw of being higher in wet areas. Its value ranges from 0 to 1, with 1 indicating perfect agreement between estimated and observed rainfall (Ebert, 2007).

$$ETS = \frac{a - a_{random}}{a + c + b - a_{random}} \quad (11)$$

The frequency bias score is a comparison of the frequency of rainfall in the satellite estimate to that of the observed rainfall (Ebert, 2007). It is a ratio of the total rain events in the satellite estimate to the total rain events observed. The bias value of one implies a perfect satellite rainfall estimate. Bias values larger than one signify a more frequent satellite rain estimate than a rain gauge record, whereas a value less than one implies a less frequent rain event in the satellite estimate (Wilks, 2011).

$$\text{Frequency bias/Bias score} = \frac{a + b}{a + c} \quad (12)$$

The continuous and categorical statistics were computed in R using the verification (NCAR - Research Applications Laboratory, 2015) and matrices (Hamner & Frasco, 2018) packages.

2.2.3.2. Methods forclimate variability analysis

In this study, variability and trend analysis of rainfall and temperature were done on a pixel by pixel basis and at three point locations representing the LWD,UWD, and *dega* agroecological zones of the Upper Gelana watershed. The mean and standard deviation were used to examine the variability of rainfall and temperature in monthly, seasonal and annual time scale. These descriptive statistics are important to get an overview of rainfall and temperature variation during the study period. Apart from the mean and standard deviation, the coefficient of variation (CV), precipitation concentration index (PCI) and standardized rainfall anomaly (SRA) were analyzed.

Coefficient of variation (CV)

The coefficient of variation is vital for understanding the degree of variability in rainfall from the long-term mean. The coefficient of variation was computed for monthly, seasonal, and annual timescales using the formula provided by (Oliver, 1980)

$$CV = \frac{\sigma}{\bar{X}} * 100 \quad (13)$$

Where σ is the standard deviation and $\bar{X}$ is the long-term mean of precipitation data

Precipitation concentration index (PCI)

To analyze the monthly rainfall distribution, the precipitation concentration index (PCI) was calculated using the formula given by (Oliver, 1980).

$$PCI = 100\ \frac{\sum xi^{\,2}}{(\sum xi)^2} \quad (14)$$

Where xi is the rainfall amount of the *i*th month, and $\sum xi$ is the sum of precipitation for twelve months. PCI values less than 10 indicate uniform distribution, values between 10 and 15 represent moderate distribution, values from 15 to 20 show irregular distribution, and values above 20 indicate strong irregularity in precipitation distribution (Oliver, 1980). These classifications were used in previous studies (Asfaw et al., 2018; Belay et al., 2021; De Luis et al., 2011).

Standardized rainfall anomaly (SRA)

Standardized rainfall anomaly (SRA) is used to examine inter-annual rainfall variability and is specifically useful to identify wet and dry years. The standardized rainfall anomaly (SRA) for a given station can be calculated as used in (Alemayehu et al., 2020; Bewket & Conway, 2007; Kassie et al., 2014).

$$SRA = \frac{Xt - \bar{X}}{\sigma} \quad (15)$$

Where Xt is the observed annual or seasonal rainfall in year t, $\bar{X}$ is the long-term mean annual or seasonal rainfall in the study period, and σ is the standard deviation of annual or seasonal rainfall. SRA values less than -1.65 indicate extreme drought; from -1.28 to -1.65, severe drought; -0.84 to - 1.28, moderate drought; and SRA greater than - 0.84, no drought (Agnew & Chappell, 1999). SRA was used for analyzing rainfall variability in previous studies (Alemayehu et al., 2020; Bewket & Conway, 2007; Kassie et al., 2014).

2.2.3.3. Trend analysis methods

Mann-Kendall (MK) trend test

Trends in timeseries climate data can be computed using parametric or non-parametric methods. In the case of the parametric method, the data must be independent and uniformly distributed, whereas non-parametric statistics do not consider distribution and can be used with non-serially correlated data. The Mann-Kendall test is one of the most commonly used non-parametric approaches for detecting statistically significant trends in rainfall and temperature (Mahmood et al., 2019; Panda & Sahu, 2019). To avoid drawing incorrect conclusions from the MK results, it is crucial to determine statistically significant autocorrelation in the data (von Storch & Navarra, 1995). When there was no serial correlation, the Mann-Kendall test was utilized in this study to detect trends in the monthly, seasonal, and yearly rainfall and temperature (Kendall, 1948; Mann, 1945;Sen, 1968). The Mann-Kendall statistic S is given as:

$$\mathrm{s} = \sum_{i=1}^{n-1} \sum_{j=i+1}^{n} sgn(x_j - x_i) \quad (16)$$

Where n is the number of data points, x_i and x_j are the data values in time series i and j (j > i), respectively, and sgn $(x_j - x_i)$ is the sign function as:

$$sgn(x_j - x_i) = \begin{cases} +1, if\ x_j - x_i > 0 \\ 0, if\ x_j - x_i = 0 \\ -1, if\ x_j - x_i < 0 \end{cases} \quad (17)$$

The variance is computed as:

$$Var(S) = \frac{n(n-1)(2n+5) - \sum_{i=1}^{m} t_i(i-1)(2ti+5)}{18} \quad (18)$$

Where n is the number of observations, m is the number of tied groups, and t_i denotes the number of ties of extent i. A tied group is a set of sample data with the same value. In cases where the sample size n >10, the standard normal test statistic Z_S can be calculated as follows:

$$Z_s = \begin{cases} \dfrac{S-1}{\sqrt{Var(S)}}, if\ S > 0 \\ 0 \quad if \ \ S = 0 \\ \dfrac{S+1}{\sqrt{Var(S)}}, if\ S < 0 \end{cases} \tag{19}$$

Positive values of Z_S indicate increasing trends, while negative Z_S values show decreasing trends.

In this study, the presence of serial-autocorrelation was assessed using the autocorrelation function (acf) of the stat package in the R program (R CoreTeam, 2021). In the presence of significant serial-correlation, pre-whitening was applied following the variance correction approach to address serial correlation in trend analysis (Yue & Wang, 2004). The pre-whitening procedure was implemented using the modifiedmk package in R (Patakamuri & O'Brien, 2021).

Sen's slope estimator

Sen's slope estimator was used to quantify the magnitude of detected trends. It is calculated using the formula given as follows (Sen, 1968).

$$\{X_{ij} = \frac{(Y_j - Y_i)}{t_j - t_i} for \ \ i = 1, \ldots, N \tag{20}$$

Where the X_{ij} are the slopes of the lines connecting each pair of points (t_i,Y_i) and (t_j, (Y_j) where ($t_j > t_i$. A positive value of X_{ij} indicates an increasing trend, while a negative value of X_{ij} indicates a decreasing trend (Gocic & Trajkovic, 2013).

For better visualization of results from coarse resolution rainfall analysis, values from each pixel were extracted and interpolated back using inverse distance weighted (IDW) interpolation using the spatstat package(Baddeley & Turner, 2005). Then, ArcGIS 10.7.1 and Origin 2022 were used to prepare the figures.

Innovative trend analysis (ITA)

The ITA is graphical approach for analyzing trends in time series data, first developed by (Sen, 2012). Non-parametric trend analysis techniques like the Mann-Kendall test need a

timeseries data that are not serially correlated. However, the ITA completely avoids such prior assumptions based on the data (Caloiero et al., 2018; Oztopal & Sen, 2017; Saini & Sahu, 2021; Sen, 2012). In this method, the data is divided into two equal parts and then plotted on a scatter plot, with the first half on the horizontal axis and the second half on the vertical axis. Data points below the 1:1 (45°) line show a decreasing trend, whereas data points above the 1:1 (45°) line show an increasing trend. Points that fall on the 45° line are considered trendless. The ITA graph can also be interpreted by dividing the data point series into three equal clusters based on the minimum and maximum value ranges of the data points on the horizontal axis. Then, the three clusters can be labeled as “low”, “medium”,and “high”, and interpretations of the trends can be provided for each cluster. The significance of the trend can be determined using ±5 % or ±10% error. If the data points are outside of ±5 % error or the maximum ±10% error from the 1:1 line, the trend is significant (Oztopal & Sen, 2017). We used the ITA method to refine the findings of the Mann-Kendall trend analysis (Ali et al., 2019; Caloiero et al., 2018; Cui et al., 2017; Saini et al., 2020; Saini & Sahu, 2021; Wu & Qian, 2017).

2.3. Results and discussions

2.3.1. Evaluation of CHIRPS and TAMSAT satellite rainfall

This section presents and discusses the validation results for the daily and monthly performances of CHIRPS and TAMSAT satellite rainfall.

2.3.1.1. Validation of CHIRPS and TAMSAT daily rainfall

For the daily timescale, the multiplicative bias statistics revealed that both satellite products are comparable to station rainfall in terms of average magnitude (Table 2.2). The multiplicative bias for TAMSAT ranges from 0.8 (Haik station) to 1.1 (Ruga station), and for CHIRPS it ranges from 0.9 (Haik station) to 1.2 (Ruga station). At Kutaber stations, CHIRPs have a perfect multiplicative bias score of 1.0. The MAE value for TAMSAT varies from 2.97 mm (Kutaber station) to 3.33 mm (Dessie station), while the MAE value for CHIRPS ranges from 3.75 mm (Ruga station) to 4.01 mm rainfall (Dessie station). The result of the MAE indicates that TAMSAT has better performance than CHIRPS. The RMSE value for TAMSAT

ranges from 6.90 mm to 8.20 mm of rainfall, and for CHIRPS, it ranges from 9.03 mm to 9.77 mm of rainfall. This implies that TAMSAT has a lower average magnitude of error than CHIRPS. As compared with CHIRPS, the daily TAMSAT rainfall has a good linear correlation (r) with the rainfall values at the four meteorological stations. The POD value of CHIRPS at the four stations ranges from 0.40 to 041, and for TAMSAT, it ranges from 0.56 to 0.60 (Table 2.2). This indicates TAMSAT has better performance in detecting daily rain events in the Upper Gelana watershed and its vicinity.The findings of this study agree with the comparison of the two products in terms of POD in the northwest part of the Rift Valley in Ethiopia (Dinku et al., 2018).

Table 2.2 Continuous and categorical validation statistics for CHIRPS and TAMSAT daily rainfall in the upper Gelana watershed and its surroundings (the unit for ME, MAE and RMSE is mm)

Stations		Bias	ME	MAE	RMSE	r	POD	TS	ETS	FAR	HSS	Bias score
Ruga	CHIRPS	1.16	0.45	3.75	9.06	0.38	0.4	0.33	0.22	0.38	0.36	0.68
	TAMSAT	1.06	0.16	2.97	7.03	0.5	0.57	0.48	0.36	0.3	0.53	0.86
Haik	CHIRPS	0.86	-0.48	3.84	9.03	0.4	0.4	0.33	0.22	0.37	0.35	0.65
	TAMSAT	0.76	-0.84	3.15	7.55	0.51	0.56	0.47	0.35	0.29	0.52	0.82
Dessie	CHIRPS	0.91	-0.31	4.01	9.77	0.42	0.41	0.32	0.21	0.4	0.35	0.69
	TAMSAT	0.84	-0.57	3.33	8.2	0.52	0.59	0.47	0.35	0.32	0.52	0.88
Kutaber	CHIRPS	1	0.01	3.79	9.24	0.43	0.41	0.33	0.22	0.37	0.37	0.67
	TAMSAT	0.89	-0.36	2.87	6.9	0.59	0.6	0.51	0.4	0.26	0.57	0.84

The TS and ETS statistics showed that CHIRPS have almost consistent performances over the four stations, while the performance of TAMSAT was more or less the same except for the Kutaber station (Table 2.2). In comparison, TAMSAT has higher TS and ETS values than CHIRPS, implying a better ability to detect rain events. The FAR values for TAMSAT are lower than CHIRPS at all stations, suggesting that TAMSAT produces fewer false alarms. This also implies that the rain events that did not occur in reality were reported as if they did by TAMSAT were smaller than those in CHIRPS. The HSS result, which measures the skill or accuracy of satellite precipitation in relation to random chances, showed that TAMSAT has better accuracy than CHIRPS for daily rainfall. Similar findings with the HSS result of this study were also reported in previous studies(Dinku et al., 2018). The comparison bias score revealed that the frequencies of TAMSAT are more similar to the frequencies of station

rainfall than those of CHIRPS (Table 2.2). In general, almost all of the continuous and categorical statistics show that TAMSAT performs better than CHIRPS in the daily rainfall estimates. Similar findings were reported by Dinku et al.(2018) who attributed the better performance of the TAMSAT daily rainfall product to the inherent algorithm adjusted based on local station data.

2.3.1.2. Validation of CHIRPS and TAMSAT monthly rainfall

The patterns in the scatterplots and the coefficient of determination (R^2) values show a significant correspondence between the monthly rainfall from satellite products and the observed rainfall patterns at all four stations (Fig. 2.2). However, both the scatter and values of (R^2) suggest that the monthly rainfall from CHIRPS (Fig. 2.2a-d) has slightly better accuracy than monthly rainfall from TAMSAT (Fig.2.2e-h). Similar pattern of scatters for both CHIRPS (less) and TAMSAT (a bit wider) over Ethiopia were reported inDinku et al. (2018).

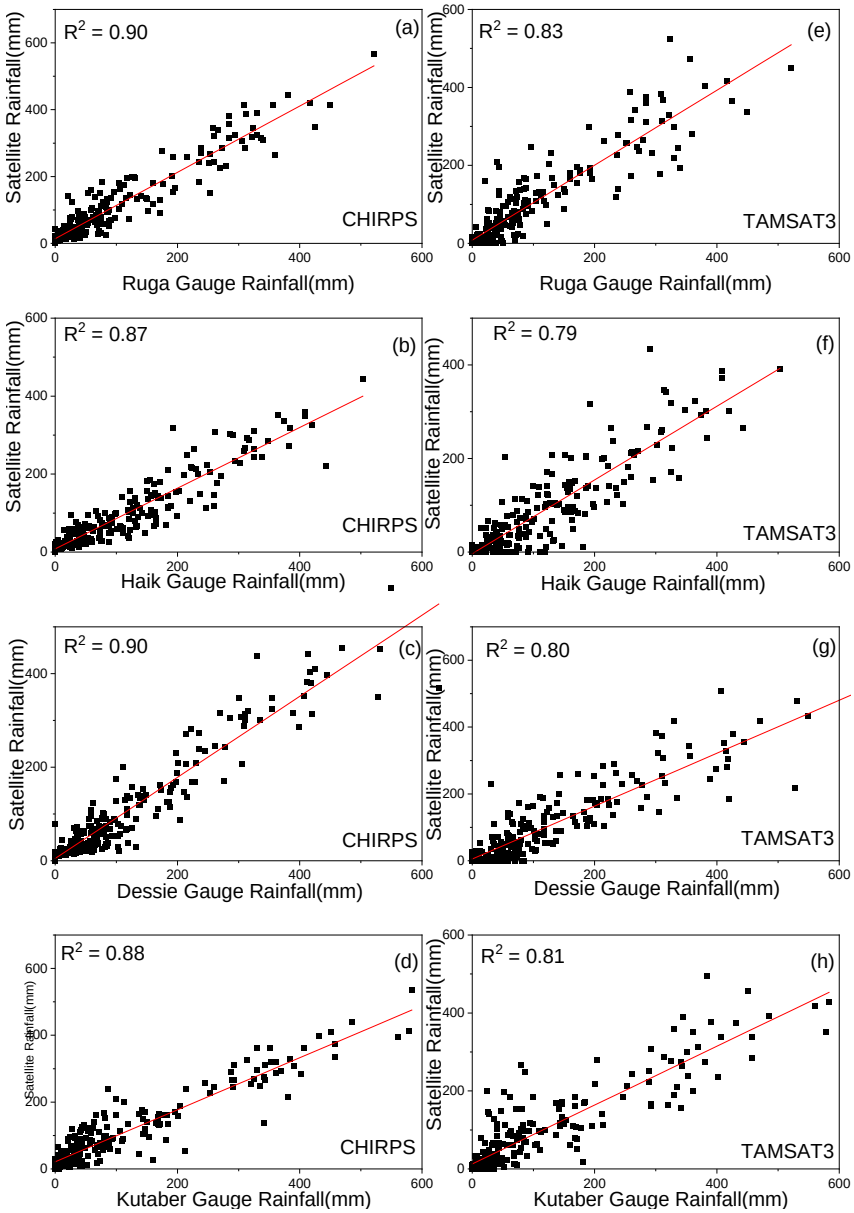

Fig. 2.2. The relationship between CHIRPS (a-d) and TAMSAT (e-h) monthly rainfalls and rain gauge data at Ruga, Haik, Dessie and Kutaber stations that are found in the upper Gelana watershed and its surroundings.

As shown in Table 2.3, the mean error at Ruga is 13.49 mm and 4.97mm for CHIRPS and TAMSAT, respectively. The result indicates that TAMSAT has a lower average error compared to CHIRPS at Ruga station. It also shows that the rainfall measured by the CHIRPS satellite is greater than the rainfall measured at the Ruga meteorological station. The mean error for CHIRPS at Haik, Dessie, and Kutaber stations, respectively, is -14.6 mm, -9.5 mm, and 0.15 mm. While the mean error for TAMSAT at Haik, Dessie, and Kutaber stations is -

25.3 mm, -17.1 mm, and -10.8 mm, respectively (Table 2.3). The findings imply that CHIRPS has a lower average error than TAMSAT at the three stations. The negative mean error values for both CHIRPS and TAMSAT suggest that the estimated rainfall by these satellite products is lower than the rainfall measured at the respective ground-based meteorological stations. For CHIRPS, the MAE values range from 25.5 mm at Dessie to 31.3 mm at Kutaber station, while TAMSAT MAE values range from 28.5 mm at Ruga to 38.9 mm at Dessie station (Table 2.3). Similar to ME, the MAE and the RMSE statistics revealed that CHIRPS is slightly better than TAMSAT in monthly rainfall estimates at all four stations. The correlation coefficient for both CHIRPS and TAMSAT monthly satellite-estimated rainfall products is larger than +0.8, which demonstrates a very strong positive association with the observed rainfall. Both CHIRPS and TAMSAT have NSE values close to one, indicating very good agreement with observed rainfall at all stations. In general, all continuous statistical tests performed on monthly data from TAMSAT and CHIRPS indicate that the two products perform well, with CHIRPS slightly outperforming the TAMSAT satellite rainfall estimate. The results of this study, specifically MAE, correlation coefficient (r), and efficiency, are in line with the findings stated by Dinku et al. (2018) for the monthly timescale in Ethiopia.

Table 2.3Validation statistics for CHIRPS and TAMSAT monthly rainfall in the upper Gelana watershed and its surroundings (the unit for ME, MAE and RMSE is mm).

Stations		ME	MAE	RMSE	*R*	NSE
Ruga	CHIRPS	13.49	25.58	36.28	0.95	0.88
	TAMSAT	4.97	28.35	45.20	0.92	0.82
Haik	CHIRPS	-14.63	29.31	42.19	0.93	0.84
	TAMSAT	-25.33	37.10	54.18	0.89	0.74
Dessie	CHIRPS	-9.46	25.54	39.39	0.95	0.90
	TAMSAT	-17.12	38.43	57.69	0.90	0.78
Kutaber	CHIRPS	0.15	31.29	46.04	0.94	0.87
	TAMSAT	-10.75	35.94	57.30	0.90	0.80

2.3.2. Spatiotemporal variability of rainfall

2.3.2.1. Variability of monthly rainfall

Based on the validation results of satellite rainfall products, TAMSAT was better than CHIRPS for daily rainfall, while they had a very close performance on monthly rainfall. As a

result, TAMSAT was chosen and, hence, used in the subsequent analyses of the variability and trend in rainfall in this study. As presented in Table 2.4, the mean monthly rainfall is high in August amounts to 268 mm, 270.9 mm, and 289.9 mm in LWD, UWD, and *dega* agroecology zones, respectively. Whereas January is the month with lowest mean monthly rainfall in all three agroecology zones. When comparing the three agroecology zones, *dega* received the highest mean monthly rainfall, followed by UWDand LWD, in the majority of the months. In the study area, the mean seasonal rainfall was high in the *kiremt* season (the main rainy season) and low in the *bega* season during the study period (1983–2021). The *belg* rainfall deviate from the mean by 96.8, 94.1 and 93.8 mm in LWD, UWD and *dega* agroecology zones, respectively. The standard deviation of annual rainfall is low (193.7mm) and high (212.4 mm) in LWD and *dega*, respectively. The coefficient of variation (CV) was higher for the *belg* season than the *kiremt* and annual rainfall in all the three agroecology zones, indicating high variability.

Table 2.4.Descriptive statistics of the monthly, seasonal, and annual rainfall (unit of measurement is mm) based TAMSAT in the LWD, UWD and *dega* agroecology zones of the upper Gelana watershed (1983-2021).

	LWD			UWD			*Dega*		
Month	Mean	SD	CV	Mean	SD	CV	Mean	SD	CV
Jan	1.7	4.0	240.0	0.7	2.6	347.1	0.3	1.5	605.4
Feb	9.8	16.3	166.3	8.6	13.8	160.6	7.8	12.5	160.7
Mar	70.1	51.7	73.7	70.0	51.5	73.7	71.5	49.0	68.6
Apr	108.3	56.0	51.7	109.8	55.5	50.5	112.4	59.1	52.6
May	61.9	48.8	78.9	66.2	52.5	79.3	70.6	56.4	79.8
Jun	26.7	28.2	105.5	30.3	30.8	101.3	31.1	32.1	103.2
Jul	238.0	102.3	43.0	243.9	103.8	42.6	264.6	111.5	42.1
Aug	268.6	92.0	34.3	270.9	93.6	34.6	289.9	97.6	33.7
Sep	108.8	40.8	37.5	111.9	43.6	39.0	123.9	49.0	39.5
Oct	45.1	47.4	105.0	45.7	47.6	104.1	46.2	49.8	107.8
Nov	17.5	29.9	171.0	17.8	30.5	170.8	19.6	29.5	150.9
Dec	7.4	12.2	166.1	7.0	11.4	162.7	7.2	13.5	186.5
Season									
Belg(FMAM)	250.0	96.8	38.7	254.5	94.1	37.0	262.3	93.8	35.8
Kiremt(JJAS)	642.1	191.3	29.8	657.1	197.7	30.1	709.5	208.7	29.4
Bega(ONDJ)	72.0	53.9	74.9	71.7	55.7	77.8	73.3	59.4	81.0
Annual	963.8	193.7	20.1	982.9	200.7	20.4	1045.1	212.4	20.3

The average monthly rainfall in the study area varies spatially and temporally across latitudes (north-south) and longitudes (east-west). The spatial variation could be related to the altitude of the study area. As we move north, the altitude drops and the agroecology shift from

dega to UWD and eventually to LWD. It increases from east to west in the northern half, but the topography is uneven in the southern half. As shown in the Hovmoller diagrams in Fig.2.3a, the southern parts (*dega*) of the study area received relatively high mean monthly rainfall in June, July, August, and September. As we moved north (LWD), the mean rainfall was high only in the July and August months. Similarly, the distribution of rainfall varies from east to west; places in the eastern part received relatively the highest mean monthly rainfall (1983–2021) in all of the *kiremt* months, but western parts do in July and August (Fig.2.3b). Furthermore, as illustrated in Fig.2.4(a-l), the mean monthly rainfall has a distinct spatial pattern that is also related to the seasons.

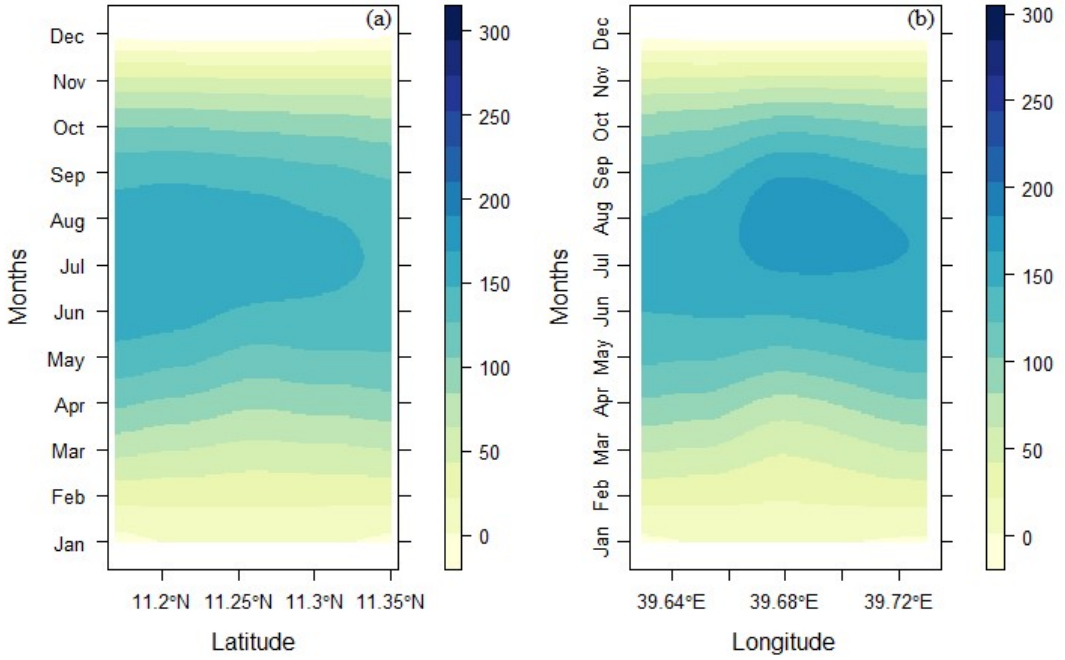

Fig.2.3.Hovmoller diagrams prepared using TAMSAT data that show latitudinal (a) and longitudinal (b) variations of mean monthly rainfall (mm) in the Upper Gelana watershed (1983–2021).

Precipitation Concentration Index (PCI)

Based on the PCI results, the LWD, UWD, and *dega* agroecology zones of the upper Gelana watershed are characterized by moderate to strong irregularities in rainfall distribution (Fig.2.5a-c). The proportion of years with a moderate rainfall distribution is 2.6% in the LWD agroecology zone and 5% in the UWD and *dega* agroecology zones. The years 1997 and 2019 exhibited moderate rainfall distributions in the UWD and *dega* agroecology zones, as did the year 2019 in the LWD (Fig.2.5). Additionally, 53.8% of study years in the LWD and UWDand

64% of the study years in *dega* had PCI values above 20, indicating a strong irregularity in the distribution of rainfall. As seen in Fig.2.5(a-c), the distribution of monthly rainfall was not uniform or homogeneous throughout the study periods (1983-2021).

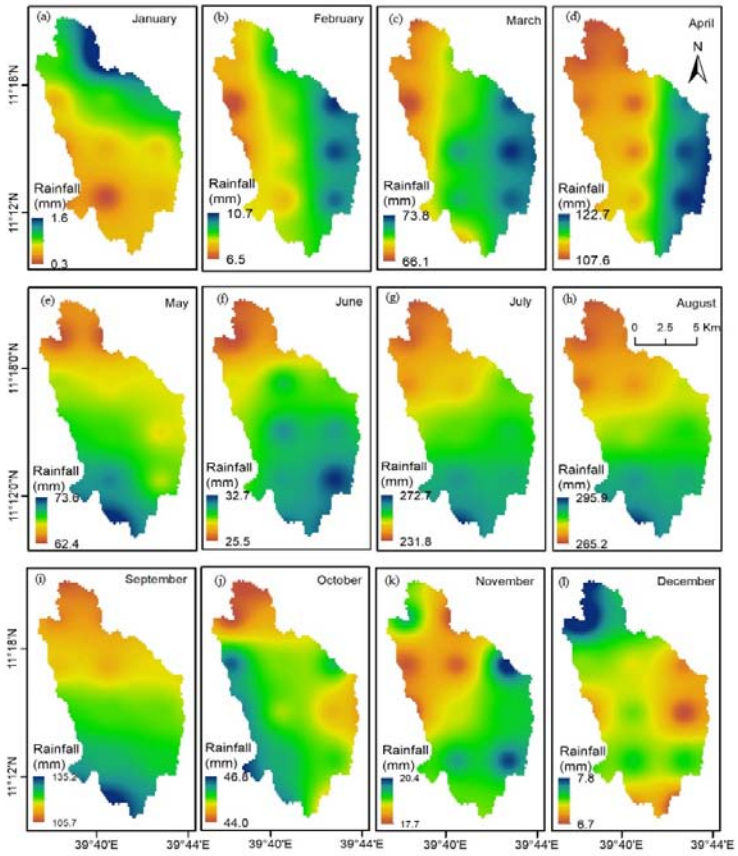

Fig. 2.4. Spatial distribution of mean monthly rainfall (mm) in the Upper Gelana Watershed (1983–2021) from January to December respectively labeled by letters a-l prepared based on TAMSAT data.

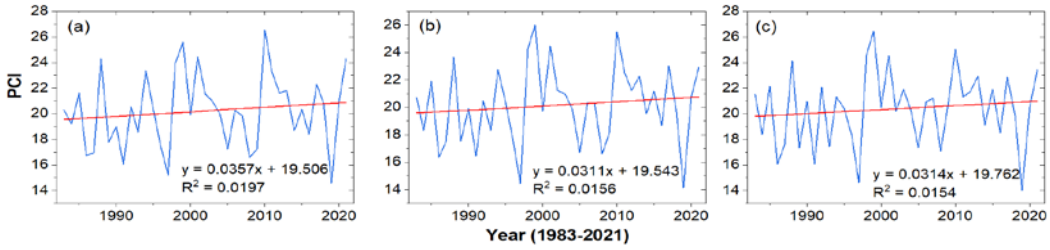

Fig. 2.5.PCI calculated from TAMSAT rainfall for LWD (a), UWD (b), and *dega* (c) agroecology zones of the Upper Gelana Watershed (1983–2021).

2.3.2.2. Variability of seasonally and annual rainfall

As depicted in Fig.2.8(a-d), the distribution of the seasonal and annual mean rainfall follows a similar pattern as the mean monthly rainfall presented in Fig.2.4(a-l). The southern parts of the Upper Gelana watershed received relatively the highest mean *kiremt* season rainfall (740 mm), while the northern part of the watershed received relatively low (616 mm) mean *kiremt* season rainfall. As in the mean monthly and seasonal rainfall, latitudinal and longitudinal variations were also visible in the annual rainfall time series (Fig.2.6a,b). The annual rainfall decreased as we moved from east to west (Fig.2.6b) and south to north (Fig.2.6a), and the patterns were consistent throughout the study period (1983–2021). As stated above, the high rainfall in the southern and eastern parts may be associated with their high altitude and better forest cover than the northern parts.

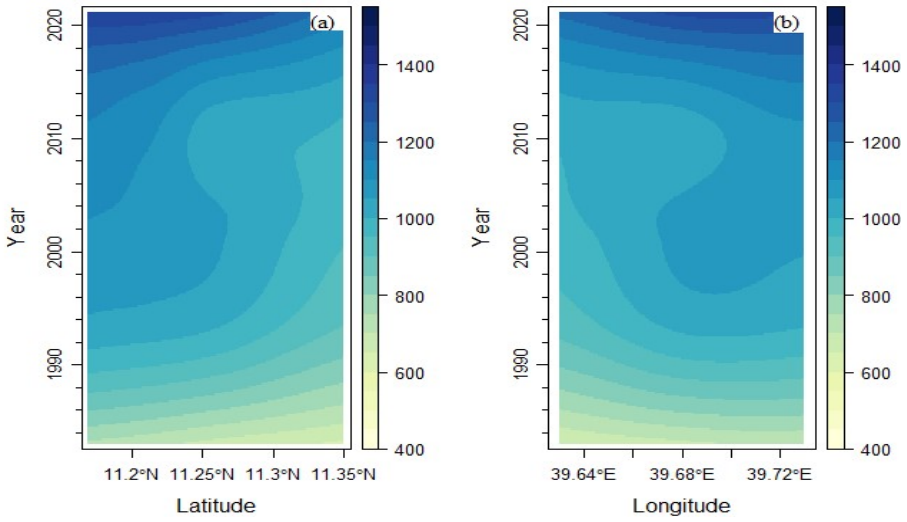

Fig. 2.6.Hovmoller diagrams prepared using TAMSAT data that show latitudinal (a) and longitudinal (b) variations of annual rainfall (mm) in the Upper Gelana watershed (1983–2021).

Standardized rainfall anomaly (SRA)

The analysis of seasonal SRA from 1983 to 2021 shows that the LWD agroecology zone experienced moderate and above drought conditions in 17.9% and 20.5% of the *belg* and *kiremt* seasons, respectively. In the UWD agroecology, 15.4% of the *belg* season and 20.5% of the *kiremt* season out of the 39 years were characterized by above-moderate drought conditions. During the study period, the proportion of dry years in the *dega* agroecology zone accounts for 15.4% and 17.9% during the *belg* and *kiremt* seasons, respectively. In all three agroecology zones, the years 1996 and 1999 were the wettest and driest of the *belg* season,

respectively (Fig.2.7a-c). The wettest *kiremt* season in the LWD and UWD occurred in 2010, but in the *dega* agroecology zone, it was in 1998. In all the agroecological zones, the driest *kiremt* season was recorded in the year 1984 (Fig.2.7d-f). According to the annual SRA statistics, both the LWD and *dega* had moderate to extreme dryness in 20.5% of the study years; the UWD agroecology, however, saw slightly more dryness (23.1%). In terms of annual rainfall, 1984 and 2019 were the driest and wettest years common to all three agroecological zones, respectively (Fig.2.7j-l). The standardized rainfall anomaly index results indicate that the study area has high inter-annual variability in seasonal and annual rainfall (Fig.2.7a-l).

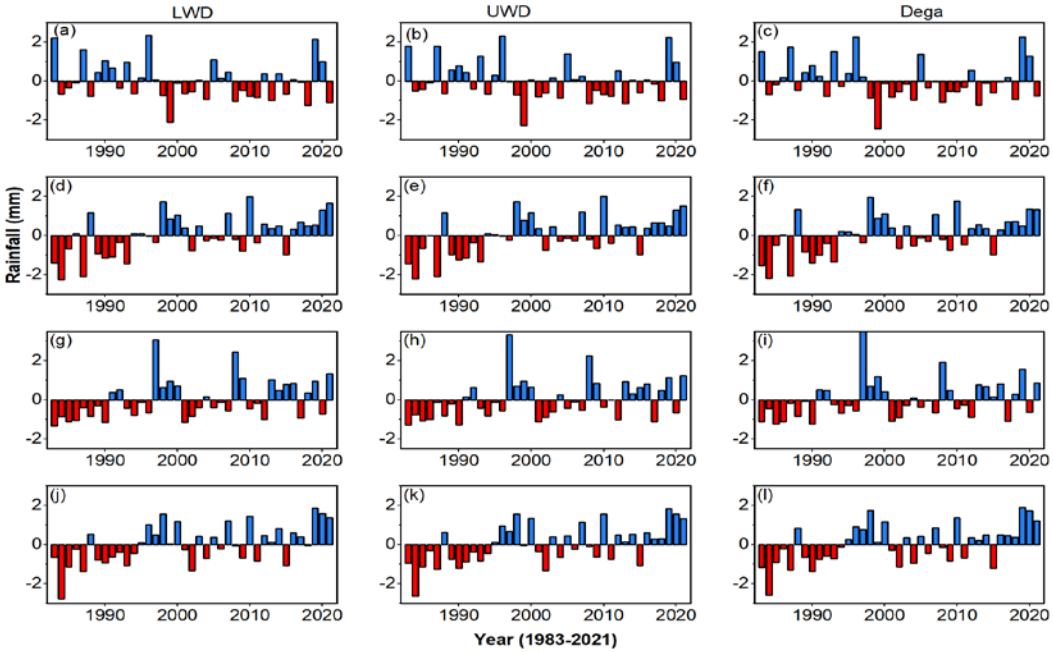

Fig. 2.7.The standardized anomaly index for the *belg* (a-c), *kiremt* (d-f), *bega* (g-i) and annual (j-l) in the LWD (first column), UWD (second column) and *dega* (third column) agroecology zone prepared using TAMSAT precipitation (1983-2021).

2.3.3. Spatiotemporal trends in rainfall

2.3.3.1. Serial-autocorrelation test

In order to get a proper result from the Mann-Kendall trend test, it is essential to assess the presence of serial autocorrelation. Thus, the lag-1 serial correlation was calculated on a pixel-by-pixel basis for monthly, seasonal, and annual rainfall. Significant autocorrelation (P = 0.05) was found in the January (Fig.2.9a) and April (Fig.2.9b) months on a few pixels. So, pre-whitening was applied for those pixels with significant autocorrelation following the variance correction approach to address serial correlation in trend analysis in R (Yue & Wang,

2004). The pixels where the point values for LWD, UWD, and *dega* agroecology zones were extracted are not serially correlated. Fig.2.9 shows the spatial autocorrelation for rainfall in January and April months.

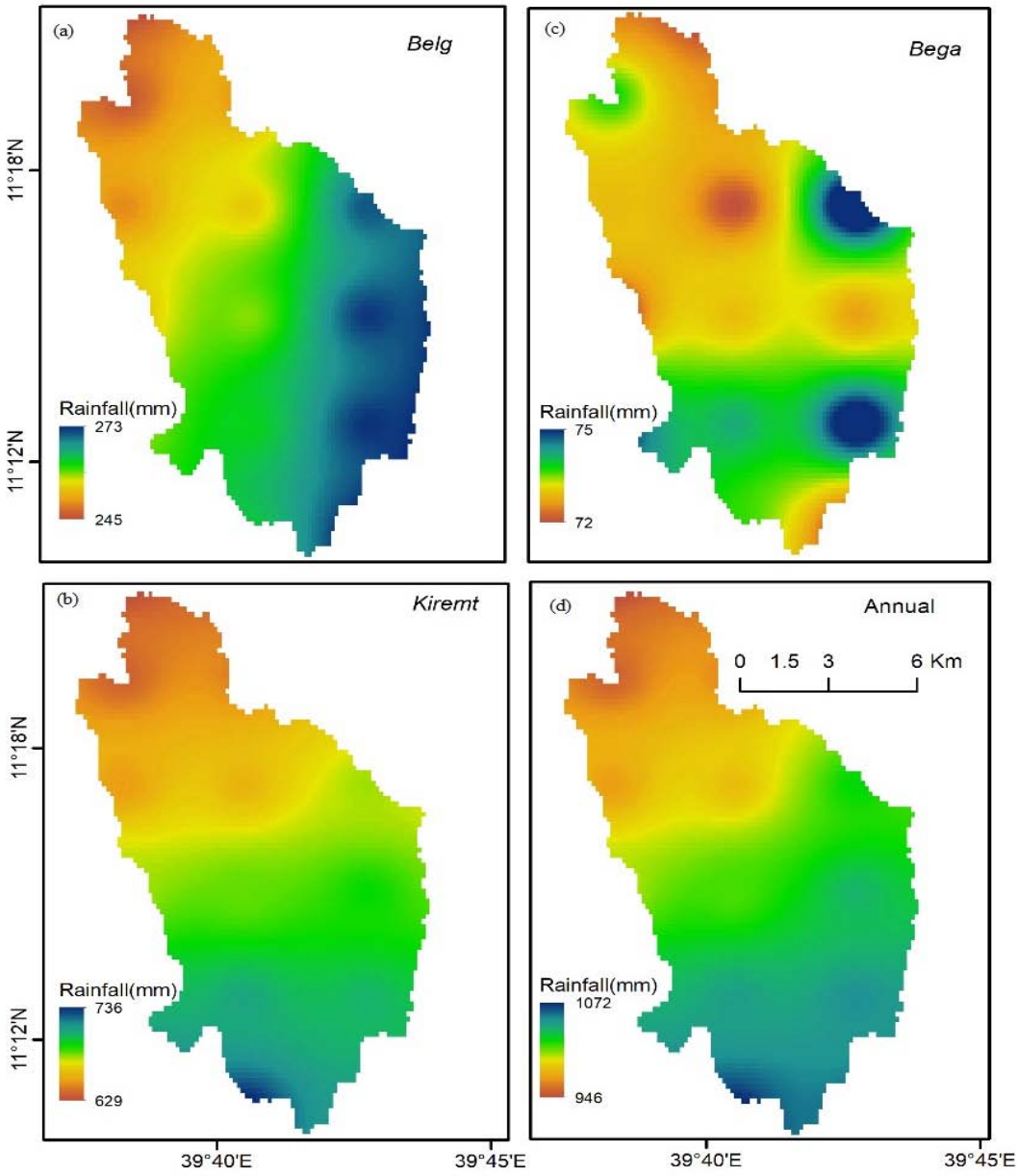

Fig. 2.8.Spatial distribution of average rainfall (1983–2021) in *belg* (a), *kiremt* (b) and *bega* (c) seasons and annual (d) timescales prepared based on TAMSAT data.

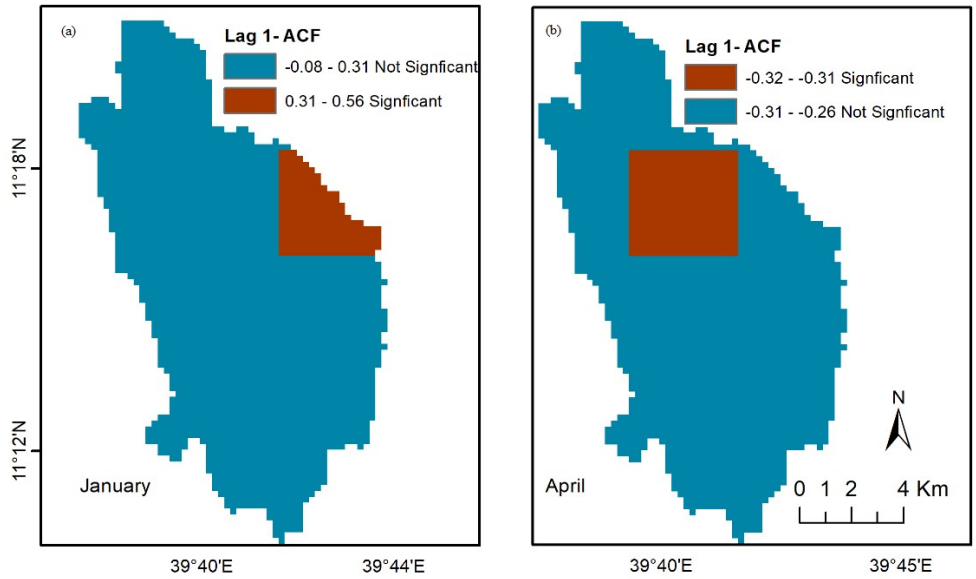

Fig.2.9.Spatial (pixel-by-pixel) lag-1 serial correlation test result for monthly TAMSAT rainfall for January (a) and April (b) in Upper Gelana Watershed (1983-2021).

2.3.3.2. Monthly rainfall Mann-Kendall trend analysis

As shown in Table 2.5, the monthly rainfall in the LWD agroecology showed statistically significant increasing trends in June (P = 0.1) and from July to November (P = 0.05). Similarly, the monthly rainfall in the *UWD* and *dega* agroecology zones shows a significant increasing trend from June to November.

Table 2.5. Mann Kendall and Sen's slope (mm/year) test statistics for monthly rainfall (1983-2021) in the upper Gelana watershed calculated using TAMSAT data.

	LWD			UWD			*Dega*		
Month	Z-Value	Sen's slope	P-value	Z-Value	Sen's slope	P-value	Z-Value	Sen's slope	P-value
Jan	-0.18	0.00	0.856	-0.60	0.00	0.548	-0.57	0.00	0.567
Feb	-1.23	0.00	0.219	-0.82	0.00	0.412	-0.67	0.00	0.504
Mar	-1.43	-1.11	0.153	-1.39	-1.03	0.164	-1.19	-0.86	0.236
Apr	-0.64	-0.50	0.521	-0.48	-0.37	0.628	-0.48	-0.50	0.628
May	0.22	0.08	0.828	0.07	0.05	0.942	0.00	0.00	1.000
Jun	1.78	0.51	0.075*	2.12	0.65	0.034**	1.88	0.67	0.061*
Jul	2.23	3.29	0.026**	2.42	3.71	0.016**	2.18	3.65	0.029**
Aug	2.85	3.79	0.004**	2.82	3.79	0.005**	2.88	3.91	0.004**
Sep	2.17	1.26	0.030**	2.27	1.50	0.023**	1.69	1.39	0.090*
Oct	2.14	0.99	0.033**	1.80	0.77	0.071*	2.45	0.72	0.014**
Nov	2.00	0.01	0.045**	2.13	0.01	0.033**	1.96	0.21	0.050**
Dec	-1.24	0.00	0.213	-1.36	0.00	0.175	-1.51	0.00	0.132

* and ** indicate statistically significant at 0.1 and 0.05 alpha levels respectively

As shown in Table 2.5, Sen's slope test result indicates that the highest magnitude of the trend for all the agroecology zones was in August. In contrast, the MK test indicates statistically non-significant downward trends in the January to April, and December months in all three agroecology zones (Table 2.5). However, Sen's slope values for January, February, and December months were nearly zero, implying that the magnitude of changes in rainfall in these months were insignificant during the study period (1983–2021).

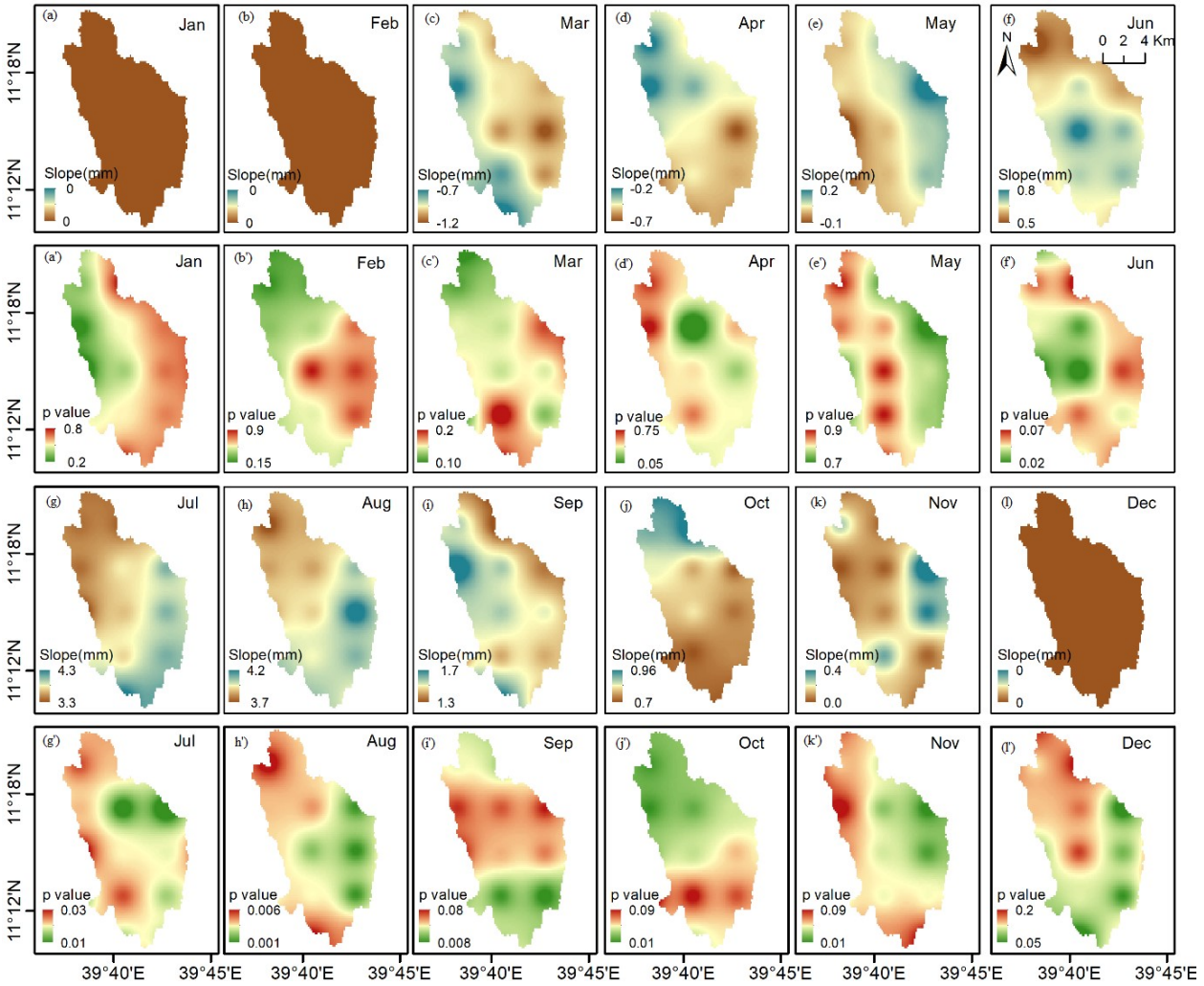

Fig. 2.10. Spatial patterns of Sen's slope expressed in mm/year (a-l) and significance of MK trends (a'-l') of monthly rainfall (1983-2021) in the upper Gelana watershed computed based on TAMSAT data.

Fig. 2.10(a-l) and (a'-l'), respectively, shows the spatial patterns of Mann-Kendall and Sen's slope test statistics of monthly rainfall for the study period (1983–2021). The pixel-wise

analysis showed the spatial variation in the magnitudes and significance levels of trends across the upper Gelana watershed. For the majority of the months, the pixel-by-pixel trend analysis results are closely related to MK and Sen's slope results presented in Table 2.5. The exceptions were the trends in the March and May months. From the spatial analysis, a statistically significant (P = 0.1) decreasing trend was found in March in the north, northwest, and a small area in the southeast part of the watershed (Fig.2.10c'). Contrary to MK and Sen's slope result for the monthly rainfall presented in Table 5, the spatial analysis shows an insignificant positive trend in May in the eastern part and negative trends in the western part (Fig.2.10e').

2.3.3.3. Mann-Kendall trend analysis for seasonal and annual rainfall

Based on the pixel-wise trends shown in Fig. 2.11(d,d',dd), statistically significant increasing trends were found in the annual rainfall for the whole upper Gelana watershed (P = 0.001). This result is in line with the findings of previous studies (Bewket & Conway, 2007; Kifle et al., 2022; Rosell, 2011). An increasing trend in annual rainfall were found for Dessie station in earlier study (Bewket & Conway, 2007). The magnitudes of the trend in annual rainfall vary spatially from 8.98 to 10.22 mm/year. It was lower in the northern part (LWD agroecology) and higher in most parts ofUWD and *dega* agroecology zones of the study area. *Kiremt* season rainfall also shows a statistically significant (P = 0.001) positive trend (Fig.2.11b,b',bb). Similar findings were reported by other researchers (Bewket & Conway, 2007; Kifle et al., 2022; Mohammed et al., 2018; Rosell, 2011; Rosell & Holmer, 2007; Wassie & Pauline, 2018). The annual increment of *kiremt* rainfall varies across the watershed from 9.38 mm (northern) to 11.4 mm (southern). Fig.2.11(a,a',aa) also shows a declining trend in *belg* season rainfall throughout the study area, but it is insignificant. The decline in *belg* season rainfall was relatively high in the southern part (*dega*) of the upper Gelana watershed. Similar findings on the decreasing trend in *belg* season rainfall were identified in previous studies (Kifle et al., 2022; Mohammed et al., 2018; Rosell, 2011; Rosell & Holmer, 2007). In all agroecology zones of upper Gelana watershed, the pattern of *bega* season rainfall shows a slight increment from 1983 to 2021 that is significant at P = 0.05 (Fig.2.11c,c'cc).

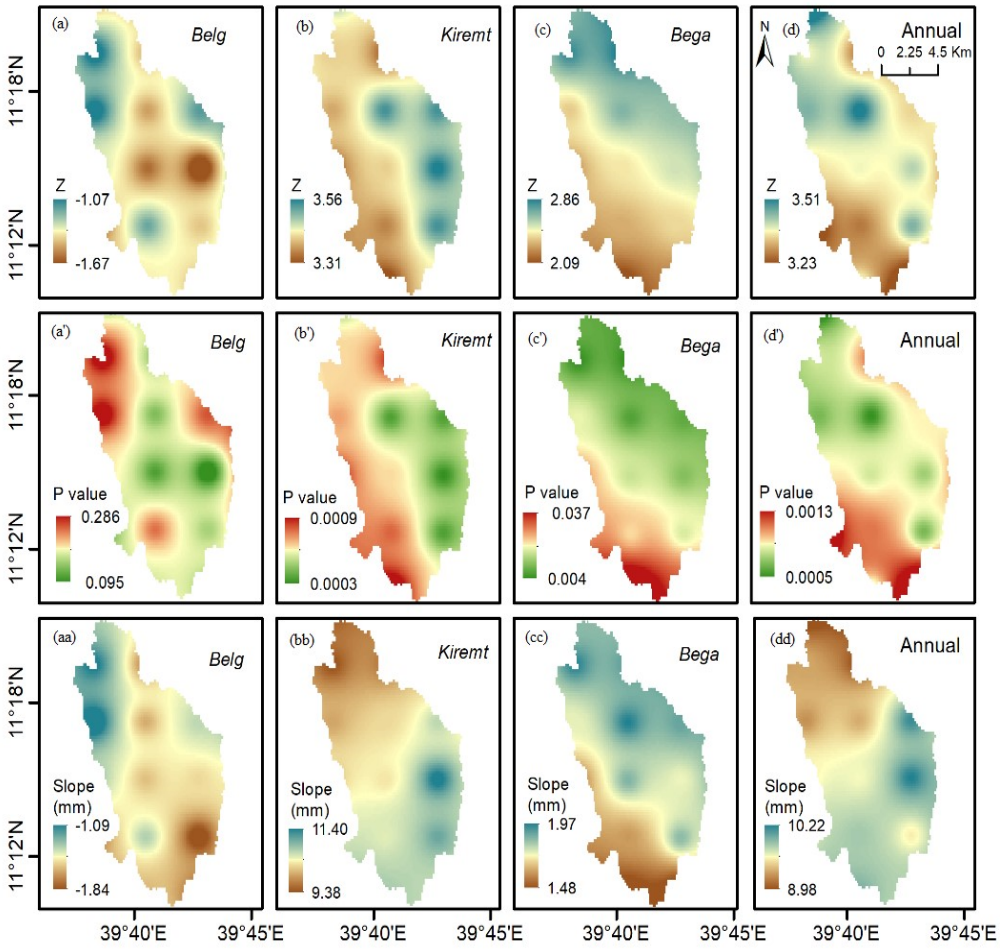

Fig. 2.11. Pixel-wise Mann Kendall trend (Z) (a-d), significance level (a'- d'), and Sen's slope in mm/year (aa-dd) for *belg*, *kiremt*, *bega* and annual rainfall (1983-2021) in the upper Gelana watershed calculated using TAMSAT data.

In all agroecological zones of the study area, the annual, *bega*, and *kiremt* season rainfall showed a significant increasing trend, whereas *belg* season rainfall exhibits a non-significant decreasing trend (Fig.2.12a-l). As determined from the Sen's slope in Fig.2.12(j-l), rate of increment in annual rainfall in the LWD, UWD and *dega* agroecology zones was 91.0, 94.4, and 99.0mm per decade, respectively. Similarly, the decadal rate of increment of rainfall during *kiremt* season was 96.1, 101.6, and 104.8 mm in the LWD, UWD and *dega* agroecological zones the order of sequence computed based on Fig.2.12(d-f). In contrast, the *belg* season rainfall in the LWD, UWD and *dega* agroecology zones decreased by 16.4, 16.2, and 14.0 mm per decade, respectively. The findings imply that the decadal rate of increase in

annual and *kiremt* season rainfall is higher in the *dega* agroecology zone and lower in the LWD.

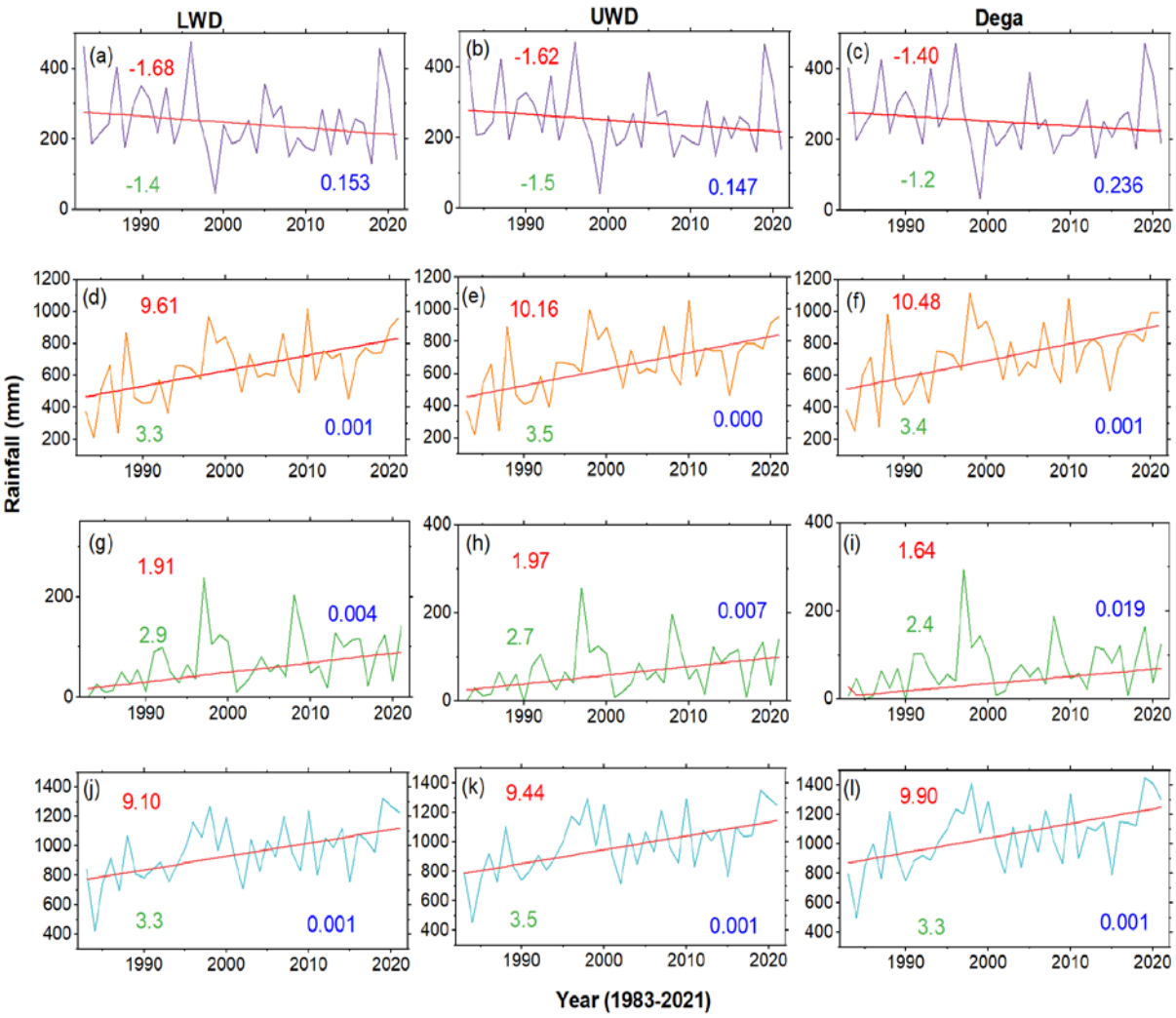

Fig. 2.12.Shows *belg* (a-c), *kiremt* (d-f), *bega* (g-i), and annual (j-l) rainfall trends (1983–2021) in the LWD (left), UWD (middle), and *dega* (right columns) agroecology zones of the upper Gelana watershed computed based on TAMSAT data. The zigzag lines represent rainfall (mm), and the straight line in red represents Sen's estimate of rainfall. In addition, the texts in green, red, and blue are the Z-value, Sen's slope (mm/year), and p-value of the MK test, respectively.

2.3.3.4. Innovative trend analysis (ITA) of seasonal and annual rainfall

The ITA results in Fig.2.13(a-l) were interpreted for the "low," "medium," and "high" clusters, as explained earlier. Accordingly, data points in the *belg* except for *dega* (Fig.2.13a-c) and *bega* season (Fig.2.13g-i) are below 1:1 (45°) line, indicating the decreasing trend of rainfall

in these seasons. In contrast, the data points series of the kiremt season except dega(Fig.2.13d-f) and annual rainfall (Fig.2.13j-l) are above the 1:1 (45°) line, suggesting an overall increasing trend in rainfall.

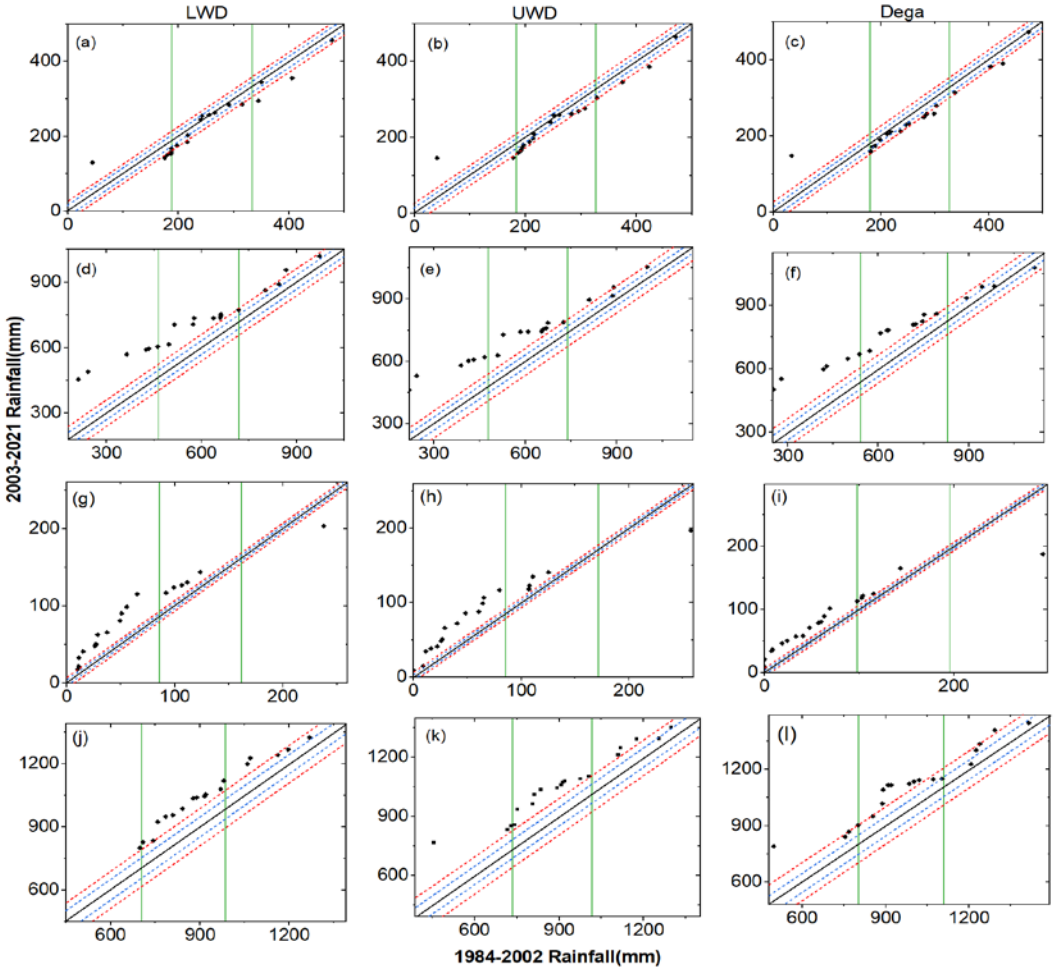

Fig. 2.13. Innovative trend analysis (ITA) results of the *belg* (a-c), *kiremt* (d-f), *bega* (g-i), and annual (j-l) rainfall (1984–2021) in the LWD (left), UWD (middle), and *dega* (right columns) agroecology zones of the upper Gelana watershed based on the TAMSAT data. Points in black color represent data points, the dash lines in red are the ±10% error and dash lines blue are ±5% error line and the line in black in between is the no-trend line. The green lines divide the data points into low, medium and high clusters.

The cluster-based interpretations of the ITA results in Fig.2.13(a-i) revealed that the trends vary in the low, medium and high clusters for seasonal rainfall. In LWD and UWD agroecology zones, a decreasing trend of *belg* season rainfall were identified in all three

clusters of data points. However, the *belg* season in the *dega* agroecology showed an increasing, decreasing and no-trends in the low, medium and high clusters respectively. *Kiremt* season rainfall exhibited an increasing trend in the low, medium, and high data points in all three agroecology zones, with the exception of the decreasing trend in the high data points in *dega* agroecology. In the case of *bega* season, an increasing trend were detected in low and medium clusters, but rainfall showed a decreasing trend in the high cluster in all the agroecology zones of the study area (Table 2.6). As presented in Table 2.6 and Fig.2.13(j–l), the ITA show that the annual rainfall exhibits an increasing trend in low, medium, and high data point clusters in all the study agroecology zones.

Table 2.6. Innovative trend analysis (ITA) statistics and cluster based interpretation of Fig.2.13(a-l) for seasonal and annual rainfall (1984–2021) in the LWD, UWD and *dega* agroecological zones of the upper Gelana watershed using the TAMSAT data.

		Interpretation		
Agroecology	Timescale	Low	Medium	High
LWD	*Belg*	-*	-*	-*
	Kiremt	+*	+*	+*
	Bega	+*	+*	-*
	Annual	+*	+*	+*
UWD	*Belg*	-*	-*	-
	Kiremt	+*	+*	+*
	Bega	+*	+*	-*
	Annual	+*	+*	+*
Dega	*Belg*	+*	-	0
	Kiremt	+*	+*	-*
	Bega	+*	+*	-*
	Annual	+*	+*	+

Note: (-), (+) and (0) signs indicates decreasing, increasing and no trend, respectively and * indicate significant trend (points are outside of the ±5 error line)

2.3.3.5. Comparison of MK and ITA results for seasonal and annual rainfall

We found almost similar findings from MK and ITA methods in the overall trend directions for *belg*, *kiremt* and annual rainfall LWD and UWD agroecological zones of the study area. However, we found a contrasting finding in the *belg* and *kiremt* season rainfall in the *dega* agroecology. In this agroecology zone, the MK test shows insignificant decreasing trend in *belg* rainfall, but the ITA revealed significant increasing trend in the low cluster and no-trend in the high cluster of the *belg* season rainfall. Likewise, we found a significant increasing trend of *kiremt* season rainfall from MK test, while ITA show significant declining trend in the

high data point clusters. Similar contrasting results were obtained for *bega* season rainfall (Fig.2.12 and Table 2.6). Other authors also noted similar discrepancies between the findings of MK and ITA (Caloiero et al., 2018). This might be viewed as an advantage of ITA method in providing detailed results about trends in hydro-climatological timeseries data.

2.3.4. Spatiotemporal variability of temperature

In the upper Gelana watershed, the temperature is spatially variable (Fig.2.14a - c). It is higher in the north (LWD) than the southern (*dega*) part. The lowest mean monthly maximum temperature was 24.1°C, 23.5 °C, and 20.3°C in the LWD, UWD, and *dega* agroecology zones, respectively, recorded in January. Whereas, the highest mean monthly maximum temperature was 30.3°C, 29.6 °C, and 25.9°C in June, in order of sequence, in the LWD, UWD, and *dega* agroecology zones. The lowest mean monthly minimum temperature is 7.3 °C (in LWD), 6.8 °C (in UWD), and 6.1°C (*dega*) - observed in December. In contrast, the mean monthly minimum temperature was high in July in the LWD (14.1 °C), UWD (13.6 °C) and *dega* (11.9°C) agroecological zones. The watershed experienced the highest seasonal average maximum and the lowest seasonal average minimum temperature in the *kiremt* and *bega* seasons, respectively (Table 2.7). The annual average maximum temperatures of the watershed were 26.6°C, 26.0°C, and 22.6°C, in order of sequence, in LWD, UWD, and *dega* agroecology zones, during the study period (1983–2018).

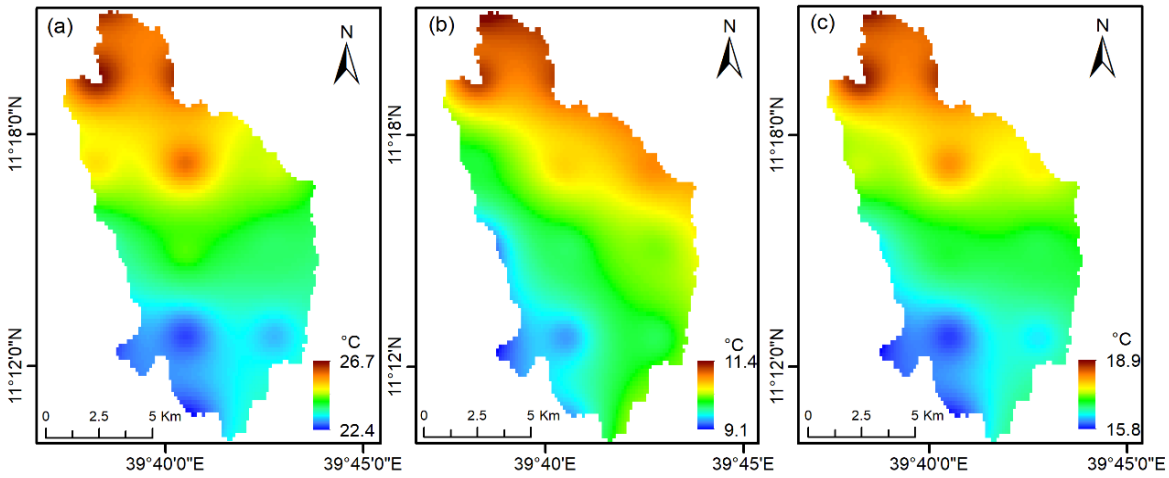

Fig. 2.14. Average maximum (a), minimum (b), and mean temperatures (°C) in the Upper Gelana watershed based on the gridded temperature from EMI (1983-2018).

Table 2.7. Descriptive statistics of seasonal and annual average maximum, minimum and mean temperature (°C) from 1983 to 2018 for the Upper Gelana watershed based on the gridded temperature from EMI.

Time-scale	LWD						UWD						*Dega*					
	Min		Max		Avg		Min		Max		Avg		Min		Max		Avg	
	Mean	SD	Mean	SD	Mean	SD	Mean	SD	Mean	SD	Mean	SD	Mean	SD	Mean	SD	Mean	SD
Belg	11.5	1.1	26.9	1.1	19.2	0.5	10.9	1.1	26.3	1.1	18.6	0.5	9.8	0.9	22.8	0.7	16.3	0.4
Kiremt	13.5	0.6	27.9	0.5	20.7	0.3	12.9	0.6	27.3	0.5	20.1	0.3	11.4	0.5	23.9	0.5	17.6	0.3
Bega	8.1	1.4	24.8	1.2	16.5	0.9	7.6	1.4	24.2	1.2	15.9	0.9	6.8	1.2	20.8	1.0	13.8	0.8
Annual	11.0	0.7	26.6	0.6	18.8	0.4	10.5	0.7	26.0	0.6	18.2	0.4	9.3	0.6	22.6	0.4	15.9	0.3

2.3.5. Spatiotemporal trends of temperature

2.3.5.1. Monthly temperature trend analysis using MK

Before running Mann-Kendall and Sen's slope test, lag-1 serial correlation was computed for the monthly, seasonal, and annual average minimum, maximum, and mean temperature. Then, the pre-whitening procedure was applied for those time scales with a significant lag-1 serial correlation.

The MK test result shows a decreasing trend of monthly minimum temperatures for all months except November in the LWD and UWD agroecology zones (Table 2.8). In *dega* agroecology, a decreasing trend of the minimum temperature was detected in January, February, March, April, August, and December. On the contrary, the monthly maximum temperature shows a significant increasing trend in all months except November in the LWD and UWD agroecology zones. As shown in Table 8, the monthly maximum temperature in *dega* agroecology showed a positive trend from February to May and September months, while the other months exhibit a negative trend. Warming trends in the maximum temperature were reported by other authors (Kifle et al., 2022; Mengistu et al., 2014; Miheretu, 2021). A rising trend was observed in the monthly mean temperature in most of the months, with the exception of February, March and Decemberin LWD and UWD and February, March, August and December in the *dega* agroecology zones. Similar trends in minimum temperature were found in recent studies for different parts of Ethiopia (Abegaz & Abera, 2020; Alemayehu et al., 2020; Mengistu et al., 2014). Abegaz & Abera (2020) noted a declining trend for the monthly minimum temperature for Dessie.

Table 2.8.Summary of Mann-Kendall and Sen's slope test statistics for the maximum, minimum and mean temperature (°C) at monthly time scales for the LWD, UWD and *dega* agroecological zones (1983-2018) based on the gridded temperature from EMI.

	LWD			UWD			Dega		
Month	Min	Max	Mean	Min	Max	Mean	Min	Max	Mean
Jan	-0.031	0.038**	0.006	-0.032	0.038**	0.006	0.003	-0.005	0.002
Feb	-0.092**	0.080***	-0.004	-0.093**	0.083***	-0.004	-0.046	0.025	-0.008
Mar	-0.085**	0.086***	-0.008	-0.084***	0.086***	-0.006	-0.032	0.032	-0.003
Apr	-0.03	0.071***	0.016	-0.029	0.072***	0.016	-0.002	0.031	0.01
May	-0.017	0.044**	0.012	-0.017	0.045**	0.013	0.018	0.005	0.008
Jun	-0.026*	0.030***	0.001	-0.026**	0.033***	0.002	0.018**	-0.0004	0.009**
Jul	-0.024**	0.027*	0.003	-0.024**	0.026*	0.004	0.007	-0.011	0.001
Aug	-0.015*	0.017*	0.001	-0.015*	0.019*	0.003	-0.004	-0.014	-0.006
Sep	-0.025**	0.035***	0.007	-0.024*	0.038***	0.007	0.001	0.01	0.008
Oct	-0.013	0.039***	0.009	-0.015	0.039***	0.01	0.017	-0.006	0.011**
Nov	0.039	0.01	0.025**	0.037	0.012	0.025*	0.047**	-0.024*	0.013
Dec	-0.043	0.022*	-0.007	-0.044	0.022**	-0.008	-0.007	-0.012	-0.009

(-) indicates decreasing trend, *, ** and *** indicate statistically significant at 0.1, 0.05 and 0.01 alpha levels, respectively

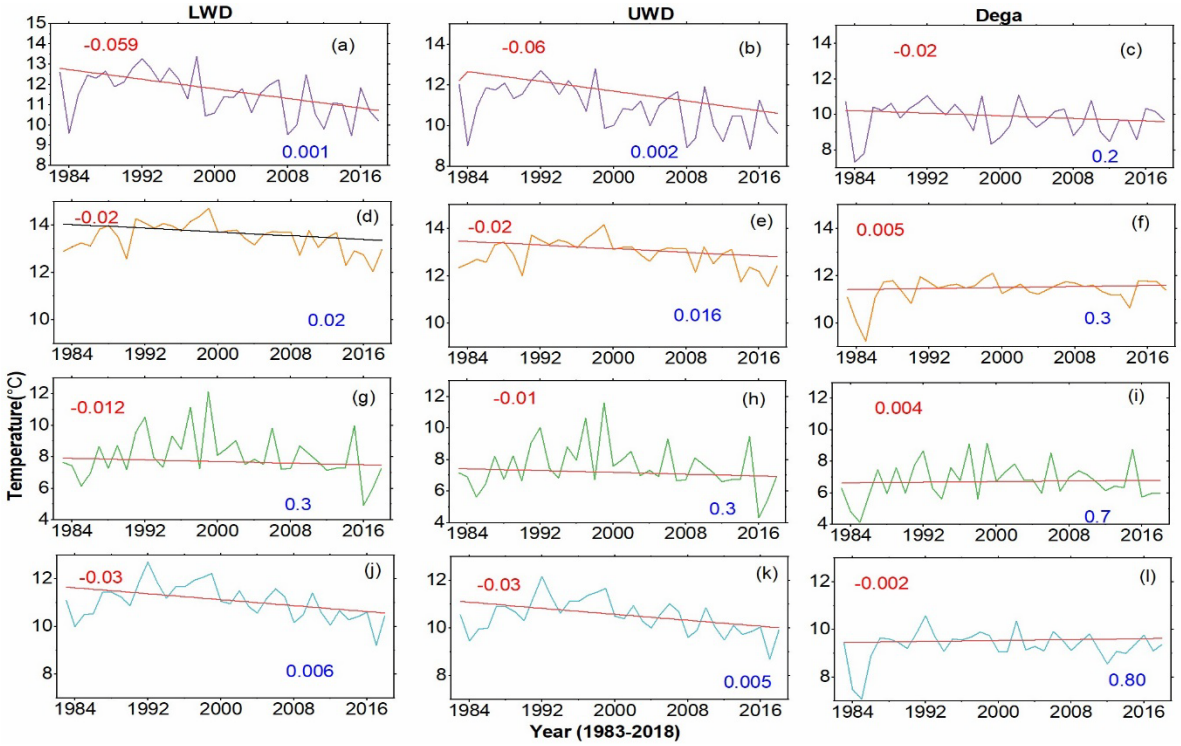

Fig. 2.15. Shows *belg* (a-c), *kiremt* (d-f), *bega* (g-i), and annual (j-l) minimum temperature trends (1983–2018) in the LWD (left), UWD (middle), and *dega* (right columns) agroecology zones of the upper Gelan watershed based on the gridded temperature from EMI. The zigzag lines represent actual temperature, and the straight line in red represents Sen's estimate. In addition, the texts red and blue are the Sen's slope (°C /year) and p-value of the MK test, respectively.

2.3.5.2. Seasonal and annual temperature trends using MK

The seasonal and annual minimum temperature in LWD and UWD agroecology zones showed a statistically significant declining trend except in the *bega* season (Fig.2.15a-l). In *dega* agroecology, declining trends were observed in the *belg* and annual timescales. Based on the Sen Slope statistics presented in Fig.2.15j-k, the annual minimum temperature declines at a rate of approximately 0.3°C per decade in both LWD and UWD agroecological zones. Similarly, declining trends in the seasonal and annual minimum temperatures were reported for the western parts of the upper Blue Nile River basin(Mengistu et al., 2014). As shown in Fig.2.16(a-l), the seasonal and annual trends in maximum temperature varies across the study agroecological zones. In the LWD and UWD agroecological zones, the annual maximum temperature showed a significant rising trend at a decadal rate of 0.4°C (Fig.2.16j-k). The increments in the *belg* and annual maximum temperature in the *dega* agroecology were insignificant. As shown in Fig.2.17(a-l), insignificant positive trends were also observed in the seasonal and annual mean temperature except in the *bega* season in all the agroecology zones.

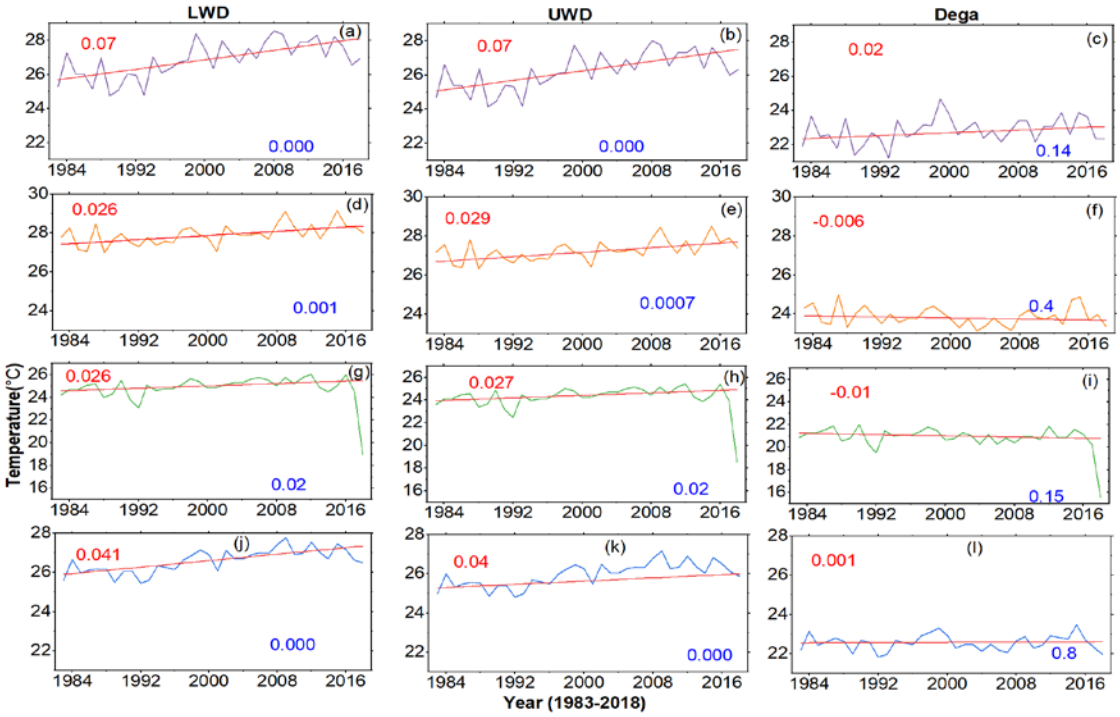

Fig. 2.16. Shows *belg* (a-c), *kiremt* (d-f), *bega* (g-i), and annual (j-l) maximum temperature trends (1983–2018) in the LWD (left), UWD (middle), and *dega* (right columns) agroecology zones of the upper Gelana watershed based on gridded temperature data from EMI. The zigzag lines represent actual temperature, and the straight line in red represents Sen's

estimate. In addition, the texts red and blue are the Sen's slope (°C /year) and p-value of the MK test, respectively.

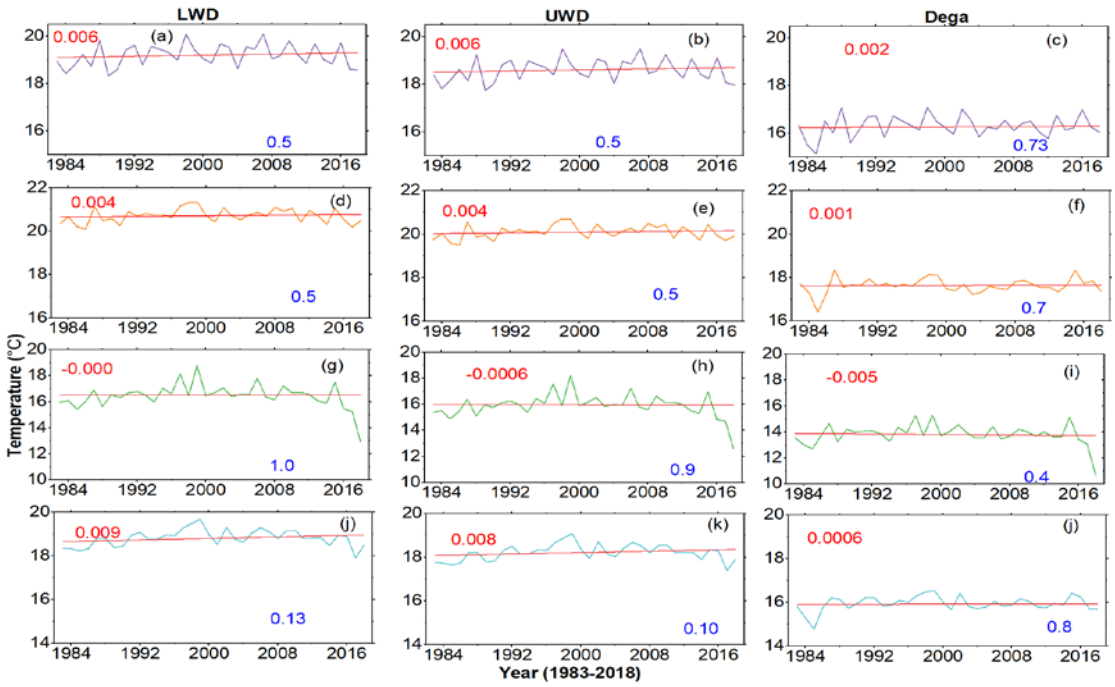

Fig. 2.17. Shows *belg* (a-c), *kiremt* (d-f), *bega* (g-i), and annual (j-l) mean temperature trends (1983–2018) in the LWD (left), UWD (middle), and *dega* (right columns) agroecology zones of the upper Gelana watershed based on the gridded temperature data from EMI. The zigzag lines represent actual temperature, and the straight line in red represents Sen's estimate. In addition, the texts red and blue are the Sen's slope (°C /year) and p-value of the MK test, respectively.

2.3.5.3. ITA for seasonal and annual temperature

As shown in Fig.2.18(a-l) and Table 2.9, the seasonal and annual minimum temperatures are consistently declining across all clusters in the LWD and UWD. The seasonal and annual minimum temperatures in the *dega* agroecology zone exhibit an increasing tendency in the low clusters, but a declining trend were identified in the high clusters except for the *belg* season. The seasonal and annual maximum temperatures in LWD and UWD showed an increasing trend in all the clusters (Fig.2.19(a-l) and Table 2.9). In the *dega* agroecology, *belg* and annual maximum temperatures showed a decreasing and increasing trend, respectively, in the high cluster (Table 2.9). In the low cluster, the annual mean temperature showed an increasing trend in all the agroecology zones (Fig.2.20(a-l) and Table 2.9). Similarly, the *belg* and *kiremt* mean temperature showed an increasing trend in the *dega* agroecology. In the

medium cluster, no trend was identified in the seasonal and annual mean temperature in all three agroecology zones. The seasonal and annual mean temperatures, with the exception of the *belg*, exhibited a declining tendency in the high cluster in the LWD and UWD agroecology zones. Whereas in *dega* agroecology, no trends were detected for seasonal and annual mean temperature in the high cluster data points (Fig.2.20 and Table 2.9).

Table 2.9. Summary interpretation of the innovative trend analysis (ITA) of minimum, maximum and mean temperatures (°C) for the Upper Gelana watershed (Fig.2.18-2.20)

		LWD				UWD				*Dega*			
	Clusters	*Belg*	*Kiremt*	*Bega*	Annual	*Belg*	*Kiremt*	*Bega*	Annual	*Belg*	*Kiremt*	*Bega*	Annual
Minimum	Low	-*	-	-*	-	-*	-	-*	-*	+	+*	+	+*
	Medium	-*	-	-*	-*	-*	-	-*	-*	-	+	0	0
	High	-*	-*	-*	-*	-*	-*	-*	-*	0	-	-*	-
Maximu	Low	+*	+	+	+	+*	+	+	+	+	-	0	0
	Medium	+	+	+	+	+	+	+	+	0	-	-	0
	High	+	+	+	+	+	+	+	+	-	0	0	+
Mean	Low	0	0	0	+	0	0	0	+	+	+	0	+
	Medium	0	0	0	0	0	0	0	0	0	0	0	0
	High	0	-	-*	-	0	-	-*	-	0	0	0	0

(-), (+) and (0) signs indicate decreasing, increasing and no trend, respectively and * indicate significant trends (points are outside of the ±5 error line)

2.3.5.4. Comparison of MK and ITA for Seasonal and annual temperature trends

The MK and ITA results completely match in the direction of trends for seasonal and annual minimum (decreasing) and maximum (increasing) temperatures in LWD and UWD agroecology zones. However, there is no clear match between the findings from the ITA and MK for the seasonal and annual minimum and maximum temperatures in the *dega* agroecology. For the seasonal and annual mean temperature, the MK shows statistically insignificant positive trends in all the agroecology zones, except for the *bega* season. Whereas the ITA results show no trends in mean temperature for the *belg* season in all the agroecology zones, except for the positive trend in the low cluster in the *dega* agroecology. The *kiremt* and annual mean temperatures also show no trend in the medium and high clusters in all agroecology zones, except for the declining trend in the high clusters in the LWD and UWD agroecology zones. Some contradicting findings of MK and ITA methods were also reported

in an earlier study (Caloiero et al., 2018). The comparison of the results shows that most of the insignificant negative and positive trends in the MK trend test tend to be trendless in the ITA method.

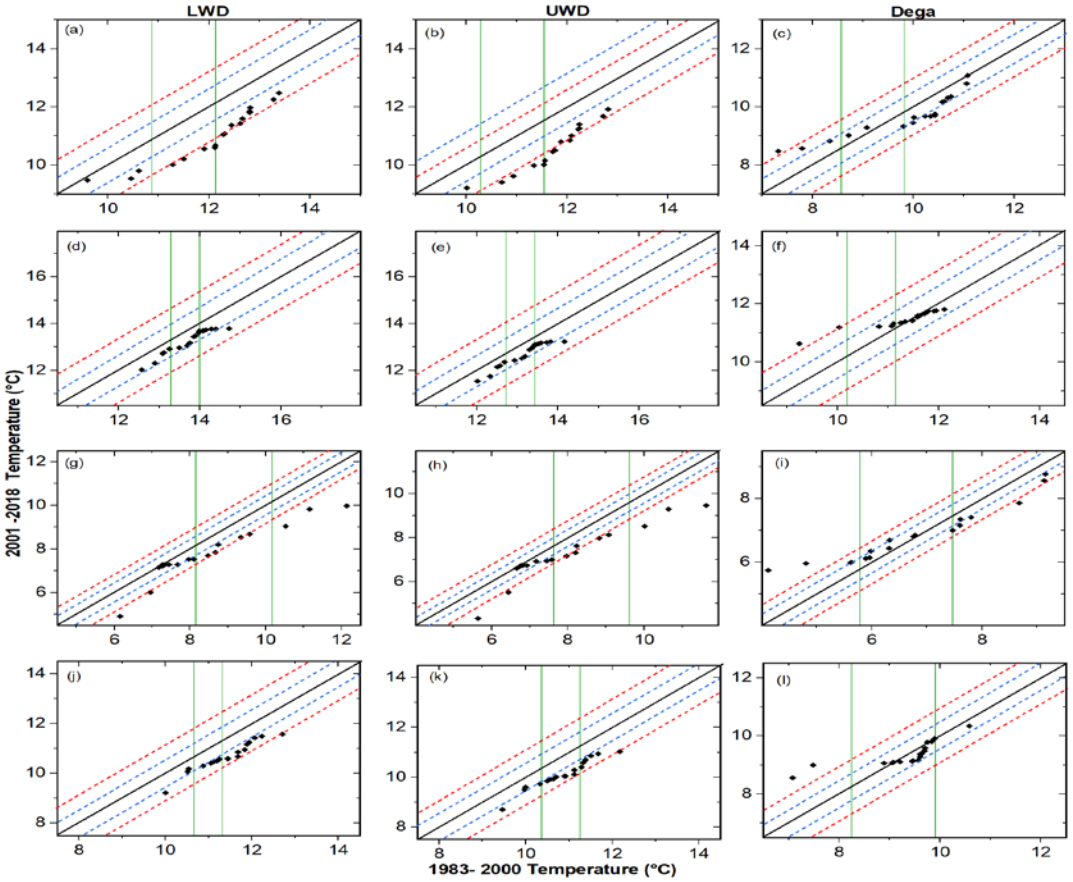

Fig. 2.18. Shows the innovative trend analysis (ITA) of the *belg* (a-c), *kiremt* (d-f), *bega* (g-i), and annual (j-l) minimum temperature (1983–2018) in the LWD (left), UWD (middle), and *dega* (right columns) agroecology zones of the upper Gelana watershed based on the gridded temperature data from EMI.

Points in black color represent data points, the dash lines in red arethe ±10% error and dash lines blue are ±5% error line and the line in black in between is the no-trend line. The green lines divide the data points into low, medium and high clusters.

2.3.6. Farmer's perception on climate variability and trends

The results of the focus group discussion and interview confirmed the decreasing trend in *belg* rainfall. The participants reported that the decreasing (or total absence, as they described) of

rainfall in the *belg* season hampered their efforts to become self-sufficient in food and caused a shortage of fodder for animals. A farmer in Amumo, a village in the upper *weina dega (UWD)* agroecology zone, told us, "In the past year, particularly before 1990, the yield we got from the *belg* season constituted a major part of food grain for household consumption, but nowadays we are not growing crops due to the lack of rainfall". Another informant also strengthens this idea by saying, "In the *belg* season it was possible to grow all the grains such as wheat (*Triticum aestivum*), barley (*Hordeum vulgare L.*), *teff* (*Eragrostis tef*) and others that we produce during the *kiremt* season, and sometimes we even harvest more than the *kiremt* season. However, the *belg* season is becoming completely dry, and we are no longer engaged in crop farming at this time".

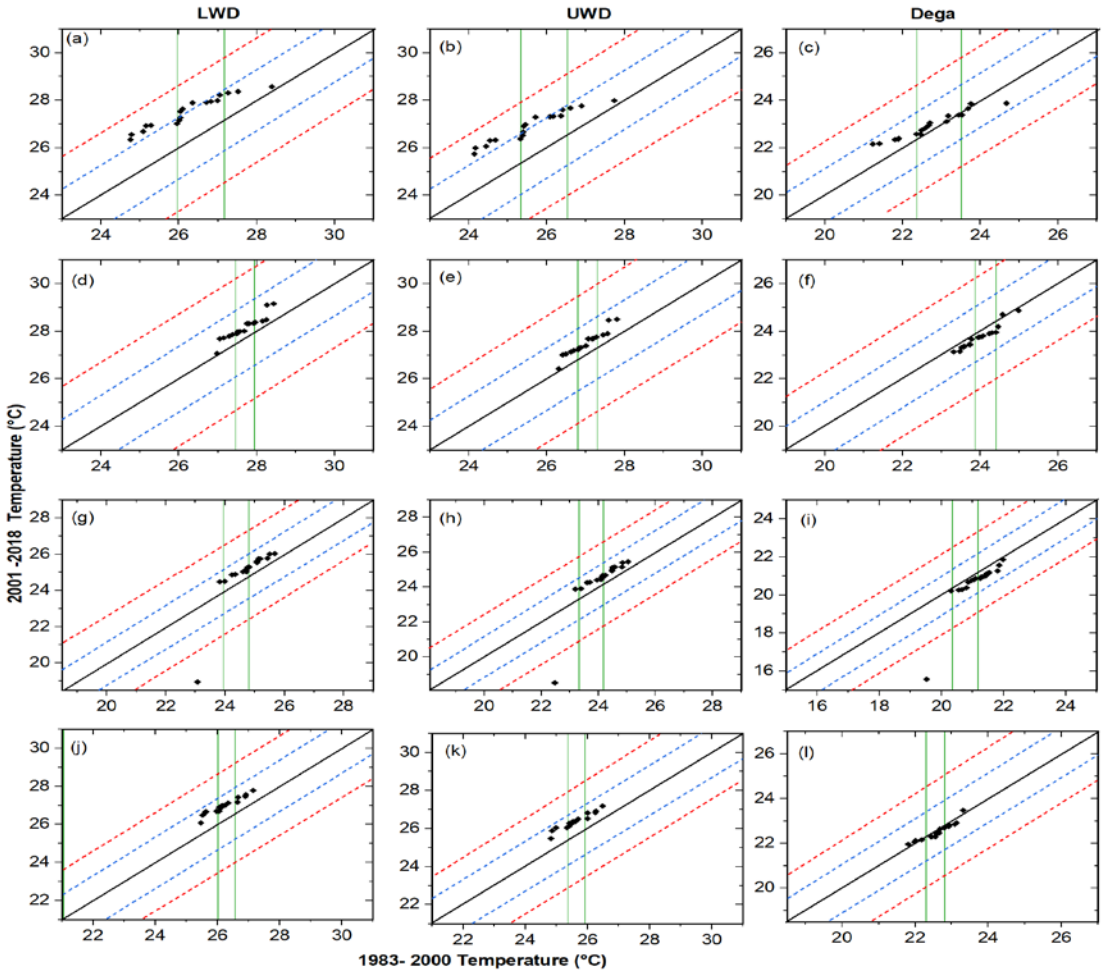

Fig. 2.19. Shows the innovative trend analysis (ITA) of the *belg* (a-c), *kiremt* (d-f), *bega* (g-i), and annual (j-l) maximum temperature (1983–2018) in the LWD (left), UWD (middle), and *dega* (right columns) agroecology zones of the upper Gelana watershed based on the gridded temperature data from EMI. Points in black color represent data points, the dash lines in red arethe ±10% error

and dash lines blue are ±5% error line and the line in black in between is the no-trend line. The green lines divide the data points into low, medium and high clusters.

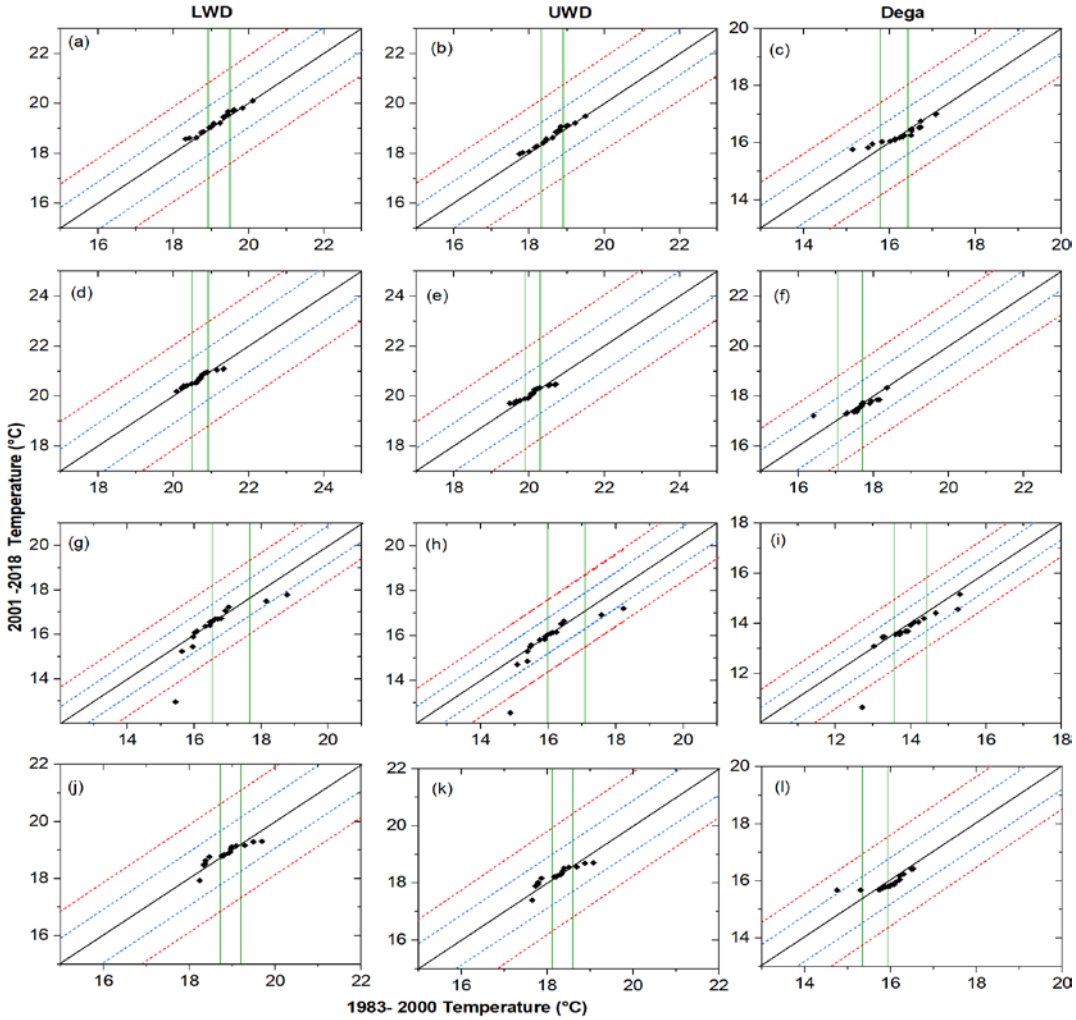

Fig. 2.20. Shows the innovative trend analysis (ITA) of the *belg* (a-c), *kiremt* (d-f), *bega* (g-i), and annual (j-l) mean temperature (1983–2018) in the LWD (left), UWD (middle), and *dega* (right columns) agroecology zones of the upper Gelana Watershed computed using the gridded temperature data from EMI. Points in black color represent data points, the dash lines in red arethe ±10% error and dash lines blue are ±5% error line and the line in black in between is the no-trend line. The green lines divide the data points into low, medium and high clusters.

Concerning the *kiremt* season, the informants' perspectives contradict the results of the statistical analysis of meteorological data. We found inconsistencies among the participants regarding the onset and termination of the *kiremt* season during the focus group discussion.

The majority of them agree on the late start of rainfall, but they have different views on the cessation of *kiremt* rainfall. Some say it ends up early, while others say it terminates late. Nevertheless, both scenarios may have an impact on the farmer's agricultural practices. "In the past year, we sowed wheat starting from the second week of July, but in recent years it has shifted to the last week of July and sometimes the first week of August," an elderly person from Lay-Golbo (*dega* agroecology) village told us. The Mann-Kendall test results, on the other hand, show an increasing trend in rainfall across all four months of the *kiremt* season. But this is apparently related to the ITA findings, which reveal a decreasing trend in *kiremt* season rainfall, especially in the high cluster for the *dega* agroecology zone. Nonetheless, the perception of farmers about climate change is dependent on personal and environmental factors, so discrepancies may occur with findings that are based on meteorological data analysis(Cherinet & Mekonnen, 2019). Most of the time, their opinions are based on the most recent event they recall or that has an impact on their farming activities, rather than the cumulative effect of a long-term event.

The focus group discussants also pointed out that the temperature in their area is becoming hot. The informants also have similar perceptions regarding the increase in temperature. An informant from the Amumo village in the UWD reported that "there is no doubt that the temperature in our area has been increasing and no evidence for this other than looking at our environment. Plants such as kinchib (*Euphorbia tirucalli* L.) and banana were growing in hot temperatures, but nowadays they can grow in our village". During the field visit, we also noticed kinchib trees used as a fence and banana trees in some homesteads.

2.4. Conclusions

In this study, we found that TAMSAT has a relatively low average magnitude of errors compared to CHIRPS, and a better correlation with the daily rainfall from ground-based stations. The POD revealed that TAMSAT has a better ability to detect daily rainfall. The ETS demonstrates that the daily rainfall estimate from TAMSAT has better correspondence with gauged rainfall. In addition, FAR was lower in TAMSAT's daily rainfall, and the frequency of daily rain events in TAMSAT was very close to the frequencies of daily gauged rainfall. Moreover, HSS suggests that TAMSAT has better skill or accuracy than CHIRPS in daily rainfall estimates. Regarding the monthly rainfall, the categorical evaluation statistics

revealed the two products have comparable performances, with CHIRPS slightly performing better than TAMSAT.

The study area is characterized by a strongly irregular distribution of rainfall throughout the study period. Based on TAMSAT rainfall product, we found a significant increasing trend in monthly rainfall from June to November in the LWD, UWD and *dega* agroecology zones using the MK test. However, a slightly different trend was detected in the pixel-wise trend analysis in the March and May months for some parts of the stud area. We found a significant positive trend in the *kiremt* season and annual rainfall that vary across the study area. In contrast, rainfall during the *belg* season shows a statistically insignificant downward trend and high variability. The increment in *kiremt* season and annual rainfall is higher in the *dega* agroecology zone and lower in the LWD. The findings from MK and ITA agree in showing the directions of trends in *belg* and *kiremt* season rainfall in the LWD and UWD and annual trends in all the agroecology zones. A few contrasting findings were found using the ITA method, which can be considered as having the ability to detect trends that are hidden in the MK test.

In all the agroecological zones of the study area, mean monthly temperatures were low in December and high in June during the study period (1983–2018). The seasonal average maximum, minimum, and mean temperatures were high in the *kiremt* season. The MK test shows that the monthly minimum and maximum temperatures, in order of sequence, showed significant declining and warming trends in most months in the LWD and UWD agroecology zones. The majority of months in *dega* agroecology exhibit an insignificant upward trend in both temperatures. With the exception of the *kiremt* and *bega* seasons in *dega* agroecology, the seasonal and annual minimum and maximum temperatures, respectively, showed decreasing and increasing trends in all the agroecology zones. However, these trends are significant only in LWD and UWD agroecology zones. The MK-based trends in seasonal and annual minimum and maximum temperatures are in agreement with the ITA-based trends in the LWD and UWD, but some discrepancies were found in the case of the *dega* agroecology zone. The findings suggest the need to implement adaptation programs to make sure communities are safe from the possible impacts of climate change and variability.

Funding statement

This research was funded by the Office of the Vice President for Research and Technology Transfer (VPRTT), Addis Ababa University, Addis Ababa, Ethiopia.

Data availability statement

The data, excluding the meteorological data from EMI, will be made available by the corresponding author upon request.

CRediT authorship contribution statement

Sileshi Tadesse: Writing – original draft, Writing – review & editing, Visualization, Validation, Software, Resources, Project administration, Methodology, Investigation, Funding acquisition, Formal analysis, Data curation, Conceptualization. Asnake Mekuriaw: Writing – original draft, Writing – review & editing, Validation, Software, Supervision, Resources, Project administration, Methodology, Investigation, Funding acquisition, Formal analysis, Conceptualization. Mohammed Assen: Writing – review & editing, Validation, Software, Resources, Project administration, Methodology, Investigation, Funding acquisition, Conceptualization.

Declaration of competing interest

The authors declare that they have no known competing financial interests or personal relationships that could have appeared to influence the work reported in this paper.

Acknowledgments

The first author expresses gratitude to Addis Ababa University and the Regional Center for Mapping of Resources for Development (RCMRD)/GMES and Africa for their financial support during this study. The authors also extend their thanks to the Tehuledera District Agricultural and Rural Development Office, development agents, and farmers who participated in the interviews and focus group discussions. Special appreciation is also extended to the Ethiopian Meteorological Institute (EMI) for providing precipitation and temperature data. Lastly, we would like to convey our heartfelt appreciation to the editor and reviewers whose contributions significantly enhanced this work.

References

Abegaz, W. B., & Abera, E. A. (2020). Temperature and Rainfall Trends in North Eastern Ethiopia. *International Journal of Environmental Sciences & Natural Resources*, *25*(3), 97–103. https://doi.org/10.19080/IJESNR.2020.25.556163

Agnew, C. T., & Chappell, A. (1999). Drought in the Sahel. *GeoJournal*, *48*(4), 299–311. https://doi.org/10.1023/A:1007059403077

Alemayehu, A., Maru, M., Bewket, W., & Assen, M. (2020). Spatiotemporal variability and trends in rainfall and temperature in Alwero watershed, western Ethiopia. *Environmental Systems Research*, *9*(22), 1–15. https://doi.org/10.1186/s40068-020-00184-3

Alemu, M. M., & Bawoke, G. T. (2020). Analysis of spatial variability and temporal trends of rainfall in Amhara region , Ethiopia Melkamu Meseret Alemu and Getnet Taye Bawoke. *Journal of Water and Climate Change*, *11*(4), 1505–1520. https://doi.org/10.2166/wcc.2019.084

Ali, R., Kuriqi, A., Abubaker, S., & Kisi, O. (2019). Long-Term Trends and Seasonality Detection of the Observed Flow in Yangtze River Using Mann-Kendall and Sen's Innovative Trend Method. *Water*, *11*(1855), 1–17. https://doi.org/doi:10.3390/w11091855

Asfaw, A., Simane, B., Hassen, A., & Bantider, A. (2018). Variability and time series trend analysis of rainfall and temperature in northcentral Ethiopia: A case study in Woleka sub-basin. *Weather and Climate Extremes*, *19*, 29–41. https://doi.org/10.1016/j.wace.2017.12.002

Ayanlade, A., Oluwaranti, A., Ayanlade, O. S., Borderon, M., Sterly, H., Sakdapolrak, P., Jegede, M. O., Weldemariam, L. F., & Ayinde, A. F. O. (2022). Extreme climate events in sub-Saharan Africa: A call for improving agricultural technology transfer to enhance adaptive capacity. *Climate Services*, *27*(100311). https://doi.org/10.1016/j.cliser.2022.100311

Aybar, C. (2021). *rgee: R Bindings for Calling the "Earth Engine" API. R package version 1.1.2*.

Ayehu, G. T., Tadesse, T., Gessesse, B., & Dinku, T. (2018). Validation of new satellite rainfall products over the Upper Blue Nile Basin, Ethiopia. *Atmospheric Measurement Techniques*, *11*(4), 1921–1936. https://doi.org/10.5194/amt-11-1921-2018

Baddeley, A., & Turner, R. (2005). spatstat: An R Package for Analyzing Spatial Point Patterns. *Journal of Statistical Software*, *12*(6), 1–42. https://doi.org/10.18637/jss.v012.i06

Bandh, S., Shafi, S., Peerzada, M., Rehman, T., Bashir, S., Wani, S. A., & Dar, R. (2021). Multidimensional analysis of global climate change: a review. *Environmental Science and Pollution Research*. https://doi.org/10.1007/s11356-021-13139-7

Belay, A., Demissie, T., Recha, J. W., Oludhe, C., Osano, P. M., Olaka, L. A., Solomon, D., & Berhane, Z. (2021). Analysis of climate variability and trends in Southern Ethiopia. *Climate*, *9*(6), 1–17. https://doi.org/10.3390/cli9060096

Bewket, W., & Conway, D. (2007). A note on the temporal and spatial variability of rainfall in the drought-prone Amhara region of Ethiopia. *International Journal of Climatology*, *27*, 1467–1477. https://doi.org/10.1002/joc.1481

Caloiero, T., Coscarelli, R., & Ferrari, E. (2018). Application of the Innovative Trend Analysis Method for the Trend Analysis of Rainfall Anomalies in Southern Italy. *Water Resources Management*, *32*, 4971–4983. https://doi.org/10.1007/s11269-018-2117-z

Chapman, S., E Birch, C., Pope, E., Sallu, S., Bradshaw, C., Davie, J., & H Marsham, J. (2020). Impact of climate change on crop suitability in sub-Saharan Africa in parameterized and convection-permitting regional climate models. *Environmental Research Letters*, *15*(094086). https://doi.org/10.1088/1748-9326/ab9daf

Cherinet, A., & Mekonnen, Z. (2019). Comparing Farmers ' Perception of Climate Change and Variability with Historical Climate Data : The Case of Ensaro District , Ethiopia. *Int J Environ Sci Nat Res*, *17*(4), 00114–00120. https://doi.org/10.19080/IJESNR.2019.17.555966

Conway, D., & Schipper, E. L. F. (2011). Adaptation to climate change in Africa: Challenges and opportunities identified from Ethiopia. *Global Environmental Change*, *21*, 227–237. https://doi.org/10.1016/j.gloenvcha.2010.07.013

Costello, A., Abbas, M., Allen, A., Ball, S., Bell, S., Bellamy, R., Friel, S., Groce, N., Johnson, A., Kett, M., Lee, M., Levy, C., Maslin, M., McCoy, D., McGuire, B., Montgomery, H., Napier, D., Pagel, C., Patel, J., … Patterson, C. (2009). Managing the health effects of climate change. Lancet and University College London Institute for Global Health Commission. *The Lancet*, *373*(9676), 1693–1733. https://doi.org/10.1016/S0140-6736(09)60935-1

Cui, L., Wang, L., Lai, Z., Tian, Q., Liu, W., & Li, J. (2017). Innovative trend analysis of annual and seasonal air temperature and rainfall in the Yangtze River Basin, China during 1960 –2015. *Journal of Atmospheric and Solar-Terrestrial Physics*, *164*, 48–59. https://doi.org/10.1016/j.jastp.2017.08.001

De Luis, M., González-Hidalgo, J. C., Brunetti, M., & Longares, L. A. (2011). Precipitation concentration changes in Spain 1946-2005. *Natural Hazards and Earth System Science*, *11*(5), 1259–1265. https://doi.org/10.5194/nhess-11-1259-2011

Dinku, T., Ceccato, P., Grover-Kopec, E., Lemma, M., Connor, S. J., & Ropelewski, C. F. (2007). Validation of satellite rainfall products over East Africa's complex topography. *International Journal of Remote Sensing*, *28*(7), 1503–1526. https://doi.org/10.1080/01431160600954688

Dinku, T., Funk, C., Peterson, P., Maidment, R., Tadesse, T., Gadain, H., & Ceccato, P. (2018). Validation of the CHIRPS satellite rainfall estimates over eastern Africa. *Quarterly Journal of the Royal Meteorological Society*, *144*(June 2017), 292–312. https://doi.org/10.1002/qj.3244

Ebert, B. (2009). *Forecast Verification - Issues, Methods and FAQ*. World Weather Research Programme Joint Working Group on Verification. https://www.cawcr.gov.au/projects/verification/verif_web_page.html

Ebert, E. (2007). Methods for Verifying Satellite Precipitation Estimates. In V. Levizzani, P. Bauer, & F.J.Turk (Eds.), *Measuring Precipitation from Space: EURAINSAT and the Future* (Vol. 28, pp. 345–356). Springer, Dordrecht. https://doi.org/10.1007/978-1-4020-5835-6_27

Funk, C., Hoell, A., Nicholson, S., Korecha, D., Galu, G., Artan, G., Teshome, F., Hailermariam, K., Segele, Z., Harrison, L., Tadege, A., Atheru, Z., Pomposi, C., & Pedreros, D. (2018). Examining the potential contributions of extreme "western v" sea surface temperatures to the 2017 March-June east african drought. *Bulletin of the American Meteorological Society*, *100*(1), S55–S60. https://doi.org/10.1175/BAMS-D-18-0108.1

Funk, C., Peterson, P., Landsfeld, M., Pedreros, D., Verdin, J., Shukla, S., Husak, G., Rowland, J., Harrison, L., Hoell, A., & Michaelsen, J. (2015). The climate hazards infrared precipitation with stations — a new environmental record for monitoring extremes. *Sci. Data*, *2*(150066). https://doi.org/10.1038/sdata.2015.66

Gebremichael, A., Quraishi, S., & Mamo, G. (2014). Analysis of Seasonal Rainfall Variability for Agricultural Water Resource Management in Southern Region , Ethiopia. *Journal of Natural Sciences Research*, *4*(11), 56–80.

Gedefaw, M., Yan, D., Hao Wang, T., Qin, I., Girma, A., Abiyu, A., & Batsuren, D. (2018). Innovative Trend Analysis of Annual and Seasonal Rainfall Variability in Amhara Regional. *Atmosphere*, *9*(326), 1–10. https://doi.org/10.3390/atmos9090326

Girma, A., Qin, T., Wang, H., Yan, D., Gedefaw, M., Abiyu, A., & Batsuren, D. (2020). Study on Recent Trends of Climate Variability Using Innovative Trend Analysis : The Case of the upper Huai River Basin. *Pol. J. Environ. Stud*, *29*(3), 2199–2210. https://doi.org/10.15244/pjoes/103448

Gocic, M., & Trajkovic, S. (2013). Analysis of changes in meteorological variables using Mann-Kendall and Sen's slope estimator statistical tests in Serbia. *Global and Planetary Change*, *100*, 172–182. https://doi.org/10.1016/j.gloplacha.2012.10.014

Gummadi, S., Rao, K. P. C., Seid, J., Legesse, G., Kadiyala, M. D. M., & Takele, R. (2017). Spatio-temporal variability and trends of precipitation and extreme rainfall events in Ethiopia in 1980 – 2010. *Theoretical and Applied Climatology*. https://doi.org/10.1007/s00704-017-2340-1

Hamner, B., & Frasco, M. (2018). *Metrics: Evaluation Metrics for Machine Learning. R package version 0.1.4.*

Hamza, I., & Iyela, A. (2012). Land Use Pattern, Climate Change, and Its Implication for Food Security in Ethiopia: A Review. *Ethiopian Journal of Environmental Studies and Management*, *5*(1), 26–31. https://doi.org/10.4314/ejesm.v5i1.4

Hurni, H. (1998). *Agroecological Belts of Ethiopia: Explanatory Notes on Three Maps at Scale of 1:1, 000,000*. Soil Conservation Research Programme and Centre for Development and Environment.

IPCC. (2018). Summary for Policymakers. In P. R. S. Masson-Delmotte, V., P. Zhai, H.-O. Pörtner, D. Roberts, J. Skea, M. I. G. A. Pirani, W. Moufouma-Okia, C. Péan, R. Pidcock, S. Connors, J.B.R. Matthews, Y. Chen, X. Zhou, & and T. W. E. Lonnoy, T. Maycock, M. Tignor (Eds.), *Global Warming of 1.5°C. An IPCC Special Report on the impacts of global warming of 1.5°C above pre-industrial levels and related global greenhouse gas emission pathways, in the context of strengthening the global response to the threat of climate change,* (pp. 3–24). Cambridge University Press, Cambridge, UK. https://doi.org/10.1017/9781009157940.001.

Joosten, K., & Grey, S. (2017). *Integrating climate change adaptation and mitigation into the watershed management approach in Eastern Africa – Discussion paper and good practices. Addis Ababa, FAO*.

Kassaye, A. Y., Shao, G., Wang, X., & Wu, S. (2021). Quantification of drought severity change in Ethiopia during 1952–2017. *Environment, Development and Sustainability*, *23*, 5096–5121. https://doi.org/10.1007/s10668-020-00805-y

Kassie, B. T., Rötter, R. P., Hengsdijk, H., Asseng, S., Ittersum, M. K. Van, Kahiluoto, H., & Keulen, D. H. Van. (2014). Climate variability and change in the Central Rift Valley of Ethiopia : challenges for rainfed crop production. *Journal of Agricultural Science*, *152*(1), 58–74. https://doi.org/10.1017/S0021859612000986

Kendall, M. G. (1948). *Rank Correlation Methods*.

Kew, S. F., Philip, S. Y., Hauser, M., Hobbins, M., Wanders, N., Jan Van Oldenborgh, G., Van Der Wiel, K., Veldkamp, T. I. E., Kimutai, J., Funk, C., & Otto, F. E. L. (2021). Impact of precipitation and increasing temperatures on drought trends in eastern Africa. *Earth System Dynamics*, *12*(1), 17–35. https://doi.org/10.5194/esd-12-17-2021

Kifle, T., Ayal, D. Y., & Mulugeta, M. (2022). Factors influencing farmers adoption of climate smart agriculture to respond climate variability in Siyadebrina Wayu District, Central highland of Ethiopia. *Climate Services*, *26*(100290), 1–10. https://doi.org/10.1016/j.cliser.2022.100290

Li, X., Zhang, Q., & Xu, C. Y. (2014). Assessing the performance of satellite-based precipitation products and its dependence on topography over Poyang Lake basin. *Theoretical and Applied Climatology*, *115*(3–4), 713–729. https://doi.org/10.1007/s00704-013-0917-x

Louis, M. E. S., & Hess, J. J. (2008). Climate Change. Impacts on and Implications for Global Health. *American Journal of Preventive Medicine*, *35*(5), 527–538. https://doi.org/10.1016/j.amepre.2008.08.023

Mahmood, R., Jia, S., & Zhu, W. (2019). Analysis of climate variability , trends , and prediction in the most active parts of the Lake Chad basin , Africa. *Scientific Reports*, *9*(6317). https://doi.org/10.1038/s41598-019-42811-9

Maidment, R. I., Grimes, D., Allan, R. P., Tarnavsky, E., Marcstringer, M., Hewison, T., Roebeling, R., & Black, E. (2014). The 30 year TAMSAT african rainfall climatology and time series (TARCAT) data set. *Journal of Geophysical Research*, *119*(18), 10619–10644. https://doi.org/10.1002/2014JD021927

Maidment, R. I., Grimes, D., Black, E., Tarnavsky, E., Young, M., Greatrex, H., Allan, R. P., Stein, T., Nkonde, E., Senkunda, S., & Alcántara, E. M. U. (2017). A new, long-term daily satellite-based rainfall dataset for operational monitoring in Africa. *Scientific Data*, *4*, 1–17. https://doi.org/10.1038/sdata.2017.63

Majedul Islam, M. M. (2022). Threats to Humanity from Climate Change. In S. A. Bandh (Ed.), *Climate Change* (pp. 21–36). Springer, Cham. https://doi.org/10.1007/978-3-030-86290-9_2

Mann, H. B. (1945). Non-parametric test against trend. *Econometrica*, *13*(3).

Mekonen, A. A., & Berlie, A. B. (2019). Spatiotemporal variability and trends of rainfall and temperature in the Northeastern Highlands of Ethiopia. *Modeling Earth Systems and Environment*. https://doi.org/10.1007/s40808-019-00678-9

Mengistu, D., Bewket, W., & Lal, R. (2014). Recent spatiotemporal temperature and rainfall variability and trends over the Upper Blue Nile River Basin, Ethiopia. *International Journal of Climatology*, *34*(7), 2278–2292. https://doi.org/10.1002/joc.3837

Mera, G. A. (2018). Drought and its impacts in Ethiopia. *Weather and Climate Extremes*, *22*, 24–35. https://doi.org/10.1016/j.wace.2018.10.002

Miheretu, B. A. (2021). Temporal variability and trend analysis of temperature and rainfall in the Northern highlands of Ethiopia. *Physical Geography*, *42*(5), 434–451. https://doi.org/10.1080/02723646.2020.1806674

Mirza, M. M. Q. (2003a). Climate change and extreme weather events: Can developing countries adapt? *Climate Policy*, *3*(3), 233–248. https://doi.org/10.3763/cpol.2003.0330

Mirza, M. M. Q. (2003b). Climate change and extreme weather events: Can developing countries adapt? *Climate Policy*, *3*(3), 233–248. https://doi.org/10.3763/cpol.2003.0330

Mohammed, Y., Yimer, F., Tadesse, M., & Tesfaye, K. (2018). Variability and trends of rainfall extreme events in north east highlands of Ethiopia. *International Journal of Hydrology*, *2*(5), 594–605. https://doi.org/10.15406/ijh.2018.02.00131

Nash, J. E., & Sutcliffe, J. V. (1970). River flow forecasting through conceptual models part I - A discussion of principles. *Journal of Hydrology*, *10*(3), 282–290. https://doi.org/10.1016/0022-1694(70)90255-6

NCAR - Research Applications Laboratory. (2015). *verification: Weather Forecast Verification Utilities. R package version 1.42*.

Negash, M. (1987). The need for meteorological information to plan agroforestry on steep slopes in Ethiopia. In W. E. Reifsnyder & T. O. Darnhofer (Eds.), *Meteorology and Agroforestry: Proceedings of an International Workshop on Application of Meteorology to Agroforestry Systems Planning and Management* (pp. 181–189).

Oliver, J. E. (1980). Monthly Precipitation Distribution: A Comparative Index. *The Professional Geographer*, *32*(3), 300–309. https://doi.org/10.1111/j.0033-0124.1980.00300.x

Oztopal, A., & Sen, Z. (2017). Innovative Trend Methodology Applications to Precipitation Records in Turkey. *Water Resour Manage*, *31*, 27–737. https://doi.org/10.1007/s11269-016-1343-5

Panda, A., & Sahu, N. (2019). Trend analysis of seasonal rainfall and temperature pattern in Kalahandi, Bolangir and Koraput districts of Odisha, India. *Atmospheric Science Letters*, *20*(10), 1–10. https://doi.org/10.1002/asl.932

Patakamuri, S. K., & O'Brien, N. (2021). *modifiedmk: Modified Versions of Mann Kendall and Spearman's Rho Trend Tests. R package version 1.6.*

R CoreTeam. (2021). *R: A language and environment for statistical computing. R Foundation for Statistical Computing, Vienna, Austria*.

Rosell, S. (2011). Regional perspective on rainfall change and variability in the central highlands of Ethiopia, 1978-2007. *Applied Geography*, *31*(1), 329–338. https://doi.org/10.1016/j.apgeog.2010.07.005

Rosell, S., & Holmer, B. (2007). Rainfall change and its implications for Belg harvest in South Wollo, Ethiopia. *Geografiska Annaler, Series A: Physical Geography*, *89*(4), 287–299. https://doi.org/10.1111/j.1468-0459.2007.00327.x

Rosell, S., Olvmo, M., & Holmer, B. (2017). Cultivated land – a scarce commodity in a densely populated rural area in South Wollo, Ethiopia. *Journal of Land Use Science*, *12*(4), 252–270. https://doi.org/10.1080/1747423X.2017.1319978

Saini, A., & Sahu, N. (2021). Decoding trend of Indian summer monsoon rainfall using multimethod approach. *Stochastic Environmental Research and Risk Assessment*. https://doi.org/10.1007/s00477-021-02030-z

Saini, A., Sahu, N., Kumar, P., Nayak, S., & Duan, W. (2020). Advanced Rainfall Trend Analysis of 117 Years over West Coast Plain and Hill Agro-Climatic Region of India. *Atmosphere*, *11*(1225), 1–25. https://doi.org/10.3390/atmos11111225

Sen, P. K. (1968). Estimates of the Regression Coefficient Based on Kendall's Tau. *Journal of the American Statistical Association*, *63*(324), 1379–1389. https://doi.org/10.1080/01621459.1968.10480934

Sen, Z. (2012). Innovative Trend Analysis Methodology. *Journal of Hydrologic Engineering*, *7*(9), 1042–1046. https://doi.org/10.1061/(ASCE)HE.1943-5584.0000556

Suryabhagavan, K. V. (2017). GIS-based climate variability and drought characterization in Ethiopia over three decades. *Weather and Climate Extremes*, *15*, 11–23. https://doi.org/10.1016/j.wace.2016.11.005

Tadese, M., Kumar, L., & Koech, R. (2020). Climate change projections in the Awash River Basin of Ethiopia using Global and Regional Climate Models. *Int J Climatol*, *40*, 3649–3666. https://doi.org/10.1002/joc.6418

Tarnavsky, E., Grimes, D., Maidment, R., Black, E., Allan, R. P., Stringer, M., Chadwick, R., & Kayitakire, F. (2014). Extension of the TAMSAT satellite-based rainfall monitoring over Africa and from 1983 to present. *Journal of Applied Meteorology and Climatology*, *53*(12), 2805–2822. https://doi.org/10.1175/JAMC-D-14-0016.1

Temesgen, D., Yehualashet, H., & Rajan, D. S. (2014). Climate change adaptations of smallholder farmers in South Eastern Ethiopia. *Journal of Agricultural Extension and Rural Development*, *6*(11), 354–366. https://doi.org/10.5897/JAERD14.0577

Upadhyay, R. K. (2020). Markers for Global Climate Change and Its Impact on Social, Biological and Ecological Systems: A Review. *American Journal of Climate Change*, *9*, 159–203. https://doi.org/10.4236/ajcc.2020.93012

von Storch, H., & Navarra, A. (1995). Misuses of statistical analysis in climate research. In H. von Storch & A. Navarra (Eds.), *Analysis of Climate Variability: Applications of Statistical Techniques* (pp. 11-26.). Springer-Verlag, New York.

Wassie, A., & Pauline, N. (2018). Evaluating smallholder farmers ' preferences for climate smart agricultural practices in Tehuledere District , northeastern Ethiopia. *Singapore Journal of Tropical Geography*, *39*(2), 300–316. https://doi.org/10.1111/sjtg.12240

Weber, T., Bowyer, P., Rechid, D., Pfeifer, S., Raffaele, F., Remedio, A. R., Teichmann, C., & Jacob, D. (2020). Analysis of Compound Climate Extremes and Exposed Population in Africa Under Two Different Emission Scenarios. *Earth's Future*, *8*(9), 1–20. https://doi.org/10.1029/2019EF001473

Wilks, D. S. (2011). *Statistical methods in the atmospheric sciences* (3rd ed.). Academic Press,Elsevier.

World Bank. (2007). *Ethiopia: Accelerating Equitable Growth, Country Economic Memorandum. World Bank, Washington, DC.*

Wu, H., & Qian, H. (2017). Innovative trend analysis of annual and seasonal rainfall and extreme values in Shaanxi, China, since the 1950s. *International Journal of Climatology*, *37*(5), 2582–2592. https://doi.org/10.1002/joc.4866

Yang, H., Xiao, H., Guo, C., Sun, Y., & Gao, R. (2020). Innovative trend analysis of annual and seasonal precipitation in Ningxia, China. *Atmospheric and Oceanic Science Letters*, *13*(4), 1–8. https://doi.org/10.1080/16742834.2020.1752616

Yue, S., & Wang, C. Y. (2004). The Mann-Kendall test modified by effective sample size to detect trend in serially correlated hydrological series. *Water Resources Management*, *18*(3), 201–218. https://doi.org/10.1023/B:WARM.0000043140.61082.60

CHAPTER THREE

3.AGROECOLOGY-BASED ANALYSIS OF METEOROLOGICAL AND AGRICULTURAL DROUGHT USING TIME SERIES REMOTE SENSING DATA IN THE UPPER GELANA WATERSHED, ETHIOPIA

Tadesse, S., Mekuriaw, A., 2024. Agroecology-based analysis of meteorological and agricultural drought using time series remote sensing data in the upper Gelana watershed, Ethiopia. Geocarto Int. 39(1), 2417881. https://doi.org/10.1080/ 10106049.2024.2417881.

3.AGROECOLOGY-BASED ANALYSIS OF METEOROLOGICAL AND AGRICULTURAL DROUGHT USING TIME SERIES REMOTE SENSING DATA IN THE UPPER GELANA WATERSHED, ETHIOPIA

Abstract

Drought, a recurring environmental hazard, poses significant challenges to Ethiopia's predominantly rainfed, agriculture-based economy, affecting millions of people. This study investigates the characteristics and interrelationships between meteorological and agricultural droughts across *lower weina dega* (LWD), *upper weina dega* (UWD), and *dega* agroecological zones (AEZs) within the upper Gelana watershed, Ethiopia. We utilized remote sensing datasets to identify drought events using the Standardized Precipitation Index (SPI), Vegetation Health Index (VHI), and Evapotranspiration Deficit Index (ETDI). The characteristics of drought events were further analyzed using run theory. The results reveal distinct seasonality in meteorological droughts, with the *kiremt* season exhibiting higher frequency compared to the *belg* season across all AEZs from 1991 to 2021. Particularly, meteorological droughts occurred during *kiremt* in 1991, 1993, 2002, 2009, and 2015. ETDI and VHI together identified *belg-season* agricultural drought in LWD and UWD during 2002, 2008, 2009, 2011, 2012, 2013, and 2021, while the *dega* zone experienced it in 2008, 2012, 2013, and 2015. The *belg-season* agricultural droughts were more frequent in LWD, followed by UWD. Agricultural droughts were also observed in all AEZs during the *kiremt* seasons in 2002, 2008, and 2009. Pixel-wise correlation analysis revealed a statistically significant positive relationship between meteorological and agricultural drought indices during both *belg* and *kiremt* seasons across large portions of the study area, indicating the potential transmission of meteorological drought into agricultural drought. The findings suggest the need to implement adaptation strategies, including soil and water conservation techniques, drought-resistant crops, and irrigation systems, to mitigate the impact of droughts on the livelihoods of rural households that primarily depend on agriculture. These strategies should be customized to suit the unique conditions of different AEZs.

Keywords: agricultural drought; meteorological drought; remote sensing; SPI; ETDI; VHI

3.1. Introduction

Drought is a recurrent climatic hazard with significant implications for both human and natural ecosystems on a global scale (Arekhi et al., 2020). In Africa, more than 250 million people live in areas susceptible to drought (Hoffman & Vogel, 2008). Specifically, in East Africa, drought is a principal driver of hunger, famine, and malnutrition(Cooper et al., 2019), as well as health crises(Bellizzi et al., 2020; Brown et al., 2014; Stanke et al., 2013) and mass migration (Lottering et al., 2021; Masih et al., 2014; Shiferaw et al., 2014). Future droughts are predicted to worsen due to natural and human-induced factors (Cook et al., 2015; Ullah et al., 2024; Zhou et al., 2023). According to the IPCC (2018) report, a global warming of 1.5°C is expected to significantly raise the frequency of extreme droughts, especially in arid and semi-arid regions. This is primarily due to the fact that even minor temperature increases lead to higher evaporation rates, intensifying soil moisture deficits (Cook et al., 2014; Trenberth et al., 2014). Additionally, global warming amplifies the El Niño-Southern Oscillation (ENSO), a climate phenomenon marked by warmer sea surface temperatures in the central and eastern Pacific, which disrupts atmospheric circulation (Shefine, 2019; Ullah et al., 2023). Such disruptions are closely associated to below-average rainfall during rainy seasons and have historically led to severe droughts in Ethiopia and the broader East African region (Gobie & Miheretu, 2021; Molla, 2020; Mulualem et al., 2024; Shefine, 2019). The impacts of drought transcend local communities, exerting both direct and indirect effects at the national level (Masih et al., 2014), disproportionately affecting vulnerable populations, such as children, women, and the elderly (Lottering et al., 2021; Shiferaw et al., 2014). The detrimental effects of drought often persist long-term, depleting surface and groundwater resources (Haile et al., 2019; Kalisa et al., 2020; Ngcamu & Chari, 2020), disrupting ecosystems (Gelorini & Verschuren, 2012), and leading to diminished agricultural productivity(Asten et al., 2011; Wang et al., 2019) and water scarcity for household and agricultural consumption. Amidst ongoing climate change, the challenge posed by drought is particularly acute in agriculture-dependent regions, especially within developing nations (Lottering et al., 2021; Shiferaw et al., 2014).

The severity of drought impact varies with the economic characteristics of individual countries (Ngcamu & Chari, 2020). In Ethiopia, where rainfed agriculture constitutes the

primary source of livelihood, drought shocks trigger a cascade of interconnected challenges. Over the past four decades, Ethiopia has experienced multiple drought events, with the 1983-1984 drought being particularly devastatingand leading to the loss of millions of lives (Mera, 2018). In the last two decades alone, the country has endured more than seven major drought episodes, including the 2015 drought, which adversely affected nearly 10 million people (Mera, 2018). Drought in Ethiopia results in a range of direct consequences, including crop failure, reduced agricultural output, water and forage shortages, disease outbreaks, and malnutrition (Dimitrova, 2021).Additionally, it imposes significant indirect costs, such as increased government expenditure to support affected populations and heightened external debt burdens.

The upper Gelana watershed, located in the South Wollo zone, is prone to frequent droughts (Mekonen et al., 2020; Mohammed et al., 2018). The livelihoods of households in this are heavily rely on agricultural production during both the *belg* (minor rainy season) from February to May and the *kiremt* season from June to September, with rainfall playing a crucial role in sustaining agricultural productivity. Drought conditions occurring in either season can have severe consequences for crop yields and food security (Orr et al., 2021). Despite the potential vulnerability, there is a notable gap in studies exploring the spatial and temporal dynamics of drought at the watershed level. Existing research has predominantly focused on zonal or regional scales, using limited meteorological station data (Demisse et al., 2022; Mekonen et al., 2020; Mohammed et al., 2018). In areas such as the upper Gelana watershed, characterized by complex topography and dynamic environmental conditions, relying solely on point-based meteorological data presents significant limitations (Arekhi et al. 2020; Shahzaman, Zhu, Ullah, et al. 2021; Burka et al. 2023). In this regard, grid-based geospatial analyses are essential for capturing the spatiotemporal variability of drought and providing insights at a local scale, thereby enabling informed decision-making to mitigate both environmental and socioeconomic risks (Vicente-serrano et al. 2012).

Moreover, previous studies(Demisse et al., 2022; Mekonen et al., 2020; Mohammed et al., 2018) have predominantly focused on meteorological drought, which is characterized by abnormal dry conditions resulting from prolonged lack of precipitation (Khan et al., 2018; Zhao et al., 2016).These studies have largely overlooked agricultural drought, which has critical implications in hydrological and socioeconomic aspects. Agricultural drought occurs

when sustained meteorological drought depletes soil moisture, adversely affecting plant growth and agricultural productivity. The assessment of agricultural drought typically involves monitoring water stress and chlorophyll content in crops and vegetation. In this regard, satellite-basedproducts such as the Tropical Applications of Meteorology using Satellite and ground-based observations (TAMSAT) and Moderate Resolution Imaging Spectroradiometer (MODIS) plays essential role (Arekhi et al., 2020; Kogan, 1995, 1997, 2002; Sholihah et al., 2016). Several drought indices have been developed to assess meteorological and agricultural drought conditions over time, with comprehensive lists and descriptions available in earlier studies (Zargar et al., 2011). Among these, the Standardized Precipitation Index (SPI), developed by(Mckee et al. 1993), is the most widely used tool for evaluating precipitation deficits over specific periods. The SPI relies solely on precipitation data, making it simple to calculate and highly effective for assessing meteorological drought. It is also recommended by the World Meteorological Organization (WMO)(Hayes et al., 2011). While the SPI is valuable for identifying meteorological droughts, further analysis is necessary to assess its impact on the agricultural sector. To address this, two agricultural drought indices were employed in this study: the Vegetation Health Index (VHI) and the Evapotranspiration Deficit Index (ETDI). The VHI is a crucial tool for evaluating vegetation health by integrating two indices: the Temperature Condition Index (TCI), which captures vegetation response to temperature variations, and the Vegetation Condition Index (VCI), which reflects the effect of soil moisture conditions on vegetation (Kogan, 1995, 2002). Numerous studies have utilized the VHI to analyze agricultural drought using satellite imagery (Ghaleb et al. 2015; Sholihah et al. 2016; Bento et al. 2018; Arekhi et al. 2020; Shahzaman, Zhu, Bilal, et al. 2021). The ETDI, on the other hand, is derived from the ratio of actual evapotranspiration (AET) to potential evapotranspiration (PET) and incorporates the effects of water stress (WS) (Narasimhan & Srinivasan, 2005). This index is instrumental in determining whether water availability for plants or crops is sufficient or deficient.

Furthermore, the study area encompasses *dega* and *weina dega* agroecological zones (AEZs), which are primarily defined by altitude and rainfall patterns. These AEZs exhibit distinct environmental characteristics that significantly influence the occurrence and severity of meteorological and agricultural droughts. The translation of meteorological droughts into agricultural droughts is further shaped by a range of factors, including land use practices,

slope, altitude, climatic conditions, water resources, and other related elements (Liu et al., 2023; Shi et al., 2022; Zhang et al., 2022). This highlights the need to examine the spatial and temporal dynamics and interconnections of droughts within the study area. Despite the significant implications for agricultural productivity and livelihoods, the interrelationships between meteorological and agricultural droughts within the AEZs of the study area remain underexplored. As a result, a comprehensive examination of the geographical variability and correlation between these drought types is essential to facilitate the development of evidence-based adaptation strategies in response to climate change. Therefore, the aim of this study was to investigate the spatial and temporal dynamics of meteorological and agricultural droughts in the Upper Gelana watershed using time series remote sensing data. Additionally, the study explored the interrelationships between agricultural and meteorological droughts in the agroecological zones (AEZs) within the Upper Gelana watershed in the northeastern highlands of Ethiopia.

3.2. Methods and materials

3.2.1. Description of the study area

This study was carried out in the Upper Gelana watershed, located in the Tehuledere district of northeast Ethiopia. Geographically, the watershed extends from 11.15 ° N to 11.35 ° N and 39.62 ° E to 39.73 ° E, encompassing a total land area of 134 km² (Fig.3.1). The study area exhibits a topographically intricate terrain, with elevations ranging from 1701 to 2886 meters (m) above mean sea level. The upper segment of the study area is characterized by prominent mountain features, traversed by a network of smaller streams that contribute to the Gelana River.

Using elevation and rainfall as a key criterion for the classification of AEZ in Ethiopia (Hurni, 1998; Negash, 1987), the study area falls into *dega* (characterized by cool and humid conditions) and *weina dega* (semi-humid) AEZs. However, a noteworthy discrepancy arises, since the district agriculture bureau designates the lower part of the *weina dega* portion of the study area as *kolla* (warm) agroecology. We also noticed during field observations of the local environment, which encompasses plant and crop characteristics that are closer to the *kolla* because the area is a fringe zone. To reconcile this disparity and better encapsulate the distinct climatic conditions prevailing in the *weina dega* AEZ of the study area, we classified it into

the lower *weina dega* (LWD) and upper *weina dega* (UWD)AEZs. This categorization aims to more accurately depict the environmental characteristics and align with our field observations.

Fig. 3.1. Location map of the study area.

The study area has a diverse array of plant species, both planted and naturally occurring. Notable among them are *Eucalyptus*, *Juniperus procera*, *Acacia abyssinica*, and *Euphorbia tirucalli*. The local economy is primarily driven by a mixed traditional subsistence agricultural system. Wheat (*Triticum aestivum*), *teff* (*Eragrostis tef*), and sorghum (*Sorghum bicolor*) stand out as the main crops grown in the *dega* and *weina dega* AEZs. In addition to these staple crops, farmers engage in the cultivation of chat (*Catha edulis*), a significant cash crop, along with various grains. Despite the richness of plant diversity, it's noteworthy that the study area is characterized by limited arable land, contributing to its status as one of the most densely populated areas in the South Wollo zone, Ethiopia (Rosell et al., 2017).

3.2.2. Data sources

In this study, TAMSAT precipitation data (Maidment et al., 2014, 2017; Tarnavsky et al., 2014) were used to compute SPI. The dataset comprises 384 monthly precipitation images covering the period from 1990 to 2021, with a spatial resolution of 0.0375 degrees (approximately 4 km). These images, available in NetCDF format, were downloaded from http://www.tamsat.org.uk/data-subset/index.html. TAMSAT is widely used precipitation data by stakeholders in climate change research. Its extensive temporal coverage and strong performance metrics, which are comparable to or surpass other satellite precipitation methods, make it particularly reliable for our analysis (Maidment et al., 2020). Additionally, a previous study conducted in the Upper Gelana watershed found TAMSAT monthly precipitation data to exhibit high reliability (Tadesse et al., 2024).

To compute agricultural drought indices, we utilized MODIS NDVI, LST, ET and PET datasets. The NDVI is based on bands 1 and 2 of the MODIS Terra/Aqua 8-day surface reflectance data from Collection 6 MOD09Q1 (Vermote, 2015) with a spatial resolution of 250 meters (Vermote et al., 2015). MODIS surface reflectance data, as noted by (Roger et al. 2015), meet stringent quality criteria, including low view angles, minimal cloud cover, and low aerosol levels. We used a total of 966 NDVI layers, along with their associated quality bands covering the period from 2001 to 2021.The MODIStsp Graphical User Interface (GUI)in the R programming language(Busetto & Ranghetti, 2016) served as a robust tool for downloading, preprocessing, and reprojecting various time series MODIS products. The data is available at https://www.earthdata.nasa.gov/. We also used 966 images of the MODIS LST (MOD11A2) with a temporal resolution of 8-days and spatial resolutions of 1 km. The 8-day LST data represent an average of daily cloud-free MOD11A1 LST values obtained from the Terra platform (Wan, 2013; Wan et al., 2015). The ET and PET products from MOD16A2GF come with a spatial resolution of 500 meters. NASA generates these products using the MOD16 algorithm from the Global Modeling and Assimilation Office (GMAO) meteorological data and MODIS satellite images(Mu et al. 2007; Mu et al. 2011), based on the Penman-Monteith equation (Monteith, 1965). This algorithm computes daily ET (sum of daytime and nighttime evaporation) using various inputs such as temperature, incoming solar radiation, specific humidity, albedo, biome type, and leaf area index (Jovanovic et al., 2015; Mu et al., 2011). Then, the 8-day ET/PET represents the sum of the ET/PET values over eight

consecutive days. These ET/PET products (Running et al., 2021)are gap-filled for cloud cover and other contaminants, enhancing their usefulness in climate studies. A summary of the datasets used in this study is presented in Table 3.1

Table 3.1Summary of the datasets used in this study.

Data	Temporal resolution	Spatial resolution	Duration	Application
Precipitation (TAMSAT)	Monthly	4 kilometers	1990-2021	SPI
NDVI (MOD09Q1)	8 day	250 meters	2001-2021	VHI
LST (MOD11A2)	8 day	1 kilometer	2001-2021	VHI
ET/PET (MOD16A2GF)	8 day	500 meters	2001-2021	ETDI

3.2.3. Data analysis

Meteorological drought was detected using the SPI, while the prevalence of agricultural drought was explored by applying the VHI and the ETDI. Recognizing that the occurrence of a meteorological drought alone may not present a significant challenge unless it transitions to other forms of drought. In this regard, understanding the connection between meteorological and agricultural droughts is important. As a result, we used the Pearson's correlation coefficient to assess the relationship between meteorological and agricultural droughts. Detailed descriptions of the procedures used in the computation of these indices are explained in this section.

3.2.3.1. Standardized precipitation index (SPI)

The SPI is determined as the precipitation deviation from the mean for a specific period, divided by the standard deviation. To ensure the reliability of the SPI results, a minimum of 30 years of precipitation data is necessary (Mckee et al., 1993). SPI can be computed on various temporal scales, typically encompassing 1-month, 3-month, 6-month, 12-month, 24-month, and 48-month accumulation periods. In this study, SPI-1, SPI-4, SPI-8 and SPI-12 were used. The SPI-1 was chosen to assess short-term meteorological drought, while the SPI-4 is crucial for understanding drought patterns during Ethiopia's four-month seasons: *belg* (February–May) and *kiremt* (June–September). Additionally, the SPI-8 provides valuable insights into meteorological drought conditions spanning the two consecutive growing periods from February to September (Mekonen et al., 2020). The monthly grid rainfall data from 1990

to 2021 served as the basis for calculating SPI values in the study area. Spatially distributed SPI at the specified time scales was calculated using the Standardized Climate Indices (SCI) package (Gudmundsson & Stagge, 2016), integrated into the SpatIndex package (Baez-Villanueva, 2023). The values corresponding to the locations of the pixels within the *lower weina dega* (LWD), *upper weina dega* (UWD), and *dega* agroecological zones illustrated in Fig.3.1, were extracted to examine how meteorological droughts vary between the agroecological zones in the study area.

3.2.3.2. Evapotranspiration deficit index (ETDI)

The Evapotranspiration Deficit Index (ETDI) is an index derived from the ratio of actual evapotranspiration (AET) to potential evapotranspiration (PET) and accounts for water stress (WS) in plants or crops. In this study, the quality of AET and PET images was meticulously assessed using quality assurance (QA) bands before computation of WS and ETDI. Subsequently, pixels exhibiting poor quality and no-data values were approximated through linear interpolation. Following the quality assessment, the WS for a given month was calculated using the formula proposed by Narasimhan & Srinivasan (2005). This multifaceted approach ensures a comprehensive evaluation of water stress conditions and facilitates the determination of the ETDI, providing valuable information on the adequacy of water resources for plants or crops.

$$\mathrm{WS} = \frac{\mathrm{PET} - \mathrm{AET}}{\mathrm{PET}} \tag{1}$$

The WS values are on a scale from 1 to 0. A WS value of 1 indicates the absence of evapotranspiration, while a value of 0 suggests the presence of evapotranspiration. This scale provides a clear representation of the extent to which evapotranspiration is absent or aligned with the reference crop's water consumption rate. The monthly stress anomaly (WSA) was computed using Equation 2.

$$\mathrm{WSA}_{\mathrm{i,j}} = \begin{cases} \dfrac{\mathrm{MWS}_{\mathrm{i}} - \mathrm{WS}_{\mathrm{i,j}}}{\mathrm{MWS}_{\mathrm{i}} - \mathrm{minWS}_{\mathrm{i}}} \times 100, \text{if } \mathrm{WS}_{\mathrm{i,j}} \leq \mathrm{MWS}_{\mathrm{i}} \\ \dfrac{\mathrm{MWS}_{\mathrm{i}} - \mathrm{WS}_{\mathrm{i,j}}}{\mathrm{maxWS}_{i} - \mathrm{MWS}_{\mathrm{i}}} \times 100, \text{if } \mathrm{WS}_{\mathrm{i,j}} > \mathrm{MWS}_{\mathrm{i}} \end{cases} \tag{2}$$

Where $\mathrm{WSA}_{\mathrm{i,j}}$ is the monthly water stress anomaly, $\mathrm{MWS}_{\mathrm{j}}$ is the long-term median of the water stress of month i, $\mathrm{maxWS}_{\mathrm{i}}$ the long-term maximum water stress of month i, $\mathrm{minWS}_{\mathrm{i}}$ the

long-term minimum water stress of month i, and WS is the monthly water stress ratio from 2001 to 2021. The water stress anomaly ranges from -100 to +100, indicating very dry to very wet conditions, respectively.

$$\mathrm{ETDI_i} = 0.5\mathrm{ETDI_{i-1}} + \frac{\mathrm{WSAi_i}}{100} \quad (3)$$

Where $\mathrm{ETDI_i}$ is evapotranspiration deficit index of month i. To obtain the ETDI values ranging from -2 to +2 to make the comparison with SPI easy, the $\mathrm{WSA_i}$ is divided by 100. An R code was developed to compute WS, WSA, and ETDI, which will be made available upon request.

3.2.3.3. Vegetation iealth Index (VHI)

Assessing drought solely using meteorological datasets may be insufficient to fully grasp the impacts of drought events (Sur & Lunagaria, 2020). As mentioned earlier, we utilized MODIS remote sensing data to explore agricultural droughts using the VHI, which is derived from the temperature condition index (TCI) and the vegetation condition index (VCI). We prefer to use MODIS datasets for the VHI calculation due to their temporal consistency with considerable resolution.

The temperature condition index (TCI) was developed to assess vegetation conditions considering the contribution of the thermal band. It is essential to understand how vegetation responds to temperature variations. For example, elevated temperatures during the mid-growing season can indicate unfavorable conditions or the onset of drought, while lower temperatures can suggest favorable circumstances (Seiler et al., 1998). The creation of TCI involved several steps. Initially, daytime and nighttime LST data, consisting of 966 images each, were downloaded along with the corresponding quality indicators. These images were projected onto a common system (WGS 1984 UTM zone 37N) and rescaled to physical values using MODIStsp. Subsequently, the bad or contaminated pixels in each image were identified and masked, designated as NA values, using quality assurance (QA) bands. The NA values were then filled using the linear interpolation method provided by the approxNA function in the raster package within the R program (Hijmans, 2022). Following this, 8-day temporal resolution LST datasets were generated by averaging preprocessed daytime and nighttime 8-day MODIS LST images, spanning from 2001 to 2021. Finally, the TCI values were computed using Equation 4.

$$TCI = 100 \times \frac{(LST_{max} - LST)}{(LST_{max} - LST_{min})} \quad (4)$$

Where LST represent the 8 day interval land surface temperature, and LSTmax and LSTmin are the maximum and minimum values of the time series from 2001 to 2021.

The VCI is important for discerning short-term weather-related NDVI fluctuations from long-term ecosystem alterations (Kogan, 1995). As mentioned previously, the MODIStsp R package facilitated the simultaneous download, calculation of NDVI from the 8-day bands 1 and 2 of MODIS land surface reflectance data, rescaling, and re-projection. Quality flags (QA) corresponding to each timestamp were used to mask pixels that were contaminated with clouds or exhibited poor quality. For pixels with no-data values, a linear interpolation method was employed using R programming (Hijmans, 2022). Subsequently, the VCI was computed in an eight-day interval from 2001 to 2021 using Equation 5 in R.

$$VCI = 100 \times \frac{(NDVI - NDVI_{min})}{(NDVI_{max} - NDVI_{min})} \quad (5)$$

NDVI, $NDVI_{max}$ and $NDVI_{min}$ are the 8-day NDVI, maximum and minimum NDVI values, respectively (Kogan, 1995).

Finally, the VHI calculated following Equation 6 proposed by (Kogan, 1995, 1997), as follows.

$$VHI = a \times VCI + (1 - a) \times TCI \quad (6)$$

Where VHI refers to an 8-day vegetation health index, a is a constant that determines the contribution of TCI most of the time it takes 0.5 and TCI and VCI refer to the 8-day temperature condition index and vegetation condition index, respectively. Table 3.2 presents the classification of the drought indices

Table 3.2Classifications on drought severity based of SPI, ETDI and VHI values.

SPI	ETDI	VHI	Severity
< -2.0	Equals -2.0	<10	Extreme drought
-1.5 to -2.0	-1.5 to -2.0	10-20	Severe drought
-1 to -1.49	-1 to -1.49	20-30	Moderate drought
0 to -0.99	0 to -0.99	30-40	Mild drought
>0	>0	>40	No drought

3.2.3.4. Pearson correlation coefficient

To examine the relationship between meteorological and agricultural droughts, we employ Pearson correlation analysis. The pixel-wise correlation coefficient (r) along with the corresponding significance value (p) for seasonal time series of meteorological and agricultural droughts was calculated using the raster package in R (Hijmans, 2022).

3.2.3.5. Run theory

The theory of run, initially proposed by (Yevjevich, 1967), stands as a fundamental tool to characterize drought and has been widely applied in numerous research papers (Burka et al., 2023; Caloiero et al., 2021; Jamro et al., 2020; Lee et al., 2017; Nam et al., 2015; Ullah et al., 2022; Wang et al., 2020; Wu et al., 2019). In time series drought analysis, a run refers to consecutive intervals during which all values consistently exceed or fall below a specified threshold, designated as positive or negative runs, respectively. Identification of these runs, along with subsequent delineation of drought events, contributes to a comprehensive understanding of various features of drought, including duration, severity, intensity, onset, and termination. The duration of drought (DD) is defined as the temporal span, measured in months, during which the drought values persistently remain below a defined threshold (Fig.3.2). The droughts were characterized on a monthly timescale to ease the comparison of VHI and ETDI with SPI. Mild droughts, SPI ranging from 0 to -0.99 exhibits insignificant deviation from normal conditions, and they used -1.0 as a threshold for meteorological drought(Degefu & Bewket, 2015; Mekonen et al., 2020). To ensure consistency, we considered droughts with a moderate and higher severity level, using a threshold value of -1.0 for both SPI and ETDI and a threshold value of 30 for VHI to characterize drought conditions. Once the duration is determined, the onset and endings are identified as the beginning and ending months of the drought event. The severity of drought (DS) involves the summation of the total values of the drought during each distinct episode. The determination of the intensity of the drought (DI) for each episode entails calculating the ratio of DS to DD (Burka et al., 2023; Caloiero et al., 2021; Nam et al., 2015).

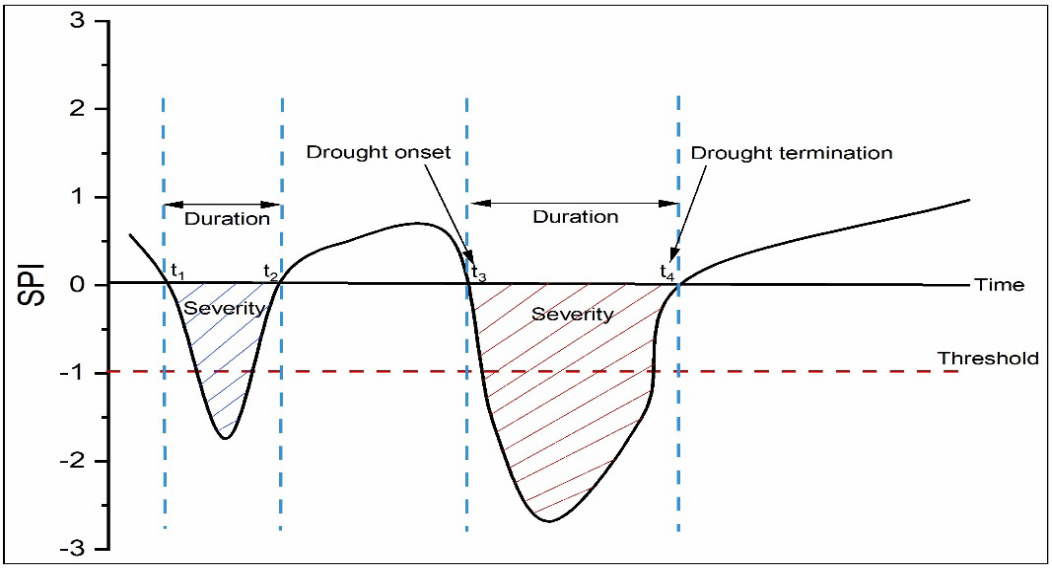

Fig. 3.2.Graphical representation of the run theory used to characterize drought features (eg, SPI), including duration, severity, onset, and termination constructed based on (Ullah et al. 2022).

3.3. Results

3.3.1. Characteristics of meteorological and agricultural drought

As mentioned earlier the duration, severity, intensity, onset and termination of both meteorological and agricultural drought were identified based on run theory and presented in the following sections.

3.3.2. Characteristics of meteorological drought

The time series values of SPI-1, SPI-4, SPI-8, and SPI-12 spanning the years 1991 to 2021 were analyzed at pixel locations corresponding to the LWD, UWD and *dega* AEZs (Fig.3.3). During the study period, some months within all three AEZs exhibited rainfall deficits or drought conditions. These months demonstrated varying degrees of severity, ranging from mild to extremely severe. The characteristics of the droughts were analyzed based on SPI-4 and SPI-8 as presented in Table 3.3.

Table 3.3. Characteristics of meteorological drought (1991-2021) in LWD, UWD and *dega* AEZS of the upper Gelana Watershed based on the standardized precipitation index (SPI-4 and SPI-8) using run theory.

	SPI-4						SPI-8					
AEZ	D	SE	I	C	O	T	D	SE	I	C	O	T
LWD	4	-6.04	-1.51	S	Aug, 1991	Nov, 1991	3	-5.85	-1.95	S	Jan, 1991	Mar, 1991
	4	-8.96	-2.24	E	Aug, 1993	Nov, 1993	7	-9.03	-1.29	M	Sep, 1991	Mar, 1992
	2	-2.69	-1.34	M	Dec, 1994	Jan, 1995	8	-13.56	-1.69	S	Aug, 1993	Mar, 1994
	3	-9.03	-3.01	E	Apr, 1999	Jun, 1999	3	-6.30	-2.10	E	May, 1999	Jul, 1999
	2	-3.29	-1.64	S	Dec, 2001	Jan, 2002	8	-11.07	-1.38	M	Aug, 2002	Mar, 2003
	4	-5.38	-1.34	M	Aug, 2002	Nov, 2002	3	-4.04	-1.35	M	Mar, 2008	May, 2008
	2	-3.27	-1.63	S	Mar, 2008	Apr, 2008	2	-2.36	-1.18	M	Jul, 2008	Aug, 2008
	2	-2.44	-1.22	M	Aug, 2009	Sep, 2009	5	-6.27	-1.25	M	Aug, 2009	Dec, 2009
	3	-4.13	-1.38	M	Nov, 2012	Jan, 2013	4	-6.30	-1.58	S	Mar, 2013	Jun, 2013
	4	-6.97	-1.74	S	Jul, 2015	Oct, 2015	5	-9.61	-1.92	S	Jul, 2015	Nov, 2015
	4	-4.98	-1.25	M	Mar, 2018	Jun, 2018	2	-2.26	-1.13	M	Jan, 2016	Feb, 2016
	2	-2.73	-1.37	M	Mar, 2021	Apr, 2021	2	-3.26	-1.63	S	May, 2018	Jun, 2018
							3	-3.56	-1.19	M	Apr, 2021	Jun, 2021
UWD	4	-5.85	-1.46	M	Aug, 1991	Nov, 1991	3	-6.16	-2.05	E	Jan, 1991	Mar, 1991
	4	-7.72	-1.93	S	Aug, 1993	Nov, 1993	8	-10.55	-1.32	M	Aug, 1991	Mar, 1992
	3	-9.03	-3.01	E	Apr, 1999	Jun, 1999	2	-2.10	-1.05	M	Aug, 1993	Sep, 1993
	2	-2.21	-1.11	M	Feb, 2000	Mar, 2000	4	-8.05	-2.01	E	Dec, 1993	Mar, 1994
	3	-3.60	-1.20	M	Dec, 2001	Feb, 2002	3	-6.23	-2.08	E	May, 1999	Jul, 1999
	4	-5.15	-1.29	M	Aug, 2002	Nov, 2002	9	-13.04	-1.45	M	Jul, 2002	Mar, 2003
	3	-5.15	-1.72	S	Mar, 2008	May, 2008	7	-8.87	-1.27	M	Mar, 2008	Sep, 2008
	4	-5.35	-1.34	M	Nov, 2012	Feb, 2013	2	-2.27	-1.13	M	Sep, 2011	Oct, 2011
	2	-2.25	-1.12	M	May, 2013	Jun, 2013	4	-6.64	-1.66	S	Mar, 2013	Jun, 2013
	4	-6.68	-1.67	S	Jul, 2015	Oct, 2015	5	-9.89	-1.98	S	Jul, 2015	Nov, 2015
	2	-2.63	-1.31	M	Mar, 2021	Apr, 2021	2	-2.56	-1.28	M	Jan, 2016	Feb, 2016
							2	-2.19	-1.10	M	Apr, 2021	May, 2021
Dega	4	-5.48	-1.37	M	Aug, 1991	Nov, 1991	3	-6.63	-2.21	E	Jan, 1991	Mar, 1991
	4	-7.60	-1.90	S	Aug, 1993	Nov, 1993	8	-9.72	-1.21	M	Aug, 1991	Mar, 1992
	3	-9.37	-3.12	E	Apr, 1999	Jun, 1999	3	-4.11	-1.37	M	Jul, 1992	Sep, 1992
	3	-4.26	-1.42	M	Dec, 2001	Feb, 2002	4	-7.09	-1.77	S	Dec, 1993	Mar, 1994
	4	-5.14	-1.28	M	Aug, 2002	Nov, 2002	2	-5.37	-2.69	E	May, 1999	Jun, 1999
	2	-2.33	-1.17	M	Jul, 2004	Aug, 2004	9	-11.99	-1.33	M	Jul, 2002	Mar, 2003
	4	-6.14	-1.54	S	Feb, 2008	May, 2008	6	-7.20	-1.20	M	Jul, 2004	Dec, 2004
	3	-3.43	-1.14	M	Sep, 2009	Nov, 2009	6	-7.97	-1.33	M	Mar, 2008	Aug, 2008
	4	-6.07	-1.52	S	Nov, 2012	Feb, 2013	2	-2.25	-1.12	M	Nov, 2009	Dec, 2009
	2	-2.29	-1.14	M	May, 2013	Jun, 2013	2	-3.00	-1.50	S	Mar, 2010	Apr, 2010
	4	-6.96	-1.74	S	Jul, 2015	Oct, 2015	4	-6.85	-1.71	S	Mar, 2013	Jun, 2013
	2	-2.57	-1.29	M	Mar, 2021	Apr, 2021	5	-9.85	-1.97	S	Jul, 2015	Nov, 2015
							2	-2.79	-1.39	M	Jan, 2016	Feb, 2016
							2	-2.11	-1.06	M	Apr, 2021	May, 2021

Note: D = duration measured in month, S= severity, I = intensity, C= drought category, O = onset and T= termination. The drought category M = moderate, S = severe and E = extremely severe.

The LWD AEZ of the study area experienced moderate to extremely severe drought events, varying in duration and intensity based on the 4-month (SPI-4) and 8-month (SPI-8). The duration of drought in the LWD ranged from two to four months according to SPI-4, while it extended up to eight months according to SPI-8. Specifically, according to SPI-4, LWD experienced two instances of extremely severe droughts during the study period: from August to November 1993 and April to June 1999, with intensity levels of 2.24 and 3.01, respectively. Furthermore, LWD encountered four instances of severe droughts, with intensity levels ranging from -1.51 to -1.74, and six instances of moderate droughts, with intensity levels ranging from -1.22 to -1.38.

In contrast, based on SPI-8 in LWD, there was only one extremely severe drought lasting from May to July 1999, with an intensity level of -2.10. In the same AEZ, there were five severe drought instances, with intensity ranging from -1.58 (March–July 2013) to -1.95 (January–March 1991). Seven instances of moderate meteorological drought also occurred in the LWD. The longest durations of drought identified according to SPI-8 were eight months from August 1993 to March 1994 (severe) and August 2002 to March 2003 (moderate) with respective intensity levels of -1.69 and -1.38 (Table 3.3).

During the study period (1991-2021), the UWD AEZ experienced moderate to extremely severe drought events that lasted 2 to 4 months according to SPI-4 and 2 to 9 months according to SPI-8 (Table 3.3). In particular, this zone faced an extremely severe three-month drought with an intensity of -3.0 from April to June 1999. However, when considering the eight-month SPI, extreme droughts occurred three times during the periods of January to March 1991, December 1993 to March 1994, and May to July 1999, with intensities of -2.05, -2.01, and -2.08, respectively. According to SPI-4, three severe and seven moderate drought events occurred between 1991 and 2021 in the UWD. The longest meteorological drought period recorded in the UWD was nine months, from July 2002 to March 2003, with moderate conditions.

In the case of the *dega* AEZ, the meteorological drought ranged from moderate to extremely severe during the study period (1991-2021). According to SPI-4, an extremely severe drought was observed from April to June 1999. However, SPI-8 detected two separate instances of extremely severe drought that occurred between January and March 1991 and

May and July 1999, with corresponding intensities of -2.21 and -2.69. Additionally, both SPI-4 and SPI-8 identified four episodes of severe drought. The intensity of these severe droughts varied from -1.52 to -1.90 in SPI-4 and from -1.50 to -1.97 in SPI-8. Furthermore, SPI-4 and SPI-8, respectively, detected seven and eight episodes of moderate meteorological drought in the *dega* AEZ.

Fig. 3.3. SPI time series for the AEZs of LWD (a-d), UWD (e-h), and dega (i-l) of the study area (1991-2021).

3.3.3. Characteristics of agricultural drought (ETDI)

The ETDI serves as a critical agricultural drought indicator, evaluating water stress based on the relationship between potential and actual evapotranspiration. Fig.3.4 illustrates the monthly time series of the ETDI values for the LWD, UWD and *dega* AEZs within the study area. The red-shaded portions signify the occurrences of mild to severe agricultural droughts spanning one to several months. During the study period, all AEZs experienced moderate and severe agricultural drought episodes at different times.

Fig. 3.4. Monthly values of ETDI for dega (a), UWD (b), and LWD(c) from 2001 to 2021 in the study area.

The characteristics of agricultural droughts were analyzed based on ETDI from 2001 to 2021 (Table 3.4). In the LWD AEZ, moderate and severe droughts that lasted 2 to 9 months were identified. Severe agricultural droughts occurred between December 2007 and August 2008, with an intensity of -1.51. Furthermore, moderate droughts occurred six times, with intensity levels ranging from -1.11 to -1.42. The longest moderate agricultural drought in this AEZ occurred from September 2012 to December 2012, with an intensity of -1.25.

Similarly, in the UWD AEZ, a severe agricultural drought was identified between December 2007 and August 2008, marking the longest drought incident with an intensity of -1.51. There were eight moderate droughts, varying in duration from two to five months, with intensities ranging from -1.12 to -1.42 (Table 3.4). Furthermore, the *dega* AEZ experienced

severe agricultural drought between February 2008 and August 2008, with an intensity of -1.60 (Table 3.4). Additionally, this AEZ encountered moderate agricultural droughts on five occasions between 2001 and 2021. The most prolonged moderate drought occurred from October 2012 to June 2013, with an intensity of -1.25.

Table 3.4. Characteristics of agricultural drought (2001-2021) in LWD, UWD, and *dega* AEZs of the study area based on time series evapotranspiration deficit index (ETDI) using run theory.

AEZ	Duration	Severity	Intensity	Category	Onset	Termination
LWD	3	-4.14	-1.38	Moderate	Jun-2002	Aug-2002
	9	-13.58	-1.51	severe	Dec-2007	Aug-2008
	3	-4.27	-1.42	Moderate	Apr-2009	Jun-2009
	2	-2.60	-1.30	Moderate	Feb-2012	Mar-2012
	4	-5.02	-1.25	Moderate	Sep-2012	Dec-2012
	2	-2.21	-1.11	Moderate	Nov-2015	Dec-2015
	3	-3.83	-1.28	Moderate	Nov-2016	Jan-2017
UWD	2	-2.24	-1.12	Moderate	Nov-2001	Dec-2001
	5	-7.36	-1.47	Moderate	May-2002	Sep-2002
	3	-3.35	-1.12	Moderate	Dec-2005	Feb-2006
	9	-13.59	-1.51	severe	Dec-2007	Aug-2008
	2	-2.27	-1.13	Moderate	Apr-2011	May-2011
	2	-2.59	-1.29	Moderate	Feb-2012	Mar-2012
	2	-2.80	-1.40	Moderate	Nov-2012	Dec-2012
	2	-2.48	-1.24	Moderate	Nov-2015	Dec-2015
	3	-4.25	-1.42	Moderate	Nov-2016	Jan-2017
Dega	2	-2.81	-1.41	Moderate	Jul-2002	Aug-2002
	7	-11.23	-1.60	severe	Feb-2008	Aug-2008
	3	-3.71	-1.24	Moderate	Feb-2012	Apr-2012
	9	-11.21	-1.25	Moderate	Oct-2012	Jun-2013
	2	-2.29	-1.15	Moderate	Nov-2015	Dec-2015
	3	-3.94	-1.31	Moderate	Nov-2016	Jan-2017

3.3.4. Characteristics of agricultural drought (VHI)

The monthly VHI values in the study area span from 2001 to 2021 (Fig.3.5). The figure highlights multiple drought incidents in the LWD, UWD, and *dega* AEZs. In particular, LWD experienced more severe droughts compared to UWD and *dega* AEZ. *Dega* agroecology had fewer drought incidents than LWD and UWD AEZs.

To gain insight into the characteristics of agricultural droughts, the monthly VHI values for LWD, UWD, and *dega* AEZs were analyzed using run theory (Table 3.5). The result shows that moderate to extremely severe agricultural drought events were detected based on the VHI for the LWD AEZ. Extremely severe agricultural droughts occurred in the LWD during May

to June 2002, December 2007 to June 2008, and March to April 2021, with respective intensities of 8.90, 7.31, and 7.43. Furthermore, LWD experienced severe agricultural droughts five times, lasting between two and ten months, with intensities ranging from 11.89 to 17.68.

Table 3.5. Characteristics of agricultural drought (2001-2021) LWD, UWD, and *dega* AEZs of the study area based on time series VHI using run theory.

AEZ	Duration	Intensity	Category	Onset	Termination
LWD	2	8.90	Extreme	May, 2002	Jun, 2002
	2	23.15	Moderate	Jan, 2006	Feb, 2006
	7	7.31	Extreme	Dec, 2007	Jun, 2008
	4	12.84	Severe	Mar, 2009	Jun, 2009
	2	14.95	Severe	Jan, 2012	Feb, 2012
	10	17.68	Severe	Sep, 2012	Jun, 2013
	2	24.64	Moderate	Mar, 2014	Apr, 2014
	3	24.00	Moderate	Feb, 2015	Apr, 2015
	2	11.89	Severe	Oct, 2016	Nov, 2016
	2	16.99	Severe	Dec, 2020	Jan, 2021
	2	7.43	Extreme	Mar, 2021	Apr, 2021
UWD	2	27.68	Moderate	Nov, 2001	Dec, 2001
	4	11.62	Severe	Apr, 2002	Jul, 2002
	2	26.75	Moderate	Dec, 2007	Jan, 2008
	5	5.73	Extreme	Mar, 2008	Jul, 2008
	2	28.61	Moderate	Sep, 2010	Oct, 2010
	3	24.54	Moderate	Feb, 2011	Apr, 2011
	2	24.28	Moderate	Oct, 2011	Nov, 2011
	2	26.13	Moderate	Jan, 2012	Feb, 2012
	2	15.53	Severe	Nov, 2012	Dec, 2012
	2	25.75	Moderate	Apr, 2013	May, 2013
	3	16.53	Severe	Oct, 2016	Dec, 2016
	2	18.33	Severe	Mar, 2021	Apr, 2021
Dega	3	28.08	Moderate	May, 2002	Jul, 2002
	7	12.37	Severe	Dec, 2007	Jun, 2008
	2	22.22	Moderate	May, 2009	Jun, 2009
	2	20.79	Moderate	Jan, 2012	Feb, 2012
	4	15.80	Severe	Nov, 2012	Feb, 2013
	2	19.00	Severe	Mar, 2021	Apr, 2021

In the UWD AEZ, an extremely severe drought and four severe droughts occurred during the study period (2001-2021). The extreme agricultural drought, with an intensity of 5.73, extended from March 2008 to July 2008. Severe agricultural droughts in the UWD ranged in intensity from 11.62 to 18.33 and lasted between two and four months. In addition, seven

moderate agricultural drought incidents that lasted two to five months were observed in the UWD.

In the *dega* AEZ, six agricultural drought incidents were identified, of which three were severe agricultural droughts and three moderate. The longest severe agricultural drought occurred from December 2007 to June 2008, with an intensity of 12.37. In contrast, the longest period of moderate drought (intensity: 28.08) occurred from May to July 2002. According to the VHI, there were fewer drought incidents in the *dega* compared to the LWD and UWD AEZs (Table 3.5).

Fig. 3.5. Monthly VHI values for dega (a), UWD (b) and LWD(c) from 2001 to 2021 in the study area.

3.3.5. Spatiotemporal seasonal metrological drought

The result shows that the *belg* and *kiremt* season SPI-4 for LWD, UWD, and *dega* AEZ covered the period 1991 to 2021(Fig. 3.6). Multiple occurrences of mild to extremely severe meteorological

Fig. 3.6. The seasonal mean values of SPI-4 from 1991 to 2021 for the belg (a) and kiremt (b) seasons in the LWD, UWD, and dega AEZs of the study area.

Fig. 3.7. Time series SPI-4 of the belg season (February to May) from 1991 to 2021 in the study area.

droughts were observed in the LWD, UWD, and *dega* AEZ throughout the study period (1991-2021). Specifically, during the *belg* season, an extremely severe drought occurred in 1999 in all AEZs. Furthermore, moderate meteorological droughts were observed in 2018 in the LWD and in 2008 and 2013 in both the UWD and the *dega* AEZ (Fig.3.6a).

In the *kiremt* season, the three AEZs experienced five droughts in 1991, 1993, 2002, 2009, and 2015. In particular, during the 1993 *kiremt* season, all AEZs encountered extremely severe incidents, while the other events were characterized as moderate and severe meteorological droughts (Fig.3.6b).

Fig. 3.8.Time series SPI-4 of the kiremt season (June to September) from 1991 to 2021 in the study area.

The spatially distributed time series seasonal meteorological drought reveals numerous dry *belg* seasons throughout the study period (1991-2021). The entire upper Gelana watershed

experienced an extremely severe meteorological drought in 1999 (Fig.3.7). The *belg* seasons of 2008 and 2013 were characterized by dry conditions in all three AEZs. However, the southern and southeastern parts of the study area, which includes the lower parts of the UWD and the *dega* AEZs, encountered relatively severe droughts. In contrast, the northern and northwest portions of the study area, including LWD and parts of UWD, were affected by a moderate *belg* season drought event in 2018.

Similar to the *belg* season, drought events during the *kiremt* seasons (1991-2021) exhibit spatial variations. The drought event in the 1993 *kiremt* season was extremely severe in the upper parts of the study area. In most of the incidents identified during the *kiremt* season, the severity of the drought appears to be higher in the northern part (LWD) compared to other parts. Furthermore, there were numerous instances of mild drought events (severity between 0 and -0.99) during the *kiremt* season throughout the study period (Fig.3.8).

3.3.6. Spatiotemporal seasonal agricultural drought

3.3.6.1. Seasonal agricultural drought (ETDI)

To identify seasonal agricultural droughts, the monthly averages of the ETDI values were analyzed (Fig.3.9). This figure provides insight into the spatial distribution of the ETDI values at pixel locations for the LWD, UWD, and *dega* AEZs. As shown in Fig.3.9a, severe agricultural drought incidents occurred in 2008 in all agroecological zones. Additionally, the *dega* AEZ was affected by moderate droughts during the *belg* season in 2012 and 2013 with intensities of -1.02 and -1.12, respectively (Fig.3.9a). The spatially distributed ETDI for the *belg* season shown in Fig.3.10 revealed moderate to extremely severe agricultural drought affected larger portion of the study area. Moderate agricultural droughts were occurred in the LWD and UWD AEZ during 2012 and 2013. However, only a small part of the LWD was affected in both years and the 2012 incident only affected the southern part of the UWD. Numerous mild agricultural drought incidents were identified in all AEZs of the study area during the study period (Fig.3.9a and Fig.3.10).

During the study period (2001-2021), the seasonal ETDI at the pixels' locations of LWD, UWD, and *dega* AEZsshowed the occurrence of drought in the *kiremt* season (Fig.3.9b). In 2008, all AEZs experienced moderate agricultural droughts during the *kiremt* season. Based on seasonal mean ETDI, in the 2002 *kiremt* season, moderate agricultural drought occurred in LWD while severe in UWD AEZ (Fig.3.9b). Because droughts vary within and between the

AEZs of the study area, incidents that are not identified at the location of the pixel in Fig.3.9b were detected from the spatially distributed ETDI of the *kiremt* season (Fig.3.11). Consequently, all AEZs experienced moderate agricultural drought incidents during the *kiremt* seasons in 2002 and 2009. Furthermore, moderate droughts were observed in 2004 in the UWD and in 2013 in the *dega* AEZ. Fig.3.11 also shows severe agricultural drought in the *kiremt* season in some parts of all AEZs in 2008 and 2002 in the LWD and UWD AEZs. Multiple mild agricultural droughts occurred during the *kiremt* season between 2001 and 2021 (Fig.3.9b and Fi.3.11).

Fig. 3.9. Seasonal mean ETDI for the belg (a) and kiremt (b) seasons from 2001 to 2021 in the LWD, UWD, and dega AEZs of the study area.

Fig. 3.10.Time series ETDI of the belg season (February to May) from 2001 to 2021 in the study area.

3.3.6.2. Seasonal agricultural drought (VHI)

To assess agricultural drought in the *belg* and *kiremt* seasons, we averaged monthly VHI values. Fig.3.12a reveals that during the *belg* season, moderate agricultural droughts occurred in the LWD in 2002, 2009, 2013, 2015, and 2021, in the UWD in 2002, 2011, and 2013, and in the *dega* AEZ in 2013. Additionally, an extremely severe agricultural drought affected all three AEZs in 2008. The spatially distributed VHI in Fig.3.13 provides further information, highlighting moderate *belg* season droughts in 2011 in the LWD, 2009 and 2015 in the UWD, and 2015 in the *dega* AEZ. Furthermore, severe agricultural droughts were observed in 2009 in the LWD and in 2013 in both the LWD and UWD AEZs.

On the basis of mean VHI values, agricultural drought events were generally less pronounced during the *kiremt* season compared to the *belg* season from 2001 to 2021 (Fig.3.12a, b). Through point-based analysis, moderately severe agricultural droughts were exclusively observed in the UWD during the 2002 and 2008 *kiremt* seasons. However, the spatially distributed VHI of the *kiremt* season in Fig.3.14 identified moderate droughts of the

*kiremt*season in 2004 and 2009 in specific areas of the LWD, in 2002, 2004, and 2008 in the UWD and in 2008 inthe *dega* AEZ.

Fig. 3.11.Time series ETDI of the kiremt season (June to September) from 2001 to 2021 in the study area.

Fig. 3.12. The seasonal mean VHI for the belg (a) and kiremt (b) seasons from 2001 to 2021 in the LWD, UWD and dega AEZs of the study area.

Fig. 3.13. VHI of the belg season (February to May) from 2001 to 2021 in the study area.

3.3.7. Relationship between meteorological and agricultural drought

Fig.3.15 illustrates the correlations between the meteorological and agricultural drought indices, revealing statistically significant positive relationships with varying strengths. The results indicate the potential influence of meteorological conditions on agricultural drought. In Fig.3.15a, a strong positive association ($r > 0.5$) between SPI and VHI is evident for the *belg* season in a substantial part of the study area. This association is statistically significant ($p < 0.05$), except in a small area (Fig. 3.15b). Similarly, the correlation coefficient for SPI and VHI during the *kiremt* season ranges between 0.3 and 0.5 for most parts of the study area, suggesting a moderate association (Fig.3.15c). The association is statistically significant ($p < 0.05$) in a large part of the study area (Fig.3.15d). This implies that as SPI values decrease in the *belg* season, VHI values also decrease, suggesting the potential translation of meteorological drought into agricultural drought.

Fig. 3.14. VHI of the kiremt season (June to September) from 2001 to 2021 in the study area.

The seasonal SPI exhibits a positive association with seasonal ETDI. SPI and ETDI for the *belg* season demonstrate moderate and strong positive correlations (Fig.3.15e). The relationship between *belg* season SPI and VHI is statistically significant at $P < 0.05$ for a large proportion, in some other areas it is significant at $p < 0.1$. The association between the SPI of the *kiremt* season SPI and ETDI shows a moderate to strong positive relationship in many parts, with a weak association in an insignificant number of pixels (Fig.3.15g). These moderate and strong relationships are statistically significant in some areas at $p < 0.05$ and at $P < 0.1$ in others (Fig.3.15h). Table 3.6 presents the correlation coefficients and corresponding significance values between SPI and VHI/ETDI at the location of the points in the LWD, UWD and *dega* AEZs.

Table 3.6. Correlation coefficients and corresponding p-values between SPI and VHI/ETDI in LWD, UWD and *dega* AEZs.

	SPI-VHI			SPI-ETDI		
Belg season	LWD	UWD	*Dega*	LWD	UWD	*Dega*
Pearson(r)	0.63	0.59	0.61	0.46	0.46	0.45
p-value	0.00	0.01	0.00	0.03	0.04	0.04
kiremt season						
Pearson(r)	0.44	0.47	0.45	0.52	0.46	0.37
p-value	0.05	0.03	0.04	0.02	0.04	0.10

Fig. 3.15. Correlation coefficients (r) between the *belg* season SPI-4 and VHI (a), the *kiremt* season SPI-4 and VHI (c), the *belg* season SPI-4 and ETDI (e), and the *kiremt* season SPI-4 and ETDI(g) with their respective significant level (p value) (b, d, f, and g) from 2001 to 2021.

3.4. Discussion

The results of meteorological drought identification using SPI-4, revealed a nearly identical number of drought incidents in the LWD, UWD, and *dega* AEZ during the period (1991–2021). For example, between 2001 and 2021, there were 8, 7, and 9 meteorological drought incidents in LWD, UWD, and *dega* AEZ, respectively, indicating minimal variation in drought occurrences across these zones.

In contrast, agricultural drought events, detected using ETDI and VHI, exhibited variability in across the AEZs. ETDI identified 7, 9, and 6 incidents in LWD, UWD, and *dega* AEZs, respectively, while VHI detected 12, 11, and 6 agricultural drought events in these zones. This suggest that the *dega* AEZ experienced fewer agricultural drought incidents compared to the LWD and UWD AEZ during the study period (2001–2021). These findings are consistent with the results reported by (Bayable & Gashaw, 2021), which highlighted a lower impact of

agricultural drought in the *dega* AEZ compared to the *weina dega* AEZ. Notably, VHI detected more drought incidents, with varying levels of severity, than ETDI, though both indices closely mirrored documented historical drought events.

Our comprehensive analysis, which included both point-based and spatially distributed methods, identified seasonal patterns of meteorological droughts during the belg and kiremt seasons. We found that meteorological droughts occurred in 1999, 2008, and 2013 during the *belg* season in all AEZs, and in 1991, 1993, 2002, 2009, and 2015 during the *kiremt* season. These results align with documented drought years reported by various authors (Gidey et al., 2018a; Kassaye et al., 2021; Mekonen et al., 2020; Tesfamariam et al., 2019). Moreover, meteorological droughts were more frequent during the kiremt season than the belg season, with spatial variation across the study area.

Additionally, agricultural droughts were identified during both the *belg* and *kiremt* seasons from 2001 to 2021. Combined analysis of ETDI and VHI revealed agricultural droughts occurrences during the *belg* season in LWD and UWD in 2002, 2008, 2009, 2011, 2012, 2013, 2015 (only in LWD) and 2021. The *dega* AEZ experienced agricultural droughts in 2008, 2012, 2013, and 2015 during the *belg* season. These drought years align with *belg*-season agricultural droughts identified by Bayable and Gashaw (2021) in the *weina dega* and *dega* AEZs of the upper Awash basin. Similarly, ETDI and VHI results for the *kiremt* season showed agricultural droughts in 2002, 2008, and 2009 in all AEZ, in 2004 in LWD and UWD, and in 2015 in *dega* AEZ. These findings partly correspond with agricultural drought occurrences in the upper Awash basin, as reported by Bayable and Gashaw (2021). The *belg*-season droughts were more frequent in LWD and less frequent in the *dega* AEZ, with severe agricultural droughts occurring more often in LWD than in the *dega* AEZ. The variation in drought occurrences across AEZs is influenced by factors such as altitude, which gradually decreases from *dega* to the LWD AEZ. This affects temperature and other climate variables. Field observations and NDVI imagery have revealed that large portions of the *dega* AEZ are covered by forests, which mitigate the severity of droughts. Additionally, the dega zone demonstrates better soil and water conservation practices, such as terracing, and rainwater harvesting, enhancing its resilience to drought conditions.

Pixel-wise Pearson correlation between SPI and ETDI/VHI indices indicates a significant, moderate to strong relationship between meteorological and agricultural droughts. These

findings align with previous studies (Gidey et al., 2018b; Wang et al., 2014) that reported a statistically significant positive association between SPI and VHI. The moderate and strong relationships identified imply the propagation of meteorological drought into agricultural drought, meaning favorable meteorological conditions lead to improved agricultural conditions, while the development of meteorological droughts often result in agricultural droughts.

The findings of this study have significant implications for farmers, government and non-governmental organizations, and policymakers. The livelihoods of most residents in the study area depend on traditional mixed agriculture, which includes both livestock rearing and rainfed agriculture. Rainfall during the *belg* season is as crucial as rain during the *kiremt* season in several aspects (Orr et al., 2021; Rosell & Holmer, 2007). Given the small size of the cultivable landholdings in the study area, less than 0.5 hectare in average (Rosell et al., 2017), the rainfall in the *belg* season is essential for compensating for low production during the kiremt season, particularly for long-cycle crops like maize and sorghum, which are predominant in the LWD and UWD AEZs (Asfaw et al., 2018; Mekonen et al., 2020). Moreover, it is indispensable for farm preparation prior to the subsequent *kiremt* season (Asfaw et al., 2018).

Drought occurrences during both the *belg* and *kiremt* seasons can severely impact crop yields (Mekonen et al., 2020), as well as forage and water availability for livestock (Degefu & Bewket, 2015). These conditions directly impact the food security of the community, necessitating appropriate climate change adaptation measures. The insights from this study provide valuable information for decision-making by farmers, agricultural extension workers, and other stakeholders, aiding in the selection of effective adaptation strategies. For instance, understanding the spatial and temporal variability of droughts can inform soil and water management efforts during the kiremt season to offset water shortages in the belg season for both crops and livestock.

3.5. Conclusions

In this study, we conducted a comprehensive analysis of meteorological and agricultural droughts in the LWD, UWD, and *dega* AEZs in the upper Gelana watershed. We utilized remote sensing data from 1991 to 2021 to examine the occurrence and severity of drought

incidents. Our findings show that although the number of meteorological drought incidents was similar across the three AEZs, the characteristics of agricultural droughts differed significantly. Through ETDI and VHI analysis, we identified a lower agricultural drought event in the *dega* AEZ compared to the LWD and UWD AEZs. This disparity underscores the importance of employing multiple metrics to analyze drought conditions effectively. The study also revealed distinct seasonal dynamics of meteorological droughts, with the *kiremt* season exhibiting more frequent instances compared to the *belg* season across all AEZs. ETDI and VHI analysis identified frequent agricultural drought incidents during the *belg* season, particularly pronounced in the LWD and UWD AEZs. In contrast, the dega agroecology experienced fewer agricultural drought incidents during the *belg* season.

Furthermore, our pixel-wise correlation analysis demonstrated a significant positive association between meteorological and agricultural indices during both the *belg* and *kiremt* seasons. These correlation coefficients, along with the characteristics of drought identified using run theory, highlight the transition from meteorological drought to its agricultural counterpart. Nevertheless, the observed spatial variation in these correlation coefficients emphasizes that this transition is not uniform across the study area.

Overall, the findings underscore the necessity of adopting pixel-wise time series analysis to comprehensively understand the spatial and temporal variations of meteorological and agricultural droughts. The results also indicate an urgent need to implement effective adaptation strategies to mitigate the impact of droughts on the agricultural sector. These strategies may include raising awareness through early warning systems, implementing soil and water conservation techniques such as water harvesting, terracing, and agroforestry, as well as introducing drought-resistant crops, irrigation systems, and related measures. Additionally, our findings provide valuable insights for developing targeted mitigation and adaptation strategies tailored to different AEZs.

Data Availability

The data used to support the findings of this study will be available from the corresponding author upon request.

Conflicts of Interest

The authors declare no conflict of interest.

Acknowledgments

The first author expresses gratitude to Addis Ababa University and the Regional Centre for Mapping of Resources for Development (RCMRD)/GMES and Africa for their financial support in this study. We also thank the National Aeronautics and Space Administration (NASA) for providing MODIS-based NDVI, LST, ET, and PET data, and the TAMSAT group at the University of Reading for providing TAMSAT rainfall data.

References

Arekhi, M., Saglam, S., & Ozkan, U. Y. (2020). Drought monitoring and assessment using Landsat TM/OLI data in the agricultural lands of Bandar - e - Turkmen and Gomishan cities, Iran. *Environment, Development and Sustainability*, *22*, 6691–6708. https://doi.org/10.1007/s10668-019-00509-y

Asfaw, A., Simane, B., Hassen, A., & Bantider, A. (2018). Variability and time series trend analysis of rainfall and temperature in northcentral Ethiopia: A case study in Woleka sub-basin. *Weather and Climate Extremes*, *19*, 29–41. https://doi.org/10.1016/j.wace.2017.12.002

Asten, P. J. A. Van, Fermont, A. M., & Taulya, G. (2011). Drought is a major yield loss factor for rainfed East African highland banana. *Agricultural Water Management*, *98*(4), 541–552. https://doi.org/10.1016/j.agwat.2010.10.005

Baez-Villanueva, O. M. (2023). *SpatIndex: Calculate spatially distributed hydroclimatological indices* (R package version 0.1.0).

Bayable, G., & Gashaw, T. (2021). Spatiotemporal variability of agricultural drought and its association with climatic variables in the Upper Awash Basin, Ethiopia. *SN Applied Sciences*, *3*(465), 1–20. https://doi.org/10.1007/s42452-021-04471-1

Bellizzi, S., Lane, C., Elhakim, M., & Nabeth, P. (2020). Health consequences of drought in the WHO Eastern Mediterranean Region: hotspot areas and needed actions. *Environmental Health*, *19*(114). https://doi.org/10.1186/s12940-020-00665-z

Bento, V. A., Trigo, I. F., Gouveia, C. M., & DaCamara, C. C. (2018). Contribution of Land Surface Temperature (TCI) to Vegetation Health Index A Comparative Stu dy Using Clear Sky and All-Weather Climate Data Record. *Remote Sensing*, *10*(9). https://doi.org/10.3390/rs10091324

Brown, L., Medlock, J., & Murray, V. (2014). Impact of drought on vector-borne diseases - how does one manage the risk? *Public Health*, *128*(1), 29–37. https://doi.org/10.1016/j.puhe.2013.09.006

Burka, A., Biazin, B., & Bewket, W. (2023). Drought characterization using different indices, theory of run and trend analysis in bilate river watershed, rift valley of Ethiopia. *Frontiers in Environmental Science*, *11*. https://doi.org/10.3389/fenvs.2023.1098113

Busetto, L., & Ranghetti, L. (2016). MODIStsp : an R package for automatic preprocessing of MODIS Land Products time series. *Computers and Geosciences*, *97*, 40–48. https://doi.org/10.1016/j.cageo.2016.08.020

Caloiero, T., Caroletti, G. N., & Coscarelli, R. (2021). IMERG-based meteorological drought analysis over Italy. *Climate*, *9*(4). https://doi.org/10.3390/cli9040065

Cook, B. I., Ault, T. R., & Smerdon, J. E. (2015). Unprecedented 21st century drought risk in the American Southwest and Central Plains. *Science Advances*, *1*(1), 1–7. https://doi.org/10.1126/sciadv.1400082

Cook, B. I., Smerdon, J. E., Seager, R., & Coats, S. (2014). Global warming and 21st century drying. *Climate Dynamics*, *43*, 2607–2627. https://doi.org/10.1007/s00382-014-2075-y

Cooper, M. W., Brown, M. E., Hochrainer-Stigler, S., Pflug, G., McCallum, I., Fritz, S., Silva, J., & Zvoleff, A. (2019). Mapping the effects of drought on child stunting. *Environmental Sciences*, *116*(35), 17219–17224. https://doi.org/10.1073/pnas.1905228116

Degefu, M. A., & Bewket, W. (2015). Trends and spatial patterns of drought incidence in the Omo-Ghibe River Basin, Ethiopia. *Geografiska Annaler, Series A: Physical Geography*, *97*(2), 395–414. https://doi.org/10.1111/geoa.12080

Demisse, U., Solomon, M., Legesse, A., Bazezew, A., Muhammad, B., & Ehsan, A. (2022). Climate Change Repercussions on Meteorological Drought Frequency and Intensity in South Wollo, Ethiopia. *Earth Systems and Environment*, *6*(3), 645–655. https://doi.org/10.1007/s41748-022-00293-2

Dimitrova, A. (2021). Seasonal droughts and the risk of childhood undernutrition in Ethiopia. *World Development*, *141*. https://doi.org/10.1016/j.worlddev.2021.105417

Gelorini, V., & Verschuren, D. (2012). Historical climate-human-ecosystem interaction in East Africa: a review. *African Journal of Ecology*, *51*(3), 409–421. https://doi.org/10.1111/aje.12045

Ghaleb, F., Mario, M., & Sandra, A. N. (2015). Regional Landsat-Based Drought Monitoring from 1982 to 2014. *Climate*, *3*, 563–577. https://doi.org/10.3390/cli3030563

Gidey, E., Dikinya, O., Sebego, R., Segosebe, E., & Zenebe, A. (2018a). Modeling the Spatio-Temporal Meteorological Drought Characteristics Using the Standardized Precipitation Index (SPI) in Raya and Its Environs, Northern Ethiopia. *Earth Systems and Environment*, *2*, 281–292. https://doi.org/10.1007/s41748-018-0057-7

Gidey, E., Dikinya, O., Sebego, R., Segosebe, E., & Zenebe, A. (2018b). Using Drought Indices to Model the Statistical Relationships Between Meteorological and Agricultural Drought in Raya and Its Environs, Northern Ethiopia. *Earth Systems and Environment*, *2*, 265–279. https://doi.org/10.1007/s41748-018-0055-9

Gobie, B. G., & Miheretu, B. A. (2021). Effects of El Nino southern oscillation events on rainfall variability over northeast Ethiopia. *Modeling Earth Systems and Environment*, *7*, 2733–2739. https://doi.org/10.1007/s40808-020-01060-w

Gudmundsson, L., & Stagge, J. H. (2016). *SCI: Standardized Climate Indices such as SPI, SRI or SPEI R package version 1.0-2*.

Haile, G. G., Tang, Q., Suna, S., Huanga, Z., Zhanga, X., & Liu, X. (2019). Droughts in East Africa: Causes , impacts and resilience. *Earth-Science Reviews*, *193*, 146–161. https://doi.org/10.1016/j.earscirev.2019.04.015

Hayes, M., Svoboda, M., Wall, N., & Widhalm, M. (2011). The Lincoln declaration on drought indices: universal meteorological drought index recommended. *Bulletin of the American Meteorological Society*, *92*(4), 485–488. https://doi.org/10.1175/2010BAMS3103.1

Hijmans, R. J. (2022). *raster: Geographic Data Analysis and Modeling* (R package version 3.5-15).

Hoffman, T., & Vogel, C. (2008). Climate Change Impacts on African Rangelands. *Rangelands*, *30*(3), 12–17. https://doi.org/10.2111/1551-501X(2008)30[12:CCIOAR]2.0.CO;2

Hurni, H. (1998). *Agroecological Belts of Ethiopia: Explanatory Notes on Three Maps at Scale of 1:1, 000,000*. Soil Conservation Research Programme and Centre for Development and Environment.

Jamro, S., Channa, F. N., Dars, G. H., Ansari, K., & Krakauer, N. Y. (2020). Exploring the evolution of drought characteristics in Balochistan, Pakistan. *Applied Sciences*, *10*(3). https://doi.org/10.3390/app10030913

Jovanovic, N., Mu, Q., Bugan, R. D., & Zhao, M. (2015). Dynamics of MODIS evapotranspiration in South Africa. *Water SA*, *41*(1), 79–90. https://doi.org/10.4314/wsa.v41i1.11

Kalisa, W., Zhang, J., Igbawua, T., Ujoh, F., John, O., Nepomuscene, J., & Yao, F. (2020). Spatio-temporal analysis of drought and return periods over the East African region using Standardized Precipitation Index from 1920 to 2016. *Agricultural Water Management*, *237*. https://doi.org/10.1016/j.agwat.2020.106195

Kassaye, A. Y., Shao, G., Wang, X., & Wu, S. (2021). Quantification of drought severity change in Ethiopia during 1952–2017. *Environment, Development and Sustainability*, *23*, 5096–5121. https://doi.org/10.1007/s10668-020-00805-y

Khan, M. M. H., Muhammad, N. S., & El-Shafie, A. (2018). A review of fundamental drought concepts, impacts and analyses of indices in Asian continent. *Journal of Urban and Environmental Engineering*, *12*(1), 106–119. https://doi.org/10.4090/juee.2017.v12n1.106-119

Kogan, F. (1995). Application of Vegetation Index and Brightness Temperature for Drought Detection. *Advances in Space Research*, *15*(11), 91–100. https://doi.org/10.1016/0273-1177(95)00079-T

Kogan, F. (1997). Global Drought Watch from Space. *American Meteorological Society*, *78*(4), 621–636. https://doi.org/10.1175/1520-0477(1997)078<0621:GDWFS>2.0.CO;2

Kogan, F. (2002). World Droughts in the New Millennium from AVHRR-based Vegetation Health Indices. *EOS,Transactions, American Geophysical Union*, *83*(48), 557–563. https://doi.org/doi:10.1029/2002EO000382

Lee, S. H., Yoo, S. H., Choi, J. Y., & Bae, S. (2017). Assessment of the impact of climate change on drought characteristics in the Hwanghae Plain, North Korea using time series SPI and SPEI: 1981–2100. *Water*, *9*(8). https://doi.org/10.3390/w9080579

Liu, Y., Shan, F., Yue, H., Wang, X., & Fan, Y. (2023). Global analysis of the correlation and propagation among meteorological, agricultural, surface water, and groundwater droughts. *Journal of Environmental Management*, *333*. https://doi.org/10.1016/j.jenvman.2023.117460

Lottering, S., Mafongoya, P., Lottering, R., Lottering, S., Mafongoya, P., & Lottering, R. (2021). Drought and its impacts on small-scale farmers in sub-Saharan Africa: a review Drought and its impacts on small-scale farmers in sub-Saharan Africa : a review. *South African Geographical Journal*, *103*(3), 319–341. https://doi.org/10.1080/03736245.2020.1795914

Maidment, R., Black, E., Greatrex, H., & Young, M. (2020). TAMSAT. In V. Levizzani et al (Ed.), *Satellite Precipitation Measurement, Advances in Global Change Research,vol 67. Springer, Cham* (pp. 393–408). Springer. https://doi.org/10.1007/978-3-030-24568-9_22

Maidment, R. I., Grimes, D., Allan, R. P., Tarnavsky, E., Marcstringer, M., Hewison, T., Roebeling, R., & Black, E. (2014). The 30 year TAMSAT african rainfall climatology and time series (TARCAT) data set. *Journal of Geophysical Research*, *119*(18), 10619–10644. https://doi.org/10.1002/2014JD021927

Maidment, R. I., Grimes, D., Black, E., Tarnavsky, E., Young, M., Greatrex, H., Allan, R. P., Stein, T., Nkonde, E., Senkunda, S., & Alcántara, E. M. U. (2017). A new, long-term daily satellite-based rainfall dataset for operational monitoring in Africa. *Nature Scientific Data*, *4*. https://doi.org/10.1038/sdata.2017.63

Masih, I., Maskey, S., Mussá, F. E. F., & Trambauer, P. (2014). A review of droughts on the African continent: a geospatial and long-term perspective. *Hydrology and Earth System Sciences*, *18*, 3635–3649. https://doi.org/10.5194/hess-18-3635-2014

Mckee, T. B., Doesken, N. J., & Kleist, J. (1993). The relationship of drought frequency and duration to time scales. *Proceedings of the 8th Conference on Applied Climatology*, 179–183.

Mekonen, A. A., Berlie, A. B., & Ferede, M. B. (2020). Spatial and temporal drought incidence analysis in the northeastern highlands of Ethiopia. *Geoenvironmental Disasters*, *7*(10). https://doi.org/10.1186/s40677-020-0146-4

Mera, G. A. (2018). Drought and its impacts in Ethiopia. *Weather and Climate Extremes*, *22*, 24–35. https://doi.org/10.1016/j.wace.2018.10.002

Mohammed, Y., Yimer, F., Tadesse, M., & Tesfaye, K. (2018). Meteorological drought assessment in north east highlands of Ethiopia. *International Journal of Climate Change Strategies and Management*, *10*(1), 142–160. https://doi.org/10.1108/IJCCSM-12-2016-0179

Molla, M. (2020). Teleconnections between Ocean-Atmosphere Coupled Phenomenon and Droughts in Tigray Region: Northern Ethiopia. *American Journal of Climate Change*, *9*, 274–296. https://doi.org/10.4236/ajcc.2020.93018

Monteith, J. L. (1965). Evaporation and environment. In *Symposia of the Society for Experimental Biology* (Vol. 19, pp. 205–234).

Mu, Q., Heinsch, F. A., Zhao, M., & Running, S. W. (2007). Development of a global evapotranspiration algorithm based on MODIS and global meteorology data. *Remote Sensing of Environment*, *111*(4), 519–536. https://doi.org/10.1016/j.rse.2007.04.015

Mu, Q., Zhao, M., & Running, S. W. (2011). Remote Sensing of Environment Improvements to a MODIS global terrestrial evapotranspiration algorithm. *Remote Sensing of Environment*, *115*(8), 1781–1800. https://doi.org/10.1016/j.rse.2011.02.019

Mulualem, G. M., Raju, U. J. P., Stojanovic, M., & Sorí, R. (2024). The phenomenon of drought in Ethiopia: Historical evolution and climatic forcing. *Hydrology Research*, *55*(6), 595–612. https://doi.org/10.2166/nh.2024.192

Nam, W. H., Hayes, M. J., Svoboda, M. D., Tadesse, T., & Wilhite, D. A. (2015). Drought hazard assessment in the context of climate change for South Korea. *Agricultural Water Management*, *160*, 106–117. https://doi.org/10.1016/j.agwat.2015.06.029

Narasimhan, B., & Srinivasan, R. (2005). Development and evaluation of Soil Moisture Deficit Index (SMDI) and Evapotranspiration Deficit Index (ETDI) for agricultural drought monitoring. *Agricultural and Forest Meteorology*, *133*, 69–88. https://doi.org/10.1016/j.agrformet.2005.07.012

Negash, M. (1987). The need for meteorological information to plan agroforestry on steep slopes in Ethiopia. In W. E. Reifsnyder & T. O. Darnhofer (Eds.), *Meteorology and Agroforestry: Proceedings of an International Workshop on Application of Meteorology to Agroforestry Systems Planning and Management* (pp. 181–189).

Ngcamu, B. S., & Chari, F. (2020). Drought Influences on Food Insecurity in Africa: A Systematic Literature Review. *International Journal of Environmental Research and Public Health Review*, *17*(16). https://doi.org/10.3390/ijerph17165897

Orr, A., Tiba, Z., Congrave, J., Porázik, P., Dejen, A., & Hassen, S. (2021). Smallholder commercialization and climate change: a simulation game for teff in South Wollo, Ethiopia. *International Journal of Agricultural Sustainability*, *19*(5–6), 595–608. https://doi.org/10.1080/14735903.2020.1792735

Roger, J. C., Vermote, E. F., & Ray, J. P. (2015). *MODIS Surface Reflectance User' s Guide*. 1–35.

Rosell, S., & Holmer, B. (2007). Rainfall change and its implications for Belg harvest in South Wollo, Ethiopia. *Geografiska Annaler, Series A: Physical Geography*, *89*(4), 287–299. https://doi.org/10.1111/j.1468-0459.2007.00327.x

Rosell, S., Olvmo, M., & Holmer, B. (2017). Cultivated land – a scarce commodity in a densely populated rural area in South Wollo, Ethiopia. *Journal of Land Use Science*, *12*(4), 252–270. https://doi.org/10.1080/1747423X.2017.1319978

Running, S., Mu, Q., Zhao, M., & Moreno, A. (2021). MODIS/Terra Net Evapotranspiration Gap-Filled 8-Day L4 Global 500m SIN Grid V061 [Data set]. *NASA EOSDIS Land Processes Distributed Active Archive Center*. https://doi.org/10.5067/MODIS/MOD16A2GF.061

Seiler, R. A., Kogan, F., & Sullivan, J. (1998). AVHRR-based vegetation and temperature condition indices for drought detection in Argentina. *Advances in Space Research*, *21*(3), 481–484. https://doi.org/10.1016/S0273-1177(97)00884-3

Shahzaman, M., Zhu, W., Bilal, M., Habtemicheal, B. A., Mustafa, F., Arshad, M., Ullah, I., Ishfaq, S., & Iqbal, R. (2021). Remote Sensing Indices for Spatial Monitoring of

Agricultural Drought in South Asian Countries. *Remote Sensing*, *13*. https://doi.org/10.3390/rs13112059

Shahzaman, M., Zhu, W., Ullah, I., Mustafa, F., Bilal, M., Ishfaq, S., Nisar, S., Arshad, M., Iqbal, R., & Aslam, R. W. (2021). Comparison of Multi-Year Reanalysis,Models, and Satellite Remote Sensing Products for Agricultural Drought Monitoring over South Asian Countries. *Remote Sensing*, *13*. https://doi.org/10.3390/rs13163294

Shefine, B. G. (2019). Analysis of Meteorological Drought Using SPI and Large Scale Climate Hydrology: Current Research Analysis of Meteorological Drought Using SPI and Large-Scale Climate Variability (ENSO) -A Case Study in North Shewa Zone , Amhara Regional. *Hydrology: Current Research*, *9*(4). https://doi.org/10.4172/2157-7587.1000307

Shi, H., Zhou, Z., Liu, L., & Liu, S. (2022). A global perspective on propagation from meteorological drought to hydrological drought during 1902–2014. *Atmospheric Research*, *280*. https://doi.org/10.1016/j.atmosres.2022.106441

Shiferaw, B., Tesfaye, K., Kassie, M., Abate, T., Prasanna, B. M., & Menkir, A. (2014). Managing vulnerability to drought and enhancing livelihood resilience in sub-Saharan Africa: Technological, institutional and policy options. *Weather and Climate Extremes*, *3*, 67–79. https://doi.org/10.1016/j.wace.2014.04.004

Sholihah, R. I., Trisasongko, B. H., Shiddiq, D., Iman, S., Kusdaryantoa, S., Manijoa, & Panujua, D. R. (2016). Identification of agricultural drought extent based on vegetation health indices of Landsat data: case of Subang and Karawang , Indonesia. *Procedia Environmental Sciences*, *33*, 14–20. https://doi.org/10.1016/j.proenv.2016.03.051

Stanke, C., Kerac, M., Prudhomme, C., Medlock, J., & Murray, V. (2013). Health effects of drought: a systematic review of the evidence. *PLoS Currents*, *5*. https://doi.org/10.1371/currents.dis.7a2cee9e980f91ad7697b570bcc4b004

Sur, K., & Lunagaria, M. M. (2020). Association between drought and agricultural productivity using remote sensing data: a case study of Gujarat state of India. *Journal of Water and Climate Change*, *11*(S1), 189–202. https://doi.org/doi:10.2166/wcc.2020.157

Tadesse, S., Mekuriaw, A., & Assen, M. (2024). Spatiotemporal climate variability and trends in the Upper Gelana Watershed, northeastern highlands of Ethiopia. *Heliyon*, *10*(5), e27274. https://doi.org/10.1016/j.heliyon.2024.e27274

Tarnavsky, E., Grimes, D., Maidment, R., Black, E., Allan, R. P., Stringer, M., Chadwick, R., & Kayitakire, F. (2014). Extension of the TAMSAT satellite-based rainfall monitoring over Africa and from 1983 to present. *Journal of Applied Meteorology and Climatology*, *53*(12), 2805–2822. https://doi.org/10.1175/JAMC-D-14-0016.1

Tesfamariam, B. G., Gessesse, B., & Melgani, F. (2019). Characterizing the spatiotemporal distribution of meteorological drought as a response to climate variability: The case of rift valley lakes basin of Ethiopia. *Weather and Climate Extremes*, *26*. https://doi.org/10.1016/j.wace.2019.100237

Trenberth, K. E., Dai, A., Van Der Schrier, G., Jones, P. D., Barichivich, J., Briffa, K. R., & Sheffield, J. (2014). Global warming and changes in drought. *Nature Climate Change*, *4*, 17–22. https://doi.org/10.1038/nclimate2067

Ullah, I., Ma, X., Asfaw, T. G., Yin, J., Iyakaremye, V., Saleem, F., Xing, Y., Azam, K., & Syed, S. (2022). Projected Changes in Increased Drought Risks Over South Asia Under a Warmer Climate. *Earth's Future*, *10*. https://doi.org/10.1029/2022EF002830

Ullah, I., Mukherjee, S., Syed, S., Mishra, A. K., Ayugi, B. O., & Aadhar, S. (2024). Anthropogenic and atmospheric variability intensifies flash drought episodes in South Asia. *Communications Earth & Environment*, *5*(267). https://doi.org/10.1038/s43247-024-01390-y

Ullah, I., Zeng, X., Mukherjee, S., Aadhar, S., Mishra, A. K., Syed, S., Ayugi, B. O., Iyakaremye, V., & Lv, H. (2023). Future Amplification of Multivariate Risk of Compound Drought and Heatwave Events on South Asian Population. *Earth's Future*, *11*. https://doi.org/10.1029/2023EF003688

Vermote, E. (2015). MOD09Q1 MODIS/Terra Surface Reflectance 8-Day L3 Global 250m SIN Grid [Data Set]. *NASA LP DAAC*. https://doi.org/10.5067/MODIS/MOD09Q1.006

Vermote, E. F., Roger, J. C., & Ray, J. P. (2015). *MODIS Surface Reflectance User's Guide*.

Vicente-serrano, S. M., Beguería, S., Gimeno, L., Eklundh, L., Giuliani, G., Weston, D., El, A., López-moreno, J. I., Nieto, R., Ayenew, T., Konte, D., Ardö, J., & Pegram, G. G. S. (2012). Challenges for drought mitigation in Africa: The potential use of geospatial data and drought information systems. *Applied Geography*, *34*, 471–486. https://doi.org/10.1016/j.apgeog.2012.02.001

Wan, Z. (2013). *MODIS Land Surface Temperature Products Users' Guide*. *December*.

Wan, Z., Hook, S., & Hulley, G. (2015). MOD11A2 MODIS/Terra land surface temperature/emissivity 8-day L3 global 1km SIN grid V006 [Data set]. *Nasa Eosdis Land Processes Daac*. https://doi.org/10.5067/MODIS/MOD11A2.006

Wang, H., Lin, H., & Liu, D. (2014). Remotely sensed drought Index and its responses to meteorological drought in Southwest China. *Remote Sensing Letters*, *5*(5), 413–422. https://doi.org/10.1080/2150704X.2014.912768

Wang, L., Zhang, X., Wang, S., Salahou, M. K., & Fang, Y. (2020). Analysis and application of drought characteristics based on theory of runs and copulas in Yunnan, southwest

China. *International Journal of Environmental Research and Public Health*, *17*(13). https://doi.org/10.3390/ijerph17134654

Wang, Q., Yang, Y., Liu, Y., Tong, L., Zhang, Q., & Li, J. (2019). Assessing the Impacts of Drought on Grassland Net Primary Production at the Global Scale. *Scientific Reports*, *9*(14041). https://doi.org/10.1038/s41598-019-50584-4

Wu, R., Zhang, J., Bao, Y., & Guo, E. (2019). Run theory and copula-based drought risk analysis for songnen grassland in Northeastern China. *Sustainability*, *11*(21). https://doi.org/10.3390/su11216032

Yevjevich, V. (1967). An Objective Approach to Definitions and Investigation of Continental Hydrologic Droughts. In *Hydrology Paper 23*. Colorado State University: Fort Collins, CO, USA.

Zargar, A., Sadiq, R., Naser, B., & Khan, F. I. (2011). A review of drought indices. *Environ. Rev.*, *19*, 333–349. https://doi.org/10.1139/A11-013

Zhang, X., Hao, Z., Singh, V. P., Zhang, Y., Feng, S., Xu, Y., & Hao, F. (2022). Drought propagation under global warming: Characteristics, approaches, processes, and controlling factors. *Science of The Total Environment*, *838*. https://doi.org/10.1016/j.scitotenv.2022.156021

Zhao, L., Wu, J., & Fang, J. (2016). Robust Response of Streamflow Drought to Different Timescales of Meteorological Drought in Xiangjiang River Basin of China. *Advances in Meteorology*, *2016*. https://doi.org/10.1155/2016/1634787

Zhou, Z., Zhang, L., Chen, J., She, D., Wang, G., Zhang, Q., Xia, J., & Zhang, Y. (2023). Projecting Global Drought Risk Under Various SSP-RCP Scenarios. *Earth's Future*, *11*. https://doi.org/10.1029/2022EF003420

CHAPTER FOUR

4.SPATIOTEMPORAL DYNAMICS OF LAND SURFACE PHENOLOGY AND ITS RESPONSE TO CLIMATE CHANGE IN THE UPPER GELANA WATERSHED, NORTHEASTERN HIGHLANDS OF ETHIOPIA

Tadesse, S., Mekuriaw, A., Assen, M., 2024. Spatiotemporal dynamics of land surface phenology and its response to climate change in the upper Gelana watershed, northeastern highlands of Ethiopia. Environmental and Sustainability Indicators. 25. https://doi.org/10.1016/j.indic.2024.100574.

4.SPATIOTEMPORAL DYNAMICS OF LAND SURFACE PHENOLOGY AND ITS RESPONSE TO CLIMATE CHANGE IN THE UPPER GELANA WATERSHED, NORTHEASTERN HIGHLANDS OF ETHIOPIA

Abstract

Land surface phenology (LSP) is a crucial indicator of climate change and its impact on ecosystems. Therefore, this study was carried out to assess the spatiotemporal variations in LSP and its response to climate change across the agroecological zones (AEZs) of the upper Gelana watershed in the northeastern highlands of Ethiopia. The LSP metrics were derived from MODIS NDVI data using TIMESAT v3.3, and trends as well as correlations were analyzed using the statistical programming language R. The results indicate that the *dega* AEZ exhibits an earlier start of the season (SOS) and a longer length of the season (LOS) compared to the *lower* and *upper weina dega* (LWD and UWD) AEZs. A delay in SOS and end of season (EOS) was observed in 71.3% and 82% of the study area, respectively, while LOS increased in nearly half of the area. There is a positive correlation between SOS and maximum temperature, and a negative correlation with *belg* season rainfall and drought indices in large parts of the study area. Similarly, EOS exhibits a direct association with *kiremt* season maximum temperature, rainfall, and drought indices. Furthermore, a shorter LOS is associated with a higher annual maximum temperature, while a longer LOS is associated with the increasing trend in annual rainfall. These findings will help raise awareness on climate change adaptation activities, including crop diversification, alteration of planting dates, soil conservation, water harvesting and irrigation, particularly within rural communities of the study area thatheavily rely on rainfed agriculture.

Keywords: Land surface phenology, start of season, end of season, length of season, NDVI, remote sensing.

4.1. Introduction

Land surface phenology (LSP) is the study of seasonal fluctuations or life cycles of plants (Caparros-Santiago et al., 2023; Stanimirova et al., 2019). It involves the analysis of time series vegetation indices or biophysical measurements derived from remote sensing data (Caparros-santiago et al., 2021; Caparros-Santiago et al., 2023; de Beurs & Henebry, 2005). Vegetation plays a crucial role in ecosystem processes, such as impacting the water cycle, carbon exchange, energy flow and species interactions (Adole et al., 2016; Caparros-santiago et al., 2021; Cleland et al., 2007; Glade et al., 2016; Kariyeva et al., 2012). In addition, vegetation offers important ecosystem services such as habitat and food security (Adole et al., 2016). However, these functions of vegetation could be negatively affected due to climate variability and change (Glade et al., 2016). As a result, a thorough understanding of the interaction between land surface phenology and climate variability is crucial to accurately assess the impacts of climate on ecosystems (Adole et al., 2016; Tang et al., 2015; Wu & Xin, 2023; Yuan et al., 2019).

Understanding these interactions requires considering how vegetation phenology varies by geographical location, temporal factor, and vegetation composition (Fitchett et al., 2015; Kariyeva & Van Leeuwen, 2011). Studies have examined the impact of various climatic variables on LSP, such as rainfall and temperature conditions (Clinton et al., 2014; Du et al., 2014; Tang et al., 2015; Zhang et al., 2018). However, no single climate variable has been identified that has the most significant influence on LSP (Clinton et al., 2014). In regions with scarce available water resources, precipitation is the main factor that affects vegetation features; however, factors such as temperature and humidity also substantially control photosynthesis and transpiration, thus affecting plant development and productivity (Glade et al., 2016; Rishmawi et al., 2016; Shen et al., 2019).

These climatic factors not only influence specific phenological events but also have cascading effects on ecosystem productivity and economic outcomes. Changes in climatic and weather elements such as rainfall and temperature conditions have a profound effect on various landscape phenological events, e.g., the onset of greenness and termination, and length of season. Several studies (Badeck et al., 2004; Fitchett et al., 2015; Jin et al., 2019; Liu et al., 2023; Yang & Fan, 2023) have shown that climate change can delay or advance the start and end of the growing season, as well as impact its duration. However, these changes

might have positive or negative consequences. For example, a longer growing season promotes vegetation productivity, while a shorter season reduces productivity (Han et al., 2015). Thus, changes can have significant implications for the overall functioning of ecosystems and economic consequences, particularly for agricultural production (Badeck et al., 2004; Caparros-santiago et al., 2021; Fitchett et al., 2015).

In countries like Ethiopia, where rainfed agriculture is the backbone of the economy, the impacts of climate change on phenology and agricultural production are particularly significant. Studies provided compelling evidence that suggest future climate change could result in a decrease in rainfed crop yields for small-scale farmers. For example, Degife et al. (2021) and Rettie et al. (2022) projected a decline of more than a third in the production of maize and wheat in different parts of Ethiopia, which would have an impact on the country's efforts to achieve food self-sufficiency and ensure food security. In this regard, understanding the nature of the long-term phenological response across the landscape to climate change can contribute to the adjustment of the timing of agricultural activities (Ruml & Vulic, 2005; Zhou et al., 2013). Furthermore, spatial and temporal variations in phenology across the different land use and land cover (LULC) in different agroecological zones are essential to gain valuable insight into vegetation response to climate change (Hwang et al., 2011). This knowledge will also help to understand and implement effective adaptation strategies (Fitchett et al., 2015) focusing primarily on the agricultural sector of Ethiopia.

To address these challenges, remote sensing emerges as a powerful tool to monitor and understand spatial and temporal dynamics in vegetation phenology and its relationship with climate variability and change (Geremew & Jebessa, 2018; Hao et al., 2016; Li et al., 2023; Tang et al., 2015; Valderrama-Landeros et al., 2021; Xu et al., 2019; Yuan et al., 2019). Vegetation indices derived from remote sensing products offer quantitative measurements that reflect vegetation vigor (Bannari et al., 1995). Various types of vegetation indices based on remote sensing data are described in previous studies (Bannari et al., 1995; Xue & Su, 2017). Among these indices, Normalized Difference Vegetation Index (NDVI) is the most widely used due to its simplicity of calculation, its sensitivity to greenness and its strong correlation with the leaf area index, among other factors (Adole et al., 2016; Bannari et al., 1995; Xue & Su, 2017). NDVI serves as an essential index to examine the impact of climate change on ecosystems (Du et al., 2014). It provides valuable information on vegetation properties that

are closely associated with climate variables such as rainfall and temperature, which are important environmental factors that affect plant growth and distribution (Revadekar et al., 2012).

While previous studies examined vegetation-climate relationships, they often overlooked the role of local agroecological differences in characterizing phenological changes (Dagnachew et al., 2020; Geremew & Jebessa, 2018; Hussien et al., 2023; Muir et al., 2021). Most researchers focused on broad-scale associations between the NDVI and climatic factors, often producing contradictory findings. To the best knowledge of the authors, the investigation of LSP and its response to climate variability, particularly in relation to local agroecological variations, remains largely unexplored in many parts of the country, including the study area, the upper Gelana basin.

Although it is crucial to understand the overall response of vegetation to climate change, we argue that further investigation is imperative in order to fully understand the impacts of climate change on agricultural activities in rural communities in the Upper Gelana watershed and its environs. This can be achieved by examining the timing of major phenological events, such as the start of the season (SOS), the end of the season (EOS) and the length of the growing season (LOS), as well as indicators of ecosystem condition (Alemayehu et al., 2023; Almeida et al., 2014; Stanimirova et al., 2019) such as the base, peak and amplitude of vegetation growth. It is also crucial to understand these long-term phenological events across various LULC categories, as they play a vital role in both crop and livestock production (Araya et al., 2018). For example, in crop production, understanding these events helps to adjust planting and harvesting schedules, while in livestock production, it allows informed decisions regarding the availability of feed and water for animals in response to climate change.

Therefore, the main objective of this study is to analyze how land surface phenological characteristics vary over time and space using long-term Moderate Resolution Imaging Spectroradiometer (MODIS) NDVI data. The study examined SOS, EOS and LOS across different LULC categories and agroecological zones in the study area. Additionally, we analyzed spatial variations and trends in maximum NDVI, base value, and amplitude, which provides useful insights into the condition of the ecosystem. Furthermore, the study aimed to assess the spatial and temporal patterns of the response of land surface phenological metrics

to climate variability and change in the Upper Gelana watershed, northeastern highlands of Ethiopia.

4.2. Methods and materials

4.2.1. Description of study area

The study was carried out in the Upper Gelana watershed of the Tehuledere district, northeastern highlands of Ethiopia. It is located between 11.15^{o} N to 11.35^{o} N and 39.62^{o} E to 39.73^{o} E with 134 square kilometer area (Fig.4.1). The area is described by uneven terrain with an elevation varying between 1701 and 2886 meters (m) above mean sea level (amsl). The Upper Gelana watershed is situated on the outskirts of the eastern Ethiopian highlands and the western escarpment of the Afar depression in the Great Rift Valley zone (Ghinassi et al., 2012), exhibiting distinct climatic conditions that are expected to have substantial implications for the vegetation ecosystem. According to Hurni (1998) classification system which is based on elevation and rainfall patterns, the study area falls into two distinct agroecological zones (AEZs). Consequently, the area from 2300 to 2886 m amsl is classified as *dega* (cool and humid) agroecology, while areas with an elevation range of 1701 to 2300 m amsl are classified as *weina dega* (semi-humid) agroecology. Taking into account the spatial variation in climate of the *weina dega* AEZ of the study area, (Tadesse et al., 2024) divided it into the *lower weina dega* (LWD, 1701 to 2000 m amsl) and the upper *weina dega* (UWD, 2001 to 2300 m amsl).

The area received mean annual rainfall ranging from 964 mm in LWD to 1072 mm in *dega* AEZ (Fig.1). In addition, it is characterized by a mean annual temperature ranging from 15.9 ^{o}C in *dega* to 18.9 ^{o}C in the LWD AEZ. All AEZs in the study area received the highest rainfall during the *kiremt* season, extending from June to September, with the highest rainfall occurring in August. As shown in Fig.4.2, the peak mean monthly maximum and mean monthly temperatures were recorded in June, while the peak for the long-term mean monthly minimum temperature was identified in July (Tadesse et al., 2024).

Farmers in the study area depend on crop and livestock production as their main sources of livelihood. A large proportion of the land in the study area is reserved for agricultural purposes. Farmers produce cereal crops such as *teff* (*Eragrostis tef*), wheat (*Triticum aestivum*), and sorghum (*Sorghum bicolor L*). Additionally, they cultivate *chat* (*Catha edulis*)

as a cash crop. The study area is home to different endemic plants, including *Acacia*, *Juniperus procera*, and *Olea africana*(Woldie & Tadesse, 2020) as well as exotic *Eucalyptus*.

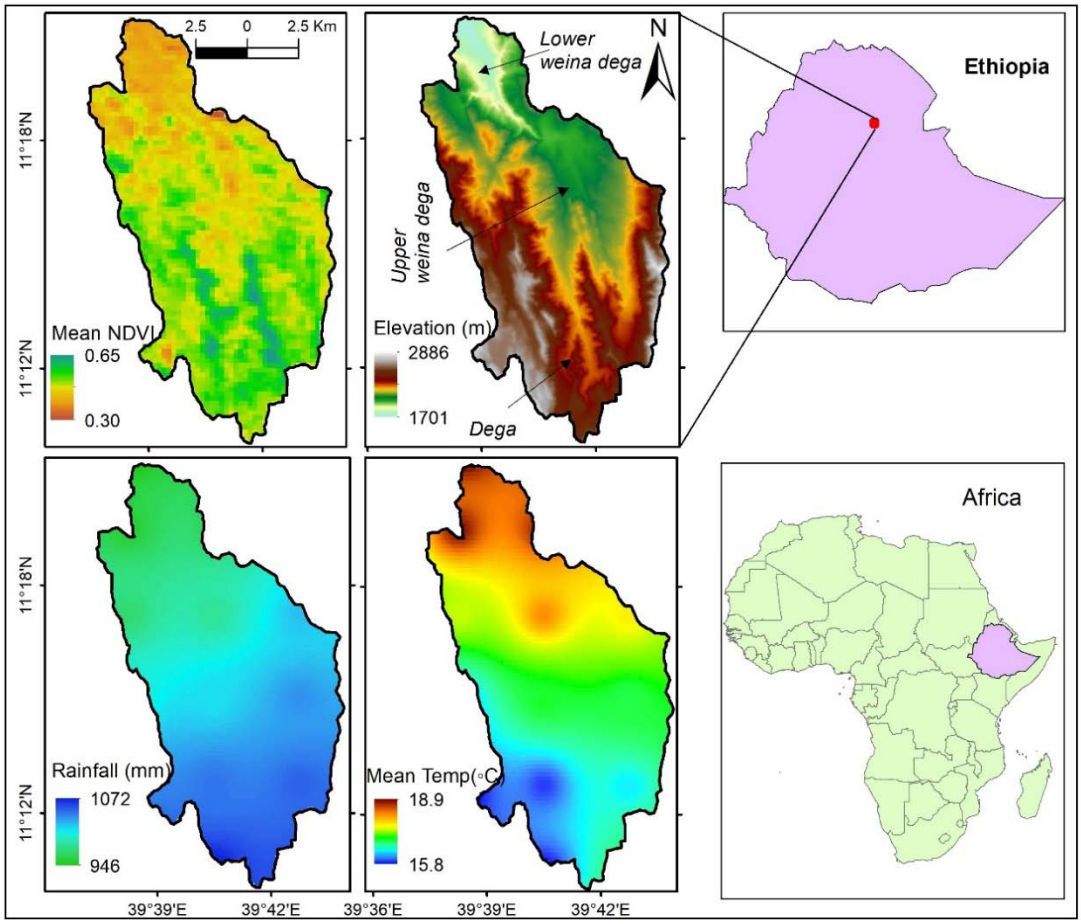

Fig. 4.1.Location map of the study area. The map shows the mean NDVI (2001-2021), the average rainfall calculated from TAMSAT data (1983-2021), and the mean temperature based on gridded data (1983–2018) obtained from the Ethiopian Meteorological Institute (EMI).

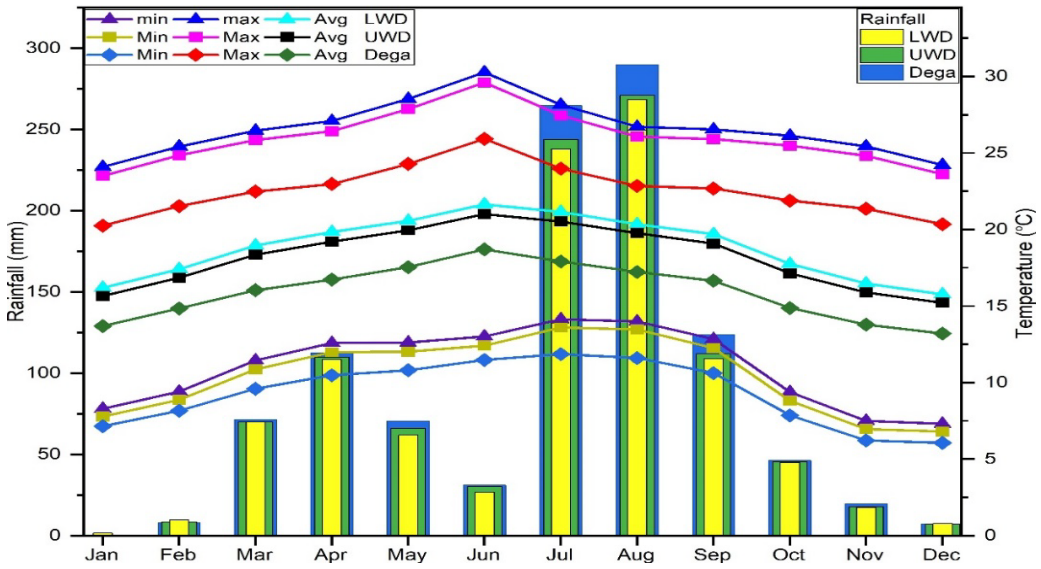

Fig. 4.2. Average monthly rainfall (1983-2021) based on TAMSAT and temperature (1983-2018) from EMI.

4.2.2. Data sources

The changes in LULC of the study area were examined to avoid uncertainties in the phonological trend analysis. For this purpose, we used Landsat 7 Enhanced Thematic Mapper Plus (ETM+) and Landsat 8 Operational Land Imager (OLI) satellite imageries for January 2001 and 2021, respectively. The years are selected to fit the temporal coverage of the phenological analysis of this study. Moreover, the images are cloud free and acquired from the National Aeronautics and Space Administration (NASA) Earthdata website https://www.earthdata.nasa.gov. The data can be accessed from the website at no cost.

We also used bands 1(red) and 2(NIR) of the MODIS Terra/Aqua 8-day surface reflectance data from Collection 6 MOD09Q1 (Vermote, 2015)to compute the NDVI. These bands have a spatial resolution of 250 m (Vermote et al., 2015). We used the MODIStsp package in R environment (Busetto & Ranghetti, 2016), to generate a total of 966 NDVI layers and their corresponding quality bands, covering the time period from 2001 to 2021 from https://www.earthdata.nasa.gov/. MODIS data are freely accessible after registering on the NASA Earthdata website. The formula for deriving NDVI from MODIS surface reflectance is as follows:

$$\mathrm{NDVI} = \frac{(\mathrm{NIR} - \mathrm{Red})}{(\mathrm{NIR} + \mathrm{Red})}, \quad (1)$$

Where, red represents band 1 and NIR represents near-infrared band 2 of the MODIS surface reflectance. The NDVI value ranges from −1.0, which indicates no vegetation to 1.0, implying high vegetation density and greenness (Revadekar et al., 2012).

We used monthly TAMSAT data (Maidment et al., 2014) from 2001 to 2021 to analyze the responses of phenology metrics to rainfall variability. TAMSAT version 3.1 monthly rainfall data with a spatial resolution of 0.0375 degrees (4 km) were downloaded from the TAMSAT group website at https://data.tamsat.org.uk/. A previous study by Tadesse et al. (2024) validated the TAMSAT monthly precipitation against station data and found a high performance in the study area and its surroundings. Additionally, to examine the responses of land surface phenology to changes in minimum and maximum temperatures, we used gridded data from 2001 to 2018 (available only up to this date) obtained from the EMI.

Moreover, we used the standardized precipitation index (SPI), the Evapotranspiration deficit index (ETDI), and the vegetation condition index (VHI) data from 2001 to 2021 produced by (Tadesse & Mekuriaw, 2024) to examine the responses of LSP to meteorological and agricultural droughts during the *belg* (February, March, April, May) and *kiremt* (June, July, August, September) seasons.

4.2.3. Data analysis

4.2.3.1. Land use and land cover (LULC) classification

Analyzing LULC using remote sensing techniques is crucial to detect changes in land use in the study area. This is important to exclude trend changes in LSP resulting from LULC dynamics and to properly model its relationship with climate change. We employed a machine learning approach to classify Landsat images to prepare LULC maps for the years 2001 and 2021. We utilized a random forest approach that combines several randomized decision trees and aggregates their predictions through averaging (Belgiu & Dra, 2016; Breiman, 2001; Parmar et al., 2019; Talukdar et al., 2020). Machine learning classifiers produce superior results as compared to conventional supervised parametric classifiers such as Maximum Likelihood Classification (MLC) (Maxwell et al., 2018). The random forest is an optimal classifier due to its capabilities, which include handling high data dimensionality and multicollinearity, rapid processing, resistance to over fitting, and high classification accuracy (Belgiu & Dra, 2016; Rodriguez-galiano et al., 2012a; Saini & Ghosh, 2017; Talukdar et al.,

2020). We followed the guidelines prepared by the Ethiopian Mapping Agency (2018) to classify the LULC classes of the study area described in Table 4.1.

Table 4.1.Description of LULC categories based on field observations and documents.

LULC categories	Descriptions
Cropland	Land used for crop production
Grazing land	Land covered with grass or herbage and used for grazing.
Forest	Area covered by dense trees with at least 2 m height and 20% canopy cover [60].
Shrubland	Land covered by shrubs and small trees
Built-up	Areas occupied by buildings, roads, and other infrastructures.
Water bodies	Area with ponds, marshes and swamps

4.2.3.2. RF model parameters and accuracy assessment

The parameters of the RF model were fine-tuned using the tuneRF function from the randomForest package in R. A grid search was performed to optimize the number of trees (ntree) and the number of variables considered at each split (mtry). The Out-of-Bag (OOB) error served as the primary evaluation metric to identify the optimal parameter settings. After testing a number of trees (Rodriguez-galiano et al., 2012b), an ntree of 300 provided the best model performance for our data sets. For the 2001 dataset, optimal performance was achieved with mtry = 2, which yielded an OOB error of 11.4%. For the 2021 dataset, the process started with mtry = 2, followed by testing mtry values of 1 and 4. The lowest OOB error of 4.67% was obtained with mtry = 1. These results demonstrate that the parameters of the RF model were effectively tuned to maximize the classification performance for each dataset.

In addition to tuning the RF model parameters, a post-classification accuracy assessment of the LULC maps was performed. This step, which involves comparing the classification results with reference data, is essential to validate the accuracy of the LULC classifications before analyzing changes in land use maps. Collecting reference data from the field can be time-consuming and expensive. As a result, aerial photographs and higher resolution satellite images can serve as viable alternatives (El-Kawy et al., 2011; Olofsson et al., 2014; Yimam et al., 2024). In this study, a total of 227 data points were collected from high-resolution Google Earth images. The accuracy of LULC maps were evaluated using unbiased estimates of the proportional area of the error matrix (Olofsson et al., 2013, 2014). The procedure is widely recognized for its superiority over kappa statistics and has been applied in numerous LULC

studies (Zoungrana et al., 2015; Mekuriaw, 2017). The unbiased estimator of the proportion of area ($\hat{p}_{ij}$) in i^{th}row and j^{th} column of the error matrix is computed using Equations (2) as follows:

$$p_{ij} = W_i \frac{n_{ij}}{n_i}, \quad (2)$$

Where, *Wi* is the proportion of area mapped as class *i*, *nij* isthe sample counts of$the\ i^{th}$ row and$the\ j^{th}$ column and n_i is the sum of samples in the i^{th} row of the error matrix. The column total error matrix (p_j) represents the proportion of area of class *j* as determined from the reference classification.

$$p_j = \sum_{i=1}^{n} W_i \frac{n_{ij}}{n_i}, \quad (3)$$

Then the standard error (*SE*) of the proportion of area of class *j* was estimated by Equation (4).

$$SE(p_j) = \sqrt{\sum_{i}^{n} Wi^2 \frac{\frac{n_{ij}}{n_i}(1-\frac{n_{ij}}{n_i})}{n_i - 1}}, \quad (4)$$

Table 4.2. Accuracy assessment report for the LULC classification of the years 2001 and 2021

Classes	1	2	3	4	5	6	wi	mapped area	PA	UA
2001										
1	0.576	0.003	0.005	0.000	0.012	0.000	0.62	80.16	96.58	93.02
2	0.007	0.095	0.000	0.000	0.016	0.000	0.11	15.92	80.1	88.24
3	0.014	0.000	0.057	0.000	0.004	0.000	0.06	10.19	75.6	92.31
4	0.000	0.000	0.000	0.003	0.000	0.000	0.00	0.38	100	94.44
5	0.022	0.009	0.000	0.000	0.172	0.000	0.20	27.28	84.69	84
6	0.000	0.000	0.000	0.000	0.000	0.003	0.00	0.44	100	100
2021										
1	0.600	0.008	0.008	0.000	0.015	0.000	0.63	83.23	96.85	95.18
2	0.003	0.111	0.000	0.000	0.007	0.000	0.12	16.56	90.49	91.89
3	0.003	0.000	0.040	0.000	0.000	0.000	0.04	6.99	77.47	92.31
4	0.001	0.000	0.000	0.009	0.000	0.000	0.01	1.15	100	94.44
5	0.012	0.004	0.004	0.000	0.173	0.000	0.19	26.23	88.79	89.36
6	0.000	0.000	0.000	0.000	0.000	0.002	0.00	0.24	100	92.86

Note: 1=Cropland, 2=Forest, 3=Grazing land, 4=Built-up, 5=Shrubland, 6=Water, PA= Producer accuracy, UA= User accuracy

Table 4.2 presents the classification accuracy of each LULC class in 2001 and 2021. LULC maps for the years 2001 and 2021 were prepared with an overall accuracy of 90.64 and 93.52, respectively. Finally, the LULC change detection was performed after the images are classified with the required level of accuracy.

4.2.3.3. Preprocessing NDVI data

As mentioned previously, the NDVI data, along with the quality assessment (QA) bit data, were obtained from the NASA Earthdata engine. Then, these QA bands were used to eliminate clouds and low-quality pixels from each image. Poor quality or contaminated pixels in each image were identified and removed. These pixels were assigned as no-data (NA) values using the quality assurance (QA) bands. The NA values were then replaced using linear interpolation, specifically using the approxNA function in the raster package of the R program (Hijmans, 2022). Furthermore, the NDVI images were converted into a binary flat format and a text file containing the list of each image was generated using R for the subsequent processes in the TIMESAT software downloaded from www.nateko.lu.se/timesat(Jonsson & Eklundh, 2004).

4.2.3.4. Extracting land surface phenology (LSP) metrics

Before computing the phenology, it is important to apply smoothing on the 8-day NDVI time series. Smoothing involves suppression of the noise or outliers in the data that makes it difficult to extract the seasons LSP metrics (Jönsson & Eklundh, 2002). We applied the Savitzky-Golay (SG) smoothing technique in TIMESAT(Chen et al., 2004; Jonsson & Eklundh, 2004; Rao et al., 2015). We utilized this smoothing technique due to its efficiency in addressing noise and imposing a bell-shaped pattern on the data (Chen et al., 2004; Jonsson & Eklundh, 2004; Rao et al., 2015). The Savitzky-Golay filtering is given in Equation (5) as follows.

$$Y_j^* = \frac{1}{N} \sum_{i=-m}^{i=m} C_i Y_{j+i,} \quad (5)$$

Where, Y and Y*represent the original and smoothed NDVI at time *j*, respectively. C_i, N, and m are the filtering coefficient, window size, and the half-width of the window in order of sequence. In this study, we used parameters such as the median filter with a spike value of 1, 2 adaption strength, and 5 SG window size in the TIMESAT graphic user interface.

Land surface phenology metrics were derived from smoothed NDVI data using the seasonal amplitude method of TIMESAT. This method determines the start and end dates of the season by identifying when the curve intersects a proportion of the seasonal amplitude, based on a specified threshold value. Threshold values ranging from 20% to 50% are commonly used in the literature on LSP (Alemayehu et al., 2023; Cheng et al., 2020; Descals et al., 2021; Egeru et al., 2020; Tang et al., 2015; C. Wang et al., 2015). In our study, we carefully examined the smoothed NDVI time series curve to determine the appropriate threshold for the start and end of the season in our specific study area. Using the TIMESAT graphical interface, we examined the resulting SOS and EOS for pixels within our study site that we are familiar with and chose a 30% threshold. Therefore, the start of the season (SOS) represents the onset of measurable photosynthesis or the onset of greenness, defined as a 30% increase on the rise of the smoothed NDVI curve measured from the left minimum level. On the contrary, the end of the season (EOS) indicates the cessation of measurable photosynthesis, marked by a 30% decrease on the right side of the smoothed NDVI curve in relation to the right minimum level. The length of the season (LOS) quantifies the duration of photosynthetic activity, ranging from SOS to EOS. Furthermore, we extracted other phenological variables, such as peak value, base value, and amplitude (Eklundh & Jonsson, 2015). The peak value indicates the highest recorded NDVI values during the season, representing the period of maximum photosynthesis. The base value is calculated by averaging the lowest values on both sides of the curve. Amplitude refers to the difference between the peak and base value (Eklundh & Jöhnsson, 2017).

The LSP metrics were extracted using TIMESAT v3.3 and a batch mode in Windows Command Prompt (CMD) for automation purposes. The time series raster LSP metrics were then post processed in R to convert pixel values to DOY (Day of the Year) to make it suitable for trend detection. Subsequently, the average for each raster LSP metrics over a period of 21 years was calculated. Furthermore, the annual average SOS, EOS, and LOS were extracted for the cropland, forest, grazing land, and shrub LULC classes in the LWD, UWD, and *dega*

agroecological zones. The division in the *weina dega* AEZ into lower (LWD) and upper (UWD) parts is aimed at capturing the spatial variation in LSP, as the lower part seems to resemble the kolla (warm, semi-arid) AEZ.

4.2.3.5. Trend analysis

Long-term shifts in phenology parameters can provide valuable insights into climate and land use changes (Davis et al., 2017). Since we are interested in exploring the relationship between LSP and climate change, we excluded areas where changes in LULC occurred to minimize uncertainties in the trends of LSP metrics resulting from such changes. We used the nearest neighbor resampling method to adjust the spatial resolution of the LULC data to match the spatial resolution of the LSP metrics derived from MODIS NDVI. This method was chosen because it preserves the original categorical values of the LULC data while ensuring spatial alignment of the pixels. Then we used the Mann-Kendall (MK) test to compute trends in the LSP parameters and determine their significance, while the Sen slope estimator is used to assess the magnitude of the trend (Davis et al., 2017; Mahmood et al., 2019). The Mann-Kendall statistic S is defined as:

$$S = \sum_{i=1}^{n-1} \sum_{j=i+1}^{n} \text{sgn}(xj - xi), \tag{6}$$

The sign function is given as:

$$sgn(x_j - x_i) = \begin{cases} +1, if\ x_j - x_i > 0 \\ 0, if\ x_j - x_i = 0 \\ -1, if\ x_j - x_i < 0 \end{cases}, \tag{7}$$

Where *n* is the number of data points, *xi* and *xj are* the data values in the time series i and j (j > i). If $S > 0$ indicates increasing trends, while $S < 0$ shows decreasing trends. The Sen slope estimator was used to measure the magnitude of trends (Sen, 1968). It is given as follows:

$$X_{ij} = \frac{(Y_j - Y_i)}{t_j - t_i} for\ \ i = 1, \ldots., N, \tag{8}$$

Where, X_{ij} slopes of the lines that connect each pair of points (t_i,Y_i) and (t_j,Y_j) where (t_j>t_i). A positive value of X_{ij}indicates an increasing trend, while a negative value indicates a declining trend (Gocic & Trajkovic, 2013).

4.2.3.6. Pixel-wise correlation coefficient

Correlation analysis is a commonly used method to evaluate the relationship between LSP metrics and climate variables, such as temperature and rainfall, as well as drought indices (Jeong et al., 2011; Luo et al., 2021; Ren et al., 2018; Tao et al., 2008). In this study, we specifically focus on pixel-wise correlations between LSP metrics and climate variables in the study area, treating each pixel as an independent unit of analysis. Since the analysis is conducted at the pixel level, spatial autocorrelation between neighboring pixels does not directly affect the correlation results. Although spatial autocorrelation may be relevant in global analyses, particularly when aggregating correlation coefficients across regions or making spatially generalized inferences, our study is descriptive and localized to pixel-level relationships. For this reason, we do not explicitly model spatial dependence.

In our study area, temperature and rainfall during the *belg* season are expected to influence the annual onset of greenness (SOS), whereas the climate conditions during the *kiremt* season could impact the EOS. Furthermore, it is expected that the annual temperature and rainfall variables will have an effect on the overall LOS. Therefore, Pearson correlation coefficients were calculated to determine the relationship between *belg* season temperature and rainfall with SOS, *kiremt* season temperature and rainfall with EOS, and annual temperature and rainfall with LOS. After resampling all climate variables to match the spatial resolution of the LSP metrics using the nearest neighbor method, the pixel-wise correlation coefficient (r_{xy}) was calculated using Equation (9).

$$r_{xy} = \frac{\sum_{i=1}^{n} (x_i - \bar{x})(y_i - \bar{y})}{\sqrt{\sum_{i=1}^{n} (x_i - \bar{x})^2}\sqrt{\sum_{i-1}^{n} (y_i - \bar{y})^2}}, \quad (9)$$

Where, x_i is the value of the i^{th}pixel in LSP metrics, y_i is the value of the i^{th} pixel in the climate variable, $\bar{x}$ is the mean LSP metrics of the i^{th}pixel, and $\bar{y}$ is the mean of the climate variable of the i^{th}pixel.Positive correlation coefficients ranging from 0-0.3, 0.3-0.5, and 0.5-1.00, in sequential order, indicate weak, moderate, and strong positive associations. Conversely, if the coefficients are negative, it indicates the presence of a negative relationship (Cohen et al., 2003). We also used partial correlation analysis to assess the effects of individual climate variables and drought indices while controlling for the influence of the others.

Due to the unavailability of gridded temperature data from EMI after 2018, we performed a correlation analysis between phenological metrics and temperature for the period 2001–2018. Furthermore, we performed a partial correlation analysis between phenological metrics and rainfall and temperature for the same period. For the correlation and partial correlation analysis between phenological metrics and drought indices, we used data that covered the entire period from 2001 to 2021.

4.3. Results

4.3.1. LULC change

As illustrated in Fig.4.3a-b, the study area is characterized by different LULC classes: cropland, forest, shrubland, grazing land, built-up, and water bodies. As seen from the figures, cropland encompasses more than half of the study area in both 2001 and 2021. The shrublands cover a large proportion next to croplands, accounting 20.3% and 19.5% in the years 2001 and 2021, respectively. The forest class is the third in terms of area coverage, accounting for 11.8% and 12.3% in 2001 and 2021, respectively. Most of the forests are found in *dega* agroecological zones. Built-up and water bodies classes cover a small proportion of the study area.

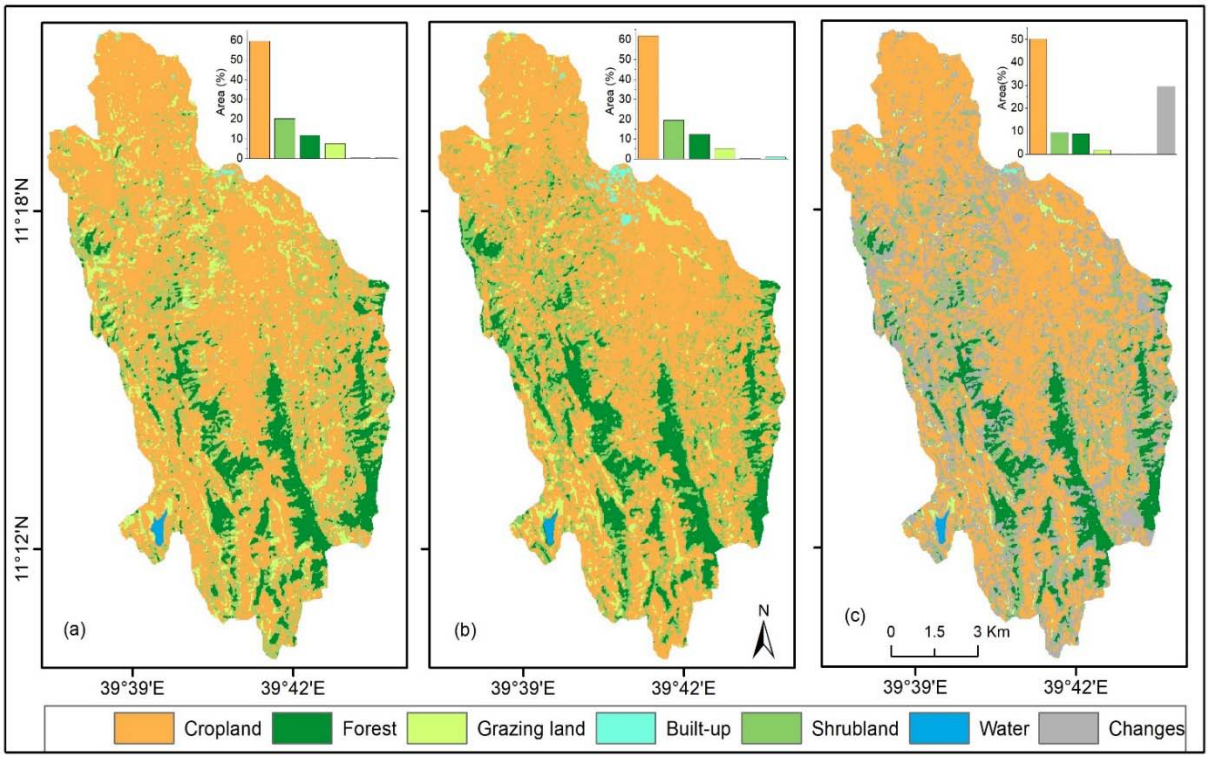

Fig. 4.3.LULC in 2001(a), 2021(b) and dynamics in between (c) in the upper Gelana Watershed

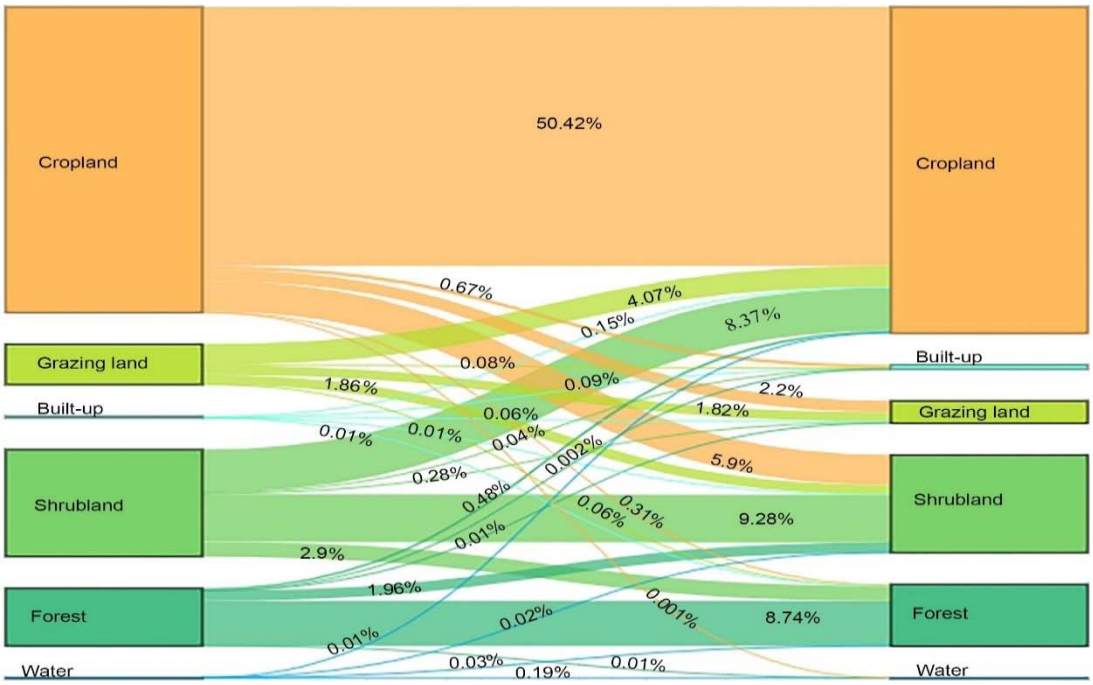

Fig. 4.4 Sankey diagram showing LULC changes matrix from the 2001(left) to 2021(right)

During the study period, the cropland, forest, and built-up LULC classes showed an increment of 2.3%, 0.5% and 0.6%, respectively. On the contrary, the grazing land, shrublands and water

bodies decreased by 2.4%, 0.8% and 0.2%, respectively. Fig.4.4, shows the proportion of land use conversion from one class to the other from 2001 to 2021. As seen in the figure, a significant conversion was observed between the cropland and shrub LULC classes.

4.3.2. Characteristics of LSP in the major LULC types across agroecological zones

During the study period (2001-2021), the mean SOS in the study area varied between 51 and 208 days (Fig.4.5a). The findings indicate that the season starts earlier in most of the *dega* and adjacent parts of the UWD. As depicted in Fig.4.5a, the early start of the season occurs in forested areas, mainly in the last week of February. Furthermore, the EOS ranges from 266 to 502 days (Fig.4.5b). The EOS days beyond 365 suggest that the growing season in a few pixels extended into the following year. During the study period, the mean LOS in the study area ranged from 186 to 295 days. As demonstrated in Fig.4.5c, the mean LOS is shorter in the LWD in the northern part, while it is longer in the *dega* agroecology zone in the southern parts of the study area. In the *dega* AEZ, characterized by relatively high altitudes, LOS was longer in the forested areas.

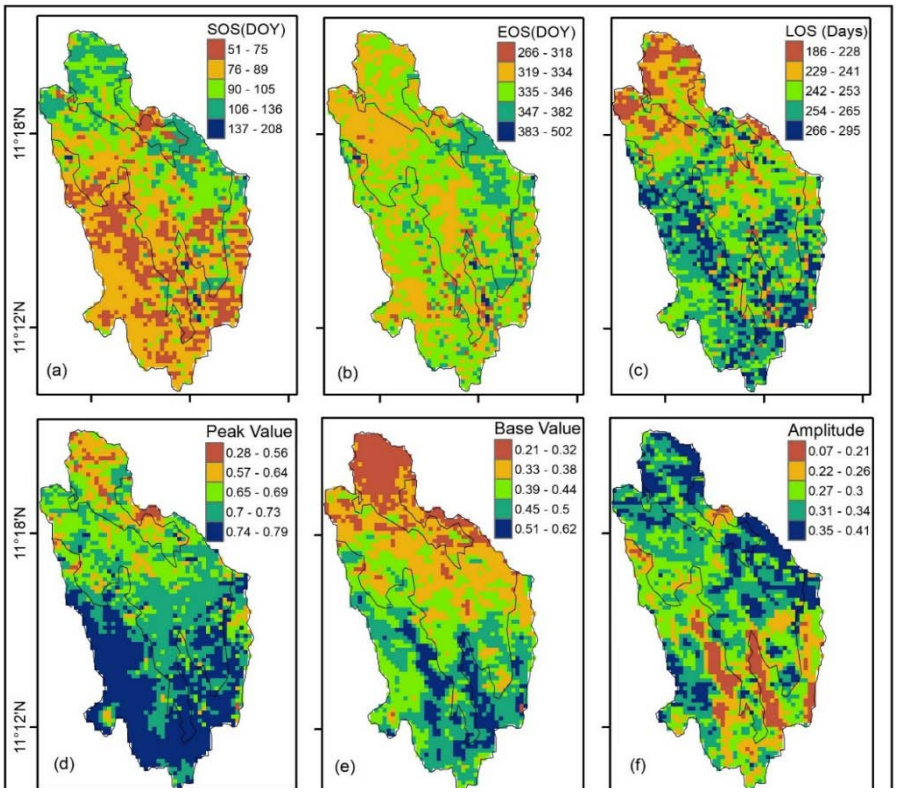

Fig. 4.5.Mean SOS (a), EOS (b), LOS (c), peak value (d), base value (e), and amplitude (f) from 2001 to 2021. Note: The higher value in the SOS indicates a late start of the season.

Similarly, we have analyzed the ecosystem condition indicators. The peak value, which represents the maximum NDVI of the growing season in Fig.4.5d, exhibits significant spatial variation across the study AEZs. It varies from 0.28 in the LWD to 0.79 in the *dega* AEZ. Similarly, the mean base value, which refers to the minimum NDVI values at the beginning of the season, varies between 0.21 in LWD and 0.62 in *dega* AEZ (Fig.4.6e). As shown in Fig.5f, the amplitude, which is an important indicator of ecosystem stability, also exhibits significant spatial variation in the study area. The amplitude values vary between 0.07 in the *dega* AEZ and 0.41 in the LWD AEZ of the study area. The lowest value of the amplitude was recorded in the forest LULC class in the *dega* AEZ.

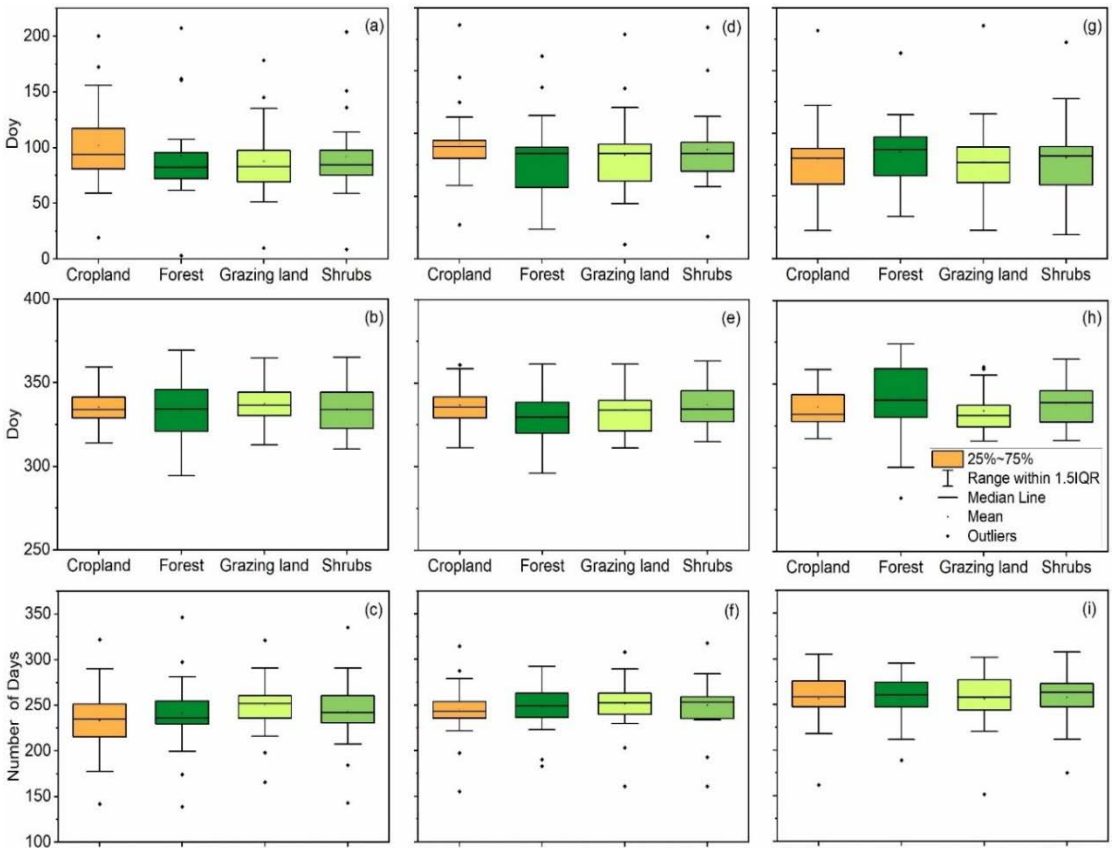

Fig. 4.6.Box plots of spatial average SOS, EOS and LOS by LULC categories in LWD (a-c), UWD (d-f), *dega* (g-h).

Fig.4.6 (a, d, g) shows the different SOS patterns in different LULC categories within the LWD, UWD, and *dega* AEZs of the study area, respectively. The cropland appears to experience late SOS in LWD and UWD than in the *dega* AEZ. The mean LOS for each LULC class exhibits variations across AEZs (Fig.4.6c, f, i). The figure shows that the grazing LULC class demonstrates a longer LOS while the cropland exhibits a relatively short LOS in the LWD and UWD AEZs. When comparing yearly LULC-specific LOS across the AEZs, it increases as we move from LWD to *dega*.As observed in the box plots, there are outliers present that suggest atypical patterns in SOS and LOS. For example, we identified the outliers for the years 2008, 2015, and 2021.

4.3.3. Spatiotemporal trends of LSP

As shown in Fig.4.7a, a significant portion of the study area exhibits an upward trend in SOS, indicating a delayed onset of greenness. This delay in the onset of greenness was observed in 71% of the pixels (Table 4.3). On the other hand, a decreasing trend in SOS was

observed in a small portion of the study area, mainly in built-up areas. A decrease in SOS was identified in nearly 6% of the pixels, while no discernible change detected for 22% of the pixels (Table 4.3).

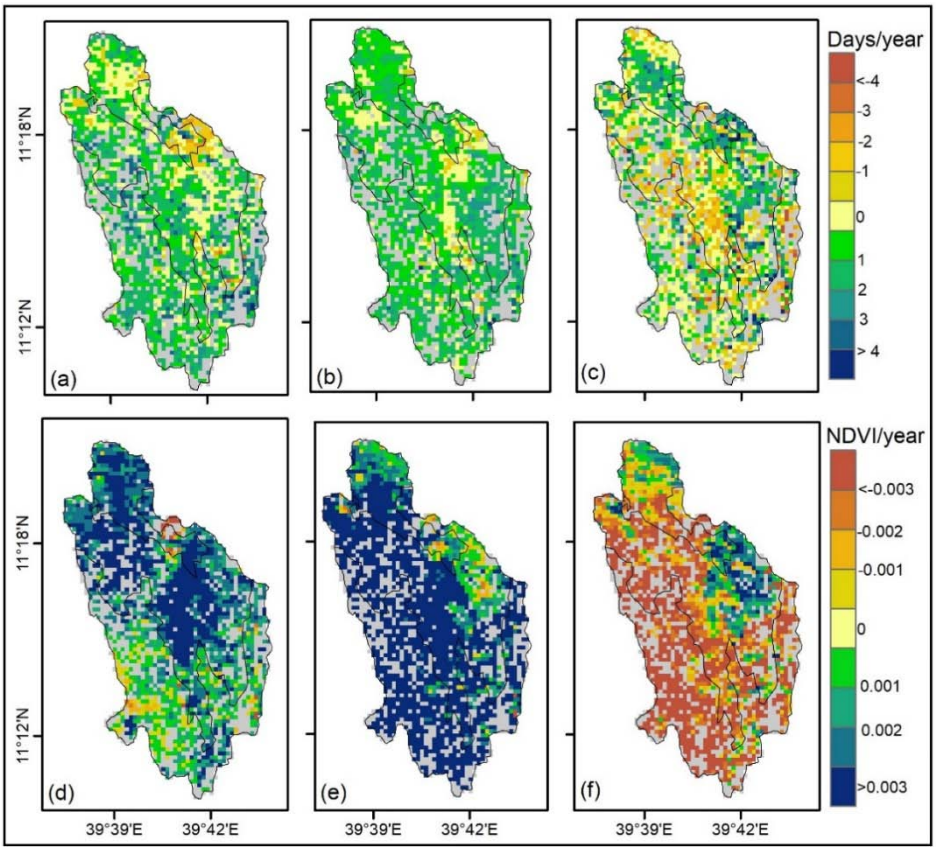

Fig. 4.7.Trends of the phenological metrics SOS (a), EOS (b), LOS (c), peak value (d), base value (e) and amplitude (f) from 2001to 2021. Trends are not valid in areas represented by grey colors in all the Sub-figures due to LULC changes.

Fig.4.7b shows that the EOS exhibits an upward trend in more than 80% of the pixels (Table 4.3). This upward trend in the EOS suggests an advancement of the end of the growing season. In addition, about 15% of the pixels, predominantly in UWD, do not show changes in EOS. Furthermore, an increasing trend in LOS was also observed in nearly 43% of the pixels, while a decreasing trend was evident in 29% (Fig.4.7c and Table 4.3). The remaining 28% of the pixels show no changes in LOS. As presented in Fig.4.7d-e and Table 4.3, the maximum NDVI (peak value) and the minimum NDVI (base value) exhibit a rising trend in more than 90% of the pixels. In contrast, the amplitude shows a decreasing trend in 81% of the pixels.

Table 4.3. Percentage of area that exhibits increasing, decreasing and no change in trends of LSP metrics.

	Area (%)		
LSP metrics	Increasing	Decreasing	No change
SOS	71.34	6.60	22.07
EOS	82.02	2.91	15.08
LOS	42.87	29.05	28.07
Peak value	90.42	9.38	0.20
Base value	95.64	4.24	0.12
Amplitude	18.92	81.00	0.08

4.3.4. Relationship between climate variables and land surface phenology

4.3.4.1. Correlation between SOS and climate variables

SOS exhibits moderate and strong positive associations with the maximum temperature of the *belg* season in 94% of the study area (Table 4.4 and Fig.4.8a). This percentage decreases slightly to 90% after controlling for the effects of the belg season minimum temperature and rainfall through partial correlation analysis (Fig.4.9a). As illustrated in the figure, the association remains moderate to strong in the LWD and UWD AEZ, indicating that an increase in maximum temperature tends to delay SOS. On the contrary, SOS exhibits a negative correlation with the *belg* season minimum temperature and rainfall in more than 80% of the pixels (Table 4.4 and Fig.4.8b-c). After controlling the effects of both minimum and maximum temperatures, SOS showed a negative association with rainfall in 74% of the area (Fig.4.9c). The relationship with minimum temperature is statistically significant and ranges from moderate to strong in most parts. Meanwhile, a weaker negative association with a declining *belg* rainfall is detected in significant portions particularly in *dega* AEZ. However, some pixels in the LWD and UWD AEZs exhibited a significant moderate association with the rainfall in the *belg* season.

Table 4.4.percentage of area for positive and negative correlations of SOS, EOS, and LOS with climate variables.

Climate Variables	SOS		EOS		LOS	
	+ve (%)	-ve (%)	+ve (%)	-ve (%)	+ve (%)	-ve (%)
Max	94	6	74	26	13	87
Min	3	97	21	79	63	37

Rain	12	88	61	39	71	29

4.3.4.2. Correlation between EOS and climate variables

In the spatial correlation patterns illustrated in Fig.8d-f, we found that a positive and negative association between EOS and the maximum and minimum temperatures of the *kiremt* season. As presented in Table 4.4, the correlation between EOS and maximum temperature was positive in 74% of the pixels. The partial correlation analysis in Fig.4.9d indicates that the proportion of the area showing a positive association has increased to 91.2%. On the other hand, we noted a negative correlation between EOS and minimum temperatures in a large proportion of the study area that accounts for 79% of the pixels.

The associations in both maximum and minimum temperatures are moderate in the southern parts mainly in *dega* AEZ; however, it is statistically significant in a very few pixels. Furthermore, EOS demonstrated a positive association with *kiremt* season rainfall in 61% of the pixels (Table 4.4 and Fig.4.8f), indicating that advances in EOS could be explained by the increasing rainfall patterns.

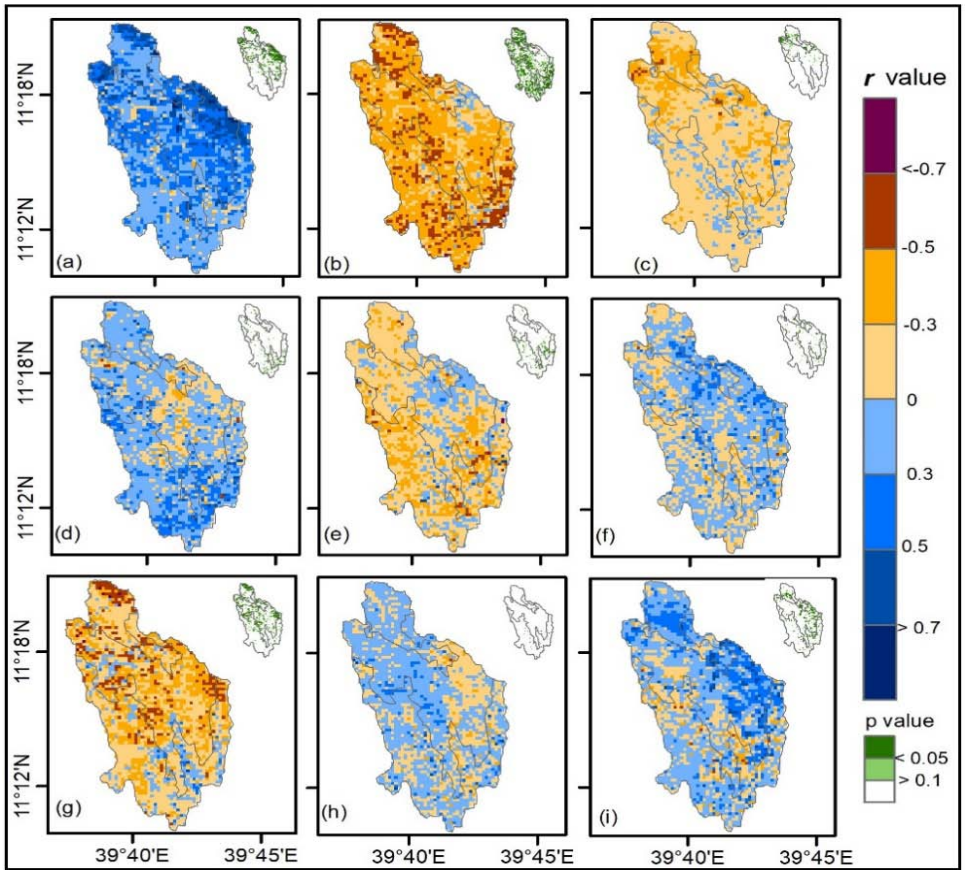

Fig. 4.8. Spatial patterns of correlation of SOS (a-c), EOS (d-f), and LOS (g-i) with maximum and minimum temperatures and rainfall. Note: correlation was computed for the climate variables of the *belg* season – SOS, the *kiremt* season – EOS and the annual mean – LOS pairs. The inset maps show the significance value (p).

The associations in both maximum and minimum temperatures are moderate in the southern parts mainly in *dega* AEZ; however, it is statistically significant in a very few pixels. Furthermore, EOS demonstrated a positive association with *kiremt* season rainfall in 61% of the pixels (Table 4.4 and Fig.4.8f), indicating that advances in EOS could be explained by the increasing rainfall patterns.

4.3.4.3. Correlation between LOS and climate variables

The LOS shows both positive and negative correlations with annual maximum and minimum temperatures, as observed in the spatial correlation patterns (Fig.4.8g-i). As presented in Table 4. 4, an inverse association between LOS and annual maximum temperature was detected in 87% of the pixels.The association is moderate and strong in most parts of LWD and UWD AEZs with statistical significance in some of the pixels. However,

when controlling for the effects of minimum temperature and annual rainfall through partial correlation analysis, the percentage of the area showing a negative association decreases slightly to 81% (Fig.4.9g). The findings indicate that as the maximum temperature rises, the length of season tends to decrease and vice versa. In contrast to this, LOS exhibited a weak positive association with minimum temperature. Furthermore, in 71% of the pixels, the LOS exhibited a positive correlation with annual rainfall.After controlling forthe effects of minimum and maximum temperatures, about 74% of the pixels exhibit a positive association between LOS and annual rainfall (Fig.4.9i). This suggests that as rainfall increases, there is a tendency for the length of the growing season to extend, indicating a potential influence of precipitation patterns on seasonal variation in LOS.

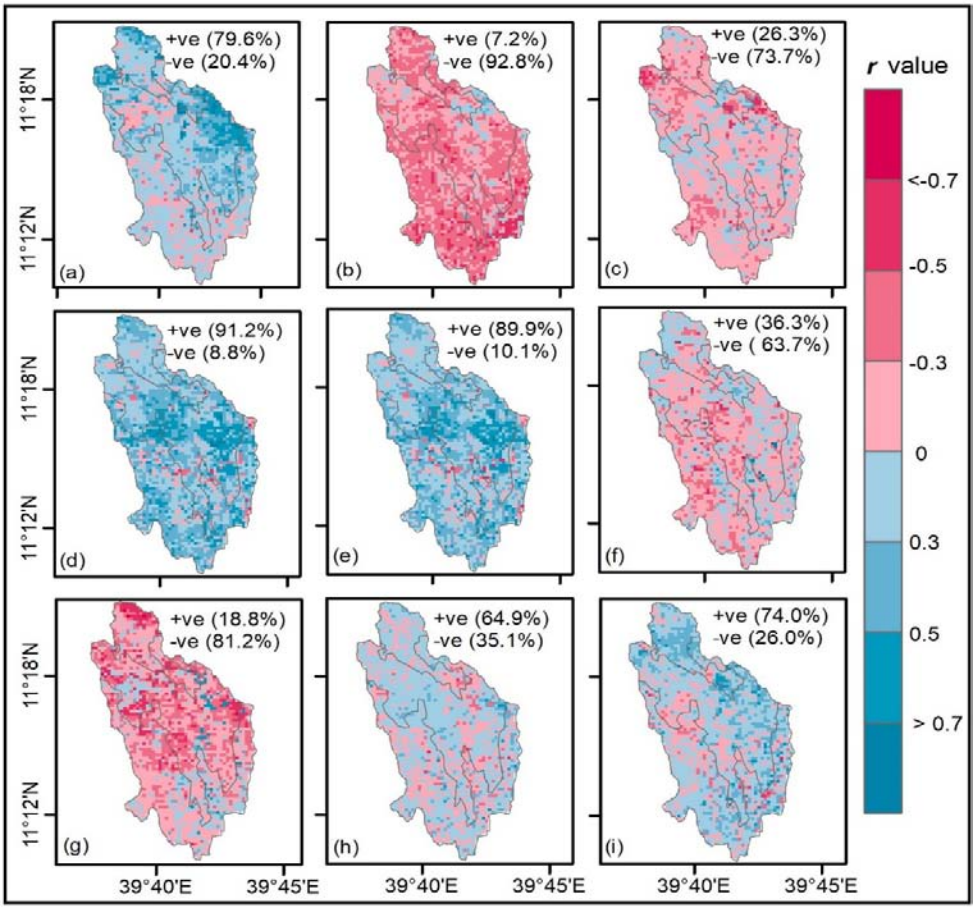

Fig. 4.9.Partial correlation of SOS (a-c), EOS (d-f), and LOS (g-i) with maximum and minimum temperatures and rainfall. Note: partial correlation was computed for climate variables of the *belg* season – SOS, the *kiremt* season – EOS and the annual mean – LOS pairs. The +ve and -ve represent positive and negative associations.

4.3.4.4. Correlations of SOS and EOS with drought indices

The SOS exhibited a negative correlation with *belg* season meteorological (SPI) and agricultural (ETDI and VHI) drought indices in more than 90% of the study area (Table 4.5 and Fig.4.10a-c). However, this figure decreased to 29% after controlling for the effects of agricultural drought indices (ETDI and VHI) (Fig.4.11a). This suggests that the negative impact of meteorological drought may become more pronounced when it is translated into agricultural drought. On the contrary, partial correlation analysis indicates that both agricultural drought indices (ETDI and VHI) exhibit a negative association with SOS in more than 75% of the study area (Fig.4.11b-c). The correlation analysis shows that EOS has a positive association with SPI in 61% of the pixels, which is reduced by half after controlling

the agricultural drought indices of the *kiremt* season (Fig.4.11d). On the other hand, EOS shows a positive correlation with ETDI and VHI in 83% of the study area. However, a partial correlation analysis reveals that the area proportion decreases to 61.4% and 66.3% for ETDI and VHI, respectively (Fig.4.11e-f). As illustrated in Fig.4.10a-c, a statistically significant moderate and strong association (at $p = 0.05$) was observed between SOS and the agricultural drought indices (ETDI and VHI) in large parts of the study area. We also found a moderate association between SOS and SPI in less than half of the study area, and this association was statistically significant only in a small proportion, particularly in the northern part of the study area. Moreover, the relationship between EOS and ETDI was found to be moderate in most parts of the LWD and UWD AEZs, with only a few of these associations being statistically significant. Furthermore, significant moderate and strong associations between EOS and VHI were identified in all AEZs.

Table 4.5. Percentage of area for positive and negative correlations of SOS and EOS with meteorological and agricultural drought indices.

Metrics	Drought indices	Positive (%)	Negative (%)
SOS	SPI	9	91
	ETDI	2	98
	VHI	3	97
EOS	SPI	61	39
	ETDI	83	17
	VHI	83	17

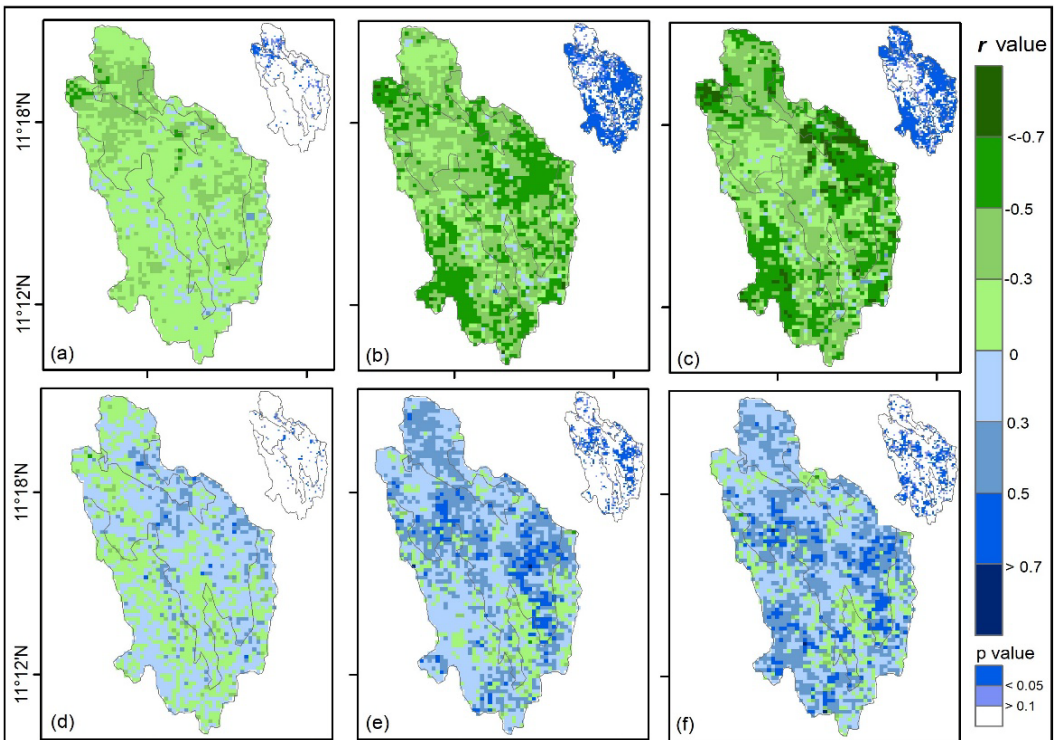

Fig. 4.10.Correlation of SOS (a-c) and EOS (d-f) with meteorological (SPI) and agricultural (ETDI and VHI) droughts. The inset maps indicate the significance values (p).

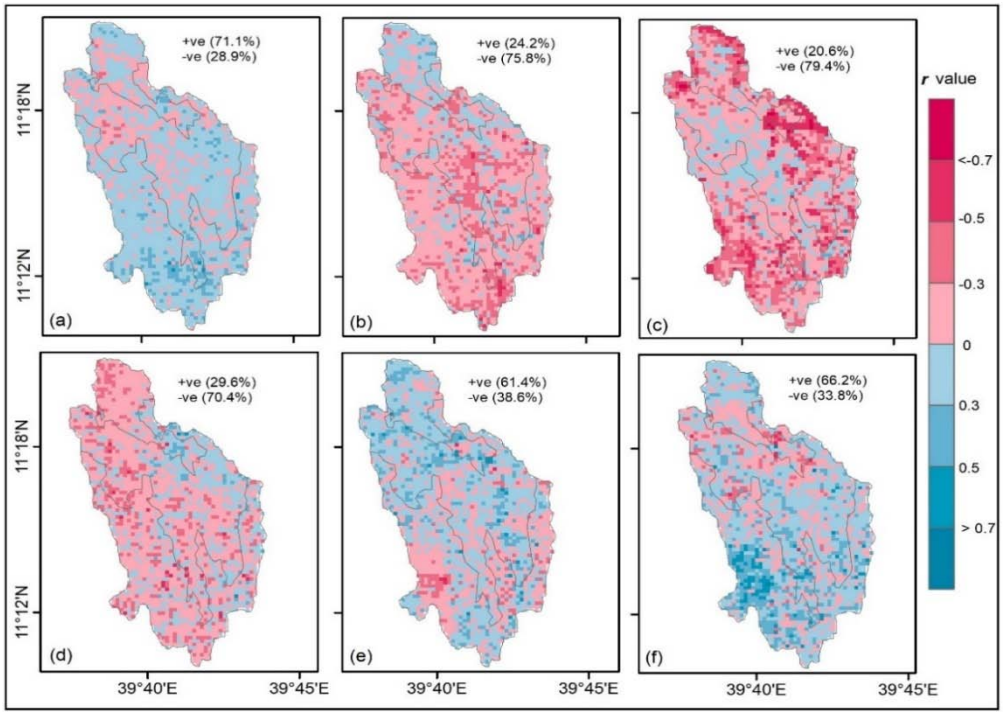

Fig. 4.11.Partial correlation of SOS (a-c) and EOS (d-f) with the SPI, ETDI and VHI drought indices, respectively.

4.4. Discussion

Phenology is a crucial indicator of changes in the timing of various stages of vegetation growth such as the start of greenness, peak growth, length, and termination of the growing season. Variability and changes in climate, such as deviations in rainfall and temperature from normal conditions (Legesse, 2016), can disrupt the proper timing of these critical stages of vegetation growth, which subsequently affects ecosystem productivity and services. Therefore, understanding the LSP is essential to safeguard the livelihoods of rural communities. It enables the implementation of appropriate measures in crop and livestock production and water management activities, such as rain water harvesting and soil moisture conservation, to adapt to seasonal variability and changes in climate, and maximize productivity.

4.4.1. Spatial variability and trends in LSP

The findings of our study revealed a spatial variation in the pixel-wise mean SOS from 2001 to 2021. The season starts relatively early in most parts of the *dega* and the adjacent parts of the UWD. In particular, a relatively early onset of greenness was observed in the forested areas.This could be attributed to the early onset of rain in the *dega* compared to other AEZs. However, an overall increasing trend was observed in SOS in a nearly three-fourth of the study area across the three AEZs from 2001 to 2021, suggesting a potential delay in the onset of growing season or greenness. The results are consistent with the findings of (Shi et al., 2023; Yang & Fan, 2023),who also identified delayed trends in SOS in South China. Similarly, (Kc et al., 2021; Liu et al., 2022; Peano et al., 2021; Shi et al., 2023) reported an overall delay in SOS on different spatial scales.

As stated in the results section, the upward trends of EOS in forest areas during the study period (2001-2021) can be attributed to various factors, such as high altitude, high rainfall, and lower temperatures. Collectively, these factors contribute to reduced moisture loss and extended periods of moisture availability.In addition, forests play a vital role in maintaining soil moisture levels through their canopy effects.Furthermore, these factors may explain the relatively longer LOS observed in forested areas.It is also important to note that the forests are predominantly located in the dega AEZ, and, as discussed earlier, the early onset of the growing season in this area may be considered an additional contributing factor. The findings of the study align with those of previous studies that have documented increasing trends in

EOS and LOS in various regions of the world (Jeong et al., 2011; Li et al., 2023; Li et al., 2020; Shi et al., 2023; Yang & Fan, 2023).

The spatial variation and trends in LSP metrics in LWD, UWD, and *dega* AEZs have significant implications on the overall conditions of the study area. Based on our field observations and information from agricultural extension workers, a significant focus has been given to sustainable land management activities in the high altitude (*dega*) and some adjacent parts of UWD. This has contributed to a relatively early SOS and longer LOS in these areas in addition to other natural factors that we mentioned in the previous section. In the remaining parts of UWD and LWD (low altitudes), forests are scarce, and soil and water conservations are not as intensive as in the *dega*. This left the soil exposed to the high temperature in the area, resulting in a high evaporation rate that in return leads to low soil moisture levels that contribute to a relatively shorter LOS. Interestingly, even in these AEZs, the presence of grass appears to have a positive impact on LOS.This is due to the fact that grass cover improves soil moisture retention compared to extensive croplands, especially after crop harvest (Atchley & Maxwell, 2011). Furthermore, the *dega* AEZ contributes to the flow of streams in the low-lying LWD and UWD AEZs which allows some smallholder farmers to use irrigation for grazing land located along the streams. This can be considered as an additional factor for a longer LOS in grazing land than the other LULC types in the LWD and UWD AEZs. In any way, these two conditions or scenarios are sufficient to emphasize the importance of soil and water conservation in improving soil water retention capacity and maintaining an extended duration of greenness as the two are directly related. Therefore, such activities should be widely practiced in other parts of the study area, similar to the *dega* AEZ.

As seen in the result section, the upward trends in base and peak value between 2001 and 2021 in more than 90% of the pixels indicates the improvements of greenness and may also signify improvements in ecosystem productivity of the study area. It is also worth noting that the decreasing trend in amplitude suggests a reduction in the disparity between the maximum NDVI and the base value over time. Furthermore, the relatively better conditions of the peak, base and amplitude values in *dega* compared to the other AEZs, can provide additional evidence of the efforts or effectiveness of sustainable land management activities, in addition to other environmental factors. Yet, these spatiotemporal variations of the trends are

suggestive that with a minimal effort or investment in land management, the ecosystem condition in LWD and UWD AEZs can also be improved.

4.4.2. LSP responses to climate variability and change

The association between SOS and both temperature and rainfall exhibits considerable variability across the study AEZs. The findings indicate that the delay in SOS was associated with warming trends in maximum temperature and decreasing in the minimum temperatures. Furthermore, the delay in SOS was associated with declining trend in the *belg* rain, although not as strong as temperature. The effects of rainfall appeared moderate and significant in some parts of the LWD and UWD AEZs, while they are weaker in the *dega* AEZ with some pixels exhibiting direct association. This may indicate that rainfall plays a significant role in areas where the temperature appears to be higher, such as in LWD and UWD, compared to dega agroecology. In a broader context, this emphasizes the importance of rainfall for an earlier start of SOS in tropical climates, as noted in previous studies (Borchert et al., 2005; Richardson et al., 2013). Similarly, Zhou et al. (2019) reported that decreased rainfall delayed plant phenology such as the date of flowering, and vice versa, in the arid and semi-arid regions of northern China. In contrast to its impact on advancing SOS in the temperate zone (Borchert et al., 2005; Huang et al., 2020; Richardson et al., 2013), the increase in maximum temperature appears to have a negative effect on SOS trends in the study area. The increasing temperature in these areas may result in higher evapotranspiration, leading to water stress. This situation can be further exacerbated by the decreasing trend in rainfall in *belg*, suggesting inadequate water availability for plants during the season. Our findings are consistent with (Shen et al., 2019), who observed a delay in the start of the growing season in the freshwater marshes of Northeast China due to reduced precipitation. However, our results contradict their findings regarding advances in SOS due to warming temperatures in some parts of their study area. Hao et al. (2016), also noted an inverse relationship, indicating that an increase in precipitation leads to earlier SOS, and vice versa.

In contrast to the effects of meteorological events on SOS, it appears that the rise in maximum temperature during the *kiremt* season has less impact on EOS in a substantial portion of the study area. This could be due to the fact that the *kiremt* season is the main rainy season in the area, and the evaporation caused by high temperature during this time does not have a pronounced effect on vegetation greenness. This can be further supported by the

observed direct association between the upward trends in EOS and precipitation during the *kiremt* season within a significant portion of the study area. This is in line with Liu et al. (2016) who found that an increase in summer temperature and rainfall was positively correlated with EOS in the northern hemisphere.Unlike EOS, the annual maximum temperature exhibits an inverse association with LOS, despite the rise in annual rainfall. This could be due to the cumulative effect that stems from variations in monthly distributions of the amount of rainfall (as it is related to the distribution of soil moisture) between the *kiremt* and annual timescales. For example, according to Tadesse et al. (2024), the months January to April exhibit a declining pattern of rainfall, coupled with an increase in maximum temperature. This suggests a substantial probability of increased evaporation as soil moisture decreases, thus contributing to the delay in SOS and the reduction of LOS. Some of the associations are moderate and statistically significant in some parts of the LWD and UWD AEZs. Our findings align with the study conducted by Hao et al. (2016),which highlights the importance of precipitation as a climatic factor in prolonging LOS. However, our results contradict the findings of Tang et al. (2015), who observed a positive correlation between temperature and longer LOS.

Drought can have a significant impact on vegetation and leads to abrupt changes in phenology (Ma et al., 2015). The findings of the correlation between SOS and both the meteorological and agricultural drought indices imply the possible impacts of drought conditions on the onset of greenness in almost all parts of the study area. The negative impacts of *belg* season meteorological drought become more pronounced when it translates into agricultural droughts. In particular, delays in spatially averaged SOS were identified in the years 2008, 2015, and 2021 for all LULC types across all AEZs. These delays coincide with meteorological and agricultural drought events that have affected the study area (Tadesse & Mekuriaw, 2024).On the other hand, advances in EOS were directly correlated with increased values of the meteorological and agricultural drought indices. This means that higher values of the indices indicate lower drought events, which positively affect EOS (Currier & Sala, 2022). Controlling for agricultural drought indices, the effect of SPI on the advancement of EOS decreased to a small area, while agricultural drought indices were associated with advances in EOS in more than half of the study area. Delays in SOS are expected during drought years due to limited availability of soil moisture. Under such

conditions, the scarcity of moisture negatively affects plant growth, resulting in a noticeable change in the timing of vegetation greenness, as evidenced by the findings. This observation is further supported by the direct correlation between the increasing EOS and *kiremt* season drought indices, which according to Tadesse & Mekuriaw (2024), indicates less pronounced droughts compared to the *belg* season.

The findings shed light on the mechanistic relationship between vegetation phenology and climate variability. Rising temperatures have been shown to significantly impact the start of the growing season, particularly when accompanied by insufficient rainfall. On the contrary, adequate rainfall along with elevated maximum temperatures can mitigate these adverse effects, highlighting the vital role of water availability in alleviating temperature-induced stress during critical growth periods. Furthermore, the findings reveal that meteorological drought alone may not severely disrupt plant growth and development unless it is translated into agricultural drought, highlighting the importance of soil moisture in sustaining vegetation greenness and productivity under changing climatic conditions.

4.4.3. Limitation of the study

The findings of this study provide valuable insights on monitoring LSP changes in response to climate change. However, uncertainties may affect the accuracy of the results. A significant source of uncertainty may arise from the relatively low spatial resolution of the NDVI data (Shen et al., 2021; Wang et al., 2021), which may not adequately capture the spatial variability of the phenological metrics within the study area, potentially oversimplifying observed patterns. Additionally, landscape-wide monitoring often captures only general trends, making it difficult to reflect finer species-level dynamics and specific land uses, such as irrigation practices in very small plots. Furthermore, while remote sensing-based findings of LSP results are valuable, their reliability can be significantly improved through validation with ground-based data.

To address these challenges, future studies in the study area should consider fusing high-temporal-resolution satellite imagery, such as MODIS, with medium-spatial-resolution imagery, such as Landsat and Sentinel. This approach allows for a balance between temporal frequency and spatial detail in monitoring vegetation changes. Furthermore, efforts to monitor phenological changes using ground-based instruments, such as phenocam, would help

validate satellite imagery-based findings. Implementing these methods can increase the reliability of future research findings and their applicability to agriculture and other related sectors in the study area.

4.5. Conclusions

This study investigated the dynamics of LULC and land surface phenology response to climate variability and change between 2001 and 2021. Our findings indicate that more than half of the study area is dedicated to croplands, with notable conversions occurring between croplands and shrublands. The spatial variability of the land surface phenology shows that the *dega* AEZ exhibits a relatively early SOS and a long LOS compared to the UWD and LWD AEZs. Additionally, we identified relatively higher values of key indicators of ecosystem condition, such as the peak (maximum NDVI) and the base value, in large part of the *dega* AEZ. These values gradually decrease as one moves towards the LWD AEZs, whereas the opposite is observed for the amplitude. The forest land cover exhibits a high peak and base value, as well as a lower amplitude, indicating the stability of the forest ecosystem.

Furthermore, we found an increasing trend for SOS and EOS between 2001 and 2021 in more than three-quarters of the study area, indicating a delay in both parameters. Furthermore, approximately half of the study area exhibited an upward trend in LOS. The peak and base values also showed an increasing trend, whereas the amplitude decreased in most parts of the study area.

The SOS and EOS showed a positive correlation with maximum temperature in most parts of the study area.This implies that the maximum temperature during the *belg* season could explain the delay in SOS, whereas the maximum temperature during the *kiremt* season has a lesser impact on EOS due to the high amount of rainfall during that period. Furthermore, SOS was found to have an inverse correlation with the *belg* season rainfall, meteorological and agricultural drought indices, while EOS demonstrated a direct association with the *kiremt* season rainfall, meteorological and agricultural drought indices. This indicates that a decrease in *belg* season rainfall postpones the start of the season, whereas an increase in *kiremt* season rainfall advances the end of the season. Furthermore, an increase in annual maximum temperature could shorten the LOS, while an increase in annual rainfall could prolong it.

The findings of this study offer valuable insight into the timing of land surface phenology events in the upper Gelana watershed, in relation to changing climate conditions.The observed

variations in LSP metrics and their responses to climate change and variability between *dega*, UWD, and LWD AEZs highlight the importance of soil and water conservation practices. These findings will improve understanding and awareness among rural communities and stakeholders about the importance of implementing adaptation strategies, specifically soil and water conservation practices such as terraces, bunds, perennial crop introduction, irrigation, reforestation, and afforestation. These strategies will help minimize the adverse effects of climate change on agricultural activities and the ecosystem at large.

References

Adole, T., Dash, J., & Atkinson, P. M. (2016). A systematic review of vegetation phenology in Africa. *Ecological Informatics*, *34*, 117–128. https://doi.org/10.1016/j.ecoinf.2016.05.004

Alemayehu, B., Suarez-Minguez, J., Rosette, J., & Khan, S. A. (2023). Vegetation Trend Detection Using Time Series Satellite Data as Ecosystem Condition Indicators for Analysis in the Northwestern Highlands of Ethiopia. *Remote Sensing*, *15*(20). https://doi.org/10.3390/rs15205032

Almeida, J., Dos Santos, J. A., Alberton, B., Torres, R. da S., & Morellato, L. P. C. (2014). Applying machine learning based on multiscale classifiers to detect remote phenology patterns in Cerrado savanna trees. *Ecological Informatics*, *23*, 49–61. https://doi.org/10.1016/j.ecoinf.2013.06.011

Araya, S., Ostendorf, B., Lyle, G., & Lewis, M. (2018). CropPhenology: An R package for extracting crop phenology from time series remotely sensed vegetation index imagery. *Ecological Informatics*, *46*. https://doi.org/10.1016/j.ecoinf.2018.05.006

Atchley, A. L., & Maxwell, R. M. (2011). Influences of subsurface heterogeneity and vegetation cover on soil moisture , surface temperature and evapotranspiration at hillslope scales. *Hydrogeology Journal*, *19*, 289–305. https://doi.org/10.1007/s10040-010-0690-1

Badeck, F. W., Bondeau, A., Böttcher, K., Doktor, D., Lucht, W., Schaber, J., & Sitch, S. (2004). Responses of spring phenology to climate change. *New Phytologist*, *162*, 295–309. https://doi.org/10.1111/j.1469-8137.2004.01059.x

Bannari, A., Morin, D., Bonn, F., & Huete, A. R. (1995). A review of vegetation indices. *Remote Sensing Reviews*, *13*(1–2), 95–120. https://doi.org/10.1080/02757259509532298

Belgiu, M., & Dra, L. (2016). Random forest in remote sensing : A review of applications and future directions. *ISPRS Journal of Photogrammetry and Remote Sensing*, *114*, 24–31. https://doi.org/10.1016/j.isprsjprs.2016.01.011

Borchert, R., Robertson, K., Schwartz, M. D., & Williams-Linera, G. (2005). Phenology of temperate trees in tropical climates. *International Journal of Biometeorology*, *50*, 57–65. https://doi.org/10.1007/s00484-005-0261-7

Breiman, L. (2001). Random forests. *Machine Learning*, *45*(1), 5–32.

Busetto, L., & Ranghetti, L. (2016). MODIStsp : an R package for automatic preprocessing of MODIS Land Products time series. *Computers and Geosciences*, *97*, 40–48. https://doi.org/10.1016/j.cageo.2016.08.020

Caparros-santiago, A, J., & Victor Dash, J. (2021). Land surface phenology as indicator of global terrestrial ecosystem dynamics: A systematic review. *ISPRS Journal of Photogrammetry and Remote Sensing*, *171*, 330–347. https://doi.org/10.1016/j.isprsjprs.2020.11.019

Caparros-Santiago, J. A., Quesada-Ruiz, L. C., & Rodriguez-Galiano, V. (2023). Can land surface phenology from Sentinel-2 time-series be used as an indicator of Macaronesian ecosystem dynamics? *Ecological Informatics*, *77*. https://doi.org/10.1016/j.ecoinf.2023.102239

Chen, J., Jönsson, P., Tamura, M., Gu, Z., Matsushita, B., & Eklundh, L. (2004). A simple method for reconstructing a high-quality NDVI time-series data set based on the Savitzky-Golay filter. *Remote Sensing of Environment*, *91*, 332–344. https://doi.org/10.1016/j.rse.2004.03.014

Cheng, Y., Vrieling, A., Fava, F., Meroni, M., Marshall, M., & Gachoki, S. (2020). Phenology of short vegetation cycles in a Kenyan rangeland from PlanetScope and Sentinel-2. *Remote Sensing of Environment*, *248*. https://doi.org/10.1016/j.rse.2020.112004

Cleland, E. E., Chuine, I., Menzel, A., Mooney, H. A., & Schwartz, M. D. (2007). Shifting plant phenology in response to global change. *TRENDS in Ecology and Evolution*, *22*(7). https://doi.org/10.1016/j.tree.2007.04.003

Clinton, N., Yu, L., Fu, H. H., He, C. H., & Gong, P. (2014). Global-Scale Associations of Vegetation Phenology with Rainfall and Temperature at a High Spatio-Temporal Resolution. *Remote Sensing*, *6*, 7320–7338. https://doi.org/10.3390/rs6087320

Cohen, J., Cohen, P., West, S. G., & Aiken, L. S. (2003). *Applied Multiple Regression/Correlation Analysis for the Behavioral Sciences*. Lawrence Erlbaum Associates.

Currier, C. M., & Sala, O. E. (2022). Precipitation versus temperature as phenology controls in drylands. *Ecology*, *103*, e3793. https://doi.org/10.1002/ecy.3793

Dagnachew, M., Kebede, A., Moges, A., & Abebe, A. (2020). Effects of Climate Variability on Normalized Difference Vegetation Index (NDVI) in the Gojeb River Catchment, Omo-Gibe Basin, Ethiopia. *Advances in Meteorology*, *2020*. https://doi.org/10.1155/2020/8263246

Davis, C. L., Hoffman, M. T., & Roberts, W. (2017). Long-term trends in vegetation phenology and productivity over Namaqualand using the GIMMS AVHRR NDVI3g data from 1982 to 2011. *South African Journal of Botany*, *111*, 76–85. https://doi.org/10.1016/j.sajb.2017.03.007

de Beurs, K. M., & Henebry, G. M. (2005). Land surface phenology and temperature variation in the International Geosphere-Biosphere Program high-latitude transects. *Global Change Biology*, *11*, 779–790. https://doi.org/10.1111/j.1365-2486.2005.00949.x

Degife, A. W., Zabel, F., & Mauser, W. (2021). Climate change impacts on potential maize yields in Gambella,Ethiopia. *Regional Environmental Change*, *21*(60). https://doi.org/10.1007/s10113-021-01773-3

Descals, A., Verger, A., Yin, G., & Peñuelas, J. (2021). A Threshold Method for Robust and Fast Estimation of Land-Surface Phenology Using Google Earth Engine. *IEEE Journal of Selected Topics in Applied Earth Observations and Remote Sensing*, *14*, 601–606. https://doi.org/10.1109/JSTARS.2020.3039554

Du, J., He, Z., Yang, J., Chen, L., & Zhu, X. (2014). Detecting the effects of climate change on canopy phenology in coniferous forests in semi-arid mountain regions of China. *International Journal of Remote Sensing*, *35*(17), 6490–6507. https://doi.org/10.1080/01431161.2014.955146

Egeru, A., Magaya, J. P., Kuule, D. A., Siya, A., Gidudu, A., Barasa, B., & Namaalwa, J. J. (2020). Savannah Phenological Dynamics Reveal Spatio-Temporal Landscape Heterogeneity in Karamoja. *Front. Sustain. Food Syst.*, *4*(541170). https://doi.org/10.3389/fsufs.2020.541170

Eklundh, L., & Jöhnsson, P. (2017). *TIMESAT 3.3 with seasonal trend decomposition and parallel processing Software Manual*. 1–92.

Eklundh, L., & Jonsson, P. (2015). TIMESAT: A Software Package for Time-Series Processing and Assessment of Vegetation Dynamics. In K. et Al (Ed.), *Remote Sensing Time Series. Remote Sensing and Digital Image Processing* (Vol. 22, pp. 141–158). Springer, Cham. https://doi.org/10.1007/978-3-319-15967-6_7

El-Kawy, O. A., Rød, J., Ismail, H., & KissSuliman, A. (2011). Land use and land cover change detection in the western Nile delta of Egypt using remote sensing data. *Applied Geography*, *31*, 483–494. https://doi.org/10.1016/j.apgeog.2010.10.012, 2011

Ethiopian Mapping Agency (EMA). (2018). *Ethiopian Land Use Land Cover Classification and Coding Standard*.

Federal Democratic Republic of Ethiopia (FDRE). (2016). *Ethiopia's Forest Reference Level Submission to the UNFCCC*.

Fitchett, J. M., Grab, S. W., & Thompson, D. I. (2015). Plant phenology and climate change: Progress in methodological approaches and application. *Progress in Physical Geography*, *39*(4), 460–482. https://doi.org/10.1177/0309133315578940

Geremew, T., & Jebessa, H. (2018). Climate change and its effects on vegetation phenology across ecoregions of Ethiopia. *Global Ecology and Conservation*, *13*. https://doi.org/10.1016/j.gecco.2017.e00366

Ghinassi, M., D'Oriano, F., Benvenuti, M., Awramik, S., Bartolini, C., Fedi, M., Ferrari, G., Papini, M., Sagri, M., & Talbot, M. (2012). Shoreline fluctuations of Lake Hayk (northern Ethiopia) during the last 3500years: Geomorphological, sedimentary, and isotope records. *Palaeogeography, Palaeoclimatology, Palaeoecology*, *365–366*, 209–226. https://doi.org/10.1016/j.palaeo.2012.09.029

Glade, F. E., Miranda, M. D., Meza, F. J., & Leeuwen, W. J. D. Van. (2016). Productivity and phenological responses of natural vegetation to present and future inter-annual climate variability across semi-arid river basins in Chile. *Environ Monit Assess*, *188*(676). https://doi.org/10.1007/s10661-016-5675-7

Gocic, M., & Trajkovic, S. (2013). Analysis of changes in meteorological variables using Mann-Kendall and Sen's slope estimator statistical tests in Serbia. *Global and Planetary Change*, *100*, 172–182. https://doi.org/10.1016/j.gloplacha.2012.10.014

Han, F., Zhang, Q., Buyantuev, A., Niu, J., Liu, P., Li, X., Kang, S., Zhang, J., Chang, C., & Li, Y. (2015). Effects of climate change on phenology and primary productivity in the desert steppe of Inner Mongolia. *J Arid Land*, *7*(2), 251–263. https://doi.org/10.1007/s40333-014-0042-4

Hao, G., Guo-hua, L., Zong-shan, L., Xin, Y., Meng, W., & Li, G. (2016). Driving force and changing trends of vegetation phenology in the Loess Plateau of Chinna from 2000 to 2010. *J. Mt. Sci.*, *13*(5), 844–856. https://doi.org/10.10007/s11629-015-3465-2

Hijmans, R. J. (2022). *raster: Geographic Data Analysis and Modeling* (R package version 3.5-15).

Huang, Y., Jiang, N., Shen, M., & Guo, L. (2020). Effect of preseason diurnal temperature range on the start of vegetation growing season in the Northern Hemisphere. *Ecological Indicators*, *112*, 106161. https://doi.org/10.1016/j.ecolind.2020.106161

Hurni, H. (1998). *Agroecological Belts of Ethiopia: Explanatory Notes on Three Maps at Scale of 1:1, 000,000*. Soil Conservation Research Programme and Centre for Development and Environment.

Hussien, K., Kebede, A., Mekuriaw, A., Beza, S. A., & Erena, S. H. (2023). Spatiotemporal trends of NDVI and its response to climate variability in the Abbay River Basin , Ethiopia. *Heliyon*, *9*. https://doi.org/10.1016/j.heliyon.2023.e14113

Hwang, T., Song, C., & Vose, J. M. (2011). *Topography-mediated controls on local vegetation phenology estimated from MODIS vegetation index*. 541–556. https://doi.org/10.1007/s10980-011-9580-8

Jeong, S.-J., Ho, C.-H., Gim, H.-J., & Brown, M. (2011). Phenology shifts at start vs . end of growing season in temperate vegetation over the Northern Hemisphere for the period 1982 – 2008. *Global Change Biology*, *17*, 2385–2399. https://doi.org/10.1111/j.1365-2486.2011.02397.x

Jin, H., Jönsson, A. M., Olsson, C., Lindström, J., Jönsson, P., & Eklundh, L. (2019). New satellite-based estimates show significant trends in spring phenology and complex sensitivities to temperature and precipitation at northern European latitudes. *International Journal of Biometeorology*, *63*, 763–775. https://doi.org/10.1007/s00484-019-01690-5

Jönsson, P., & Eklundh, L. (2002). Seasonality extraction by function fitting to time-series of satellite sensor data. *IEEE Transactions on Geoscience and Remote Sensing*, *40*(8), 1824–1832. https://doi.org/10.1109/TGRS.2002.802519

Jonsson, P., & Eklundh, L. (2004). TIMESAT — a program for analyzing time-series of satellite sensor data. *Computers & Geosciences*, *30*, 833–845. https://doi.org/10.1016/j.cageo.2004.05.006

Kariyeva, J., & Van Leeuwen, W. J. D. (2011). Environmental Drivers of NDVI-Based Vegetation Phenology in Central Asia. *Remote Sensing*, *3*, 203–246. https://doi.org/10.3390/rs3020203

Kariyeva, J., van Leeuwen, W. J. D., & Woodhouse, C. A. (2012). Impacts of climate gradients on the vegetation phenology of major land use types in Central Asia (1981–2008). *Frontiers of Earth Science*, *6*, 206–225. https://doi.org/10.1007/s11707- 012-0315-1

Kc, A., Acharya, T. D., Wagle, N., & Lee, D. H. (2021). Tracking Long-term Phenological Shift in Response to Climatic Parameters in Chitwan National Park , Nepal. *Sensors and Materials*, *33*(11), 3787–3799. https://doi.org/10.18494/SAM.2021.3449

Legesse, S. A. (2016). The outlook of Ethiopian long rain season from the global circulation model. *Environmental Systems Research*, *5*(16). https://doi.org/10.1186/s40068-016-0066-1

Li, X., Du, H., Zhou, G., Mao, F., Zhu, D., Zhang, M., Xu, Y., Zhou, L., & Huang, Z. (2023). Spatiotemporal patterns of remotely sensed phenology and their response to climate change and topography in subtropical bamboo forests during 2001-2017 : a case study in Zhejiang Province, China. *GIScience & Remote Sensing*, *60*(1). https://doi.org/10.1080/15481603.2022.2163575

Li, Y., Qin, Y., & Pan, Z. (2020). Climate change: vegetation and phenological phase dynamics. *International Journal of Climate Change Strategies and Management*, *12*(4), 495–509. https://doi.org/10.1108/IJCCSM-06-2019-0037

Liu, E., Zhou, G., He, Q., Wu, B., Zhou, H., & Gu, W. (2022). Climatic Mechanism of Delaying the Start and Advancing the End of the Growing Season of Stipa krylovii in a Semi-Arid. *Agronomy*, *12*, 1906. https://doi.org/10.3390/agronomy12081906

Liu, Q., Fu, Y. H., Zhu, Z., Liu, Y., & Liu, Z. (2016). Delayed autumn phenology in the Northern Hemisphere is related to change in both climate and spring phenology. *Global Change Biology*, *22*, 3702–3711. https://doi.org/10.1111/gcb.13311

Liu, Y., Shen, X., Zhang, J., Wang, Y., Wu, L., Ma, R., Lu, X., & Jiang, M. (2023). Variation in Vegetation Phenology and Its Response to Climate Change in Marshes of Inner Mongolian. *Plants*, *12*. https://doi.org/10.3390/plants12112072

Luo, M., Meng, F., Sa, C., Duan, Y., Bao, Y., Liu, T., & De Maeyer, P. (2021). Response of vegetation phenology to soil moisture dynamics in the Mongolian Plateau. *Catena*, *206*. https://doi.org/10.1016/j.catena.2021.105505

Ma, X., Huete, A., Moran, S., Ponce-campos, G., & Eamus, D. (2015). Abrupt shifts in phenology and vegetation productivity under climate extremes. *Journal of Geophysical Research: Biogeosciences*, *120*, 2036–2052. https://doi.org/10.1002/2015JG003144

Mahmood, R., Jia, S., & Zhu, W. (2019). Analysis of climate variability,trends, and prediction in the most active parts of the Lake Chad basin, Africa. *Scientific Reports*, *9*(6317). https://doi.org/10.1038/s41598-019-42811-9

Maidment, R. I., Grimes, D., Allan, R. P., Tarnavsky, E., Marcstringer, M., Hewison, T., Roebeling, R., & Black, E. (2014). The 30-year TAMSAT african rainfall climatology

and time series (TARCAT) data set. *Journal of Geophysical Research*, *119*(18), 10619–10644. https://doi.org/10.1002/2014JD021927

Maxwell, A. E., Warner, T. A., & Fang, F. (2018). Implementation of machine-learning classification in remote sensing: an applied review sensing: an applied review. *International Journal of Remote Sensing*, *39*(9), 2784–2817. https://doi.org/10.1080/01431161.2018.1433343

Mekuriaw, A. (2017). Assessing the effectiveness of land resource management practices on erosion and vegetative cover using GIS and remote sensing techniques in Melaka watershed. *Environmental Systems Research*, *6*(16). https://doi.org/10.1186/s40068-017-0093-6

Muir, C., Southworth, J., Khatami, R., Herrero, H., & Akyapı, B. (2021). Vegetation dynamics and climatological drivers in ethiopia at the turn of the century. *Remote Sensing*, *13*. https://doi.org/10.3390/rs13163267

Olofsson, P., Foody, G. M., Herold, M., Stehman, S. V, Woodcock, C. E., & Wulder, M. A. (2014). Good practices for estimating area and assessing accuracy of land change. *Remote Sensing of Environment*, *148*, 42–57. https://doi.org/10.1016/j.rse.2014.02.015

Olofsson, P., Foody, G. M., Stehman, S. V., & Woodcock, C. E. (2013). Making better use of accuracy data in land change studies: Estimating accuracy and area and quantifying uncertainty using stratified estimation. *Remote Sensing of Environment*, *129*, 122–131. https://doi.org/10.1016/j.rse.2012.10.031

Parmar, A., Katariya, R., & Patel, V. (2019). A Review on Random Forest: An Ensemble Classifier. In Hemanth et al. (Ed.), *ICICI 2018, LNDECT* (Vol. 26, pp. 758–763). Springer Nature. https://doi.org/10.1007/978-3-030-03146-6_86

Peano, D., Hemming, D., Materia, S., Delire, C., Fan, Y., Joetzjer, E., Lee, H., Nabel, J. E. M. S., Park, T., Peylin, P., Wårlind, D., & Wiltshire, A. (2021). Plant phenology evaluation of CRESCENDO land surface models – Part 1: Start and end of the growing season. *Biogeosciences*, *18*, 2405–2428. https://doi.org/10.5194/bg-18-2405-2021

Rao, Y., Zhu, X., Chen, J., & Wang, J. (2015). An improved method for producing high spatial-resolution NDVI time series datasets with multi-temporal MODIS NDVI data and Landsat TM/ETM+ images. *Remote Sensing*, *7*, 7865–7891. https://doi.org/10.3390/rs70607865

Ren, S., Yi, S., Peichl, M., & Wang, X. (2018). Diverse responses of vegetation phenology to climate change in different Grasslands in Inner Mongolia during 2000-2016. *Remote Sensing*, *10*. https://doi.org/10.3390/rs10010017

Rettie, F. M., Gayler, S., Weber, T. K. D., Tesfaye, K., & Streck, T. (2022). Climate change impact on wheat and maize growth in Ethiopia: A multi-model uncertainty analysis. *PLoS ONE*, *17*(1). https://doi.org/10.1371/journal.pone.0262951

Revadekar, J. V., Tiwari, Y. K., & Kumar, K. R. (2012). Impact of climate variability on NDVI over the Indian region during 1981-2010. *International Journal of Remote Sensing*, *33*(22), 7132–7150. https://doi.org/10.1080/01431161.2012.697642

Richardson, A. D., Keenan, T. F., Migliavacca, M., Ryu, Y., Sonnentag, O., & Toomey, M. (2013). Climate change, phenology, and phenological control of vegetation feedbacks to the climate system. *Agricultural and Forest Meteorology*, *169*, 156–173. https://doi.org/10.1016/j.agrformet.2012.09.012

Rishmawi, K., Prince, S. D., & Xue, Y. (2016). Vegetation Responses to Climate Variability in the Northern Arid to Sub-Humid Zones of Sub-Saharan Africa. *Remote Sensing*, *8*(910). https://doi.org/10.3390/rs8110910

Rodriguez-galiano, V. F., Ghimire, B., Rogan, J., Chica-olmo, M., & Rigol-sanchez, J. P. (2012a). An assessment of the effectiveness of a random forest classifier for land-cover classification. *ISPRS Journal of Photogrammetry and Remote Sensing*, *67*, 93–104. https://doi.org/10.1016/j.isprsjprs.2011.11.002

Rodriguez-galiano, V. F., Ghimire, B., Rogan, J., Chica-olmo, M., & Rigol-sanchez, J. P. (2012b). An assessment of the effectiveness of a random forest classifier for land-cover classification. *ISPRS Journal of Photogrammetry and Remote Sensing*, *67*, 93–104. https://doi.org/10.1016/j.isprsjprs.2011.11.002

Ruml, M., & Vulic, T. (2005). Importance of phenological observations and predictions in agriculture. *Journal of Agricultural Sciences*, *50*(2), 217–225. https://doi.org/10.2298/jas0502217r

Saini, R., & Ghosh, S. K. (2017). Ensemble Classifiers in Remote Sensing: A Review. *International Conference on Computing, Communication and Automation (ICCCA2017)*, 1148–1152.

Sen, P. K. (1968). Estimates of the Regression Coefficient Based on Kendall's Tau. *Journal of the American Statistical Association*, *63*(324), 1379–1389. https://doi.org/10.1080/01621459.1968.10480934

Shen, X., Jiang, M., Lu, X., Liu, X., Liu, B., Zhang, J., Wang, X., Tong, S., Lei, G., Wang, S., Tong, C., Fan, H., Tian, K., Wang, X., Hu, Y., Xie, Y., Ma, M., Zhang, S., Cao, C., & Wang, Z. (2021). Aboveground biomass and its spatial distribution pattern of herbaceous marsh vegetation in China. *Science China Earth Sciences*, *64*(7), 1115–1125. https://doi.org/10.1007/s11430-020-9778-7

Shen, X., Liu, B., Xue, Z., Jiang, M., Lu, X., & Zhang, Q. (2019). Spatiotemporal variation in vegetation spring phenology and its response to climate change in freshwater marshes of Northeast China. *Science of the Total Environment*, *666*, 1169–1177. https://doi.org/10.1016/j.scitotenv.2019.02.265

Shi, S., Yang, P., & Tol, C. Van Der. (2023). Spatial-temporal dynamics of land surface phenology over Africa for the period of 1982 – 2015. *Heliyon*, *9*, e16413 Contents. https://doi.org/10.1016/j.heliyon.2023.e16413

Stanimirova, R., Cai, Z., Melaas, E. K., Gray, J. M., Eklundh, L., Jönsson, P., & Friedl, M. A. (2019). An empirical assessment of the MODIS land cover dynamics and TIMESAT land surface phenology algorithms. *Remote Sensing*, *11*(2201). https://doi.org/10.3390/rs11192201

Tadesse, S., & Mekuriaw, A. (2024). Agroecology-based analysis of meteorological and agricultural drought using time series remote sensing data in the upper Gelana watershed, Ethiopia. *Geocarto International*, *39*(1), 2417881. https://doi.org/10.1080/10106049.2024.2417881

Tadesse, S., Mekuriaw, A., & Assen, M. (2024). Spatiotemporal climate variability and trends in the Upper Gelana Watershed, northeastern highlands of Ethiopia. *Heliyon*, *10*(5), e27274. https://doi.org/10.1016/j.heliyon.2024.e27274

Talukdar, S., Singha, P., Mahato, S., Shahfahad, Pal, S., Yuei-An, L., & Rahman, A. (2020). Land-Use Land-Cover Classification by Machine Learning Classifiers for Satellite Observations — A Review. *Remote Sensing*, *12*(1135). https://doi.org/doi:10.3390/rs12071135

Tang, H., Li, Z., Zhu, Z., Chen, B., Zhang, B., & Xin, X. (2015). Variability and climate change trend in vegetation phenology of recent decades in the Greater Khingan Mountain area, Northeastern China. *Remote Sensing*, *7*, 11914–11932. https://doi.org/10.3390/rs70911914

Tao, F., Yokozawa, M., Zhang, Z., Hayashi, Y., & Ishigooka, Y. (2008). Land surface phenology dynamics and climate variations in the North East China Transect (NECT), 1982 – 2000. *International Journal of Remote Sensing*, *29*(19), 5461–5478. https://doi.org/10.1080/01431160801908103

Valderrama-Landeros, L., Flores-Verdugo, F., Rodríguez-Sobreyra, R., Kovacs, J. M., & Flores-de-Santiago, F. (2021). Extrapolating canopy phenology information using Sentinel-2 data and the Google Earth Engine platform to identify the optimal dates for remotely sensed image acquisition of semiarid mangroves. *Journal of Environmental Management*, *279*. https://doi.org/10.1016/j.jenvman.2020.111617

Vermote, E. (2015). MOD09Q1 MODIS/Terra Surface Reflectance 8-Day L3 Global 250m SIN Grid [Data Set]. *NASA LP DAAC*. https://doi.org/10.5067/MODIS/MOD09Q1.006

Vermote, E. F., Roger, J. C., & Ray, J. P. (2015). *MODIS Surface Reflectance User's Guide*.

Wang, C., Guo, H., Zhang, L., Liu, S., Qiu, Y., & Sun, Z. (2015). Assessing phenological change and climatic control of alpine grasslands in the Tibetan Plateau with MODIS time series. *IntJ Biometeorol*, *59*, 11–23. https://doi.org/10.1007/s00484-014-0817-5

Wang, Y., Shen, X., Jiang, M., Tong, S., & Lu, X. (2021). Spatiotemporal change of aboveground biomass and its response to climate change in marshes of the Tibetan Plateau. *International Journal of Applied Earth Observations and Geoinformation*, *102*, 102385. https://doi.org/10.1016/j.jag.2021.102385

Woldie, B. A., & Tadesse, S. A. (2020). Composition and Structure of Woody Vegetation in Community Compared to State Forests in Tehuledere District, South Wollo, Ethiopia. *Journal of Sustainable Forestry*. https://doi.org/10.1080/10549811.2020.1772826

Wu, W., & Xin, Q. (2023). Characterizing Spring Phenological Changes of the Land Surface across the Conterminous United States from 2001 to 2021. *Remote Sensing*, *15*(3). https://doi.org/10.3390/rs15030737

Xu, X., Du, H., Fan, W., Hu, J., Mao, F., & Dong, H. (2019). Long-term trend in vegetation gross primary production, phenology and their relationships inferred from the FLUXNET data. *Journal of Environmental Management*, *246*, 605–616. https://doi.org/10.1016/j.jenvman.2019.06.023

Xue, J., & Su, B. (2017). Significant Remote Sensing Vegetation Indices: A Review of Developments and Applications. *Journal of Sensors*, *2017*. https://doi.org/https://doi.org/10.1155/2017/1353691

Yang, Y., & Fan, F. (2023). Land surface phenology and its response to climate change in the Guangdong-Hong Kong-Macao Greater Bay Area during 2001 – 2020. *Ecological Indicators*, *154*. https://doi.org/10.1016/j.ecolind.2023.110728

Yimam, A., Mekuriaw, A., Assefa, D., & Bewket, W. (2024). Impact of Eucalyptus plantations on ecosystem services in the Upper Blue Nile basin of Ethiopia. *Environmental and Sustainability Indicators*, *22*. https://doi.org/10.1016/j.indic.2024.100393

Yuan, M., Wang, L., Lin, A., Liu, Z., & Qu, S. (2019). Variations in land surface phenology and their response to climate change in Yangtze River basin during 1982–2015. *Theoretical and Applied Climatology*, *137*(3–4), 1659–1674. https://doi.org/10.1007/s00704-018-2699-7

Zhang, Q., Kong, D., Shi, P., Singh, V. P., & Sun, P. (2018). Vegetation phenology on the Qinghai-Tibetan Plateau and its response to climate change (1982–2013). *Agricultural and Forest Meteorology*, *248*, 408–417. https://doi.org/10.1016/j.agrformet.2017.10.026

Zhou, L., He, H. L., Sun, X. M., Zhang, L., Yu, G. R., Ren, X. L., Wang, J. Y., & Zhao, F. H. (2013). Modeling winter wheat phenology and carbon dioxide fluxes at the ecosystem scale based on digital photography and eddy covariance data. *Ecological Informatics*, *18*, 69–78. https://doi.org/10.1016/j.ecoinf.2013.05.003

Zhou, Z., Li, Y., Song, J., Ru, J., Lei, L., Zhong, M., Zheng, M., Zhang, A., Hui, D., & Wana, S. (2019). Growth controls over flowering phenology response to climate change in three temperate steppes along a precipitation gradient. *Agricultural and Forest Meteorology*, *274*, 51–60. https://doi.org/10.1016/j.agrformet.2019.04.011

Zoungrana, B. J. B., Conrad, C., Amekudzi, L. K., Thiel, M., Da, E. D., Forkuor, G., & Löw, F. (2015). Multi-temporal landsat images and ancillary data for land use/cover change (LULCC) detection in the Southwest of Burkina Faso, West Africa. *Remote Sensing*, *7*(9), 12076–12102. https://doi.org/10.3390/rs70912076

CHAPTER FOUR

4.FARMERS' PERCEPTION AND CHOICES OF ADAPTATION STRATEGIES TO CLIMATE VARIABILITY AND CHANGE IN THE UPPER GELANA WATERSHED, NORTHEASTERN HIGHLANDS OF ETHIOPIA

Tadesse, S., Mekuriaw, A., Assen, M., 2025. Farmers' perception and choices of adaptation strategies to climate change in the upper Gelana watershed, northeastern highlands of Ethiopia. Theoretical and Applied Climatology. 156. https://doi.org/10.1007/s00704-025-05629-2.

CHAPTER FIVE

5.FARMERS' PERCEPTION AND CHOICES OF ADAPTATION STRATEGIES TO CLIMATE VARIABILITY AND CHANGE IN THE UPPER GELANA WATERSHED, NORTHEASTERN HIGHLANDS OF ETHIOPIA

Abstract

Climate change and its impacts are increasing, which requires the timely implementation of adaptation measures. This study aimed to assess smallholder farmers' perceptions of climate change and determinants in the adoption or choice of adaptation strategies in the upper Gelana watershed, located in the northeastern highlands of Ethiopia. This research employed mixed research methods, involving both qualitative and quantitative approaches. Empirical data were gathered from 165 randomly selected households using structured questionnaires, complemented by 12 key informant interviews to provide in-depth qualitative insights. We used descriptive statistics, chi-square test and multivariate probit (MVP) models to analyze the data. The findings revealed that a significant proportion of farmers in all agroecological zones (AEZs) perceive increasing temperature and declining precipitation. However, key informants noted a decreasing trend in rainfall, mainly observed in the *belg* season. The majority of the respondents also perceived an increase in the occurrence of drought, disease incidence, erosion hazards, pests, and a decline in crop yields due to climate change and variability. There is a significant variation in the adaptation strategies to climate change

implemented across the AEZs particularly in soil and water conservation (SWC), agroforestry, and irrigation. The MVP models indicated that farming in the lower and upper *Weina Dega* AEZs, education status, extension support, and access to climate information significantly affect the choices of most climate adaptation strategies in the study area. The findings will help improve climate adaptation measures by leveraging the positive contributions of agroecology, demographic, socioeconomic, and institutional factors and addressing negative influences, ultimately benefiting stakeholders in the upper Gelana watershed.

Keywords: climate variability, climate change, perceptions, adaptation strategies, smallholder farmers

5.1. Introduction

Climate change is a serious problem throughout the world, especially in developing countries. Globally, natural disasters caused 1.19 million deaths and affected 3.25 billion people between 1980 and 1999 (Donatti et al., 2024; UNDRR, 2019). In the subsequent period, from 2000 to 2019, these numbers rose to 1.23 million deaths, with 4.2 billion people affected. Economic losses increased from 1.63 trillion USD in the first period to 2.97 trillion USD in the second. Climate-related events accounted for 86.8% of these disasters between 1980 and 1999, increasing to 90.9% between 2000 and 2019 (UNDRR, 2019).

The frequency and damages from climate-related disasters such as droughts and floods have been increasing over time, with more pronounced effects in low-income countries (Jonkman et al., 2024; Rentschler & Salhab, 2022; UNDRR, 2019). Between 1998 and 2017, global economic losses from droughts were estimated at 124 billion USD (UNCCD, 2022), while floods caused more than 1.3 trillion USD economic losses from 1990 to 2022, affecting more than 3.2 billion people in 168 countries (Liu et al., 2024). In 2022 alone, about 2.3 billion people experienced a shortage of water (UNCCD, 2022).

Studies have revealed that climate change will significantly impact agricultural production in African countries (Akinnagbe & Irohibe, 2015; Becker & Elliot, 2022; Fauzel, 2021; Gwambene et al., 2023; Mbow et al., 2019; Muluneh, 2021; Serdeczny et al., 2017; Zhao et al., 2017). It affects the length of growing seasons and reduces suitable areas for cultivation,

negatively affecting food availability and increasing the risk of hunger in sub-Saharan Africa (Bedeke, 2023; Kotir, 2011; Newman & Noy, 2023; Omotoso et al., 2023; Saleem et al., 2024; Serdeczny et al., 2017). Although the number of climate-related events in African countries is comparable to other regions, the number of affected people has increased. This trend underscores the urgency of implementing adaptation measures, particularly in developing countries, to reduce the impacts of climate change (Akinnagbe & Irohibe, 2015; Donatti et al., 2024; Raihan, 2023).

In Ethiopia, climate change and variability pose significant threats to food security, particularly for rural populations depending on agriculture (Asfaw et al., 2018a,b; Bewket, 2012; Gezie, 2019; Moges & Bhat, 2021; Tibebe et al., 2022; Tofu et al., 2022). Previous studies suggest that climate change will severely impact the production of key crops such as *teff*, maize, sorghum, and barley (Bouteska et al., 2024; Mohammed et al., 2022; Solomon et al., 2021; Zhao et al., 2017). According to Solomon et al. (2021), in Ethiopia, climate change will lead to reductions in the production of *teff*, maize and sorghum by 25.4%, 21.8 %, and 25.2%, respectively, which will result in a 31.1% decrease in agricultural GDP by 2050. It impacts not only agriculture but also other sectors, such as health. According to Simane et al. (2016a), due to the impacts of adverse climatic conditions, trends in respiratory, waterborne, and vector-borne diseases are increasing, posing significant threats to societal well-being in Ethiopia.

Although the need for climate change adaptation is more urgent than ever, adaptation efforts have not kept up with the rate of escalating risks (Donatti et al., 2024; Eisenack et al., 2014). Since the impact of climate change is unevenly distributed across agroecological zones (AEZs) of Ethiopia (Solomon et al., 2021), adaptation and mitigation strategies must be tailored to local contexts to be effective (Adom, 2024). Studies suggest that measures related to human capital development, land management, governance, irrigation, infrastructure, and the adoption of modern agricultural practices should be prioritized to reduce the adverse effects of climate change (Donatti et al., 2024; Fauzel, 2021).

In the upper Gelana watershed of northeastern Ethiopian highlands, recent studies indicate that the temperature and rainfall patterns are changing (Mohammed et al., 2018; Rosell & Holmer, 2015; Tadesse et al., 2024). Meteorological data analysis shows that maximum

temperature during the *kiremt* season and annual rainfall have shown a significant increase, whereas a notable decreasing trend was observed in the amount of belg season rainfall over the past 30 years (Tadesse et al., 2024). These unprecedented changes in climate patterns have affected the agriculture sector dependent livelihood of people and are expected to face greater impacts in the future. The increase in temperature and rainfall coupled with the rugged topography of the area makes the area more susceptible to soil erosion and soil fertility reduction. On the other hand, the decreasing rainfall in the *belg* season poses a serious challenge to production and on the efforts of smallholder farmers to become self-sufficient in food. It was evidenced that the area was affected by meteorological and agricultural drought events in 2002, 2004, 2008, 2015 and 2021, which also affected other parts of Ethiopia (Mera, 2018; Tadesse & Mekuriaw, 2024).

Although several studies (Addis & Abirdew, 2021; Asrat & Simane, 2018; Bedeke, 2023; Deressa et al., 2009; Tesfaye & Nayak, 2023), have examined farmers' climate change perceptions and adaptation responses, notable research gaps remain. Much of the existing literature tends to generalize findings across larger regions, often overlooking the micro-level variability in exposure, perception, and adaptation practices within diverse agroecological zones. Specifically, there is limited empirical evidence from the Upper Gelana watershed, with its complex topography, varied AEZs, and vulnerability to drought, on how local ecological, socio-economic, and institutional contexts shape adaptation decisions. This study addresses that gap by applying a comparative agroecological lens, using data collected from multiple zones to assess both perception and adaptation strategies.

Given the severity of climate-related challenges, we argue that studies on perception and adaptation strategies to climate change should be conducted in different localities and geographical settings. As the factors influencing perception and the choice of adaptation strategies vary from one place to another, there is no one-size-fits-all approach. Additionally, perceptions of climate change and choices of adaptation strategies are not constant; they evolve over time. In doing so, this study contributes new insights that are locally grounded and policy-relevant. Moreover, most of the previous studies rile on multinominal logistic regression (Deressa et al., 2009) or Heckman selection model (Asrat & Simane, 2018), our study applied a Multivariate Probit (MVP) model that allow to capture the simultaneous

nature of farmers adopting multiple strategies, which provides a more realistic representation of adaptation behavior.

Therefore, following the agroecological systems approach, which integrates socioecological systems and focuses on local context, diversity, and sustainability, this study aims to analyze farmers' perceptions of climate change and its impacts. In addition, it seeks to explore the factors that influence the choice of adaptation strategies to address climate variability and change across the agroecological zones in the Upper Gelana watershed, northeastern highlands of Ethiopia.

5.2. Methods and materials

5.2.1. Description of the study area

This research was conducted in the Upper Gelana watershed, situated within the Tehuledere district of Ethiopia's northeastern highlands. Geographically, the watershed stretches between 11.15° and 11.35° north latitude and 39.62° and 39.73° east longitude, encompassing an area of 134 km² (Fig. 5.1). Elevation in the region ranges from 1,701 to 2,886 meters above sea level, contributing to significant climatic variability. Earlier investigations have identified two primary AEZs in this area: *Dega* and *Weina Dega*. To capture finer spatial variations within the *Weina Dega* zone, it has been subdivided into *Lower Weina Dega* (LWD; 1,701–2,000 m) and *Upper Weina Dega* (UWD; 2,001–2,300 m) (Tadesse et al., 2024; Tadesse & Mekuriaw, 2024). Temperature patterns vary with both elevation and agroecological zone: minimum temperatures range between 9.1°C (in *Dega*) and 11.4°C (in LWD), while maximum temperatures range from 22.4°C (*Dega*) to 26.7°C (LWD). The mean annual temperature is cooler in the *Dega* zone

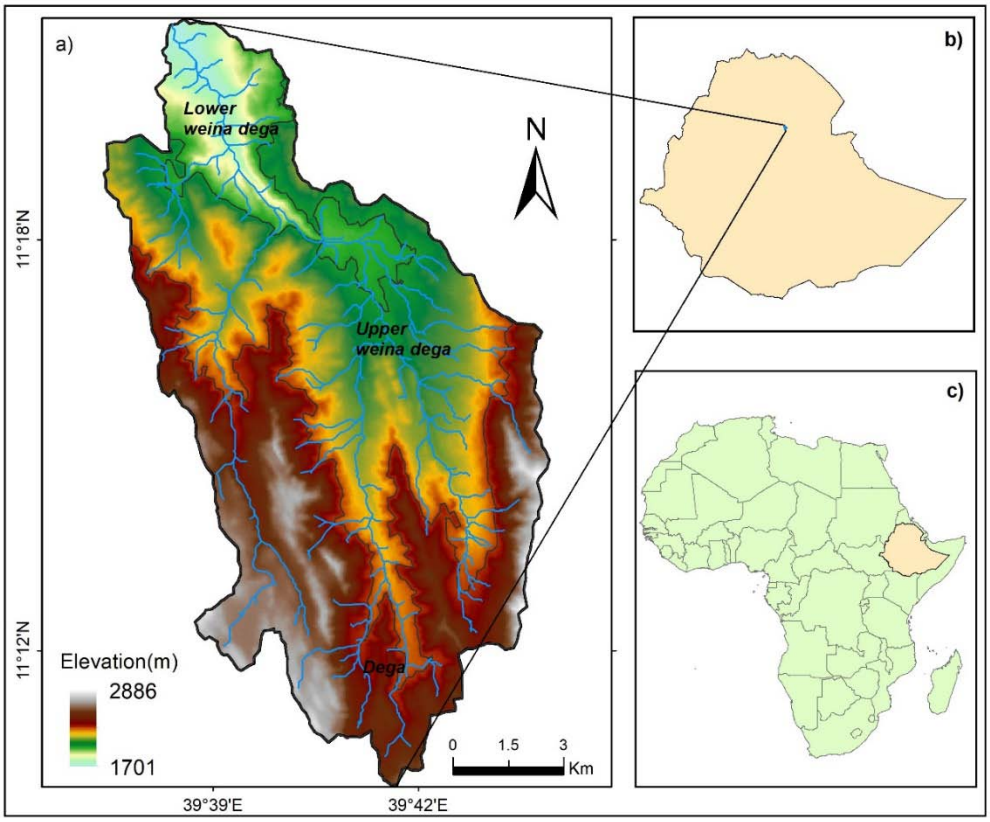

Fig. 5.1. Location map of the study area: a) upper Gelana watershed, b) Ethiopia and c) Africa.

(15.9°C) compared to the LWD (18.9°C). The hottest month, in terms of both mean maximum and average temperatures, is June, while July records the highest long-term minimum temperatures. Rainfall distribution is bimodal, characterized by a short rainy season (belg) from February to May, and a main rainy season (kiremt) stretching from June to September. Annual precipitation ranges between 964 mm in LWD and 1,072 mm in the *Dega* zone, with August being the wettest month across all AEZs (Tadesse et al., 2024; Tadesse & Mekuriaw, 2024).

In the study area, mixed subsistence agriculture, encompassing both crop farming and livestock rearing serves as the main source of income. Farmers typically grow staple crops such as teff (*Eragrostis tef*), wheat (*Triticum aestivum*), sorghum (*Sorghum bicolor* L) and *chat* (*Catha edulis*). Additionally, they raise livestock, primarily cattle, sheep, and goats, alongside other domestic animals, integrating both crop and animal production to sustain their livelihoods.

5.2.2. Data collection

A multistage sampling procedure was employed, aligned with the hierarchical structure of the study area. First, the watershed was stratified into three AEZs: *Dega*, UWD, and LWD. In the second stage, one representative village was purposively selected from each AEZ: Gishen-Welager from the *Dega* zone, Lekole from the UWD zone, and Kofo from the LWD zone. These villages were selected based on factors such as accessibility and resource constraints, with the primary aim of ensuring representativeness across different AEZ and elevation gradients. The selected sites reflect varied climatic conditions, land use systems, and access to adaptation options, thereby capturing the diversity of challenges and responses within the watershed. In the third stage, households were selected from each of the chosen villages. According to data obtained from the respective kebele (the smallest administrative units) there were 80 households in Gishen-Welager, 98 in Lekole, and 231 in Kofo, in sum of 409 household heads (HHHs). The sample size was then determined using the Yamane (1967) formula as follows:

$$n = \frac{N}{1+N(e^2)} \quad \ldots\ldots 1$$

Where *n* is the sample size, *N* is the total number of households, and *e* is the margin of error. A margin of error of 6% was chosen, which falls within the commonly accepted range of 5% to 10% for social science studies (Israel, 1992; Tesfahun et al., 2024). This resulted in a sample size of 165 households (40.3% of the total), selected through a proportionate stratified random sampling technique. The sample was proportionally distributed between the villages accordi.ng to the size of households: 32 households in Gishen-Welager, 40 in Lekole, and 93 in Kofo. Then, the survey data were collected through a questionnaire from these households, and only six questionnaires were not returned, resulting in 159 responses. In addition to the survey, interviews were conducted with 12 key informants, with four informants from each AEZ. The key informants include community leaders, elders, experienced farmers and extension workers. They were selected purposively based on their long-term experience and familiarity with local agricultural practices and challenges. Survey data collection took place between March and May 2022.

5.2.3. Data analysis

The collected data were carefully coded and organized to facilitate subsequent analysis. Basic descriptive statistics, including frequency and percentage, as well as chi-square (X^2) and one-way ANOVA tests, were employed to examine the characteristics of respondents, assess the perceptions of farmers and the impacts of climate variability and change, and analyze the variation in adaptation strategies in different AEZs.

The multivariate probit model (MVP) was used to analyze the factors that influence farmers' decision-making regarding adaptation strategies. The MVP model builds upon the binary probit model, which is utilized when the outcome is a single binary variable. It is ideal for complex decisions involving multiple correlated binary outcome variables (Cappellari & Jenkins, 2003, 2006; Greenberg, 1998; Ting et al., 2022). In rural farming communities, farmers often choose to implement several adaptation strategies simultaneously. Therefore, the commonly used multinomial logistic regression falls short because it assumes that farmers select only one adaptation strategy that maximizes profit, which is not realistic. It is common for farmers to use multiple adaptation techniques, such as soil conservation, agroforestry, crop diversification, irrigation and adjusted planting dates. In such cases, the MVP model accurately captures the choices by predicting the combined probability of implementing different strategies based on a set of explanatory factors. This approach provides a comprehensive and unified perspective, as decisions are made considering the combined effects and interrelationships of each option (Addis & Abirdew, 2021; Mengistu & Assefa, 2019; Teklewold et al., 2019). In other words, the MVP model can handle correlated dependent variables that are non-mutually exclusive. For example, selecting an adaptation measure may increase the probability of choosing another strategy, such as SWC measures, potentially increasing the likelihood of using irrigation. For each adaptation choice, Y_{im} is determined by an underlying latent variable Y_{im}*, which represents the farmer's propensity to adopt the strategy. We computed the MVP model as follows (Cappellari & Jenkins, 2003):

$$Y_{im}{}^{*} = \beta_m{}' X_{im} + \epsilon_{im}, m = 1, \dots\dots.., M \quad \dots\dots\dots 2$$

$Y_{im}{}^{*} = 1$ if $Y_{im}{}^{*} > 0$ *and* 0 *otherwise*

Where:

Y_{im} is a binary variable indicating whether farmer i adopts the adaptation strategy$m$; $Y_{im}{}^{*}$ is an unobserved latent variable representing the underlying propensity for the outcome y_{ij}; X_i is a vector of explanatory variables for individual i;β_m is the vector of coefficients representing the effect of each explanatory variable on the m^{th} adaptation choice; ϵ_{im} is the error term that follows a multivariate normal distribution across strategies, capturing interdependencies between adaptation choices.

The probability that a farmer adopts a specific combination of adaptation strategies were calculated following equation 3.

$$\mathrm{P}(Y_{i1} = y_{i1}, \ldots, Y_{iM} = y_{iM} \mid \mathrm{X}_i) = \phi M(X_i\beta \ ; \Omega) \quad \ldots\ldots 3$$

Where:

ϕM is the cumulative distribution function (CDF) of an M-dimensional multivariate normal distribution; Ω is the covariance matrix of the error terms, capturing correlations between adaptation strategies.

It is crucial to understand the probability of adopting a specific adaptation strategy in relation to a unit change in the explanatory variables. Hence, the marginal effect of an explanatory variable X_{ij} on the probability of adopting a specific adaptation strategy m is calculated as follows(Mullahy, 2011):

$$\frac{\partial \mathrm{P}(Y_{im}=1|\mathrm{X}_i)}{\partial X_{ij}} = \phi M(X\beta_m \, ; \Omega) * \beta_{mj} \quad \ldots\ldots 4$$

Where:ϕM is the probability density function (PDF) of the multivariate normal distribution, evaluated at $X\beta_{m;}$ β_{mj} is the coefficient for X_{ij}, showing the effect of the j^{th}explanatory variable on the m^{th} adaptation strategy.

The MVP model and marginal effects were calculated using the CMP package in Stata version 15 (Roodman, 2011), focusing on five adaptation strategies practiced by nearly half or more of the residents in the area: SWC, irrigation, agroforestry, changing crop varieties and adjusting planting dates. These strategies were coded as binary variables, with 1 indicating adoption and 0 otherwise. Fourteen explanatory variables, both binary and continuous, were used as described in Tables 5.1 and 5.2, respectively.

Before running the MVP model, the multicollinearity of the data was checked by fitting the Ordinary Least Squares model (OLS). The results imply that the variance inflation factor (VIF) values of all the explanatory variables are less than 1.5 which indicates no collinearity. The MVP model was computed with 159 observations to examine the joint impact of the explanatory variables on the five widely used adaptation strategies. We obtained Wald chi-square statistic of 724.16 with 75 degree of freedom which is significant at $p < 0.01$, suggesting that the explanatory variables meaningfully explain the variance in the dependent variables and that the model fits the data reasonably well.

5.3. Results and discussion

5.3.1. Characteristics of the respondents

Analysis of the demographic and socioeconomic characteristics of the respondents across the three AEZs reveals notable differences that help contextualize their adaptation strategies. More than half of the households in all AEZs are male-headed, accounting 74.2% (Table 5.1). The education level of respondents varies significantly across AEZs ($X^2 = 11.87$, $p < 0.1$). UWD has the highest proportion of illiterate household heads (55.3%), while *Dega* has a larger share of respondents with education levels between grades 5 and 8 (31.3%). This variation in education may influence households' access to and use of climate information, as well as their capacity to implement adaptation strategies. Approximately 74.2% of respondents reported membership in local social groups, while 54.7% had received extension support. Access to climate information was relatively low (43.4% overall), with minimal differences among AEZs. Market linkage was highest in *Dega* (81.3%) and lowest in LWD (65.2%).

Table 5.1 Selected characteristics of the respondents (%)

Dependent variables	Measurements	LWD	UWD	*Dega*	Total	X^2
Sex	Categorical					
Male		76.4	73.7	68.8	74.2	0.728
Female		23.6	26.3	31.3	25.8	
Education level	Categorical					
Illiterate		31.5	55.3	28.1	36.5	11.87*
Grades 1-4		32.6	23.7	21.9	28.3	
Grades 5-8		18	7.9	31.3	18.2	
Grade 9 and above		18	13.2	18.8	17	
Memberships in social groups	Binary	73	73.7	78.1	74.2	0.326
Extension support	Binary	51.7	60.5	56.3	54.7	0.878
Climate info	Binary	40.4	50	43.8	43.4	0.991
Market linkage	Binary	65.2	71.1	81.3	69.8	2.925
Credit access	Binary	50.6	44.7	46.9	48.4	0.4

*, ** and *** indicate statistically significant at 0.1, 0.05 and 0.01 alpha levels, respectively.

As shown in Table 5.2, the mean age of household heads is 53.2 years, which varies significantly across AEZs ($F = 5.34$, $p < 0.05$), with UWD having slightly younger household heads (mean = 49.8 years) compared to LWD (54.0) and *Dega* (55.0). The mean household size is 4.97 people, with no significant difference across AEZs and the mean farm size is 0.50 hectares, with a standard deviation of 1.17 (Table 5.2). The chi-square test indicates the presence of significant variation in the number of tropical livestock units (TLU) across the study area, with a mean of 2.85 TLUs and a standard deviation of 1.41. Regarding income, the mean annual farm income is 14,904 Birr (1 USD ~ 51.5 Birr during the survey period), with the highest average in UWD (15,976 Birr), though the variation is not statistically significant. In contrast, non-farm income shows a significant difference ($F = 2.329$, $p < 0.1$), with UWD again leading (7,920 Birr), suggesting greater income diversification in this AEZ (Table 5.2). These economic disparities may influence the capacity of households to adopt certain adaptation measures that require upfront investment, such as irrigation or use of different crop varieties.

Table 5.2. Characteristics of the respondents based on continuous variables

Variables	Indicators	LWD	UWD	*Dega*	Total	F
Age of HHH (year)	Mean	54.03	49.82	55.03	53.23	5.34**
	Std	6.9	8.78	7.57	7.72	
HH size (number)	Mean	4.97	5.08	4.87	4.97	0.191
	Std	1.301	1.617	1.338	1.382	

Land holdings (ha.)	Mean	0.49	0.47	0.54	0.5	1.03
	Std	0.23	0.22	0.21	0.22	
livestock ownership (TLU)	Mean	3	2.3	3.2	2.85	4.30**
	Std	1.46	1.04	1.5	1.41	
Farm income (Birr)	Mean	14386.52	15976.32	15071.88	14904.4	0.51
	Std	7291	9091.56	9457.01	8181.94	
Non-farm income (Birr)	Mean	6651.12	7919.74	7743.75	7174.21	2.329*
	Std	2702.33	4491.91	3938.96	3491.42	

Note: 1 USD ~ 51.5 Birr during the survey time. *, ** and *** indicate statistically significant at 0.1, 0.05 and 0.01 alpha levels, respectively.

5.3.2. Farmers perception on climate variability and change

A large proportion of the respondents have observed the presence of changes in rainfall and temperature patterns over the past several years. About 82%, 78.9% and 75% of farmers in the LWD, UWD and *Dega* AEZ, respectively, reported a decreasing pattern in the amount of annual rainfall (Fig.5.2). In contrast, a significant number of respondents reported an increase in temperature conditions in recent years, accounting for 88.8%, 81.6% and 78.1% in the LWD, UWD, and *Dega* AEZ of the upper Gelana watershed, respectively. These slight variations in smallholder farmers' perceptions of rainfall and temperature could be attributed to differences in the local agroecological setting, which is characterized by variations in topography and other specific environmental conditions (Gezie, 2019). Their perceptions of temperature conditions and the amount of annual rainfall changes align with earlier studies (Ayal & Filho, 2017; Sertse et al., 2021). Specifically, farmer observations of increasing temperature conditions are consistent with meteorological analysis reported in a previous study (Tadesse et al., 2024). However, a discrepancy arises regarding the amount of annual rainfall trends. As indicated by key informants, there was variation in the rainfall amount between the *belg* and *kiremt* rainy seasons. KII indicated that the amount of rainfallin *belg* season has been declining and becoming more unpredictable over time, which has significant implications for local agricultural activities and adverse effects on food security. On the other hand, KII observed an increase in the amount of rainfall during the *kiremt* season. However, *belg* rains often cease unexpectedly, forcing farmers to use a significant portion of their *belg* cultivated crops as animal feed, which poses a major food security challenge. These negative impacts, experienced more acutely by smallholder farmers, likely influence their perception of changes in amount of annual rainfall, as such changes are often the most noticeable and memorable when prompted. Furthermore, the frequent agricultural drought in the *belg* and

less agricultural drought in the *kiremt* season(Tadesse & Mekuriaw, 2024) may also influence perceptions about rainfall and temperature. The mismatches between farmers' perceptions and meteorological rainfall analysis have been reported in previous studies (Asfawet al.,2018b; Ayal & Filho, 2017).

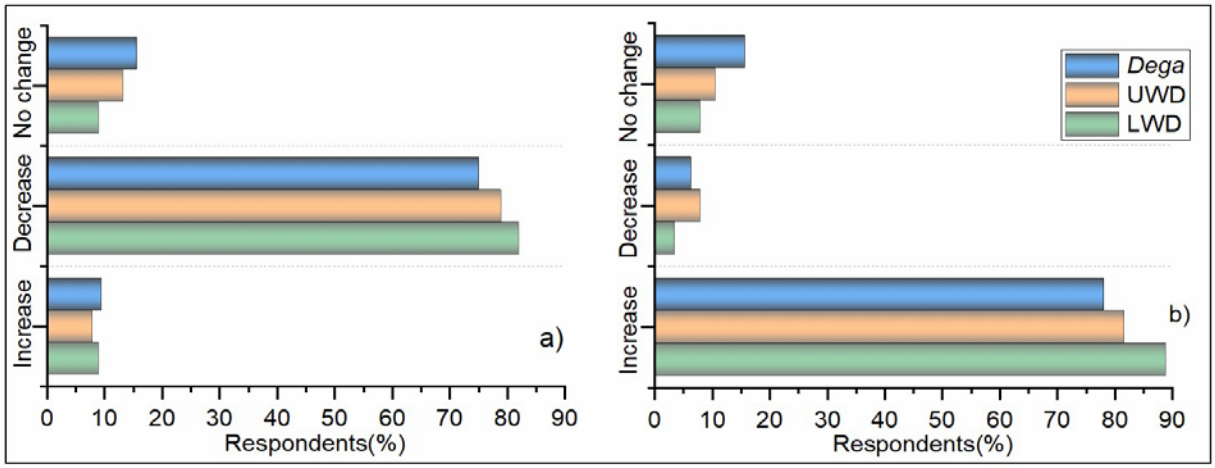

Fig. 5.2. Smallholder farmer perceptions of changes in the amount of annual rainfall (a) and temperature (b) in LWD, UWD and *dega* AEZs of the upper Gelana watershed.

5.3.3. Perceived impacts of climate variability and change

A significant proportion of respondents across the study area perceived the impacts of climate variability and change. Nearly 82% of the respondents reported that climate change and variability have led to increased incidences of droughts and crop diseases. Specifically, a large proportion of respondents in the LWD zone perceived a rise in drought incidences, followed by those in the UWD and *Dega* zones, while the reverse was observed for crop diseases. This may imply the need to customize interventions across AEZs, which might include SWC, irrigation, and promoting drought-resistant crops. On the other hand, better disease management strategies are essential for AEZs with higher crop disease incidence perceptions. These results coincide with the findings of previous studies conducted in different parts of Ethiopia (Likinaw et al., 2023; Tofu et al., 2022).

More than half of the respondents in the study area perceived an increased incidence of diseases, erosion hazards, pests, and declining crop yields. Key informants highlight the

growing prevalence of pests across all three zones, noting that pests such as locusts have become more frequent, posing risks to crops and other plants. They believed that crop pests are becoming a critical concern, driven increasingly by changing climatic conditions. They also revealed that some farmers resort to using malathion to manage pests in chickpea, vetch, *chat*, and use gasoline for *teff* and wheat, despite human, animal health and environmental risks. Farmers reported that most crops now require pesticides to survive, and the cost of these products has increased sharply.

Table 5.3.Impacts of climate change and variability in the study area.

Perceived impacts	LWD	UWD	*Dega*	Total	X^2
Increase in drought incidences	89.9	73.7	68.8	81.8	9.237***
Increase in flooding events	30.3	47.4	37.5	35.8	3.406
Increase in storms and hailstones	24.7	31.6	34.4	28.3	1.346
Increase in erosion hazards	67.4	52.6	43.8	59.1	6.324**
Growing prevalence in pests	74.2	57.9	46.9	64.8	8.716**
Increase in crop diseases	78.7	84.2	87.5	81.8	1.437
Rise in invasive weed species	30.3	28.9	25	28.9	0.326
Decline in crop yields	70.8	68.4	56.3	67.3	2.289
Increase in livestock diseases	39.3	63.2	53.1	47.8	6.517**
Growing prevalence of diseases (e.g., malaria)	69.7	44.7	37.5	57.2	13.13***
Reduction in water availability	51.7	34.2	28.1	42.8	6.832**
Decline in fodder availability	49.4	39.5	31.3	43.4	3.483

*, ** and *** indicate statistically significant at 0.1, 0.05 and 0.01 alpha levels, respectively.

About 70.8%, 68.4% and 56.3% of farmers in the LWD, UWD, and *Dega* zones, respectively, perceived reductions in yield due to the impacts of climate change (Table 5.3). One of the informants noted, “In the past, cereal yields during the *belg* season were comparable to or even exceeded those in the *kiremt* season, but this is no longer the case due to erratic or absent *belg* rains.” The absence of *belg* rainfall has also led to forage shortages, which limit livestock as a reinsurance option. A key informant from the UWD shared, “There has been no rain this year; it only started in the last two days, but the sowing time has already passed. This has led to a severe forage shortage, and buying forage is costly except for dairy farms, forcing many of us to sell our cattle.” Discussions with key informants revealed that crops such as chickpeas, vetch, and lentils, which were once resistant to rainfall and temperature fluctuations, now often fail to reach maturity and produce viable yields, reflecting increased stress from climate variability on agricultural productivity in recent years.

These findings are consistent with existing empirical literature. Studies by Deressa et al. (2009) and Simane et al. (2016b) reported that changes in rainfall patterns are critical drivers of declining crop productivity in Ethiopia. The reported impacts of climate change on forage scarcity and livestock stress are also consistent with the findings of Ayal and Filho (2017), Godde, et al. (2021), and Thornton et al. (2009), who highlight how climate change undermine the reliability of livestock as a traditional coping mechanism. The combined impacts of reduced crop yields and limited livestock resources have far-reaching consequences for household food security and income. Declining agricultural productivity compromises the ability of households to sustain their livelihoods, reducing their purchasing power for food crops and critical agricultural inputs such as fertilizers. This economic strain diminishes households' adaptive capacity, leaving them more vulnerable to the impacts of climate change and variability. Over time, these challenges erode the resilience of farming communities, threatening their long-term sustainability and overall well-being.

5.3.4. Farmers choice of adaptation strategies

Respondents in the study area employ various strategies to adapt to climate variability and change. About 43.8%, 44.7%, and 65.6% of the respondents in the LWD, UWD, and *Dega* AEZ, respectively, implement SWC practices (Table 5.4). On average, almost half of the respondents in the study area reported adopting SWC as an adaptation strategy. According to key informants, the SWC methods used within each AEZ differ. In the *Dega* AEZ, common practices include terracing, soil bunds, soil covering (particularly for *chat* cultivation), rainwater harvesting, and the use of compost to enhance soil fertility, among other methods. Respondents also use chemical fertilizers to improve soil fertility. Those who own livestock produce compost for their own farmland; some even sell compost to others. In UWD and LWD, farmers rely heavily on chemical fertilizers to achieve desired yields, as it can be challenging to do so without artificial fertilizer. Key informants noted that in the past, elevated and steep areas in the *Dega* and parts of the UWD faced challenges from floods and various forms of soil erosion. However, SWC efforts have reduced soil erosion, filled gullies, and reduced flood hazards, significantly improving conditions in these areas compared to other parts of the UWD and LWD AEZs. The findings align with existing empirical literature

that are conducted in Ethiopia. For example, Bewket (2007), Hengsdijk et al. (2005) and Teshome et al. (2016) reported that SWC practices substantially reduce soil erosion and enhance crop yields and water retention in the Ethiopian highlands.

Table 5.4. Proportion of farmers who implement different adaptation strategies in the three study AEZs.

Adaptation strategies	LWD	UWD	*Dega*	Total	χ^2 value
Soil and water conservation	43.8	44.7	65.6	48.4	4.75*
Agroforestry	47.2	65.8	65.6	55.3	5.44*
Irrigation	44.9	68.4	56.3	52.8	6.08**
Change in crop varieties	66.3	73.7	59.4	66.7	1.61
Changing in planting dates	64	57.9	56.3	61	0.8

*, ** and *** indicate statistically significant at 0.1, 0.05 and 0.01 alpha levels, respectively.

As shown in Table 5.4, almost equal proportions of respondents in *Dega* and UWD AEZs (65.6%) practice agroforestry, compared to 47.2% in the LWD. The *Dega* AEZ has large forest stands, where farmers cultivate on the fringes, planting tree crops such as apples and growing *chat*. They also grow trees, such as alfalfa and elephant grass, for cattle feed. In the UWD, agroforestry focusses mainly on *chat* crops and other plants used as animal feed, whereas in the LWD, farmers grow *chat* along with fruit crops such as papaya, mango, and lemon. About 55.3% of the respondents practice agroforestry in the Upper Gelana watershed. The chi-square test indicates significant variation in agroforestry practices in the study area. Previous studies have also reported variations in agroforestry practices across agroecological zones (Mbow et al., 2014; Zeratsion et al., 2024). Moreover, these studies highlight that agroforestry improves livelihoods and can serve as an effective climate change adaptation strategy (Dawide et al., 2022; Mbow et al., 2014; Zeratsion et al., 2024).

Irrigation is a crucial strategy for reducing the impact of erratic rainfall on crop and livestock production. Nearly 44.9%, 68.4%, and 56.3% of respondents in the LWD, UWD, and *Dega* AEZ, respectively, use irrigation from rainwater harvesting and stream diversion. The chi-square test shows significant variation in irrigation use between the three AEZs. Key informants highlighted that rainwater harvesting is practiced in the *Dega* and parts of the UWD AEZs, primarily for *chat* cultivation and livestock feed production. However, they noted both opportunities and limitations with water harvesting in the area. An informant shared a case of a model farmer in another village with three ponds cultivating *chat* on a plot

of less than 0.1 hectare plot and generating nearly 90,000 ETB per annum, which is about three times the average income of other *chat* farmers. Despite such opportunities, challenges include the increased cost of geomembranes (plastic sheets) and their short durability, and the increasingly unaffordable water pump generators, essential for transferring water from ponds and streams in areas where topography limits direct river diversion. Plastic sheets play a crucial role in water harvesting by preventing infiltration and reducing evaporation. Smallholder farmers often use geomembranes for long-term purposes; however, if these materials are short-lived, prone to rupture, or fail to perform as intended, farmers may struggle to replace them due to financial constraints. Similarly, the cost, quality, and availability of water pumps are critical factors for effective irrigation in the study areas. These challenges pose significant obstacles to improving irrigation practices among smallholder farmers. The findings of our study align with the importance of small-scale irrigation and water harvesting practices as climate change adaptation strategies, as well as the associated challenges, reported in previous studies (Maru et al., 2023; Rockström, 2003; Roba et al., 2022).

The key informants also raised concerns about misconceptions about irrigation. Despite available irrigation resources for some corners of the study sites, some farmers hesitate to grow cereal crops with irrigation, fearing that it will degrade the quality of black soil, making it unsuitable for *teff* cultivation during the rainy season. An illustrative case is the government-constructed irrigation canal in Aloma, in the UWD, which remains underutilized due to such misconceptions. Informants emphasized the need for education and enforcement, referencing Proclamation No. 456/2005 (Federal Democratic Republic of Ethiopia, 2005), which allows for land revocation if farmers do not adhere to expert guidelines. This underscores the importance of awareness and regulatory measures to overcome barriers to irrigation adoption and optimal land use.

Most respondents in all study AEZs cultivate a variety of crops to reduce the impacts of climate change. Accordingly, about 66.3%, 73.7%, and 59.4% of respondents in LWD, UWD, and *Dega*, respectively, diversify their crops as a coping mechanism for impacts of climate change. Farmers grow perennial and cereal crops, with distinct crops in each zone. In the *Dega* AEZ, wheat and barley are commonly cultivated; in the UWD, wheat and teff dominate; while in the LWD, sorghum, maize, and fast-maturing *teff* varieties are popular. Furthermore,

chat is grown across all AEZs, being more prevalent in the UWD than in the LWD and *Dega*, due to favorable climate conditions for its growth. However, key informants expressed concern that highly fertile farmlands, suitable for cereal production, are increasingly being converted to *chat* farms, which may threaten future cereal crop production. They believe that *chat* depletes soil fertility, gradually reducing yields. Although chat production helps reduce risks associated with climate variability and change(Tofu & Wolka, 2023a), it may force households to rely on distant markets for food. Additionally, the income generated from chat is not always sufficient to cover household cereal purchases. Similar concerns about the negative impact of chat cultivation on cereal production have also been raised in eastern Ethiopia (Tofu & Wolka, 2023b).

5.3.5. Factors affecting the choice of adaptation strategies

As discussed earlier, the choice of adaptation strategies is influenced by various household characteristics. These factors can be broadly categorized into agroecological, demographic, socioeconomic and institutional dimensions. To assess the significance and contributions of these factors, we employed the MVP model, and the results are presented in the following sections.

5.3.5.1. Agroecology

Agroecology reflects the spatial variation in socioeconomic and environmental conditions which might have different requirements for small holder farmers to adapt to climate change. To elaborate further, rainfall, temperature, soil fertility and the way of living between the *Dega* and *Kolla* areas differ, which might influence the choice of adaptation strategies.

The MVP model revealed that the probability of choosing specific adaptation strategies varies across the AEZs. Specifically, farming in both LWD and UWD zones is significantly negatively associated with the adoption of SWC practices, indicating that farmers in these zones are less likely to implement SWC measures compared to those in the *Dega* AEZ (Table 5.5). This may be due to the variation in topographic conditions across these AEZs in which the *Dega* area is steeper and greater emphasis is placed on these areas by the agricultural extension workers. However, farming in the UWD zone positively influences the choices of other adaptation strategies, with statistically significant effects on the implementation of

irrigation and crop variety changes. This is due to the relatively moderate slope or topography as well as water availability, which is collected from the upstream *Dega* AEZs, and also due to infrastructure like irrigation canals; farmers also use pipe water for growing chat. In addition to this, this agroecology zone has a moderate climate condition and supports a variety of crops

Table 5.5. Parameter estimates of the multivariate probit model for climate change adaptation strategies.

Explanatory	SWC		Irrigation		Agroforestry		Change in crop varieties		Changing planting dates	
variables	**Coef.**	**p value**	**Coef.**	**p value**	**Coef**	**p value**	**Coef**	**p value**	**CoeF.**	**p value**
AEZ										
UWD	-1.75	0.000***	1.34	0.001***	0.268	0.475	0.923	0.007***	0.155	0.681
LWD	-1	0.001***	-0.043	0.888	-0.479	0.092*	0.496	0.076*	0.408	0.178
Age	-0.01	0.739	-0.005	0.777	-0.024	0.09*	0.012	0.444	-0.014	0.342
Gender	0.338	0.296	0.189	0.469	0.238	0.389	-0.203	0.453	0.027	0.918
Household size	0.237	0.013**	0.025	0.778	0.044	0.623	0.099	0.326	0.161	0.07*
Education	0.303	0.038**	0.661	0.000***	0.285	0.01**	0.6	0.000***	0.352	0.003***
Farm size	0.53	0.51	0.288	0.69	0.876	0.208	0.649	0.352	0.852	0.158
Farm income	1.763	0.017**	0.902	0.197	-2.538	0.000***	0.305	0.619	-0.426	0.485
Livestock ownership	0.134	0.232	0.044	0.612	0.103	0.179	-0.092	0.278	-0.073	0.37
Non-farm income	1.034	0.221	0.913	0.242	1.136	0.104	-0.426	0.494	0.769	0.192
Memberships in social institution	0.28	0.345	-0.115	0.674	0.218	0.433	0.452	0.101	-0.036	0.882
Extension support	1.345	0.000***	0.431	0.072*	0.787	0.001***	0.718	0.006***	0.408	0.095*
Market linkage	0.387	0.27	0.726	0.009***	0.041	0.879	0.075	0.784	0.081	0.766
Climate info	1.18	0.000***	0.589	0.022**	0.662	0.006***	0.521	0.042**	0.444	0.062*
Credit access	1.622	0.000***	0.518	0.052*	0.258	0.283	0.172	0.503	0.178	0.468
_cons	-5.08	0.000***	-3.616	0.000***	-0.633	0.5	-3.131	0.007***	-1.598	0.108
Rho 12	0.72***	Rho 13	0.54*	Rho 14	0.69***	Rho 15	0.33	Rho 23	0.64***	Rho 24	0.60***	Rho 25	0.34**	Rho34	0.75***	Rho 35	0.24	Rho 45	0.08								

*, ** and *** indicate statistically significant at 0.1, 0.05 and 0.01 alpha levels, respectively.

better than the two other AEZs. In contrast, farming in the LWD zone has a statistically significant negative effect on adopting agroforestry, but a positive effect on changing crop varieties as an adaptation strategy. The topography in the LWD is relatively steeper than in the UWD, and water availability and diversion are more difficult, limiting the implementation of irrigation and agroforestry. However, smallholder farmers in these areas choose to implement varieties of crops to avoid loses due to highly fluctuated climate and drought conditions in the area.

Marginal effects further clarify these relationships. Farming in the UWD zone significantly decreases the likelihood of adopting SWC by 27.2%, while the probabilities of adopting

irrigation and crop varieties increase by 28.4% and 22.6%, respectively (Table 5.6). In contrast, farmers in the LWD zone are 13.6% and 13.2% less likely to adopt SWC and agroforestry, respectively. However, farming in the LWD AEZ increases the probability of adopting crop varieties by 12.8% (p = 0.1). These findings underscore the differentiated impacts of AEZs on the adoption of various adaptation strategies, with distinct patterns emerging in the UWD and LWD zones (Table 5.6).

5.3.5.2. Demographic factors

MVP estimates indicate that the age of the household head negatively affected the choice of adaptation strategies such as SWC, agroforestry, irrigation, and adjusting planting dates. However, this effect is statistically significant only for agroforestry (p = 0.1). Changes in crop varieties were not negatively affected by age. This may be attributed to the fact that adaptation strategies like SWC, agroforestry and irrigation require significant manpower and effort. Consequently, older farmers may be less inclined to adopt these labor-intensive and physically demanding strategies.

Larger household sizes positively influence the adoption of all strategies likely due to the availability of more labor within the household. However, this effect is statistically significant only for SWC and changing crop variety. As shown in Table 5.6, an increase in household size significantly increases the likelihood of adopting SWC and changing crop variety by 3.9% and 4.8%, respectively. This suggests that the availability of labor, closely associated with household size, plays a crucial role in farmers' decisions to adopt these strategies.

Table 5.6. Parameter estimates of the multivariate probit model for climate change adaptation strategies.

Explanatory	SWC		Irrigation		Agroforestry		Change in crop varieties		Changing planting dates	
Variables	Coef.	p value	Coef.	p value	Coef	p value	Coef	p value	CoeF.	p value
AEZ										
UWD	-1.75	0.000***	1.34	0.001***	0.268	0.475	0.923	0.007***	0.155	0.681
LWD	-1	0.001***	-0.043	0.888	-0.479	0.092*	0.496	0.076*	0.408	0.178
Age	-0.01	0.739	-0.005	0.777	-0.024	0.09*	0.012	0.444	-0.014	0.342
Gender	0.338	0.296	0.189	0.469	0.238	0.389	-0.203	0.453	0.027	0.918

Household size	0.237	0.013**	0.025	0.778	0.044	0.623	0.099	0.326	0.161	0.07*
Education	0.303	0.038**	0.661	0.000***	0.285	0.01**	0.6	0.000***	0.352	0.003***
Farm size	0.53	0.51	0.288	0.69	0.876	0.208	0.649	0.352	0.852	0.158
Farm income	1.763	0.017**	0.902	0.197	-2.538	0.000***	0.305	0.619	-0.426	0.485
Livestock ownership	0.134	0.232	0.044	0.612	0.103	0.179	-0.092	0.278	-0.073	0.37
Non-farm income	1.034	0.221	0.913	0.242	1.136	0.104	-0.426	0.494	0.769	0.192
Memberships in social institution	0.28	0.345	-0.115	0.674	0.218	0.433	0.452	0.101	-0.036	0.882
Extension support	1.345	0.000***	0.431	0.072*	0.787	0.001***	0.718	0.006***	0.408	0.095*
Market linkage	0.387	0.27	0.726	0.009***	0.041	0.879	0.075	0.784	0.081	0.766
Climate info	1.18	0.000***	0.589	0.022**	0.662	0.006***	0.521	0.042**	0.444	0.062*
Credit access	1.622	0.000***	0.518	0.052*	0.258	0.283	0.172	0.503	0.178	0.468
_cons	-5.08	0.000***	-3.616	0.000***	-0.633	0.5	-3.131	0.007***	-1.598	0.108
Rho 12 0.72*** Rho 13 0.54* Rho 14 0.69*** Rho 15 0.33 Rho 23 0.64*** Rho 24 0.60*** Rho 25 0.34** Rho34 0.75*** Rho 35 0.24 Rho 45 0.08										

*, ** and *** indicate statistically significant at 0.1, 0.05 and 0.01 alpha levels, respectively.

5.3.5.3. Socioeconomic factors

As expected, the level of education of household heads has a statistically significant positive effect on the adoption of all climate change adaptation strategies. The findings indicate that with each additional level of education, the probability of adopting SWC, agroforestry, irrigation, changing crop varieties, and adjusting planting dates increases by 4.9%, 14.5%, 7.7%, 14.9% and 10.4%, respectively (Table 5.6). This aligns with the findings of previous studies, which emphasize that human capital development is crucial for improving climate adaptation (Akinnagbe & Irohibe, 2015). The MVP estimates in Table 5.5 show that farm size has a generally positive but insignificant impact on the adoption of all adaptation strategies. Income from farm activities has a statistically significant positive effect ($p = 0.05$) on the adoption of SWC but a statistically significant negative effect ($p = 0.01$) on the adoption of agroforestry. Specifically, a unit increase in farm income increases the probability of adopting SWC by 31% and decreases the probability of choosing agroforestry by 68.7% (Table 5.6). The negative association between farm income and agroforestry may be due to the prominence of *chat* cultivation, which is often considered a form of agroforestry. This emphasis on *chat* production may reduce crop production by reallocating land from crops to chat. Non-farm income, on the other hand, positively influences the adoption of all adaptation strategies except changes in crop variety. As shown in the marginal effects in Table 5.6, a unit increase in non-farm income significantly ($p = 0.1$) increases the probability of adopting agroforestry by 30.5%.

Table 5.7. Marginal effects of multivariate probit model for climate change adaptation strategies.

Explanatory	SWC		Irrigation		Agroforestry		Chang in crop varieties		Changing planting dates	
Variables	Coef.	p value	Coef.	p value	Coef	p value	Coef	p value	CoeF.	p value
AEZ										
UWD	-0.272	0.000***	0.284	0.000***	0.071	0.473	0.226	0.005***	0.047	0.68
LWD	-0.156	0.003***	-0.01	0.888	-0.132	0.091*	0.128	0.078*	0.122	0.179
Age	-0.001	0.738	-0.001	0.776	-0.006	0.087*	0.003	0.439	-0.004	0.343
Gender	0.055	0.301	0.042	0.471	0.064	0.391	-0.05	0.453	0.008	0.917
Household size	0.039	0.011**	0.006	0.78	0.012	0.623	0.024	0.318	0.048	0.061*
Education	0.049	0.033**	0.145	0.000***	0.077	0.006**	0.149	0.000***	0.104	0.002***
Farm size	0.086	0.519	0.063	0.687	0.235	0.197	0.161	0.35	0.251	0.153
Farm income	0.287	0.017**	0.198	0.188	-0.682	0.000***	0.076	0.619	-0.126	0.483
Livestock ownership	0.022	0.243	0.01	0.608	0.028	0.167	-0.023	0.267	-0.022	0.368
Non-farm income	0.168	0.209	0.2	0.242	0.305	0.095*	-0.106	0.493	0.227	0.187
Memberships in social institution	0.046	0.348	-0.025	0.672	0.059	0.438	0.112	0.089*	-0.011	0.882
Extension support	0.219	0.000***	0.095	0.071*	0.211	0.001***	0.178	0.004**	0.12	0.088*
Market linkage	0.063	0.251	0.159	0.008***	0.011	0.879	0.019	0.784	0.024	0.766
Climate info	0.192	0.000***	0.129	0.014**	0.178	0.004***	0.129	0.035**	0.131	0.056*
Credit access	0.264	0.000***	0.114	0.048**	0.069	0.281	0.043	0.507	0.053	0.466

*, ** and *** indicate statistically significant at 0.1, 0.05 and 0.01 alpha levels, respectively.

5.3.5.4. Institutional factors

MVP estimates indicate that institutional factors significantly influence the adoption of most climate change adaptation strategies. The results highlight the crucial role of extension support in promoting the adoption of all adaptation strategies, with a statistically significant impact on all strategies (Table 5.5). The marginal effects presented in Table 5.6 explain these relationships. Specifically, extension support is associated with a 21.9% increase in the probability of adopting SWC, a 9.5% increase for irrigation, a 21.1% increase for agroforestry, and a 17.8% increase for changing crop variety, and a 12.0% increase for changing planting dates. This highlights the importance of expert advice in motivating farmers to implement climate change adaptation strategies. Choosing an effective adaptation strategy requires considering various factors. The guidance of extension workers on suitable conservation measures, improved seed selection, intensity of irrigation, and locally compatible agroforestry practices is invaluable. Furthermore, advice on selecting optimal planting dates aligned with seasonal rainfall and temperature patterns can strengthen farmers' confidence in their decisions. This targeted support not only improves the relevance of

adaptation choices, but also promotes more effective and resilient agricultural practices in response to climate variability (Berrang-ford et al., 2011a; Di Falco et al., 2012; Obsi et al., 2023a).

Furthermore, market linkages exhibit a positive association with the adoption of all strategies, although the effect is statistically significant ($p = 0.01$) only for irrigation. Market linkages enhance the probability of adopting irrigation by 15.9%. Irrigation demands substantial investment from farmers, which includes expenses for land preparation, seeds, fertilizers, water pumps, and other inputs. Farmers typically focus on perishable cash crops, such as tomatoes, cabbage, onions, and potatoes, which require timely market access to avoid losses. Consequently, before committing to irrigation, farmers often assess available market opportunities to ensure a profitable return. Therefore, it is essential to ensure reliable market access, as it enhances farmers' confidence and willingness to invest in irrigation, ultimately fostering the growth of high value, perishable crops that contribute to their livelihoods.

Access to climate information has a statistically significant positive effect on the probabilities of choosing all adaptation strategies. Specifically, it increases the likelihood of adopting SWC by 19.2%, irrigation by 12.9%, agroforestry by 17.8%, changing crop variety by 12.9% and adjusting planting dates by 13.1%. Timely access to climate information is crucial for allowing farmers to make informed and proactive decisions. For example, when forecasts indicate an increase in rainfall during the *kiremt* season, farmers can implement measures to mitigate potential flooding and soil erosion, such as constructing barriers or improving drainage. This information also helps in selecting the appropriate crop types and adjusting planting dates to optimize plant growth conditions. By anticipating seasonal weather patterns, farmers can better protect their fields, maximize yields, and enhance resilience against climate-related risks (Obsi et al., 2023b).

Similarly, access to credit positively influences the adoption of all adaptation strategies, with significant effects on SWC and irrigation. Specifically, access to credit significantly ($p < 0.05$) increases the likelihood of adopting SWC by 26.4% and irrigation by 11.4%. As noted above, both SWC and irrigation require substantial financial investment from farmers. Access to credit helps alleviate the financial burden associated with these expenses, facilitating the implementation of SWC and irrigation practices (Berrang-ford et al., 2011b).

5.4. Limitations of the study

This study was conducted in three representative villages across different AEZs using a relatively small sample size. While the sample is considered representative for the upper Gelana watershed, including more villages, increasing the number of surveyed households, and expanding the range of explanatory variables could improve the robustness and generalizability of the findings. Additionally, future studies should incorporate livelihood vulnerability analysis to quantify the degree of exposure, sensitivity, and adaptive capacity of farming households. Research could also explore the long-term effectiveness of different adaptation strategies and examine the roles of gender and youth in decision-making and climate resilience.

5.5. Conclusion and policy implications

This study examined farmers' perceptions of climate change and their choices of adaptation strategies in the upper Gelana watershed. The findings reveal that a substantial proportion of farmers across all AEZs perceived an increase in temperature and a decrease in precipitation patterns in the study area. However, there are seasonal variations in rainfall patterns, with a decline in *belg* rainfall (short rainy season) and an increase in *kiremt* (main rainy season) rainfall. The majority of the respondents perceived an increment in the occurrence of drought, the incidence of diseases, erosion hazards, pests, and the decline in crop yields as impacts of climate change. Analysis of adaptation strategies in different AEZs shows significant variation, particularly in the adoption of SWC, agroforestry, and irrigation. SWC and agroforestry are more commonly practiced in the *Dega* AEZ, while irrigation and changes in crop variety are more prevalent in the UWD, and adjustments in planting dates are more frequently practiced in the LWD AEZ.

The study identifies a variety of factors that influence the choice of climate adaptation strategies. Farming across the three AEZs determines the choice of strategies. Among socioeconomic factors, the education status of the household head significantly affects the choices of all adaptation strategies. In addition, farm income significantly influences SWC, while it has a significant negative effect on the adoption of agroforestry. Institutional factors, such as extension support, access to climate information, market linkages, and credit access, have a significant positive effect on the choice of most climate adaptation strategies.

These findings offer important insights for administrators at various levels, government organizations (GOs), and non-government organizations (NGOs) working in the area, as well as policymakers. First, understanding farmers' perceptions of climate change and its impact provides a foundation for responsive policy measures. Additionally, recognizing the gaps in adaptation strategy choices and the limiting factors is crucial to implement immediate actions to mitigate the effects of climate change. Specifically, more emphasis should be given on the AEZ-specific adaptation strategies to effectively minimize the impacts climate change. Given the positive role of education in adaptation, awareness-raising and capacity-building training programs and support from extension workers should be prioritized. Strengthening local meteorological stations and providing timely climate information will also enhance the implementation of adaptation strategies.

Based on the findings of this study, particularly those related to rainfall unpredictability, technology adoption, and uneven access to information and support, the following recommendations are proposed:

- Enhance the role of extension services and invest in awareness-raising and capacity-building training programs for smallholder farmers.
- Strengthen local meteorological stations and ensure the timely dissemination of localized climate forecasts and advisories to support informed decision-making.
- Facilitate access to credit and affordable technologies (e.g., water pumps, geomembranes) that are essential for improving water harvesting and irrigation in light of rainfall variability.
- Establish and improve market linkages, particularly for high-value crops such as chat and fruits, to increase the economic to incentivizes for the adoption of sustainable practices.
- Replicate best practices in natural resource management, such as those successfully implemented in the Dega AEZ, across UWD and LWD through farmer-to-farmer exchanges, organized field visits, and learning platforms.

Funding statement

This research was received financial support from the Office of the Vice President for Research and Technology Transfer (VPRTT), Addis Ababa University, Addis Ababa,

Ethiopia and Regional Center for Mapping of Resources for Development (RCMRD)/GMES and Africa, Nairobi, Kenya.

Data Availability

The data used to support the findings of this study will be available from the corresponding author upon request.

Conflicts of Interest

The authors declare no conflict of interest.

Acknowledgments

The first author expresses gratitude to Addis Ababa University, Kotebe University of Education, and the Regional Centre for Mapping of Resources for Development (RCMRD)/GMES and Africa for their financial support for this study. The authors also extend their appreciation to the Tehuledere District Agricultural and Rural Development Office, as well as the development agents and farmers who participated in the focus group discussions and surveys.

References

Addis, Y., & Abirdew, S. (2021). Smallholder farmers' perception of climate change and adaptation strategy choices in Central Ethiopia. *International Journal of Climate Change Strategies and Management*, 13(4/5), 463–482. https://doi.org/10.1108/IJCCSM-09-2020-0096

Adom, P. K. (2024). The socioeconomic impact of climate change in developing countries over the next decades: A literature survey. *Heliyon*, *10*(15), e35134. https://doi.org/10.1016/j.heliyon.2024.e35134

Akinnagbe, O., & Irohibe, I. (2015). Agricultural adaptation strategies to climate change impacts in Africa: a review. *Bangladesh Journal of Agricultural Research*, *39*(3), 407–418. https://doi.org/10.3329/bjar.v39i3.21984

Asfaw, A., Simane, B., Bantider, A., & Hassen, A. (2018). Determinants in the adoption of climate change adaptation strategies evidence from rainfed - dependent smallholder farmers in north - central Ethiopia (Woleka sub-basin). *Environment, Development and Sustainability*, *21*, 2535–2565. https://doi.org/10.1007/s10668-018-0150-y

Asfaw, A., Simane, B., Hassen, A., & Bantider, A. (2018). Variability and time series trend analysis of rainfall and temperature in northcentral Ethiopia: A case study in Woleka sub-basin. *Weather and Climate Extremes*, *19*, 29–41. https://doi.org/10.1016/j.wace.2017.12.002

Asrat, P., & Simane,B.(2018).Farmers' perception of climate change and adaptation strategies in the Dabus watershed, North-West Ethiopia. *Ecological Processes.7(7). https://doi.org/10.1186/s13717-018-0118-8*

Ayal, D. Y., & Filho, W. L. (2017). Farmers ' perceptions of climate variability and its adverse impacts on crop and livestock production in Ethiopia. *Journal of Arid Environments*, *140*, 20–28. https://doi.org/10.1016/j.jaridenv.2017.01.007

Becker, R., & Elliot, P. (2022). Climate change a friend or foe to food security in Africa? *Environment, Development and Sustainability*, *24*, 4387–4412. https://doi.org/10.1007/s10668-021-01621-8

Bedeke, S. B. (2023). Climate change vulnerability and adaptation of crop producers in sub - Saharan Africa: a review on concepts , approaches and methods. In *Environment, Development and Sustainability* 25, 1017–1051. https://doi.org/10.1007/s10668-022-02118-8

Berrang-ford, L., Ford, J. D., & Paterson, J. (2011a). Are we adapting to climate change? *Global Environmental Change*, *21*, 25–33. https://doi.org/10.1016/j.gloenvcha.2010.09.012

Berrang-ford, L., Ford, J. D., & Paterson, J. (2011b). Are we adapting to climate change? *Global Environmental Change*, *21*, 25–33. https://doi.org/10.1016/j.gloenvcha.2010.09.012

Bewket, W. (2007). Soil and water conservation intervention with conventional technologies in northwestern highlands of Ethiopia: Acceptance and adoption by farmers.Land Use Policy, 24: 404–416. https://doi.org/10.1016/j.landusepol.2006.05.004

Bewket, W. (2012). Climate change perceptions and adaptive responses of smallholder farmers in central highlands of Ethiopia. *International Journal of Environmental Studies*, *69*(3), 507–523. https://doi.org/10.1080/00207233.2012.683328

Bouteska, A., Sharif, T., Bhuiyan, F., & Zoynul, M. (2024). Impacts of the changing climate on agricultural productivity and food security: Evidence from Ethiopia. *Journal of Cleaner Production*, *449*(May 2023), 141793. https://doi.org/10.1016/j.jclepro.2024.141793

Cappellari, L., & Jenkins, S. P. (2003). Multivariate Probit Regression using Simulated Maximum Likelihood. *The Stata Journal*, *3*(3), 278–294. https://doi.org/10.1177/1536867x0300300305

Cappellari, L., & Jenkins, S. P. (2006). Calculation of multivariate normal probabilities by simulation , with applications to maximum simulated likelihood estimation. *The Stata Journal*, *6*(2), 156–189.

Dawide, T.A., Zeleke, F. and Ebro, M.M. (2022) Impact of Khat Production and Marketing on the Livelihood of Smallholder Households in Ethiopia. *Agricultural Sciences* , 13, 1309-1320. https://doi.org/10.4236/as.2022.1312080

Deressa, T. T., Hassan, R. M., Ringler, C., Alemu, T., & Yesuf, M. (2009). Determinants of farmers' choice of adaptation methods to climate change in the Nile Basin of Ethiopia. *Global Environmental Change*, *19*(2), 248–255. https://doi.org/10.1016/j.gloenvcha.2009.01.002

Di Falco, S., Yesuf, M., Kohlin, G., & Ringler, C. (2012). Estimating the Impact of Climate Change on Agriculture in Low-Income Countries: Household Level Evidence from the Nile Basin, Ethiopia. *Environmental Resource Economics*, *52*, 457–478. https://doi.org/10.1007/s10640-011-9538-y

Donatti, C. I., Nicholas, K., Fedele, G., Delforge, D., Speybroeck, N., Moraga, P., Blatter, J., Below, R., & Zvoleff, A. (2024). International Journal of Disaster Risk Reduction Global hotspots of climate-related disasters. *International Journal of Disaster Risk Reduction*, *108*(April), 104488. https://doi.org/10.1016/j.ijdrr.2024.104488

Eisenack, K., Moser, S. C., Hoffmann, E., Klein, R. J. T., Oberlack, C., Pechan, A., Rotter, M., & Termeer, C. J. A. M. (2014). Explaining and overcoming barriers to climate change adaptation. *Nature Climate Change*, *4*, 867–872. https://doi.org/10.1038/NCLIMATE2350

Fauzel, S. (2021). Economic Impact of Climate Change on Agriculture: Case of Africa. In D. Luetz, J.M., Ayal (Ed.), *Handbook of Climate Change Management* (pp. 1913–1937). Springer, Cham. https://doi.org/10.1007/978-3-030-57281-5_34

Federal Democratic Republic of Ethiopia. (2005, July 15). Federal Democratic Republic of Ethiopia Rural Land Administration and Use Proclamation No. 456/2005. *Negarit Gazeta*, 44.

Gezie, M. (2019). Farmer ' s response to climate change and variability in Ethiopia : A review. *Cogent Food & Agriculture*, *5*(1), 1613770. https://doi.org/10.1080/23311932.2019.1613770

Godde,C.M. , Mason-D'Croz, D., Mayberry,D.E., Thornton,P.K., Herrero,M. (2021). Impacts of climate change on the livestock food supply chain; a review of the evidence. *Global Food Security*, 28,100488. https://doi.org/10.1016/j.gfs.2020.100488

Greenberg, E. (1998). Analysis of Multivariate Probit Models. *Biometrika Trust*, *85*(2), 347–361.

Gwambene, B., Liwenga, E., & Mung'ong'o, C. (2023). Climate Change and Variability Impacts on Agricultural Production and Food Security for the Smallholder Farmers in Rungwe,Tanzania. *Environmental Management*, *71*, 3–14. https://doi.org/10.1007/s00267-022-01628-5

Hengsdijka,H. , Meijerinkb,G.W., & Mosugu, M.E.(2005). Modeling the effect of three soil and water conservation practices in Tigray, Ethiopia. *Agriculture, Ecosystems and Environment*, 105: 29–40. https://doi.org/10.1016/j.agee.2004.06.002

Israel, G.D. (1992) Determining Sample Size. University of Florida Cooperative Extension Service, Institute of Food and Agriculture Sciences, EDIS, Florida.

Jonkman, S. N., Curran, A., & Bouwer, L. M. (2024). Floods have become less deadly: an analysis of global flood. *Natural Hazards*, *120*(7), 6327–6342. https://doi.org/10.1007/s11069-024-06444-0

Kotir, J. H. (2011). Climate change and variability in Sub-Saharan Africa: A review of current and future trends and impacts on agriculture and food security. *Environment, Development and Sustainability*, *13*(3), 587–605. https://doi.org/10.1007/s10668-010-9278-0

Likinaw, A., Bewket, W., & Alemayehu, A. (2023). Smallholder farmers ' perceptions and adaptation strategies to climate change risks in northwest Ethiopia. *International Journal of Climate Change Strategies and Management*, *15*(5), 599–618. https://doi.org/10.1108/IJCCSM-01-2022-0001

Liu, Q., Du, M., Wang, Y., Deng, J., Yan, W., Qin, C., Liu, M., & Liu, J. (2024). Global, regional and national trends and impacts of natural floods,1990–2022. *Bull World Health Organ*, *102*(6), 410–420. https://doi.org/10.2471/BLT.23.290243

Maru, H., Haileslassie, A., & Zeleke, T. (2023). Impacts of small-scale irrigation on farmers' livelihood: Evidence from the drought-prone areas of upper Awash sub-basin, Ethiopia. *Heliyon*, 9(3), e16354. https://doi.org/10.1016/j.heliyon.2023.e16354

Mbow, C., Van Noordwijk, M., Luedeling, E., Neufeldt, H., Minang, P. A., & Kowero, G. (2014). Agroforestry solutions to address food security and climate change challenges in Africa. *Current Opinion in Environmental Sustainability*, 6, 61–67. https://doi.org/10.1016/j.cosust.2013.10.014

Mbow, C., Rosenzweig, C., Barioni, L. G., Benton, T. G., Herrero, M., Krishnapillai, M., Liwenga, E., Pradhan, P., Rivera-Ferre, M. G., Sapkota, T., Tubiello, F. N., & Xu, Y. (2019). Food security. In P. R. Shukla, J. Skea, E. C. Buendia, V. Masson-Delmotte, H.-O. Pörtner, D. C. Roberts, P. Zhai, R. Slade, S. Connors, R. van Diemen, M. Ferrat, E. Haughey, S. N. S. Luz, M. Pathak, J. Petzold, J. P. Pereira, P. Vyas, E. Huntley, K. Kissick, … J. Malley (Eds.), *Climate Change and Land: an IPCC special report on climate change, desertification, land degradation, sustainable land management, food security, and greenhouse gas fluxes in terrestrial ecosystems* (pp. 437–550). https://doi.org/https://doi.org/10.1017/9781009157988.007

Mengistu, F., & Assefa, E. (2019). Farmers' decision to adopt watershed management practices in Gibe basin, southwest Ethiopia. *International Soil and Water Conservation Research*, *7*(4), 376–387. https://doi.org/10.1016/j.iswcr.2019.08.006

Mera, G. A. (2018). Drought and its impacts in Ethiopia. *Weather and Climate Extremes*, *22*, 24–35. https://doi.org/10.1016/j.wace.2018.10.002

Moges, D. M., & Bhat, H. G. (2021). Climate change and its implications for rainfed agriculture in Ethiopia. *Journal of Water and Climate Change*, *12*(4), 1229–1244. https://doi.org/10.2166/wcc.2020.058

Mohammed, A., Yimer, E., Gessese, B., & Feleke, E. (2022). Environmental and Sustainability Indicators Predicting Maize (Zea mays) productivity under projected climate change with management options in Amhara region , Ethiopia. *Environmental and Sustainability Indicators*, *15*, 100185. https://doi.org/10.1016/j.indic.2022.100185

Mohammed, Y., Yimer, F., Tadesse, M., & Tesfaye, K. (2018). Variability and trends of rainfall extreme events in north east highlands of Ethiopia. *International Journal of Hydrology*, *2*(5), 594–605. https://doi.org/10.15406/ijh.2018.02.00131

Mullahy, J. (2011). *Marginal Effects in Multivariate Probit and Kindred Discrete and Count Outcome Models, with Applications in Health Economics* (17588; NBER Working Paper Series).

Muluneh, M. G. (2021). Impact of climate change on biodiversity and food security : a global perspective - a review article. *Agriculture & Food Security*, *10*(36). https://doi.org/10.1186/s40066-021-00318-5

Newman, R., & Noy, I. (2023). *The global costs of extreme weather that are attributable to climate change*. *October 2022*. https://doi.org/10.1038/s41467-023-41888-1

Obsi, D., Korecha, D., & Garedew, W. (2023a). Determinants of climate change adaptation strategies and existing barriers in Southwestern parts of Ethiopia. *Climate Services*, *30*, 100376. https://doi.org/10.1016/j.cliser.2023.100376

Obsi, D., Korecha, D., & Garedew, W. (2023b). Determinants of climate change adaptation strategies and existing barriers in Southwestern parts of Ethiopia. *Climate Services*, *30*, 100376. https://doi.org/10.1016/j.cliser.2023.100376

Omotoso, A. B., Letsoalo, S., Olagunju, K. O., Tshwene, C. S., & Omotayo, A. O. (2023). Climate change and variability in sub-Saharan Africa: A systematic review of trends and impacts on agriculture. *Journal of Cleaner Production*, *414*, 137487. https://doi.org/10.1016/j.jclepro.2023.137487

Raihan, A. (2023). A review of the global climate change impacts, adaptation strategies, and mitigation options in the socio-economic and environmental sectors. *Journal of Environmental Science and Economics*, *2*(3), 36–58. https://doi.org/10.56556/jescae.v2i3.587

Rentschler, J., & Salhab, M. (2022). Flood exposure and poverty in 188 countries. *Nature Communications*, *13*, 3527. https://doi.org/10.1038/s41467-022-30727-4

Roba, N. T., Kassa, A. K., Geleta, D. Y., & Hishe, B. K. (2022). Achievements, challenges, and opportunities of rainwater harvesting in the Ethiopian context: A review. *Water Supply*, 22(2), 1611–1627. https://doi.org/10.2166/ws.2021.330

Rockström, J. (2003). Resilience building and water demand management for drought mitigation. *Physics and Chemistry of the Earth*, *28*(20–27), 869–877. https://doi.org/10.1016/j.pce.2003.08.009

Roodman, D. (2011). Fitting fully observed recursive mixed-process models with cmp. *The Stata Journal*, *11*(2), 159–206. https://doi.org/10.1177/1536867X1101100202

Rosell, S., & Holmer, B. (2015). Erratic rainfall and its consequences for the cultivation of teff in two adjacent areas in South Wollo, Ethiopia. *Norsk Geografisk Tidsskrift*, *69*(1), 38–46. https://doi.org/10.1080/00291951.2014.992805

Saleem, A., Anwar, S., Nawaz, T., Fahad, S., Saud, S., & Ur, T. (2024). Securing a sustainable future : the climate change threat to agriculture , food security , and sustainable development goals. *Journal of Umm Al-Qura University for Applied Sciences*. https://doi.org/10.1007/s43994-024-00177-3

Serdeczny, O., Adams, S., Baarsch, F., Coumou, D., Robinson, A., Hare, W., Schaeffer, M., Perrette, M., & Reinhardt, J. (2017). Climate change impacts in Sub-Saharan Africa: from physical changes to their social repercussions. *Regional Environmental Change*, *17*(6), 1585–1600. https://doi.org/10.1007/s10113-015-0910-2

Sertse, S. F., Khan, N. A., Shah, A. A., Liu, Y., & Naqvi, S. A. A. (2021). Farm households ' perceptions and adaptation strategies to climate change risks and their determinants

Evidence from Raya Azebo district , Ethiopia. *International Journal of Disaster Risk Reduction*, *60*, 102255. https://doi.org/10.1016/j.ijdrr.2021.102255

Simane, B., Hunachew Beyene, Wakgari Deressa, Abera Kumie, Kiros Berhane, & Jonathan Samet. (2016a). Review of Climate Change and Health in Ethiopia: Status and Gap Analysis. *Ethiop J Health De*, *30*, 28–41.

Simane, B., Zaitchik, B.F., & Foltz, J. D.(2016b). Agroecosystem specific climate vulnerability analysis: application of the livelihood vulnerability index to a tropical highland region. *Mitig Adapt Strateg Glob Change*, 21:39–65.https://doi.org/10.1007/s11027-014-9568-1

Solomon, R., Simane, B., & Zaitchik, B. F. (2021). *The Impact of Climate Change on Agriculture Production in Ethiopia: Application of a Dynamic Computable General Equilibrium Model*. 32–50. https://doi.org/10.4236/ajcc.2021.101003

Tadesse, S., & Mekuriaw, A. (2024). Agroecology-based analysis of meteorological and agricultural drought using time series remote sensing data in the upper Gelana watershed, Ethiopia. *Geocarto International ISSN:*, *39*(1), 2417881. https://doi.org/10.1080/10106049.2024.2417881

Tadesse, S., Mekuriaw, A., & Assen, M. (2024). Spatiotemporal climate variability and trends in the Upper Gelana Watershed, northeastern highlands of Ethiopia. *Heliyon*, *10*(5), e27274. https://doi.org/10.1016/j.heliyon.2024.e27274

Tesfahun, T., Abegaz A, & Abate, E.(2024). quantitative analysis on the adoption of soil, water, and forest conservation technologies in the upper Gelana watershed, Northeast Ethiopian highlands. *Heliyon*, *10*(17), e36794. https://doi.org/10.1016/j.heliyon.2024.e36794

Teshome, A., Jan de Graaff, & Kassie, M.(2016). Household-Level Determinants of Soil and Water Conservation Adoption Phases: Evidence from North-Western Ethiopian Highlands. *Environmental Management*, 57:620–636. https://doi.org/10.1007/s00267-015-0635-5

Teklewold, H., Mekonnen, A., & Kohlin, G. (2019). Climate change adaptation a study of multiple climate-smart practices in the Nile Basin of Ethiopia. *Climate and Development*, *11*(2), 180–192. https://doi.org/10.1080/17565529.2018.1442801

Tesfaye, T., & Nayak, D. (2023). Climate Change Adaptation Measures by Farm Households in Gedeo Zone , Ethiopia An Application of Multivariate. *Environment, Development and Sustainability*, *25*(4), 3183–3209. https://doi.org/10.1007/s10668-022-02185-x

Tibebe, D., Teferi, E., Bewket, W., & Zeleke, G. (2022). Climate induced water security risks on agriculture in the Abbay river basin: A review. *Frontiers in Water*, *4*, 961948. https://doi.org/10.3389/frwa.2022.961948

Ting, B., Wright, F., & Zhou, Y.-H. (2022). Fast Multivariate Probit Estimation via a Two-Stage Composite Likelihood. *Statistics in Biosciences*, *14*(3), 533–549. https://doi.org/10.1007/s12561-022-09338-6

Tofu, D. A., Woldeamanuel, T., & Haile, F. (2022). Smallholder farmers' vulnerability and adaptation to climate change induced shocks: The case of Northern Ethiopia highlands. *Journal of Agriculture and Food Research*, *8*, 100312. https://doi.org/10.1016/j.jafr.2022.100312

Tofu, D. A., & Wolka, K. (2023a). Climate change induced a progressive shift of livelihood from cereal towards Khat (Chata edulis) production in eastern Ethiopia. *Heliyon*, *9*(1), e12790. https://doi.org/10.1016/j.heliyon.2022.e12790

Tofu, D. A., & Wolka, K. (2023b). Climate change induced a progressive shift of livelihood from cereal towards Khat (Chata edulis) production in eastern Ethiopia. *Heliyon*, *9*(1), e12790. https://doi.org/10.1016/j.heliyon.2022.e12790

Thornton, P.K. , van de Steeg, J., Notenbaert, A. & Herrero, M. (2009). The impacts of climate change on livestock and livestock systems in developing countries: A review of what we know and what we need to know. *Agricultural Systems,* 101, 113–127.https://doi.org/10.1016/j.agsy.2009.05.002

UNCCD. (2022). *DROUGHT IN NUMBERS 2022 - restoration for readiness and resilience*.

UNDRR. (2019). *Human cost of disasters:An overview of the last 20 years 2000-2019*.

Yamane, T. (1967). *Statistics, An Introductory Analysis* (2nd ed.). Harper and Row.

Zeratsion, B., Manaye,A., Gufi,Y., Tesfaye,M., Werku,A., & Anjulo, A.(2024). Agroforestry practices for climate change adaptation and livelihood resilience in drylands of Ethiopia, *Forest Science and Technology*, 20:1, 47-57, https://doi.org/10.1080/21580103.2023.2292171

Zhao, C., Liu, B., Piao, S., Wang, X., Lobell, D. B., Huang, Y., Huang, M., Yao, Y., Bassu, S., Ciais, P., Durand, J.-L., Elliott, J., Ewertp, F., Janssens, I. A., Li, T., Lin, E., Liu, Q., Martre, P., Müller, C., … Asseng, S. (2017). Temperature increase reduces global yields of major crops in four independent estimates. *PNAS*, *114*(35), 9326–9331. https://doi.org/10.1073/pnas.1701762114

CHAPTER SIX

6.SUMMARY, CONCLUSIONS AND RECOMMENDATIONS

6.1. Summary

This study analyzes climate variability and changes over the past three decades, focusing on trends in rainfall and temperature, droughts and dynamics of land surface phenology in response to climate variability across the lower *weina dega* (LWD), upper *weina dega*(UWD), and *dega* agroecological zones (AEZs) of the Upper Gelana watershed. In addition, it explores farmers' perceptions of climate variability and change, its impacts, and the factors that determine the choices adaptation strategies.

The rainfall and temperature trends from 1983 to 2021 were examined using satellite remote sensing precipitation and gridded temperature data. First, evaluation of the performance of two widely used satellite precipitation datasets, CHIRPS and TAMSAT, in the Upper Gelana watershed. Then TAMSAT was selected because of its resolution and better performance. Trends were then assessed using Mann-Kendall, Sen's Slope estimator, and ITA methods. Results reveal high inter-annual and spatiotemporal variability, with strong irregularities in monthly rainfall. The Mann-Kendall test shows statistically significant positive trends in *kiremt* and annual rainfall, while negative trend was observed in *belg* rainfall. During *kiremt*, rainfall increased by 96.1, 101.6, and 104.8 mm per decade in LWD, UWD, and *dega*, respectively, whereas *belg* season rainfall declined by 16.4, 16.2, and 14.0 mm per decade in these zones. Annual minimum and maximum temperatures show significant decreasing and increasing trends in LWD and UWD, respectively, while no significant trend detected in *dega*AEZ. The ITA method uncovered additional trends not detected by the Mann-Kendall test.

The study examined meteorological and agricultural drought events using remote sensing datasets using SPI, VHI, and ETDI. The results indicate notable meteorological droughts during the *belg* season in the LWD in 2018 and in the UWD and *dega* in 2008 and 2013, with an extreme drought in 1999 affecting all AEZ. Similarly, there were meteorological droughts during the *kiremt* season in 1991, 1993, 2002, 2009, and 2015. The ETDI and VHI jointly identified *belg*-season agricultural droughts in LWD and UWD in the years 2002, 2008, 2009, 2011, 2012, 2013 and 2021, while the *dega*AEZ experienced itin 2008, 2012, 2013, and 2015. Furthermore, all AEZs experienced agricultural droughts in the *kiremt* season in 2002, 2008, and 2009. The findings revealed that *belg*

season agricultural droughts were more frequent in LWD, followed by UWD. Pixel-wise correlation analysis shows a statistically significant positive relationship between meteorological and agricultural drought indices during both *belg* and *kiremt* seasons, indicating potential transmission of meteorological drought into agricultural drought.

The study also examined spatiotemporal dynamics of land surface phenology and its association with climate variability and drought events across AEZs using MODIS NDVI data. The findings indicate that the *dega* AEZ has an earlier SOS and a longer LOS compared to LWD and UWD. Delays in SOS and EOS were observed in 71.3% and 82% of the study area, respectively, with LOS increasing in nearly half of the area. SOS is positively correlated with maximum temperature and negatively correlated with *belg* season rainfall and drought indices. Similarly, EOS shows a direct correlation with *kiremt* season maximum temperature, rainfall, and drought indices. A shorter LOS is associated with higher annual maximum temperatures, while a longer LOS correlates with increased annual rainfall.

Significant proportion of smallholder farmers across all AEZs of the Upper Gelana watershed perceive increasing temperatures and declining precipitation, particularly in the *belg* season. They also perceived the negative impacts of climate change. Notable variations in climate change adaptation strategies were observed across the AEZs, with soil and water conservation (SWC) and agroforestry more prevalent in the *dega* AEZ, irrigation and crop variety changes more common in UWD, and adjustments in planting dates practiced more in the LWD AEZ. In addition to the agroecology settings various demographic, socioeconomic and institutional factors play a significant role in choice of climate change adaptation strategies.

6.2. Conclusion

This study analyzed climate variability, drought occurrences, and land surface phenology dynamics across the LWD, UWD, and *dega* AEZs of the upper Gelana watershed. The analysis revealed that study area is characterized by a strongly irregular distribution of rainfall throughout the study period (1983-2021). We found a significant increasing trend in monthly rainfall from June to November in the LWD, UWD and *dega* AEZs using the MK test. The findings also showed a significant positive trend in the *kiremt* season and annual rainfall that vary across the study area. In contrast, rainfall during the *belg* season shows downward trend and high variability. The increment in *kiremt* season and annual rainfall is higher in the *dega*

agroecology zone and lower in the LWD. The findings from the MK test were corroborated by the ITA, with both methods aligning in their assessment of *belg* and *kiremt* seasonal rainfall trends in the LWD and UWD, as well as annual rainfall trends across all AEZs.

Temperature analysis highlighted a general warming trend, with significant increases in maximum temperatures in the LWD and UWD AEZs. However, in the *Dega* AEZ, *belg* and annual maximum temperatures exhibited insignificant upward trends, while bega (dry season) and *kiremt* maximum temperatures showed decreasing trends. The MK test also indicated upward trends in *belg*, *kiremt*, and annual mean temperatures. Some discrepancies were noted between the MK and ITA results, particularly in the trends of mean temperature.

The study revealed that meteorological droughts were more frequent during the *kiremt* season, while agricultural droughts were more prevalent during the *belg* season, particularly in the LWD and UWD AEZs. A pixel-wise correlation analysis demonstrated a strong positive association between meteorological and agricultural drought indices, highlighting the potential for drought conditions to propagate from meteorological to agricultural systems. This interconnection underscores the importance of integrated drought monitoring and early warning systems to mitigate cascading impacts across ecological and agricultural domains.

The analysis of land surface phenology revealed that the *dega* AEZ experienced an earlier SOS and a longer LOS compared to the LWD and UWD AEZs. Positive correlations between SOS and EOS with maximum temperature, and negative correlations with *belg* rainfall, suggest that warming temperatures delay SOS, while increased *kiremt* rainfall advances EOS. Key ecosystem indicators, such as maximum NDVI and base NDVI values, exhibit a gradual declining pattern from the *dega* AEZ to the LWD AEZ. These findings highlight the sensitivity of phenological dynamics to climatic variables and the varying ecological productivity across the AEZs.

Farmers perceptions of climate change aligned with observed trends, particularly regarding increasing temperatures and declining *belg* rainfall. Climate change adaptation strategies varied across AEZs, with SWC and agroforestry being practiced more in the *dega* AEZ, while irrigation and crop variety changes were more commonly practiced in the UWD AEZ. The education level of household heads, support from extension workers, and access to climate information were found to have a significant positive influence on the adoption of all climate adaptation strategies. Additionally, market linkages and access to credit specifically enhanced

the use of irrigation as an adaptation measure in the study area. These findings underscore the importance of strengthening institutional support, improving market access, and facilitating financial services to enhance adaptive capacity.

6.3. Recommendations

The study findings reveal significant shifts in rainfall patterns, temperature trends, drought occurrences, and land surface phenology dynamics within the upper Gelana watershed. They also highlight the different adaptation strategies employed by farmers, which are shaped by socio-economic, institutional, and agroecological factors. Drawing from these insights, the following recommendations are proposed to support effective adaptation measures and enhance resilience in the study area.

- Given the unpredictable nature of climate in the study area, the advancement in GIS and remote sensing technologies can play a significant role in detecting such changes, particularly the pattern of rainfall and temperature over space and time. In this regard, future research should leverage geospatial artificial intelligence to improve predictions of climate variability and trends in areas where meteorological data is scarce, so as to facilitate data driven decision making among farmers, administrators at different level and other stakeholders.
- Taking into account the prevalence of meteorological and agricultural drought in the *belg* and *kiremt* seasons, administrators and development partners must support smallholder farmers to implement and strengthen rainwater harvesting and soil conservation practices, agroforestry, irrigation activities and the use of drought-resilient crops and animal feed. These strategies should be tailored to the specific climate and drought conditions of each AEZto minimize the cascading impacts, particularly on agricultural production.
- Continuous monitoring of LSP is required to understand the effects of climate variability and extreme drought events across agroecological zones. Thus, future researchers should focus on the use of ground-based instruments such as phenocam to monitor the LSP across LULC and even at species level. This will provide deeper insights into how climate variability and drought affect the SOS, EOS, LOS and

other ecosystem condition indicators at a finer scale, thus informing adaptation strategies suited to different LULC types and specific crop types.

- Strengthening and devising appropriate adaptation strategies is essential. This can be achieved by increasing awareness and providing timely climate information to smallholder farmers. In this regard, extension workers can play a significant role in shaping the understanding and building capacities of smallholder farmers, which will empower farmers to adopt these strategies effectively.
- Enhancing institutional support by establishing frameworks for climate change adaptation and providing continuous assistance to smallholder farmers can help build a resilient agricultural community. This requires strengthening local administrations with the necessary human and financial resources to support the implementation of sustainable climate-smart farming practices in the area.
- Increasing market linkage and access to finance for smallholders will promote the adoption of appropriate climate change adaptation strategies such as irrigation practices. Improved access to credit will allow farmers to invest in water harvesting technologies and irrigation infrastructure. Strengthened market linkages will incentivize smallholder farmers to adopt more resilient agricultural practices and encourage them to diversify into non-farm activities, that increase their adaptive capacity in case of crop failure or yield reduction due to climate variability or extreme drought events.
- The best practices observed in the *dega* zone, such as natural resource management practices, should be shared with farmers in the UWD and LWD zones. Organized field visits and knowledge-sharing initiatives among smallholder farmers and experts at the local level can facilitate the dissemination of successful strategies and foster their implementations across AEZs.

These recommendations will help to build a climate-resilient agricultural system in the upper Gelana watershed, equipping farmers with the tools, knowledge, and support needed to adapt effectively to climate variability and change.

APPENDICES

Appendix A: Questionnaires

Addis Ababa University
School of Graduate Studies
Department of Geography and Environmental Studies

Dear respondents,

This research aims to assess the implication of spatiotemporal dynamics of climate variability, drought, land surface phenology and farmers' adaptation strategies across the agroecology zones of upper Gelana watershed, northeastern highlands of Ethiopia.So, this questionnaire is designed to obtain data on farmers' perception on climate variability and change as well as the impacts and adaptation strategies. Responding to the question accurately will greatly help me in completing my research and enhancing the understanding of the research under focus. I assure you that I will keep the information confidential and only use it for academic purposes. Thank you for taking your time in assisting me with this research. Thank you!

Survey No: _____Date of interview _____Time _____
Name of Kebele _____ Name of Village_____

Part One: General characteristics of the respondents

1. Sex of family head 1. Male □ 2. Female □
2. Education level of family head
   1.Illiterate □ 2. Grades 1-4 □
   3. Grades 5-8 □ 4.Grade 9 and above □
3. Age of the family head_____
4. Marital status 1. Single □ 2. Married □ 3. Widowed □ 4. Divorced □
5. Total number of the family members _____
6. Do you have your own farm land? 1. Yes □ 2. No □
7. If your answer for question 6 is yes, what is the size in hectare? _____
8. What is the estimated annual farm income in Birr? _____
9. What is the estimated annual non-farm income in Birr? _____
10. Please provide the number of animals owned in the table below?

1. Calf		6. Donkey (young)	
2. Heifer		7. Sheep and goat (adult)	
3. Cow and oxen		8. Sheep and goat (young)	
4. Horse		9. Camel	
5. Donkey (adult)		10. Chicken	

Part Two: farmers perception aboutclimate variability and change, its impacts and adaptation strategies.

11. How long have you been here? _____
12. Have you observed any long-term changes in the mean of climate variables specifically temperature and rainfall,since 2000? 1. Yes □ 2. No □
13. If your answer for question 12 is yes, indicate (x) what have been the changes.

No.	Long-term changes in mean climate variables	Response		
		1.Increased	2.Decreased	3.No change
1.	Temperature	□	□	□
2.	Rainfall Amount	□	□	□
3.	Others please specify			

14. What have you observed to be the negative impacts of these long-term changes in the mean of climate variation since 2000? Mark your answer by (x)

No.	Perceived impacts	1.Yes	2. No
1.	Increase in drought incidences	□	□
2.	Increase in flooding events	□	□
3.	Increase in storms and hailstones	□	□
4.	Increase in erosion hazards	□	□
5.	Growing prevalence in pests and insects	□	□
6.	Increase in crop diseases	□	□
7.	Rise in invasive weed species	□	□
8.	Decline in crop yields	□	□
9.	Increase in livestock diseases	□	□
10.	Growing prevalence of diseases (e.g., malaria)	□	□
11.	Reduction in water availability	□	□
12.	Decline in fodder availability	□	□

15. Would you please name the crop disease, livestock disease and pests occurred in your area?

    1.crop disease _____
    2.livestock disease_____
    3.pests _____

16. What kind of adaptation measures you used to reduce these impacts of climate change/ variability? Mark your answer by (x)

No.	Adaptation strategies	1.Yes	2.No
1.	Soil and water conservation (SWC)	□	□
2.	Changing crop variety	□	□
3.	Changing planting/harvesting dates	□	□
4.	Using irrigation	□	□
5.	Implementing agroforestry	□	□

17. Are you a member of social institutions in your village? 1.Yes □ 2.No □
18. If your answer for question 17 is yes in which social institutions you participate? 1.Iddir □ 2.Equb □ 3. Religious groups □ 4. None □ 5. Others, specify _____
19. Did you get help from extension workers on crop and livestock? 1. Yes □ 2. No □
20. Do you have any market linkage for selling your product? 1. Yes □ 2. No □
21. Do you get climate information that helps for your agricultural activities? 1. Yes □ 2.No □
22. Do you have access to credit services? 1. Yes □ 2. No □

Appendix B: Questions for the interview guide

1. What are the observed changes in rainfall and temperature since 2000
2. What are the impacts of changes in rainfall and temperature?
3. Do you perceive the changes in drought patterns? Do you think droughts affect agricultural activities, both livestock and crop production?
4. Have you ever noticed the shifts in planting and harvesting dates?
5. What adaptation strategies did you used to lessen the impacts of climate change?
6. What major factors affect the choices of these adaptation strategies?